FUEL PRODUCTION FROM THERMOCHEMICAL PROCESSING OF WASTE PLASTICS AND BIOMASS

By

Kaltume Akubo

Submitted in accordance with the requirements for the degree of
Doctor of Philosophy

The University of Leeds
School of Chemical and Process Engineering

October 2019

The candidate confirms that the work submitted is her own, except where work which has formed part of jointly authored publications has been included. The contribution of the candidate and the other authors to this work has been explicitly indicated below. The candidate confirms that appropriate credit has been given within the thesis where reference has been made to the work of others.

Journal papers

Chapter 4 was based on the following published paper:

Akubo, K., Nahil, M.A. and Williams, P.T. (2017) Aromatic fuel oils produced from the pyrolysis-catalysis of polyethylene plastic with metal-impregnated zeolite catalysts. Journal of the Energy Institute, 92, p. 195-202.

Chapter 5 was based on the following published paper:

Akubo, K., Nahil, M.A. and Williams, P.T. (2018) Pyrolysis-catalytic steam reforming of agricultural biomass wastes and biomass components for production of hydrogen/syngas. Journal of the Energy Institute, 92, p.1987-1996.

Conference/posters:

Akubo, K., Nahil, M.A. and Williams, P.T. (2016) Production of methane from waste plastics for high value aromatic products. 21st International Symposium on Analytical and Applied Pyrolysis; Nancy, Francis May, 2016.

Akubo, K., Nahil, M.A. and Williams, P.T. (2017) Pyrolysis-catalysis of waste plastics to produce high value fuel and aromatic compounds; 5th International Conference on Sustainable Solid Waste Management, Athens, Greece, June 2017.

The candidate Kaltume Akubo performed the experimental and analytical work, wrote the initial drafts of the papers along with supporting material including Tables and

Figures, and carried out the calculation and summarisation of the results and developed the discussion section.

The co-authors, Professor P.T Williams, and M.A. Nahil, supervised the entire research work and made suggestions, Professor P.T Williams proofread the drafts and made corrections to the draft papers.

Acknowledgements

Foremost, I would like to thank God; my Lord Jesus Christ and to give him all the glory for his endless love in my life. My appreciation goes to the Federal Government of Nigeria, specifically the administration of His Excellency, President Goodluck Ebele Jonathan who offered me an NYSC President Honours Award in 2010 with automatic employment and full scholarship for both masters and doctorate degrees. Special recognition must be given to Petroleum Trust Development Fund (PTDF) for following through with the presidential award.

My sincere and deepest gratitude goes out to my supervisor Professor Paul T. Williams for all the support, guidance, encouragement, direction and assistance granted me during the study. Thank you for always been accessible, speedy in responding to every issue and for always being patient. Also, thank you for enabling me to access the fund and to acknowledge the EU-RISE FLEXI-PYROCAT grant to carry out experiments in Tsinghua University, Beijing, China.

Likewise, my co-supervisor Dr Mohammad Nahil Anas for all the support and assistance during the laboratory work. Thank you for your patience, positive criticism and suggestions. On this note, I would equally like to thank Dr. Jude Onwudili for the positive encouragement to join the group. I would like to thank all my colleagues for their friendship; Ganiyu, Efosa, Simon, Cynthia, Japheth, Julius, Kenneth, Juniza, Amal, Yeshui, Andrew, Elle, Musaab, Idris, and Rayed.

My deepest gratitude goes to my family, first to my husband: Arome O. Akubo for his endless love, support, prayers and encouragement. Also, to my lovely daughters Emmaneulla O. Akubo and Tehillah O. Akubo. I am so blessed by God to have given birth to you both during my PhD research studies. I sincerely want to show my appreciation to my sisters, particularly Fatima Binta Abutu for your kindness and sacrifice towards us just like a mother and your endless calls of care. Also, Amina Charity Abutu for all your assistance, visits and support during the course of this study. I also wish to sincerely thank all my brothers and sisters, too numerous to name. Special thanks to my father-in-law for his encouragement to bring the certificate and all my in-laws. To all my friends, family friends, Pastors and well-wishers, I say a big thank you.

Lastly, with so much deep-rooted hearty emotion, I recognise my late parents, Alhaji A. D. O Abutu and Hajiya Salamatu A. Abutu, I wish you were alive to see me, you left too soon and your memories will last a lifetime, I love you both.

Abstract

Thermochemical conversion through pyrolysis and pyrolysis-catalysis in addition to gasification methods of processing plastic wastes and biomass have attracted research interest. Likewise, co-pyrolysis catalytic steam reforming of lignocellulosic biomass with plastic wastes for converting these wastes into high-value fuel and chemicals remains a novel option as it offers several advantages such as cost reduction for waste management, improvement in product quality and quantity, prevention of wastes into the landfill, etc.

In this research, pyrolysis-catalysis of high-density polyethylene (HPDE) was carried out in a fixed-bed two-stage reactor for the production of up-graded aromatic pyrolysis oils. The catalysts investigated were Y-zeolite impregnated with transition metal promoters with 1 wt.% and 5 wt.% metal loading of Ni, Fe, Mo, Ga, Ru and Co to determine the influence on aromatic fuel composition. Loading of metals on the Y-zeolite catalyst led to a higher production of aromatic hydrocarbons (about 98%) in the product oil with greater concentration of single ring aromatic hydrocarbons (up to 99%) produced. The single ring aromatic compounds consisted mainly of toluene, ethylbenzene and xylenes, while the 2-ring hydrocarbons were mainly naphthalene and their alkylated derivatives. There was a reduction in the production of multiple ring aromatic compounds such as phenanthrene and pyrene. However, there was significant carbon deposition on the catalysts in the range 14-22 wt.% for the 1% metal-Y-zeolite catalysts and increased to 18-26 wt.% for the 5 wt.% metal-Y-zeolite catalysts which were mainly filamentous type carbon.

In addition, steam reforming of six agricultural biomass waste samples and the three main components of biomass were investigated in a two-stage fixed bed pyrolysis-catalytic reactor. The waste biomass samples consisted of; rice husk, coconut shell, sugarcane bagasse, palm kernel shell, cotton stalk and wheat straw while the biomass components included: cellulose, hemicellulose (xylan) and lignin. The TGA results showed distinct peaks for the individual biomass components, which were also evident in the biomass waste samples reflecting the existence of the main biomass components in the biomass wastes. The results for the two-stage pyrolysis-catalytic steam reforming showed that introduction of steam and catalyst into the pyrolysis-catalytic steam reforming process significantly increased gas yield and syngas production notably hydrogen. For instance, hydrogen composition increased from

6.62 to 25.35 mmol/g by introducing steam and catalyst into the pyrolysis-catalytic steam reforming of palm kernel shell. Lignin produced the most hydrogen compared to cellulose and hemicellulose at 25.25 mmol/g. The highest residual char production was observed with lignin which produced about 45 wt.% char, more than twice that of cellulose and hemicellulose.

Co-pyrolysis gasification of biomass components (lignin and cellulose) with plastic wastes (HDPE and PS) using novel metal catalysts in a fixed bed two-stage reactor was equally investigated. The introduction of steam and temperature increase, as well as the presence of metal catalysts, markedly increased the yield of hydrogen and syngas. Likewise, in the analyses of the different metals (Ni, Co, Mo and the bimetal NiCe) supported on MCM-41 catalysts presented the 10%Ni/MCM-41 (up to ~52 mmol/g and syngas ~ 79 mmol/g) to have a slightly higher yield of hydrogen compared with the other metals. The temperature increase from 750 to 850^{0}C showed an increase in hydrogen yield from ~52 to 61 mmol/g and increased syngas yield from ~ 74 to 87 mmol/g. Likewise, as the steam flow rate was increased from 0 to 9.7 ml/h, the hydrogen yield increased from ~ 32 to 68 mmol/g and the syngas yield increased from ~ 45 to 96 mmol/g but decreases slightly from 7.7 to 9.7 ml/h steam rate. The blend of lignocellulosic biomass and plastic wastes in co-pyrolysis appears to be a novel option for tackling the problem of waste disposal in landfill, coupled with the production of petrochemical products, and in addition the generation of carbon neutral fuels.

Table of Contents

List of Figures

List of Tables

Abbreviations

ABS	Acrylonitrile-Butadiene-Styrene
BET	Brunauer-Emmett-Teller
BTX	Benzene, Toluene and Xylenes
CH_4	Methane
CHP	Combine Heat and Power generation
CHNS–O	Carbon, Hydrogen, Nitrogen, Sulphur, Oxygen
CO_2	Carbon dioxide
CO	Carbon monodioxide
CNT	Carbon Nanotubes
DCM	Dicloromethane
DTG	Differential thermogravimetry
EDXS	Energy Dispersive X-Ray Spectrometer
EIA	Energy Information Administration
EJ	Exajoule
EPS	Expanded Polystyrene
ER	Equivalent Ratio
EVA	Ethylene Vinyl Acetate
Exp	Experiment
FC	Fixed carbon
FEGSEM	Field Electron Gun Scanning Electron Microscopy
GCV	Gross Calorific Value
GC-MS	Gas Chromatograph-Mass Spectrometry
GC	Gas Chromatograph
GC-TCD	Gas Chromatograph-Thermal Conductivity Detector

GC-FID	Gas Chromatography-Flame Ionization Detector
HC	Hydrocarbon
HHV	Higher Heating Value
HIPS- Br	High Impact Polystyrene with Brominated Flame Retardant
HDPE	High-Density Polyethylene
H_2	Hydrogen
IEA	International Energy Agency
LDPE	Lower Density Polyethylene
LLDPE	Linear Low Density Polyethylene
LHV	Low Heating Value
MDPE	Medium density polyethylene
MCM-41	Mobil Composition of Matter No. 41
MC	Moisture content
MSW	Municipal Solid Waste
NYSC	National Youth Service Corps
ND	Not detected
PAHs	Polycyclic Aromatic Hydrocarbons
PE	Polyethylene
PET	Polyethylene terephthalate
PP	Polypropylene
PS	Polystyrene
PTDF	Petroleum Trust Development Fund
PVC	Polyvinylchloride
RF	Response factor
RSTD	Relative Standard Deviation
STD	Standard Deviation
SPI	Society of Plastics Industry

SEM	Scanning electron microscopy
Syngas	Mixture of permanent and hydrocarbon gas in different concentrations composed of mainly H_2 and CO.
Tar	Mixture of aromatic and oxygenated compounds in gaseous or liquid phase
TCD	Thermal Conductivity Detector
TGA	Thermogravimetry analysis
TPO	Temperature program oxidation
VM	Volatile matter
XRD	X-ray diffraction
XLPE	Cross-Linked Polyethylene
XPS	Extruded Polystyrene

Chapter 1

Introduction

1.1 Global Energy Demand

Currently, the production of energy will not be sufficient for future global requirements. In addition, the problem of fossil fuel depletion, increase in fuel price, difficulty in accessing petroleum sources as well as global warming and environmental degradation pose a threat to global energy demand and production. Therefore, sustainable development of energy is essential. Energy demand around the world has been increasing progressively due to population growth and increased economic development. The desire for the production of energy from renewable sources rather than fossil fuels has been stimulated by concerns over global warming linked to greenhouse gas emissions from fossil fuel use and issues of sustainability [1, 2]. The world population is estimated by the United Nations to increase to about 8.1 billion by 2050. The world energy use will grow by 56 per cent between 2010 and 2040 [3]. About 80% of the global energy demands are produced from fossil fuels such as oil, gas and coal [4]. Renewable energy and nuclear power contributes 13.5% and 6.5% of the total energy demand respectively [4]. It has also been reported that renewable energy and nuclear power are the fastest growing energy sources, each increasing by 2.5 per cent per year [3]. It is, therefore, very necessary to concentrate on improving alternative energy (renewable sources such as biomass and wastes) rather than depending solely on fossil fuel, which is fast depleting. Existing reserves of fossil fuels all around the world are becoming rapidly exhausted as compared to new ones being discovered [1, 5]. Furthermore, worldwide energy-related carbon dioxide emissions are estimated to increase by 46 per cent by 2040. This has prompted a proposed greenhouse gas emissions reduction (from 1990) by at least 40%, with at least a 32% share of renewable energy and at least a 32.5% improvement in energy efficiency target set up by the EU for year 2030 [6]. Likewise, the European commission further advocate for a climate-neutral Europe by 2050 in long-term strategy with the objective to keep the global temperature increase below 2 ^{o}C and, with effort, to keep it to 1.5 ^{o}C [6].

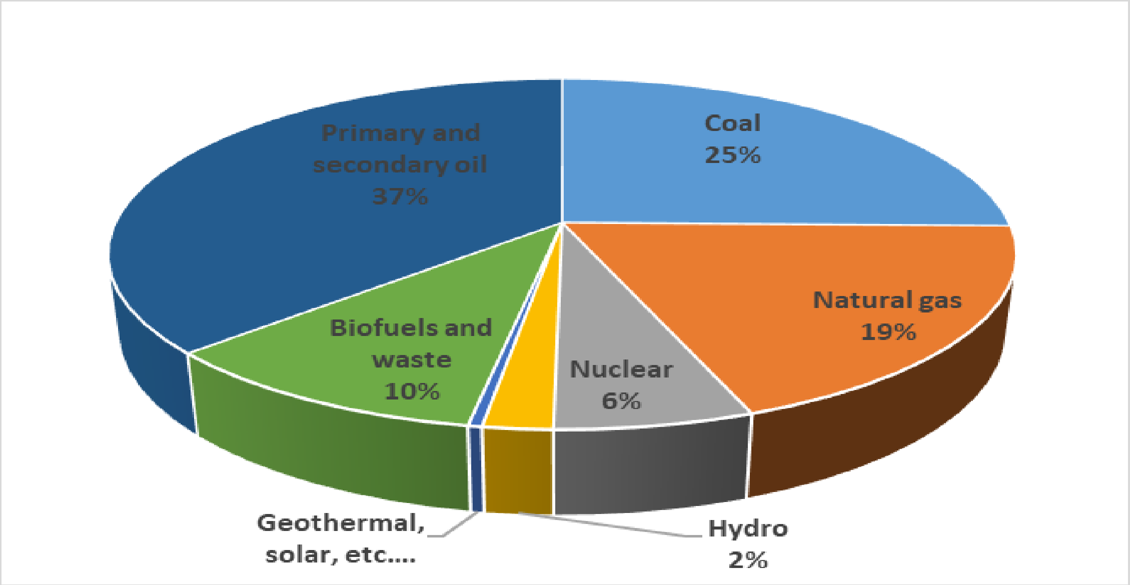

Figure 1.1. World total primary energy supply by fuels, 2018 [7].

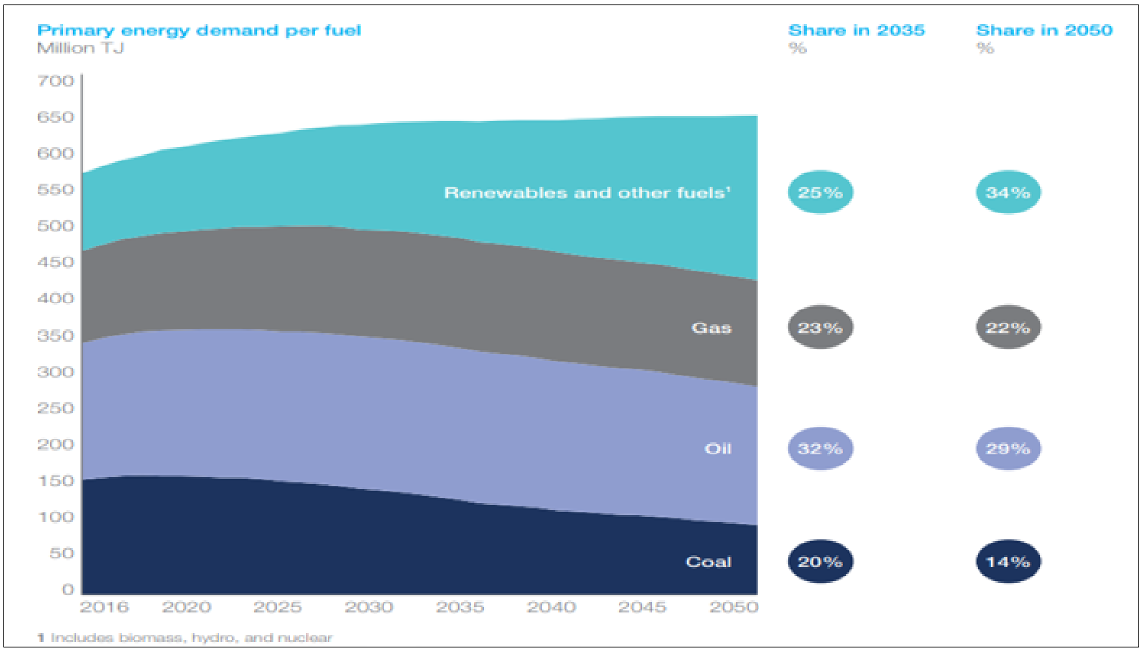

Figure 1.2. Global energy demand per fuel projection in 2019 [8].

As shown in Figures 1.1 and 1.2, renewable energy sources including biomass are currently estimated to be about 19% and suggested to increase to about 34% by the year 2050. Fossil fuels which include oil, gas and coal are predicted to drop (especially coal) to about 14% in 2050 and carbon emissions are projected to decrease due to the decline in coal usage by 2050 [8]. Consequently, global energy demand is stipulated by two major issues of more energy production and less of carbon production, to mitigate these challenges attributed to fossil fuel production, an alternative energy from wastes as a sustainable resource and renewable energy pathway seem to be the solution.

1.2 Production of Alternative Energy from Wastes

The global solid waste generation is estimated to increase because of population and urbanization. Global solid-waste generation has risen by tenfold and been suggested to double to more than 6 million tonnes per day by 2025 [9]. Also, the World Bank has estimated that about 1.2 kg per person per day (i.e. 1.3 billion tonnes per year) of MSW from 3 billion urban residents was generated in 2012 and this is to increase to 4.3 billion urban residents generating about 1.42 kg/capita/day (2.2 billion tonnes per year) of MSW by 2025 [10]. Solid waste generation has created global environmental issues. Some of the problems associated with solid waste generation includes, air and water contamination, public health issues due to breeding of disease vector and exposure to people living near the waste and toxic substances (dioxins and furans) discharged by incineration of wastes which causes harm to both human and ecological health. Waste disposal by landfill also tends to emit greenhouse gases such as methane, as the organic waste decomposes. Therefore, a sustainable energy source and vital waste management is necessary to tackle these challenges. Waste to energy seems to afford a sustainable path for solving waste management issues. Hence, creating a process for converting wastes into energy is a promising route and sustainable for solving waste disposal by landfill. There are different classifications of solid waste generation. Some components of municipal solid waste (MSW) include plastics and biomass [11] which represent a significant proportion of the total solid waste generation. According to a World Bank report, plastic wastes are the second and third largest fractions of MSW [10] and organic waste being the highest as shown in Figure 1.3. According to Elif [12], the most important biomass energy sources and their estimated energy production includes wood and wood waste (64%), agricultural crops (5%) and their waste, municipal solid waste (MSW-24%), food processing waste, aquatic plants and algae, and animal wastes.

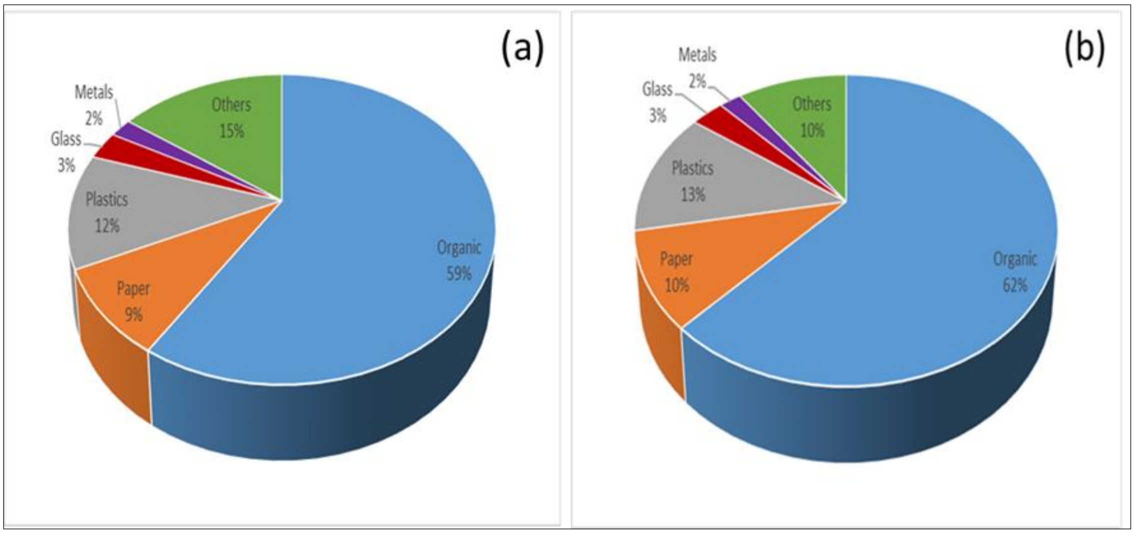

Figure 1.3. Global solid waste composition projections for 2025 (a) by lower middle income (369 MT), (b) by region EAP [10].

1.2.1 Biomass production

Biomass is an organic waste that originates from plants consisting of trees, crops and algae. Biomass does not contribute to the greenhouse effect, because the CO_2 absorbed by the plant during photosynthesis is the same CO_2 returned to the atmosphere during combustion. The process occurs regularly, as CO_2 is available and absorbed by new plant growth forming a closed loop cycle. Therefore, biomass does not release CO_2, which can accumulate in the atmosphere to alter climate change as fossil fuel, and others do.

Biomass has potential in all sectors which accounts for about 60% of total entire renewable use [13]. Global primary biomass potential has been estimated at 33-1135 EJ/year with the largest contribution coming from energy crops (0-988 EJ/y) produced in surplus agricultural land [14]. It has also been reported that global agricultural production of 2005 will have to increase from 70-110 percentage points (pp) to meet the demand in 2050 [15]. Global biomass demand is estimated to double to 108 EJ by 2030, a third of this total to be used to produce power and district heat generation, 30% in biofuel production for transportation while the remaining is to be shared equally between manufacturing industry and building sectors [13]. It was also reported, of the global biomass supply in 2030 to be estimated from a range of 97-147 EJ per year with approximately 40% originating from agricultural residues and wastes (37-66 EJ) while the remainder is divided between energy crops (33-39 EJ) and forest residues (24-43 EJ) [13]. According to an IEA report, about 9% of world total primary energy supply comes from bioenergy, with more than half of this being attributed to traditional inefficient open fires or on cooking stoves in developing countries with impact on the environment and health due to indoor smoke pollution [16]. Therefore, it is very necessary to improve energy production from biomass as more than half of the world is impoverished by energy, as shown in Figure 1.4. Developments in the biomass sector of the UK has been estimated to be a 400 MW cap on subsidy eligibility for non-CHP biomass projects [17]. In addition, UK electricity generation is estimated to deliver 38-50 terawatt-hours (TWh) of biomass power conversion and other sustainable biomass in the year 2020, biomass heat with a total of 223-230 TWh estimated demand across the electricity sector as well as the heat and transport sectors to meet the UK's 15% renewable energy target [18]. The expected biomass conversion capacity to range from about 1.7 GW to 3.4 GW by 2020 [18].

Biomass availability for energy is reported to depend on some important factors such as: (1) Future demand for food, determined by the population growth and the future diet; (2) Availability of degraded land; (3) Productivity of forest and energy crops, (4) Surplus agricultural land used for reforestation; (5) The increased use of bio-materials; (6) The type of food production systems that can be adopted world-wide over the next 50 years [14]. The drive for bio-energy production necessitated by rising prices of energy, climate change, energy security and rural development, etc. as bio-energy could contribute to CO_2 reduction leading to a low-carbon energy future. Biomass uses includes power and electricity generation, transportation, heating, cooking and combined heat and power generation (CHP) for use in the manufacturing industry and power sectors.

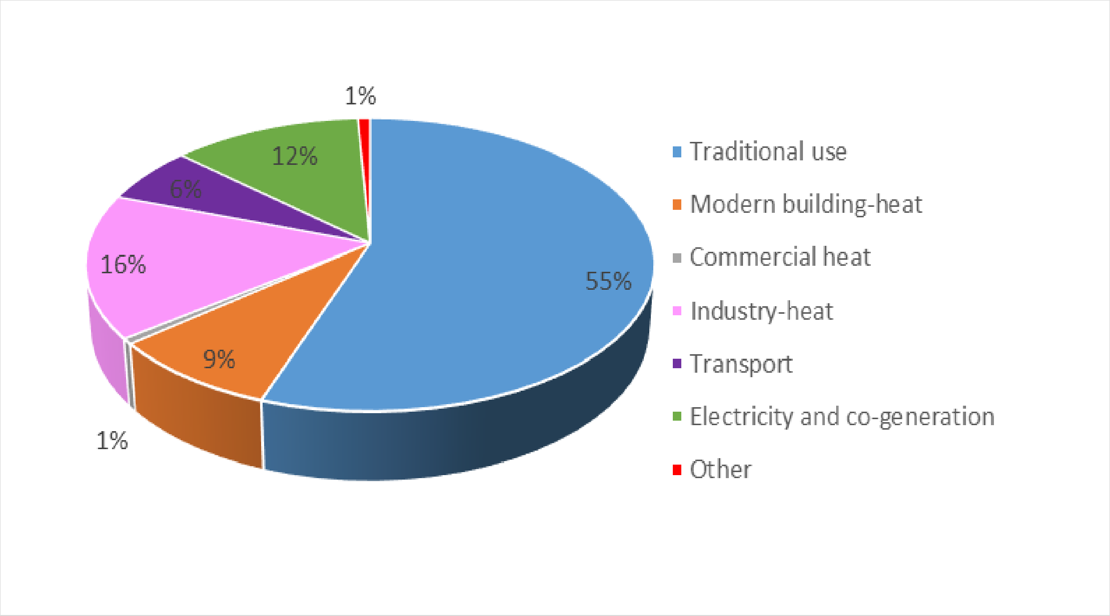

Figure 1.4. Consumption of biomass and waste resources (Total: 51 EJ) IEA report, 2015 [16].

1.2.1.1 Biomass potential for energy production

Biomass sources of fuel are abundantly available all over the world in both rural and urban environments. It is a renewable source because it does not become extinct as long as plants and animals exist, they will continually generate waste. The feedstock includes agricultural wastes, wood/forestry, food processing industries, aquatic waste, animal and human waste, municipal and industrial waste. Materials with the potential for energy production from biomass include woody crops, grasses, herbaceous plants (all perennial crops), starch and sugar crops and oilseeds with characteristics such as high yield, low energy input to produce, low cost, low nutrient requirements [19], that is not an edible crop. These biomass sources for the production of energy (hydrogen fuel and chemicals), can be divided into edible and non-edible sources. The edible sources are the starch-based biomass such as corn crops, cassava, and sugar cane bagasse etc. The non-edible sources are the lignocellulosic biomass such as wood, grass and agricultural waste, energy crops, etc., which are preferable because they do not compete with food resources [20].

Biomass energy can be converted into a usable form directly and indirectly, e.g. combusted to generate heat, converted into electricity directly and indirectly through processing into biofuel. However, biomass needs to be dried before it can be used and it can also be processed into a coal-like material through torrefaction with better fuel characteristics than the original biomass. It can be compressed into briquettes-moulded block, then combusted directly (direct firing) and the steam produced during the firing process powers a turbine that operates a generator to produce electricity. Hence, energy can be produced from biomass plant through physical conversion such as combustion, biological conversion as fermentation and anaerobic digestion, as well as thermochemical conversion, e.g. combustion, pyrolysis and gasification, see Figure 1.5.

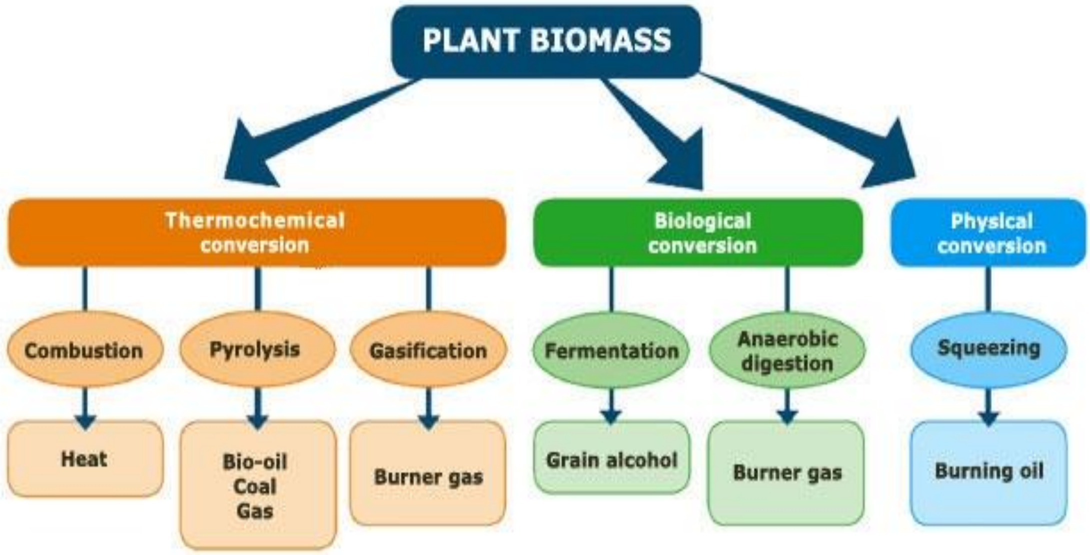

Figure 1.5. Illustration of the biomass process pathway for biomass [21].

1.2.2 Plastics production

Plastic production over the years has increased due to high demand and its use in various fields. It has been reported that plastics production had increased annually by 5% since 1990 and had attained the largest global capacity of about 260 million tonnes (260 x10^6 t) since 2007 [22, 23]. Wong et al. [24], stated annual production for each type of plastic in 2012 to be 65.41, 52.75, 37.98, 19.80, 10.55 and 2.8 million tonnes for polyethylene (PE), polypropylene (PP), polyvinylchloride (PVC), polyethylene terephthalate (PET), polystyrene (PS) and ethylene vinyl acetate (EVA) respectively. In 2006, the principal manufacturers of plastics in the world were in Europe (EU25 + Norway and Switzerland), producing about 25% in a total of 245 million tonnes in 2006 while the USA are the largest consumer of plastics, estimated at 27.3 million tonnes as compared with 170 million tonnes global consumption in 2000, and reaching about 39 million tonnes in 2010 [25]. In 2014, it was reported that the largest manufacturer of plastic materials globally is China followed by Europe [26]. Plastics consumption investigation per capita shows about 100 kg per resident in Western Europe and North America, and this may grow to about 140 kg per occupant by 2015. In addition, emergent parts of Asia excluding Japan, also have the utmost growth potential with a current consumption per capita of about 20 kg, New European Union Member states have witnessed the highest potential for growth in Europe with an average consumption rate ranging between 50 to 55 kg per capita [27].

1.2.2.1 Plastic waste generation

There are two major groups of plastic waste: industrial and municipal. Industrial plastic waste involve homogeneous wastes, uncontaminated wastes that can easily be recycled while that of municipal waste is very heterogeneous. MSW contains about 10.62 +/- 5.12 wt.% of plastic waste and these are more difficult to recycle due to the different content of the waste [23, 28]. It was also estimated by the World Bank that about 8-9% of plastics waste is contained in municipal solid wastes as generated by different countries around the globe and this may increase to about 9-13% by the year 2025 [24]. The total plastics waste in municipal solid waste consists of about 50-70% packaging materials mainly of polyethylene (high and low density polyethylene, HDPE and LDPE), polyethylene terephthalate (PET), polypropylene (PP), polyvinyl chloride (PVC), and polystyrene (PS). Polypropylene and polyethylene plastics are the most widely used plastics and in an estimate of all plastics waste, 69% is made up of polyethylene [23]. According to Wrap [29] in 2016, the total UK plastics post-consumer waste treatment is projected to be about 3.8 million tonnes, packaging is the major source of plastic waste generation valuing about 2.3 million tonnes and non-packaging plastics are estimated to be approximately 1.5 million tonnes, as shown in Figure 1.6. In 2017, an estimate of the breakdown by format and polymer showed that the consumer plastics packaging film totalled about 32% and rigid plastics totalled about 68% while for non-consumer plastics packaging film the total was about 69% while rigids totalled about 31%, as shown in Tables 1.1 and 1.2.

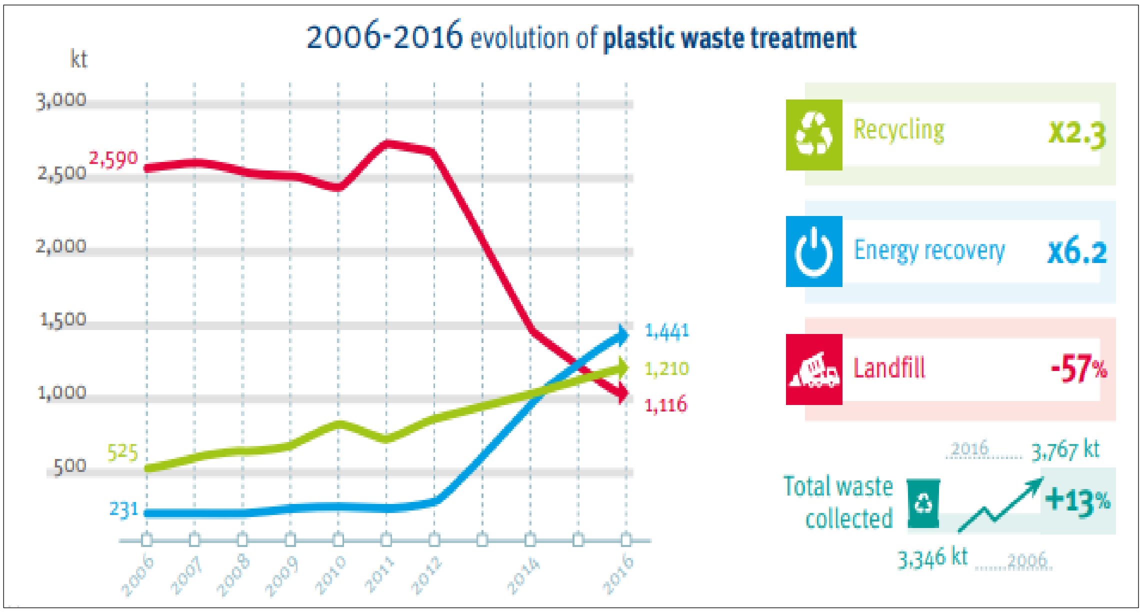

Figure 1.6. UK plastic packaging treatment (million tonnes), 2016 [30].

Table 1.1. Breakdown of UK consumer plastic packaging by format and polymer (thousand tonnes), 2017 [29].

Consumer plastic packaging	**LDPE/ LLDPE**	**HDPE**	**OPP**	**PP**	**PET**	**PS**	**PVC**	**Other**	**Grand Total (Tonnes)**	**Grand Total (%)**
Film Total (k)	**164**	**159**	**18**	**106**	**66**	**2**	**7**	**108**	**629**	**32**
Film (k)	67	32	13	66	56	0	6	75	315	16
Film-Bags (k)	97	127	5	40	10	2	1	32	314	16
Rigids Total (k)	**12**	**218**	**4**	**170**	**778**	**75**	**47**	**16**	**1320**	**68**
Bottles (k)	1	179	0	5	376	0	2	0	563	29
Consumer closures (k)	4	36	4	19	23	0	1	3	91	5
Consumer PTTs (k)	5	0	0	139	372	60	44	8	629	32
Thermoformed packs (k)	3	0	0	27	331	8	44	2	416	21
Injection moulded Rigids (k)	2	0	0	113	41	52	0	5	213	11
Others (k)	1	2	0	6	7	15	0	5	37	2
Grand Total (tonnes)	**176**	**377**	**22**	**275**	**845**	**77**	**54**	**124**	**1950**	
Grand total (%)	9	19	1	14	43	4	3	6		

Table 1.2. Breakdown of UK non-consumer plastic packaging by format and polymer (thousand tonnes), 2017. [29].

Consumer plastic packaging	**LDPE/ LLDPE**	**HDPE**	**OPP**	**PP**	**PET**	**PS**	**PVC**	**Other**	**Grand Total (Tonnes)**	**Grand Total (%)**
Film Total (k)	**546**	**5**	**0**	**57**	**15**	**4**	**8**	**3**	**637**	**69**
Film (k)	508	5	0	42	9	4	7	3	578	63
Film-Bags (k)	38	0	0	11	0	0	0	0	50	5
Film-strapping/Tape/Bands (k)	0	0	0	3	6	0	0	0	9	1
Rigids Total (k)	**1**	**82**	**0**	**87**	**48**	**25**	**38**	**1**	**280**	**31**
Bottles (k)	1	50	0	1	4	0	1	0	57	6
Consumer closures (k)	0	0	0	0	0	0	0	0	0	0
Consumer PTTs (k)	0	0	0	0	0	0	0	0	0	0
Non-Consumer Rigids (k)	**0**	**21**	**0**	**86**	**34**	**25**	**0**	**0**	**167**	**18**
Closures (k)	0	1	0	1	1	0	0	0	3	0
Injection moulded pallets, crates, etc. (k)	0	0	0	25	0	0	0	0	25	3
EPS Transit Packaging (k)	0	0	0	0	0	10	0	0	10	1
Parts, Drums, Industrial	0	20	0	13	0	0	0	0	33	4
Non-Consumer PTTs	0	1	0	47	33	15	0	0	96	10
Others (k)	0	11	0	0	9	0	36	1	57	6
Grand Total (tonnes)	**546**	**87**	**0**	**143**	**63**	**29**	**45**	**4**	**918**	
Grand total (%)	60	6	0	17	7	4	6	0		

Recycling provides the avenue for reduction of waste plastics disposal in landfill, hydrocarbon usage and reduced carbon dioxide emissions. Amidst all the recycling methods, chemical recycling [31-33] seems to be most effective and efficient method of waste plastics recycling because of its capability to form the raw materials from which it is made.

1.2.2.2 Potential for energy recovery from plastic waste

Plastics are polymer materials with large molecular weight that can be moulded and remoulded into different shapes and sizes. They can also combine with other substances to form different products. Plastics using different criteria classified as thermoplastics or thermosetting plastics, synthetic or natural, non-biodegradable or biodegradable, crystalline or non-crystalline (amorphous). However, there are two major types of plastics: thermoplastics and thermosetting polymers. Thermoplastics are plastics that do not change in their chemical composition when subjected to heat, they usually melt when heated and harden when cooled thus can be moulded and remoulded. While thermosetting plastic dimensional structures decompose thermally during heating, it undergoes irreversible chemical reaction, has infinite molecular weight, and thus cannot be remoulded. Examples of thermoplastics include: polyethylene, polypropylene, polyvinyl chloride which are usually used for packaging while examples of thermosetting plastics are vulcanisation process of rubber, epoxy, phenolic, polyester, silicone, fiberglass, etc.

There are wide applications of plastics in various fields such as in domestic use, agriculture, medical, construction, electrical and electronics, transportation (automobile parts, aviation, space technology, etc.), entertainment and parks (amusement parks, toys, games and event centers, etc.), fashion and styles (clothing, shoes, decoration, hair extensions and accessories, etc.), and a variety of different types of packaging. According to Panda et al. [34], plastics usage saves energy and results in CO_2 emission reduction.

The production of plastic materials from hydrocarbons consumes about 4%-8% of the world’s total annual oil production [31, 35, 36]. Petroleum-based hydrocarbons contain both hydrogen and carbon atoms with the variation of shorter and longer carbon chain molecules, which can be incorporated into plastics. This implies that plastic materials can equally be converted back to produce petroleum products such as diesel, petrol, gases as well as aromatics and chemicals. The use of waste plastics for production of high value aromatics and chemicals is of enormous benefit in that it helps to serve a dual purpose: on the one hand, plastic recycling provides a solution for waste treatment thereby leading to a cleaner environment. On the other hand, the conversion of waste plastics to high-value chemicals, hydrogen and fuels avoids the loss of valuable resources, provides an avenue for job creation and revenue generation. This process of conversion of plastics to hydrocarbons involves pyrolysis-catalytic which is a type of chemical recycling process [31, 33, 37].

1.3 Thermochemical Conversion of Wastes for Fuel Production

Amidst the conversion routes, thermochemical conversion provides an effective system. Pyrolysis and pyrolysis-catalysis in addition to gasification methods of processing biomass and plastic wastes have attracted research interest [37-39] as it is considered a feasible and sustainable alternative energy source to meet supply and demand. Pyrolysis-catalysis of plastics and biomass yield three distinct products which include gases, liquids and solids [31, 32]. The proportion for each of the three products greatly depends on the type of feedstock (plastics, biomass, etc.) and the pyrolysis-catalytic reaction conditions. Furthermore, co-pyrolysis of the combination of biomass with hydrogen-rich feedstock (like plastics waste) [40-42] is a vital alternative in terms of the quality and quantity of products produced.

In this work, pyrolysis-catalytic of waste plastics, biomass and co-pyrolysis of both feedstocks were studied in a two-stage fixed bed reactor for producing liquid fuels and high value aromatic chemicals or hydrogen and syngas.

1.4 Research Aim and Objectives

The main aim of this project is to convert plastic wastes and biomass into valuable hydrocarbon chemicals and fuels; aromatic chemicals, hydrogen and syngas production which have significant importance in the world today such as for power and electricity generation, and industrial chemical production.

The research objectives listed as follows:

- To evaluate and characterise the feedstock in order to understand the composition of various samples and the degradation pattern/profile of the feedstock.
- To investigate the most suitable process parameters such as feedstock type, pyrolysis and catalytic bed temperature, steam injection rate, etc., for the modification and determination of appropriate product yield and distribution.

- To analyse the influence of catalyst type, catalyst ratio and metal loading on different catalysts for maximising production of aromatic chemicals and fuel from plastics waste and biomass.
- To understand the reaction mechanism involved in the processing of pyrolysis-gasification of biomass and plastics waste, and to further manipulate the yield of hydrogen/syngas production.
- To explore the synergistic effect on co-pyrolysis of biomass with high hydrogen-rich feedstock (plastics waste) for enhancement of product yield and composition.
- To characterise both fresh and used catalysts from the pyrolysis-catalytic process for identification of solid carbon deposition and to minimise catalyst deactivation.

References

1. Shafiee, S. and E. Topal, *When will fossil fuel reserves be diminished?* Energy policy, 2009. 37(1): p. 181-189.
2. Böhringer, C., T.F. Rutherford, and R.S. Tol, *The EU 20/20/2020 targets: An overview of the EMF22 assessment.* Energy economics, 2009. 31: p. S268-S273.
3. Briefing, U.S.J.U.E.I.A., *International energy outlook 2013.* 2013.
4. Asif, M., T.J.R. Muneer, and S.E. Reviews, *Energy supply, its demand and security issues for developed and emerging economies.* 2007. 11(7): p. 1388-1413.
5. Ahuja, S., ed. *Food, Energy, and Water: The Chemistry Connection*. 2015: Calabash, NC.
6. Union, E. *Climate strategies & targets*. European Commission 2018 revised; Available from: https://ec.europa.eu/clima/policies/strategies/2050_en.
7. Agency, I.E., *IEA World Energy Balances* 2018.
8. insights, M.E., *Global Energy Perspective.* 2019.
9. Hoornweg, D., P. Bhada-Tata, and C.J.N.N. Kennedy, *Environment: Waste production must peak this century.* 2013. 502(7473): p. 615.
10. Bhada-Tata, D.H.a.P., *WHAT A WASTE: A Global Review of Solid Waste Management.* World Bank, 2012. No. 15.
11. Zhou, H., et al., *Classification of municipal solid waste components for thermal conversion in waste-to-energy research.* 2015. 145: p. 151-157.
12. Kırtay, E., *Recent advances in production of hydrogen from biomass.* Energy Conversion and Management, 2011. 52(4): p. 1778-1789.
13. IRENA, *Global Bioenergy Supply and Demand Projections.* International Renewable Energy Agency (IRENA), 2014.
14. Hoogwijk, M., et al., *Exploration of the ranges of the global potential of biomass for energy.* 2003. 25(2): p. 119-133.
15. Mauser, W., et al., *Global biomass production potentials exceed expected future demand without the need for cropland expansion.* 2015. 6: p. 8946.
16. Agency, I.E., *Bioenergy and biofuels.* 2015.
17. CONSULTING, T., *UK Dedicated Biomass Statistics - 2017.* The Waste and Bioenergy Experts, 2017.
18. Association, R.E., *UK Biomass Sector:an overview of developments,challenges and opportunities.* 2014.
19. McKendry, P., *Energy production from biomass (part 1): overview of biomass* Bioresource Technology 2002. 83: p. 37–46.
20. Zhang, X., et al., *Catalytic co-pyrolysis of lignocellulosic biomass with polymers: a critical review.* Green Chemistry, 2016. 18(15): p. 4145-4169.
21. Ambiente, I. *Biomass processing pathway*. Available from: http://www.imamambiente.com/en/biomass/.

22. Lettieri, P. and S.M. Al-Salem, *Thermochemical treatment of plastic solid waste.* WASTE: a handbook of waste management and recycling. Elsevier, Amsterdam, The Netherlands, 2011: p. 233-242.

23. Kunwar, B., et al., *Plastics to fuel: a review.* Renewable and Sustainable Energy Reviews, 2016. 54: p. 421-428.

24. Wong, S., et al., *Current state and future prospects of plastic waste as source of fuel: A review.* Renewable and Sustainable Energy Reviews, 2015. 50: p. 1167-1180.

25. Panda, A.K., R.K. Singh, and D.K. Mishra, *Thermolysis of waste plastics to liquid fuelA suitable method for plastic waste management and manufacture of value added products—A world prospective.* Renewable and Sustainable Energy Reviews, 2010. 14(1): p. 233-248.

26. Europe, P. *An analysis of European plastics production, demand and waste data*. 2015; Available from: http://www.plasticseurope.org/Document/plastics---the-facts-2015.aspx.

27. Sartorius, I. *Materials case study 4:plastics* in *OECD Global Forum on Environment*. 2010. Mechelen,Belgium: OECD Environment Directorate,OECD.

28. Zhou, C., et al., *Characteristics and the recovery potential of plastic wastes obtained from landfill mining.* Journal of Cleaner Production, 2014. 80: p. 80-86.

29. Wrap. *PlasFlow report*. 2017; Available from: http://www.wrap.org.uk/sites/files/wrap/PlasFlow%202017%20Report.pdf.

30. Europe, P. *Plastics_the facts*. 2018; Available from: https://www.plasticseurope.org/application/files/6315/4510/9658/Plastics_the_facts_2018_AF_web.pdf.

31. Donaj, P.J., et al., *Pyrolysis of polyolefins for increasing the yield of monomers' recovery.* Waste Manag, 2012. 32(5): p. 840-6.

32. Adrados, A., et al., *Pyrolysis of plastic packaging waste: A comparison of plastic residuals from material recovery facilities with simulated plastic waste.* Waste Manag, 2012. 32(5): p. 826-32.

33. Kaminsky, W. and J.-S. Kim, *Pyrolysis of mixed plastics into aromatics.* Journal of Analytical and Applied Pyrolysis, 1999. 51(1): p. 127-134.

34. Panda, A.K., R.K. Singh, and D. Mishra, *Thermolysis of waste plastics to liquid fuel: A suitable method for plastic waste management and manufacture of value added products—A world prospective.* Renewable and Sustainable Energy Reviews, 2010. 14(1): p. 233-248.

35. Al-Salem, S., P. Lettieri, and J. Baeyens, *The valorization of plastic solid waste (PSW) by primary to quaternary routes: From re-use to energy and chemicals.* Progress in Energy and Combustion Science, 2010. 36(1): p. 103-129.

36. Brems, A., et al., *Gasification of plastic waste as waste-to-energy or waste-to-syngas recovery route.* Natural Science, 2013. 05(06): p. 695-704.

37. Achilas et al, *Recent Advances in the Chemical Recycling of Polymers (PP, PS, LDPE, HDPE, PVC, PC, Nylon, PMMA),*. 2015.

38. Uddin, M.N., W.W. Daud, and H.F. Abbas, *Effects of pyrolysis parameters on hydrogen formations from biomass: a review.* RSC Advances, 2014. 4(21): p. 10467-10490.
39. Kirkels, A.F. and G.P. Verbong, *Biomass gasification: Still promising? A 30-year global overview.* Renewable and Sustainable Energy Reviews, 2011. 15(1): p. 471-481.
40. Brebu, M., M.J.C.C. Nistor, and TECHNOLOGY, *Co-pyrolysis of various lignins with polycarbonate.* 2014. 48(1-2): p. 69-74.
41. Brebu, M., et al., *Co-pyrolysis of pine cone with synthetic polymers.* 2010. 89(8): p. 1911-1918.
42. Abnisa, F., et al., *Co-pyrolysis of palm shell and polystyrene waste mixtures to synthesis liquid fuel.* Fuel, 2013. 108: p. 311-318.

Chapter 2

Literature Review

2.1 Plastic wastes processing/management

For plastic waste treatment, there are four main methods which include primary, secondary, tertiary and quaternary recycling, (Figures 2.1 and 2.2). Tertiary/chemical recycling of waste plastic conversion into fuel or chemical feedstock has been acknowledged as being the ideal option [1, 2].

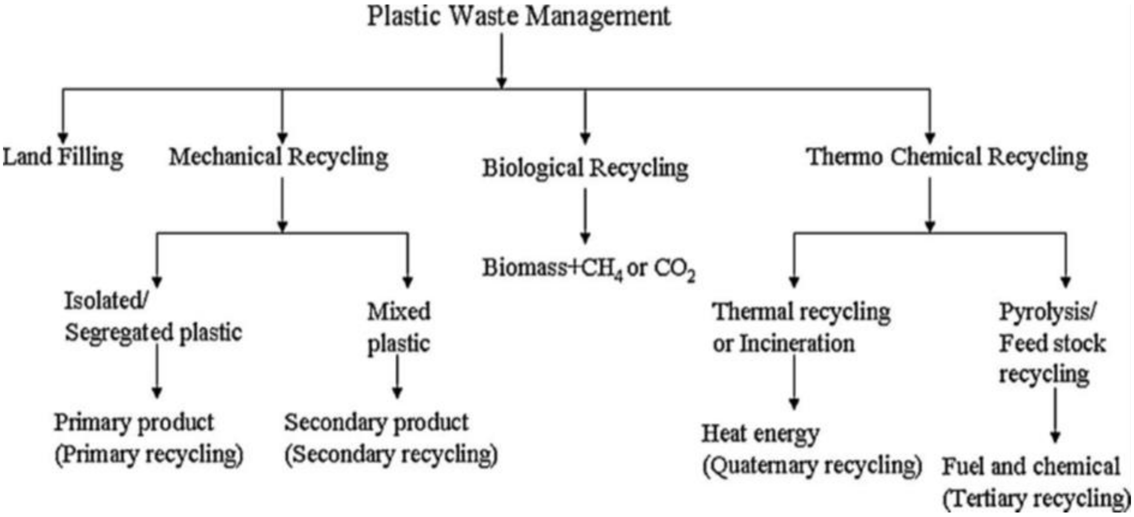

Figure 2.1. Illustration of different recycling methods [2].

a). Primary (re-extrusion) method: this is basically the reintroduction of single polymer plastic edges, scrap and other parts of the extrusion cycle in order to produce products of similar materials. According to Al-Salem [3], this process utilizes scrap plastics that have similar features to the original products. This process is only effective and feasible with semi clean scrap, not too popular with recyclers as many waste items hardly meet this criteria.

b). Secondary (mechanical) method: This process involves size reduction of the plastic to a more suitable form (pellets or powder) which is achieved by milling, grinding or shredding. The large plastics are cut into smaller sizes or shreds and contaminants such as paper or dust separated before floating, which separates plastic flakes of different density. Kaminsky and Kim [4], stated that the mechanical method is used on only one type of plastic waste (e.g. HDPE) and a market can only be found if the reprocessed products exactly match the primary product property and quality.

c). Tertiary (chemical) method: this is also known as the cracking process and refers to the technology used for processes which breakdown materials into smaller molecules at high temperatures, commonly gases, liquids and solids which are appropriate for further use as a feedstock for the production of other products, chemicals and fuel. Usually, the original raw material is lost in the process of conversion. Kaminsky and Kim [4] argued that chemical recycling such as pyrolysis is preferable due to the high rate and volume of plastic waste consumed during the conversion process to fuel and chemicals.

d). Quaternary (energy recovery) method: This procedure involves the recovery of energy content only and generation of heat energy is the only one advantage this process ensures. In Western Europe, 22.5% of overall waste plastics collectable are treated by the method of energy recovery, the residual involved incineration of about 20 wt.% and 10 vol.% of the initial wastes are dumped in landfills which shows that the problems of air pollution and solid waste are not resolved by this process [1, 5].

Figure 2.2. Illustration of polymer recycling techniques [6].

All the products generated by waste plastic conversion such as gases, liquid and solid residues are very useful, the gases and liquid can be used for fuel and chemicals while the residues can find uses as carbon black or to produce carbon nanotubes (CNT). There are diverse means of obtaining fuel and feedstock from waste plastics, the major ones include: pyrolysis/thermal degradation, gasification and catalytic cracking.

2.2 Pyrolysis/thermal degradation of plastic wastes

Pyrolysis is the thermal decomposition at high temperatures in enclosed atmospheres, which involves a chemical compositional change of the materials processed, and it is irreversible. The process involves the breaking down of the materials into gases, liquid and solid residue (char) thus obtaining high molecular weight and high boiling fraction in the absence of oxygen. According to Al-Salem [3], the pyrolysis process is an advanced technology that converts various types of wastes and biomass to produce a clean and high-calorific value fuel gas subject to the type of waste material being processed. Pyrolysis conditions can be varied to take advantage of producing a desired yield; higher temperatures for instance cause oil species of the higher molecular weight to thermally decompose into lower molecules and more of the gaseous phase is favoured [7]. Further processing and refining of liquids and gaseous yield generates petrochemical feedstock [5]. Pyrolysis is effectively applied to polyolefin plastics - polyethylene (PE), polypropylene (PP), polystyrene (PS) and other forms of waste plastics. Brems et al. [8], reported the use of polyethylene as feedstock for gasoline production and waxes for synthetic lubricants. Pyrolysis offers environmental, financial and operational advantages; some of the environmental benefits include a reduction in greenhouse gases (GHGs) such as CO_2 and a substitute for cleaning wastes dumped into landfill. The financial advantage of pyrolysis is due to the fact that the production of high calorific value fuel can easily be marketed whilst operationally, pyrolysis products are used as feedstock for the production of chemicals and the fuel gas produced is usually treated before utilisation [3].

The different type of plastics vary in chemical composition and properties. Proximate analysis techniques are used to measure the chemical composition and properties; these properties include moisture content, fixed carbon, volatile matter and ash content [9]. According to Sharuddin et al. [9], the volatile matter and ash content are the major factors that influence the liquid oil yield in the pyrolysis process. High volatile matter is reported to favour production of liquid oil while high ash content decreases the amount of liquid oil produced with a corresponding increase in the gaseous yield and char production. Table 2.1 shows that the ash content is relatively low and the volatile matter is high for all the plastics, thus presenting good potential for large amounts of liquid oil production through a thermal degradation process.

Table 2.1. Proximate analysis of different plastics, adopted from [10].

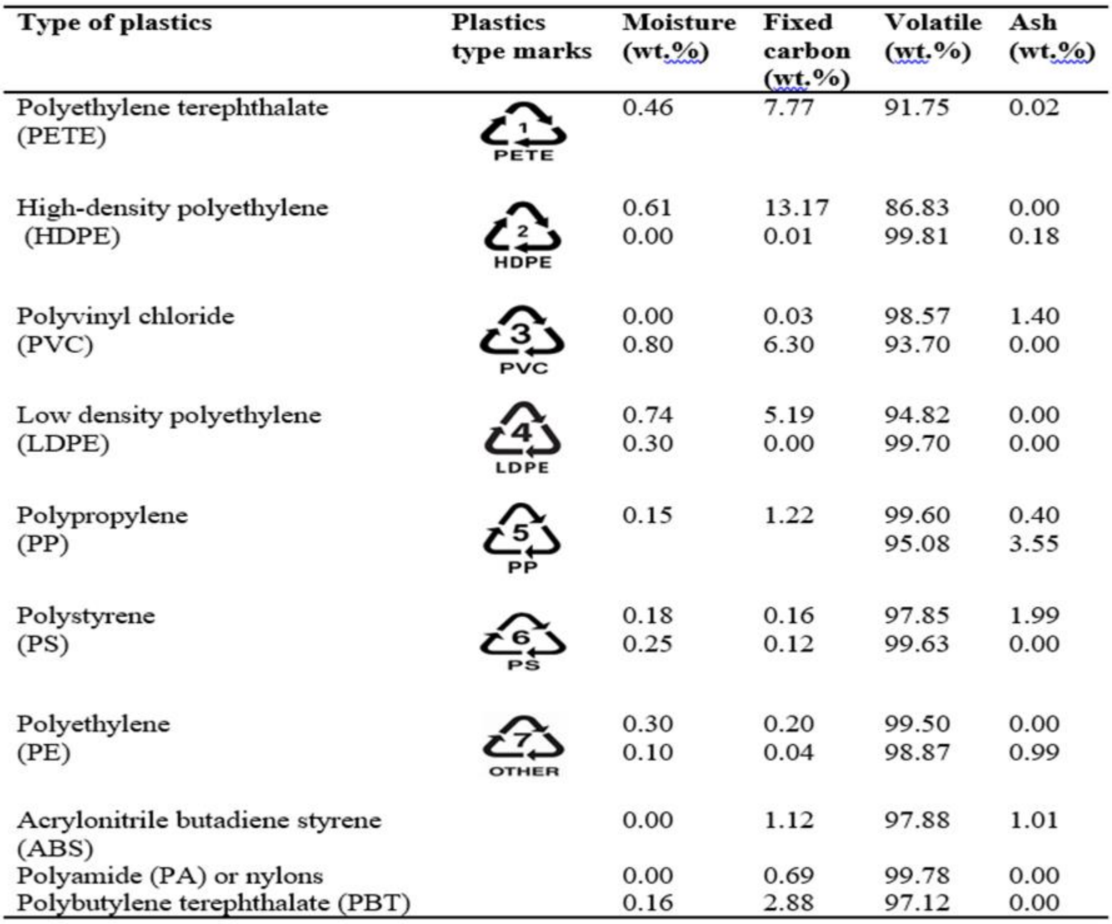

Type of plastics	Plastics type marks	Moisture (wt.%)	Fixed carbon (wt.%)	Volatile (wt.%)	Ash (wt.%)
Polyethylene terephthalate (PETE)	1 PETE	0.46	7.77	91.75	0.02
High-density polyethylene (HDPE)	2 HDPE	0.61 0.00	13.17 0.01	86.83 99.81	0.00 0.18
Polyvinyl chloride (PVC)	3 PVC	0.00 0.80	0.03 6.30	98.57 93.70	1.40 0.00
Low density polyethylene (LDPE)	4 LDPE	0.74 0.30	5.19 0.00	94.82 99.70	0.00 0.00
Polypropylene (PP)	5 PP	0.15	1.22	99.60 95.08	0.40 3.55
Polystyrene (PS)	6 PS	0.18 0.25	0.16 0.12	97.85 99.63	1.99 0.00
Polyethylene (PE)	7 OTHER	0.30 0.10	0.20 0.04	99.50 98.87	0.00 0.99
Acrylonitrile butadiene styrene (ABS)		0.00	1.12	97.88	1.01
Polyamide (PA) or nylons		0.00	0.69	99.78	0.00
Polybutylene terephthalate (PBT)		0.16	2.88	97.12	0.00

Several authors have reported on the influence of thermal degradation of plastic wastes. Uddin et al. [11] conducted studies on thermal degradation of four different types of polyethylene (PE) plastics; high density polyethylene (HDPE), low density polyethylene (LDPE), linear low density PE (LLDPE), and cross-linked PE (XLPE) operated in a batch reactor at a temperature of 430 ^{o}C. HDPE and XLPE produced substantial amounts of wax-like components and the liquid products (58-63 wt.%), lower than that of LDPE and LLDE (76-77 wt.%) due to a smaller amount of the wax-like compound being produced. Hence, the structure of the polymers influenced the pyrolysis product yields. The same tendency was observed by Demirbas et al. [12], who pyrolysed three types of plastic wastes; polyethylene (PE), polypropylene (PP) and polystyrene (PS). The results showed that PS yielded higher liquid oil with the dominant pyrolytic liquid produced as styrene. Likewise, PE and PP produced higher concentrations of gaseous product yield as compared with PS. The liquid oil produced from the plastics wastes suggested it contained a mixture of naphtha (C_7-C_{10}) fractions, gasoline and light gas oil (C_{10}-C_{20}) fractions as well as gaseous products, mostly containing C_1-C_4 paraffinic hydrocarbons with some olefins. A similar trend was observed by Kiran et al. [13], who studied the pyrolysis of plastic wastes; PE and PS using a thermogravimetric analyser (TGA) at temperatures from ambient to 700 ^{o}C using a heating rate of 5 ^{o}C/min in a nitrogen atmosphere. The results showed that the waste PS yielded more liquid while higher gaseous products were produced by waste PE. The dominant liquid produced is styrene ~ 37% by PS waste alongside mono-aromatics up to 63% such as toluene, xylene and naphthalene while prophenylbenzene was the most common product from PE waste. Angyal et al. [14] equally investigated thermal cracking of plastic wastes (polypropylene and polystyrene) to obtain petrochemical feedstock using a horizontal tube reactor at a temperature of 510-520 ^{o}C and a residence time of 15-39 min. The properties of the cracking products were observed to be mainly dependant on the type of feedstock material. It was observed that the concentration of polystyrene influences the quality and quantity of degraded products due to an increased reaction rate coefficient leading to improvement in the degradation rate of polypropylene. A higher concentration of polystyrene increased the yield of light products as well as an increase in the concentration of aromatics hydrocarbon as the product properties changed in the presence of PS addition to the feedstock.

The characteristics of thermal degradation of heavy hydrocarbon products are highlighted as; high production of C_{1s} and C_{2s} in the product gas, olefins were less branched, high temperatures lead to the production of some diolefins, production of high gas and coke products, slow reactions compared to catalytic reactions and a wide distribution of molecular weight as gasoline selectivity is low [15]. The species from the initial degradation reaction are transformed into secondary products through the existence of the inter- and intra-molecular reactions as it depends on the reaction temperature and the residence time of the products in the reactor chamber [15]. Therefore, the proportion of each product fraction and composition depends primarily on the type of plastic wastes as well as process conditions to certain extent.

2.2.1 Factors that affect pyrolysis

Pyrolysis parameters play a major key role in the modifying of the product yield and composition. In the pyrolysis of plastics waste, the process conditions influence the production of final end products such as gaseous, liquid oil and char yields. These pyrolysis products can be directed towards producing appropriate products by adjusting the parameters. The main important factors that affect pyrolysis of plastics waste includes temperature, the type of reactor, feedstock chemical composition, catalyst, heating rate, residence time, reaction agents, pressure and other influencing factors.

2.2.1.1 Temperature

Temperature is one of the most significant factors in pyrolysis of waste plastics. Increasing temperature aids in breaking down the van der Waal forces between polymers [16] as well as breaking down of heavy molecular hydrocarbons into lighter/smaller hydrocarbons. Different plastics have different van der Waal forces bonding the molecules together and there are differences in decomposition temperature of different types of plastics. The thermal decomposition temperature of plastics is determined by the use of thermogravimetric analysis (TGA). The degradation temperature for plastics is suggested to range between 350-550 ^{o}C. According to Marcilla et al. [17], who conducted studies on thermogravimetric analysis of the pyrolysis behaviour of high-density polyethylene (HDPE) and polypropylene (PP), the maximum decomposition temperature for PP was observed at about 447 ^{o}C while the highest thermal degradation peak for HDPE was ~ 467 ^{o}C. This suggests that PP degraded faster than HDPE. Likewise, Chin et al. [18], carried out kinetic studies on the co-pyrolysis of high density polyethylene (HDPE) with rubber seed shell. It was reported that the thermal degradation of HDPE commenced at 378-404 ^{o}C but complete decomposition was observed in the range of 517-539 ^{o}C. Increase in reaction temperature and heating rate promote conversion of a higher molecular carbon chain to a lower carbon chain, thereby disintegrating the volatile plastics into component phases such as gas, liquid and char, respectively [16]. Many researchers have reported an increase in reaction temperature, which results in an increased gaseous yield, and a decrease in liquid phase [12, 19]. In the study performed by Acomb et al. [20], they investigated the influence of increased temperature on low density polyethylene (LDPE) feedstock in a two stage fixed bed using a catalytic temperature from 700 to 900 ^{o}C, the result showed that there was an increase in gaseous and hydrogen yield with a corresponding decrease in liquid yield due to the cracking of heavy hydrocarbons into lighter one. High temperatures favour the production of gaseous product and composition, as shown in Figure 2.3.

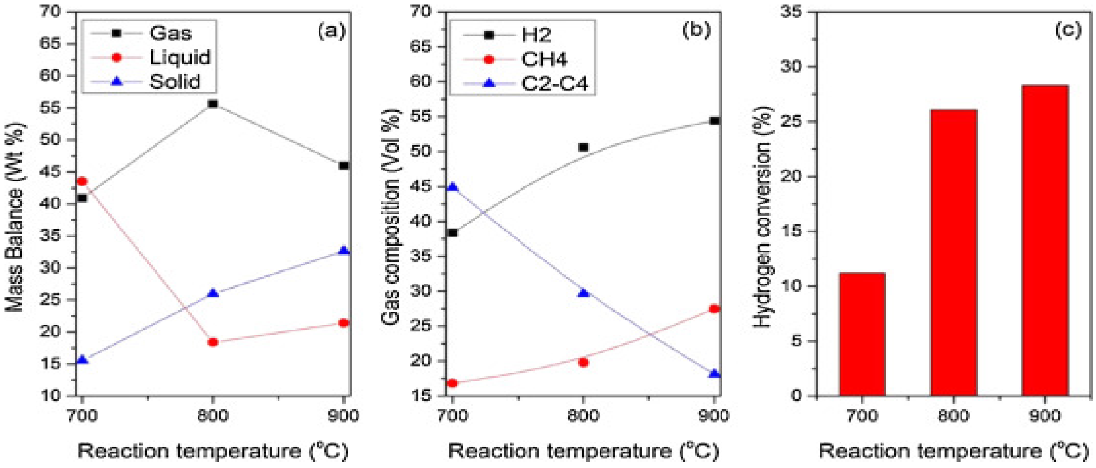

Figure 2.3. Effect of increase in temperature on (a) mass balance (b) gas composition and (c) hydrogen yield from a two stage fixed bed pyrolysis-catalysis of LDPE [20].

Table 2.2. Pyrolysis product yields obtained from polypropylene (PP) at different temperatures (K).

Fraction/ Temperature (K)	675	725	800	875
Total-paraffin	30.4	28.2	24.9	29.6
Total-olefin	44.7	42.1	39.5	35.5
Naphthene	21.5	22.8	24.4	23.5
Aromatics	1.4	4.5	8.6	10.2
Others	2.0	2.4	2.6	1.2

Likewise, Demirbas [12], pyrolysed three types of plastic wastes; polystyrene (PS), polyethylene (PE) and polypropylene (PP) conducted in a stainless steel tube pyrolyser. The result showed that as the temperature increases, the yield of aromatics fraction increases from 1.4 to 10.2 wt.% from PP (see Table 2.2), also the gas yield increases as the temperature increases. In another study, at the lowest temperature (460 °C) investigated it was found to contain highly viscous liquids with long chain hydrocarbons but at the highest temperature tested (600 °C) it resulted in low molecular fraction liquid with high aromatic content due to cracking of C-C bonds of the heavy hydrocarbon molecules leading to lighter hydrocarbons with shorter carbon chains [16]. Temperature does affect the composition of products as aromatic hydrocarbon compounds were produced due to secondary reactions at a higher temperature [21, 22]. In addition, Sharuddin et al. [9] conducted review studies on pyrolysis of plastic wastes, it was highlighted that temperature has the greatest effect on reaction rate which influences the composition of the products: gases, liquid and char. It was suggested that for gaseous products a temperature > 500 ^{o}C is recommended while for liquid yield preference, a lower temperature range between 300-500 ^{o}C is a suitable temperature for all plastics.

2.2.1.2 Heating rate

The effect of heating rate is also very important in pyrolysis. The heating rate is defined as increase in temperature per unit time. There are two types of pyrolysis: fast and slow pyrolysis. Fast or flash pyrolysis is characterised by a high heating rate of about 10,000 K/s, the reaction takes place very quickly, within a few seconds, thereby accumulating a lot of char while slow pyrolysis is characterised by a low heating rate with a range of about 10-100 ^{o}C/min [23]. In some of the investigations conducted on pyrolysis of waste plastics, many researchers have reported different heating rates [24-26]. Encinar and Gonzalez [27], investigated kinetic study on the pyrolysis of synthetic polymer and plastic wastes at temperatures of 415-490 ^{o}C under nitrogen flow rate of 200-300 cm^{3}/min and heating rate of 5-30 ^{o}C/min. The experiment showed that there was a greater weight loss of the polystyrene as the heating rate increases. The heating rate was reported to have a positive effect on the production of gases while the liquid yield decreases, the component fraction includes: H_2, CO, CH_4, C_2-C_3, and CO_2. In the work of FakhrHoseini and Dastanian [28], they analysed the NRTL activity coefficient model for predicting pyrolysis products from PE, PP and PET at a temperature of 500 ^{o}C with different heating rates (6 ^{o}C/min, 8 ^{o}C/min, 10 ^{o}C/min, 12 ^{o}C/min and 14 ^{o}C/min). The results showed that PP with the maximum liquid product of about 82% was obtained at the lowest temperature rate (lowest heating rate) (6 ^{o}C/min). Likewise, all the results indicate that as heating rate increases, the liquid product and solid product decreases with a consequent increase in gaseous yield and vice versa, as shown in Table 2.3. This is due to cracking of the polymer and secondary reactions occurring in the reactor, which convert liquid oil product/tar into gaseous products and char.

Table 2.3. Plastic wastes pyrolysis reaction at different temperature increasing rates [28].

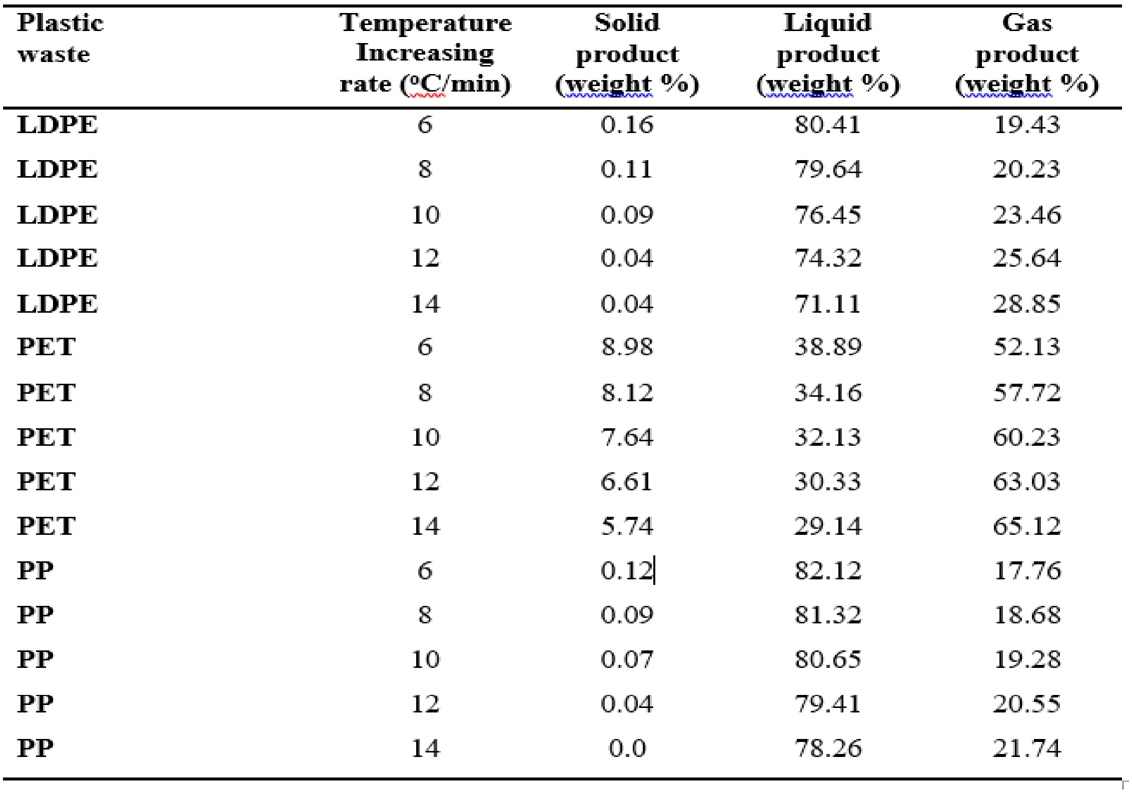

Plastic waste	Temperature Increasing rate (°C/min)	Solid product (weight %)	Liquid product (weight %)	Gas product (weight %)
LDPE	6	0.16	80.41	19.43
LDPE	8	0.11	79.64	20.23
LDPE	10	0.09	76.45	23.46
LDPE	12	0.04	74.32	25.64
LDPE	14	0.04	71.11	28.85
PET	6	8.98	38.89	52.13
PET	8	8.12	34.16	57.72
PET	10	7.64	32.13	60.23
PET	12	6.61	30.33	63.03
PET	14	5.74	29.14	65.12
PP	6	0.12	82.12	17.76
PP	8	0.09	81.32	18.68
PP	10	0.07	80.65	19.28
PP	12	0.04	79.41	20.55
PP	14	0.0	78.26	21.74

2.2.1.3 Residence time

Residence time is the amount of time the product is inside the pyrolysis chamber. In addition, it is explained as the average time the volatile particles spend inside the reactor, which have impact on the product distribution and composition. It is very important in pyrolysis but this is majorly determined by reaction temperature. It has been reported that conversion increases with residence time at lower temperatures as the influence of residence time is more obvious compared to temperatures [2]. In the study by Mastral et al. [29], pyrolysis of HDPE in a fluidised bed reactor was conducted in a range of residence times from 0.64 to 2.6 s from temperatures of 650 to 850 °C. The residence time of gas in the reactor chamber was found to have an influence on the product distribution and gas composition which become vital as the pyrolysis temperature increases. The residence time had a slight effect on gas composition at higher temperatures (685 and 730 °C). At 780 °C temperature, C_2H_4 (with maximum yield of 41.9 wt.% at residence time of 1.34 s) and CH_4 increases while C_3, C_4 and C_4 decreases with a corresponding increase in residence time. At a temperature of 850 °C, H_2 and CH_4 yields increased (from 11.8 to 22.2 wt.% and from 1 to 3.6 wt.%), C_2H_4 yield reached a maximum (40.5 wt.%) at a residence time of 0.86 s, C_2H_2 and C_2H_6 were not affected by residence time while the C_3, C_4 and C_5 fraction decreased with increasing residence time. In other work by Palafox and Chase [30] they investigated a microwave-induced pyrolysis process for the degradation of high-density polyethylene at 500 and 700 ^oC for determination of the relationship between temperature and residence time of the pyrolytic products in the reactor. The yield of gases and liquid between 500 and 700 ^oC did not vary with respect to temperature due to the change in reaction rate that affected the residence time. At 700 ^oC, the average molecular weight for the oils/waxes presented values similar to those produced at 500 ^oC due to the same extent of cracking being accomplished in a shorter time. Similarly, Scheirs and Kaminsky [31], stated that longer residence time supports secondary conversion of principal products leading to formation of additional tar, coke and thermally stable products such as methane, hydrogen and aromatics, while shorter residence time results in the formation of primary products like monomers. According to Al-Salem et al. [32], the secondary reactions in pyrolysis of plastics rely on the residence time and favours the production of gases. Also, that the condensable liquid fraction increases with residence time in end of life tires (ELTs).

2.2.1.4 Feedstock composition

Pyrolysis primary products directly relates to the chemical composition, structure and decomposition mechanism of pyrolysed plastics, thus product distribution depends on time, temperature, rates of bond breakage and other resultant processes [31]. In a chemical reaction, the law of conservation of mass states that the mass of the products is equal to the mass of the reactants. This means that the quantity of the plastics pyrolysed is equal to the products yield (gas, liquid and char), both the raw materials and pyrolytic products have the same elements. According to Angyal et al. [14], pyrolysis of polyolefin will usually produce paraffins and olefins as primary products, therefore having an insight into the type of plastics leads to anticipation of a product’s chemical composition. For example, polyethylene (PE) supports formation of alkanes, polypropylene (PP) results in alkenes formation, polyvinyl chloride (PVC) leads to hydrogen chloride (HCl) production while polystyrene increases aromatics formation such as styrene monomers. However, products from a mixture of plastics may exhibit different compositions, differing from individual polymers due to an interaction of the components mixture of plastics [14]. For example, Panda et al. [2], conducted studies on waste plastics to liquid fuel, the decomposition of polyolefin mixtures occurs similarly as the virgin plastics (350-500 ^oC) in the cracking mechanism of different polyolefins. The waste polyolefins may degrade at a relatively lower temperature with a higher conversion than that of the virgin polyolefins, but the effect of catalyst on the pyrolysis of virgin polyolefins notably influence the product yields as well as the conversion rate. The pyrolysis of polyethylene (PE) and polypropylene (PP) was characterised by low monomer yield while polystyrene (PS) presents a monomeric unit as the major product, high yields of aromatics up 97 wt.% of liquid were produced due to the polycyclic nature of PS and the thermodynamic challenge in the converting cyclic. In the mixture of PE and PS decomposition, H_2 is provided by PE and the decomposition of PE is accelerated by PS presence because of radicals during PS decomposition. The decomposition of PS seems to be resistant to the effect of the other polyolefins (PE and PP). Likewise, the pyrolysis of PE favours the formation of paraffins but increasing addition of PS or PP content will result in the yield of aromatic and alkenic products and vice versa. Likewise, in the pyrolysis study conducted on different plastics; polypropylene (PP), polyethylene (PE), polystyrene (PS), poly(vinylchloride) (PVC), high impact polystyrene with brominated flame retardant (HIPS- Br) plastics mixed with poly(ethylene terephthalate) (PET) at a temperature of 430 ^{o}C, observed that the formation of gaseous products increased while the liquid product decreased [33].

2.2.1.5 Pressure

Reaction pressure has a substantial effect on both rate and the distribution of products during thermal degradation of polyethylene, thus at higher pressure carbon number allocation of gaseous products, liquid products and molecular weight distribution of reactor constituents shifted to the lower molecular weight side [34]. High pressures tend to increase the production of non-condensable gases, decrease average molecular weight of gas products and also decrease liquid product yield [23]. Ismadji et al. [35], investigated pore structure characterisation and development of activated carbon obtained from vacuum pyrolysis char of sawdust. It was observed that BET surface area and pore volume of activated carbon prepared by vacuum pyrolysis char were higher than that from atmospheric pyrolysis char. In the study performed by Paradela et al. [36], on co-pyrolysis of plastics waste and biomass in an autoclave reactor at a temperature of 350-450 ^{o}C using reaction time from 5-30 min and initial pressure of 0.2-1.0 MPa. The change of initial pressure varying from 0.21 to 1.03 MPa had no effect on the gas and solid yield but led to a decrease in the production of liquid yield as the initial pressures increased. There was no obvious impact on gas composition but aromatic compounds formation was favoured as the initial pressure increased as shown in Figure 2.4.

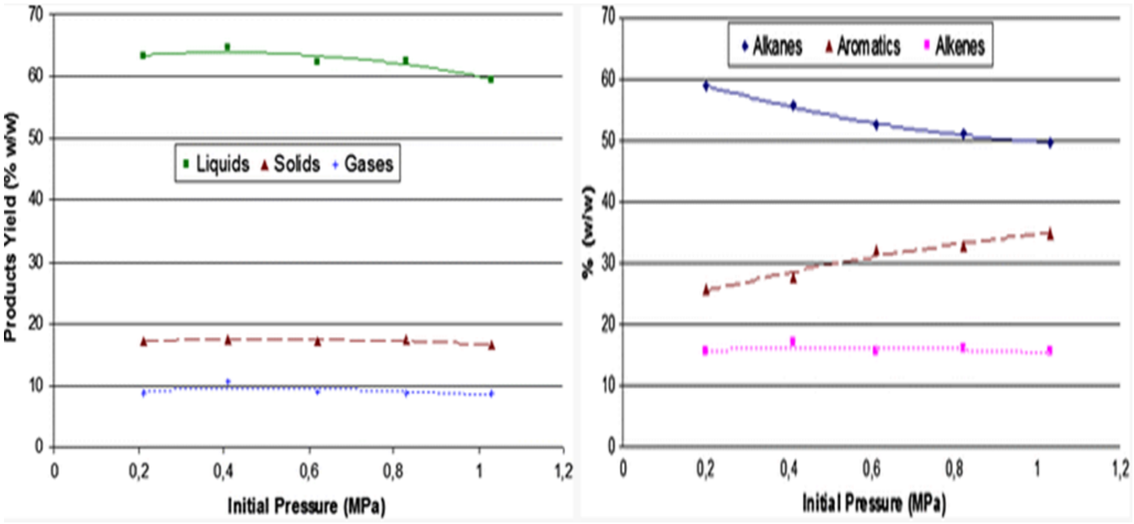

Figure 2.4. Influence of initial pressure on product yield and oil composition at 400 °C and 15 min. [36].

In pyrolysis, atmospheric pressure usually drives product in the direction of the desired product production, pressure reaction is generated by using either an inactive gas like nitrogen or hydrogen in the case of hydrocracking. The work by Al-Salem et al. [32], who conducted review studies on thermal and catalytic pyrolysis of plastic solid wastes (PSW), confirmed that most experimental work in the pyrolysis field is conducted under an atmospheric pressure. It was reported that pressure has its greatest effect at lower temperatures and diminishes with its increase. Hence, pressure is a time dependent factor in pyrolysis. The influence of pressure has also been reported by other researchers [9, 33] and most research has been conducted under atmospheric pressure [37].

2.2.2 Types of reactors in pyrolysis

There are different types of reactors used in pyrolysis of waste plastics and biomass, the choice of reactor determines the quality of heat transfer, residence time, mixing and principal products outflow [2]. Reactors are categorised into batch reactor, semi-batch reactors and continuous-flow reactor while all others are based on modification or a combination of these [2]. These reactors include fixed bed reactors, fluidized bed reactors, rotary/screw kiln reactors, plug flow reactors, etc. Serrano et al. [38], mentioned fixed bed and batch reactors to be the first types of reactors to be used for plastic wastes cracking. Likewise, another reactor is a fluidised bed reactor characterised by possessing homogeneous temperature and composition throughout the bed but the main drawback associated with its usage is the requirement for high amounts of catalysts to achieve complete polymer cracking.

2.2.2.1 Batch reactors

Batch reactors are closed systems and operate under unsteady-state conditions. The reactors are easy to clean, flexible to operate and have the advantage of high conversion obtained due to reactant being left in the reactor for a long period of time but has the drawback of difficulty in large-scale production and labour cost per batch is high [39]. They are used in a variety of processes such as solid dissolution, product mixing, crystallisation, chemical reactions, pharmaceutical, fermentation, liquid/liquid extraction and polymerisation, etc. Batch reactors include stirred tank batch reactor (STR), constant-volume batch reactor, constant-pressure batch reactor, pressurized reactors or autoclave reactors. Onwudili et al. [40], utilised the autoclave batch reactor for the study of carbon reinforced composite plastic waste (CRCP). Van Grieken et al. [41], employed a batch reactor for the investigation of thermal-catalytic degradation of high density polyethylene (HDPE) and low density polyethylene LDPE as well as Manos et al. [42], who also utilised a semi-batch reactor for catalytic cracking of polyethylene over clay catalyst.

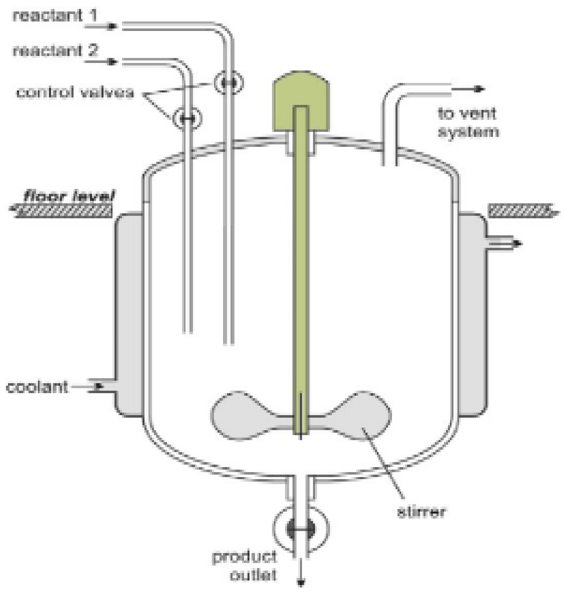

Figure 2.5. Illustration of a batch reactor [43].

2.2.2.2 Continuous flow reactor

These are open systems and often referred to as a flow system. They are classified into continuous-stirred tank reactor (CSTR), tubular reactor (plug flow reactor), and packed bed reactor (PBR).

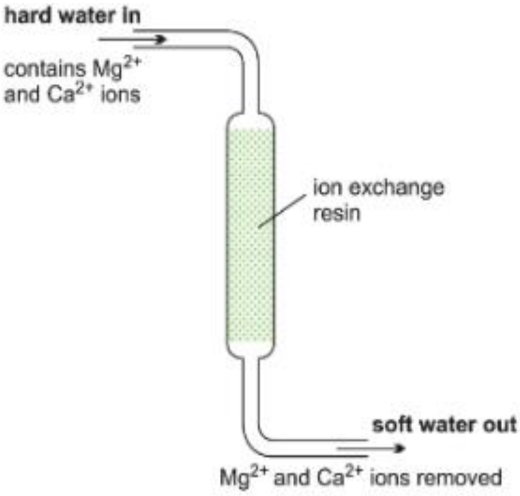

Figure 2.6. Illustration of continuous flow reactor [43].

2.2.2.3 Plug flow reactor

Plug flow reactors (PFR) are also called tubular reactors, fluids such as gases and/or liquid flow at high velocities inside it. It has the advantage of high conversion per reactor volume of any choice of the flow reactors, it is easy to maintain, simple to operate, has low pressure drop and large capacity. Its drawback include: hot spots during exothermic reaction, difficulty in temperature control inside the reactor and variations in composition. It has been reported that most homogeneous gas-phase flow reactors are tubular which are made up of a certain amount of smaller reactors arranged in a tube bank manner or just in one long tube [39]. Westerhout et al. [44], carried out an experimental investigation for the determination of pyrolysis products from polyethylene (PE) and polypropylene (PP) using a tubular reactor. Lee and Oh [45], employed the use of tubular reactor for thermal and catalyst cracking of pyrolytic waxy oil.

2.2.2.4 Fluidised-bed reactor

Fluidised-bed reactors can be used for heterogeneous catalyst reactors that permit broad mixing in all directions enabling a steadiness of temperature, increased reaction rate, increased mass-transfer and the mass of the catalyst is fluidised. There are very large, can be controlled automatically and are used in catalytic cracking processes where a separate unit for regeneration of the catalyst exists. They are very expensive to construct and maintain, large pressure drop, erosion of reactor walls and deactivation of catalyst may exist which are some drawbacks of fluidised-bed reactors. Lin et al. [46], analysed catalytic pyrolysis of commingled plastic waste over the FCC process using a fluidized-bed reactor which was categorized by outstanding heat and mass transfer, offers almost constant temperature throughout the reactor, and was less prone to clogging with molten polymer. Kaminsky et al. [47], utilised a fluidised bed reactor for pyrolysis of feedstock recycling from polymer. Williams and Brindle [48], carried out an investigation on catalytic pyrolysis of scrap tyres for the determination of catalyst temperature and tyre ratio using a fluidised bed reactor.

2.2.2.5 Continuous-stirred tank reactor (CSTR)

CSTRs are open systems, they operate on the principle of steady state due to no change in conditions with time in the reactor, there is also an input of material into the system and outlet for product discharge. There is constant composition all over the reactor due to vigorous stirring by impellers to ensure a good mix of reactants. The reactor construction is economical, has a large heat capacity, sustains good temperature control and effortless accessibility to the reactor internal but has the drawback of small product yield per volume of reactor as compared to other flow systems. Murata et al. [49], carried out an investigation using a continuous stirred tank reactor (CSTR) for thermal degradation of polyethylene (PE), polypropylene (PP), and polystyrene (PS) mixture, it was reported that CSTR is suitable for converting plastic wastes into hydrocarbon feedstock. Uppal et al. [50], carried out an investigation on continuous stirred tank reactor (CSTR) for classification of dynamic behaviour and has stated that the reactor residence time is the most easily varied. Murata et al. [34], conducted analysis using a continuous stirred tank reactor (CSTR) for thermal degradation of polyethylene at elevated pressure, it was discovered that the carbon number distribution of gaseous and liquid products as well as the molecular weight distribution of the reactor contents shifted to the lower molecular weight side.

2.2.2.6 Rotary kiln/screw kiln reactor

Serrano et al. [51], carried out an investigation by means of a screw kiln reactor for thermal and catalytic cracking of low density polyethylene (LDPE), it was stated that a screw kiln is adequate for cracking LDPE, a comparison with a batch reactor showed that the screw kiln reactor led to lower formation of gaseous products and cracking of heavy hydrocarbon component fraction. Fantozzi et al. [52] , analysed the production of syngas and char from biomass and waste using rotary kiln slow pyrolysis. Serrano et al. [53], utilised a screw kiln reactor with two different reaction temperature regions for pyrolytic thermal and catalytic degradation of low density polyethylene (LDPE), with the addition of lubricating oil leading to a decrease in its viscosity which favoured almost complete conversion of about 90% product range (C_1-C_{40}) hydrocarbon.

2.2.2.7 Fixed-bed reactor

The fixed-bed reactor, also known as a packed-bed reactor, is basically a tubular reactor which is packed with solid catalyst particles loaded into the bed, it is regularly used for gas catalyse reaction and the system is heterogeneous reaction [39]. It results in high conversion rate per weight of the catalyst, more products are formed due to increased reactant: catalyst contact, easier to build, the cost of construction, maintenance and operation is equally low. Fixed-bed reactors are simple, flexible and easy to scale up. In addition, they have the advantages of high pressure and temperature but have drawbacks of temperature control problems like other tubular reactors. Hall et al. [54], utilised a fixed bed reactor for investigation of removal of contaminated brominated compounds from pyrolysis products of flame-retarded high-impact polystyrene (HIPS) and acrylonitrile-butadiene-styrene (ABS) [55].

2.2.2.8 Two-stage fixed-bed reactor

A two-stage fixed-bed reactor, as investigated in this study, has been reported to be the best reactor configuration for pyrolysis catalytic of plastic wastes with the first stage of thermal cracking followed by catalytic cracking (on the catalytic bed) in the second stage reactor [38]. The suggested advantages include: control and optimization of temperature for each stage of the process, improvement of contact between pyrolysis products and the catalyst, ease of recycling of the used catalyst, reduction in mass transfer and heat transfer problem [19, 38]. Wu and Williams [56], carried out an experimental investigation for pyrolysis gasification of plastics, mixed plastics and real world waste plastics using a two-stage reactor. The first stage involved pyrolysis of plastic at a reaction temperature of 500 ^{o}C, the product volatiles were passed through to the second stage with Ni-Mg-Al catalyst for cracking as well as steam reforming at a temperature of 800 ^{o}C, it was discovered that an increase in gasification temperature and water injection rate resulted in an increase in total gas yield and hydrogen production. Marcilla et al. [57], analysed catalytic pyrolysis of LDPE over HZSM-5 and H-beta zeolites using horizontal fixed bed reaction. Uemichi et al. [58], investigated using a two stage reactor for catalytic degradation of polyethylene over silica-alumina and HZSM-5 zeolite catalysts, the degradation reaction temperature was 375-425 ^{o}C, the conclusion was drawn to an increase in concentration of aromatics and isoparaffins which presented an improvement.

2.2.3 Presence of catalyst in pyrolysis

Catalysts are substances that increase the rate or accelerate a chemical reaction without itself being affected or undertaking any permanent chemical change. Therefore, in pyrolysis-catalytic reaction, addition of catalyst to pyrolysis reaction aid in speeding up the rate of reaction by lowering pyrolysis temperature, residence time, it enhances selectivity of products, boosts conversion, and increases quality of product yield [59]. According to Kunwar et al. [59], higher conversion occurs with acidic catalysts having mesopores and micropores (examples include zeolite catalyst, silica-alumina, etc.), thus use of a strong catalyst results in the generation of shorter chain hydrocarbons such as C_3-C_5. It has been reported that microporous materials have pore diameters less than 2 nm, mesopores pore diameters are between 2 nm and 50 nm while macroporous materials pore diameters are above 50 nm. It was presumably reported that, primary cracking reactions of waste polymer may proceed on the macroporous surface of a catalyst, while the smaller fragments are cracked on its microporous surface because it was found that the difference in catalyst pore structure could result to variance of product yield as examined with ZSM-5 [60]. According to Miskolczi [60], common catalysts used for plastics waste pyrolysis include: FCC, ZSM-5, USY, etc., however FCC and ZSM-5 were mentioned to support optimum hydrocarbon productions in gasoline boiling point range. Catalysts used for plastic conversion can be grouped into three sections and these include: fluid catalytic cracking (FCC), catalysts for reforming, and activated carbon, etc. [61]. The two major catalysts employed in this study were reforming and zeolite catalysts.

2.2.3.1 Reforming catalyst

Reforming catalyst is a chemical process that converts low octane rating straight chain (paraffins) hydrocarbons naphtha distilled from crude oil into branched chain alkanes (isoparaffins) and cyclic naphthenic hydrocarbons, which to a certain extent dehydrogenated to produce high-octane aromatic hydrocarbons and substantial amounts of hydrogen gas as a by-product. Reforming catalysts are bi-functional catalysts based on transition metal supported on such as silica-alumina as an example; Pt/SiO_2-Al_2O_3 [61, 62] and Ni-based catalysts. Hence, the two functioning parts that include the metal sites drive hydrogenation/dehydrogenation reactions, while the acid sites on the support catalyses isomerisation reactions. The combination of these two functions promotes reforming reaction such as isomerisation where straight-chain paraffins are isomerised to branched-chain molecules, and dehydrocyclisation (cyclisation) where straight-chain paraffins are converted to cycloparaffins and dehydrogenation where naphthenes are dehydrogenated to aromatic hydrocarbon [61]. Several studies have been reported on reforming catalysts, Uddin et al. [11] conducted studies on thermal and catalytic degradation of polyethylene (PE), low density polyethylene (LDPE), linear low density PE (LLDPE), and cross-linked PE (XLPE) in a batch reactor over silica-alumina catalyst at a temperature of 430 ^{o}C. The result showed that all the polyethylene was converted to light hydrocarbon liquid yielding about 77-83 wt.% (mostly C_5-C_{12}) without any wax production over the silica:alumina catalyst. According to Buekens and Huang [61], the use of reforming catalysts applied in plastics cracking enhance aromatic production. For instance, in an experiment conducted with Al_2O_3 the catalyst yielded an aromatic fraction of about 4% due to inadequate acidic activity but increased to about 12% with the use of Pt/Al_2O_3 catalyst. Likewise, the use of SiO_2-Al_2O_3 catalyst increased the yield of iso-alkanes and alkenes while Pt/SiO_2-Al_2O_3 led to an increase in aromatics yield from 13.5 to 22 wt.% respectively as shown in Table 2.4.

Table 2.4. Polyethylene (PE) products distribution over reforming and activated carbon catalyst at reaction temperature of 526 ^{o}C [63].

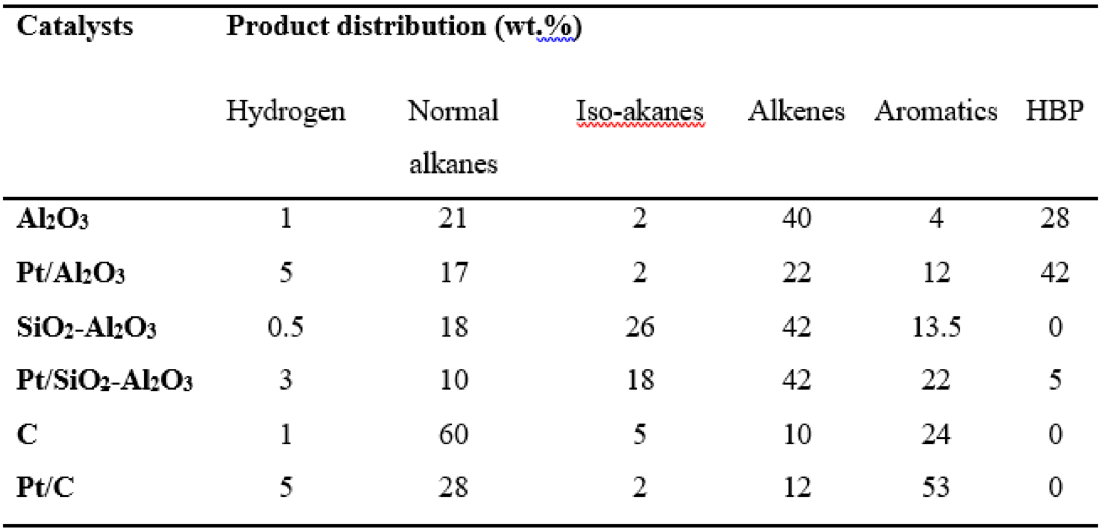

Catalysts	**Product distribution (wt.%)**					
	Hydrogen	Normal alkanes	Iso-akanes	Alkenes	Aromatics	HBP
Al_2O_3	1	21	2	40	4	28
Pt/Al_2O_3	5	17	2	22	12	42
SiO_2-Al_2O_3	0.5	18	26	42	13.5	0
Pt/SiO_2-Al_2O_3	3	10	18	42	22	5
C	1	60	5	10	24	0
Pt/C	5	28	2	12	53	0

Rahimpour et al. [62], reviewed studies on catalytic naphtha reforming which is a very important process in refinery of hydrocarbon components, the naphtha reforming catalyst is a bifunctional catalyst consisting of a metal function, mainly platinum, and an acid function such as chloride alumina. The metal function catalyses the hydrogenation and dehydrogenation reactions and the acid function drives isomerisation and cyclisation reactions. Modification of both the acid and metal function will lead to improvement in the stability, selectivity and deactivation of the catalyst for enhancement of product yields. For example, germanium and tin are active metals for hydrogenolysis reactions; Pt-Ge/Al_2O_3 and Pt-Sn/Al_2O_3 bimetal catalysts are good for use in novel low-pressure naphtha reforming processes utilizing continuous regeneration of the catalyst.

These precious metals are very expensive and as such are not economical for waste plastics reforming. Therefore, a more cost competitive metal for catalytic reforming catalysts such as nickel-based catalysts are appropriate. For example Huang et al. [64], investigated a method of liquid hydrocarbon fuels production from solid waste plastics by reacting the plastic wastes with metal hydride and supported catalyst. The noble metal-based catalysts are active for aromatization and hydrogenation of hydrocarbons, especially Pt. The pyrolysis of LDPE over Pt/γ-Al_2O_3 (1.0 wt.% Pt content) at 750 ^oC temperature increased the production of gasoline and jet fuel range up to 19.67% and 9.03% with the decrease in the heavier hydrocarbon fractions (diesel 10.00% and heavy oil to 9.03%). However, the Ni-based catalysts are less expensive industrial catalysts; the Ni catalysts were reported to show similar properties to those of Pt. For example, the use of Ni/SiO_2 increased gasoline range products up to 29.56% and 9.03% with a corresponding decrease in the heavier hydrocarbon fractions (diesel 10.43%, heavy oil to 10.28%) and jet fuel 8.85%. Compared with Pd noble metal catalyst at the same pyrolysis temperature of 850 ^oC, Ni/SiO_2 catalyst resulted in a higher increase in gasoline production as well as a reduction in heavy oil hydrocarbons as shown in Table 2.5.

Table 2.5. Production of liquid fuels over Ni and Pd based catalyst at temperature of 850 °C.

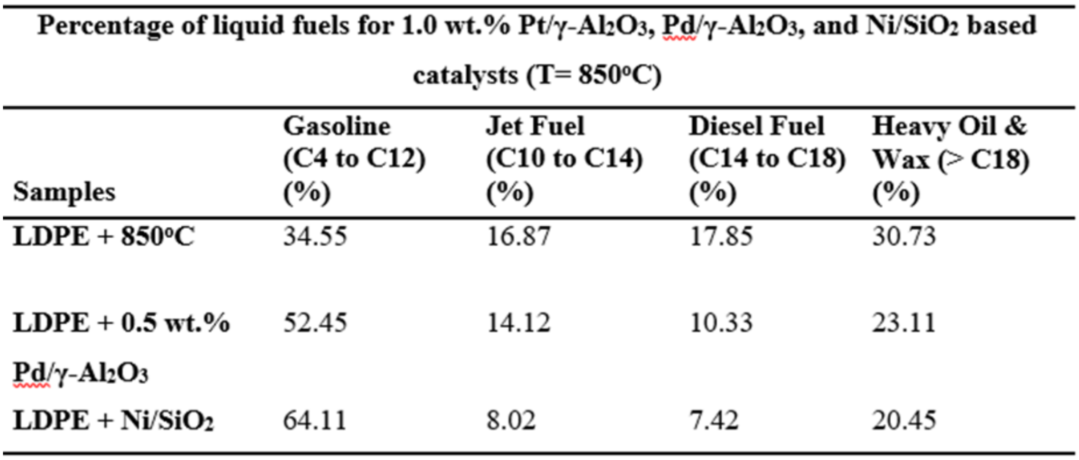

Percentage of liquid fuels for 1.0 wt.% Pt/γ-Al_2O_3, Pd/γ-Al_2O_3, and Ni/SiO_2 based catalysts (T= 850°C)

Samples	Gasoline (C4 to C12) (%)	Jet Fuel (C10 to C14) (%)	Diesel Fuel (C14 to C18) (%)	Heavy Oil & Wax (> C18) (%)
LDPE + 850°C	34.55	16.87	17.85	30.73
LDPE + 0.5 wt.% Pd/γ-Al_2O_3	52.45	14.12	10.33	23.11
LDPE + Ni/SiO_2	64.11	8.02	7.42	20.45

Nickel metal is considered one of the best transition metals for the reforming of hydrocarbons, which are cost effective as compared to other metal-based catalysts. Nickel-based catalysts are used in thermochemical processing of waste plastics and biomass for the production of hydrogen and aromatics fuel oils. They are very stable at high temperature with high selectivity for hydrogen production. Wang et al. [65] worked on nickel-based catalysts impregnated on diverse supports of Al_2O_3, Al_2O_3-SiO_2, Al_2O_3-MgO, Al_2O_3-CaO and discovered that the Ni on MgO and CaO were more stable while Ni on Al_2O_3, Al_2O_3-SiO_2, Al_2O_3-CaO resulted in high conversion reaction of CO_2/CH_4 (methane reforming) in the temperature range of 870-1040 °C for syngas production. Likewise, He et al. [37], investigated catalytic steam gasification of waste polyethylene (PE) for the production of syngas (H_2 + CO) over NiO/γ- Al_2O_3 catalyst in a bench scale downstream fixed-bed reactor in the temperature range of 700-900 °C. The NiO/γ-Al_2O_3 reported to be an active catalyst for steam gasification of polyethylene waste. Also, in the range of parameters studied, temperature is an important factor in the yield and composition. The content of syngas increased from 37.25% to 64.35% with the increase of H_2 greater than CO content in the ratio of H_2/CO from 0.83 to 1.35 as the temperature increased from 700 to 900 °C, with a consequent decrease in the tar and char yield respectively. The efficiency of nickel-based catalysts in the reforming process majorly depends on the temperature reaction; also, the introduction of steam in the pyrolysis process enhances water gas-shift as well as methane reforming reactions leading to the product gas yield and expedite the conversion of polyethylene waste.

2.2.3.2 Zeolites catalysts

Zeolite catalysts are crystalline aluminosilicates with microporous structure while silica-alumina are amorphous aluminosilicates having pore structures that comprise mesoporous and macroporous structures [38]. Zeolite catalysts are formed by joining SiO_4 and AlO_4 tetrahedra, which exhibit mono-dimensional, bi-dimensional or tri-dimensional pore channel structure with a range of 0.4-1.0nm pore sizes changing zeolites into molecular sieves (shape selectivity), furthermore the existence of aluminium in the zeolite is responsible for the acidic properties (Lewis and Bronsted) that differ from one zeolite to another due to topology [66]. The Si/Al ratio is an essential parameter used to classify zeolite catalyst, high Si/Al indicate zeolites with high acidity while lower Si/Al infers zeolites with lower acidity and smaller crystal size of zeolite catalyst which leads to greater conversion efficiency [23]. It is also stated that the high content of silica in zeolite catalysts enables its suitability for high temperature pyrolysis and regeneration cycles due to the framework ability to endure high temperatures. According to Muhammad et al. [19], the surface acidity of catalysts is controlled by the Si/Al ratio, lower Si/Al ratio leads to higher relative surface alumina concentration and higher surface acidity of the catalyst consequently providing greater catalytic conversion activity. Examples of such zeolite catalysts which will be considered in this work includes ZSM-5, Y-Zeolite, etc.

Many researchers have investigated the use of zeolite catalysts for aromatics fuel oil production. For example, Lerici et al. [67], analysed H-Y zeolite catalyst on the pyrolysis of polyethylene (HDPE and LDPE), polypropylene (PP) and polystyrene (PS) in a batch reactor at a temperature of 500 ^{o}C. The liquid product yield ranged from ~ 42 wt.% for PE and ~ 44 wt.% for PP while the production of PS resulted in ~71 wt.%. The gaseous products are in the ranges of 46, 52, and 24 wt.% for PE, PP and PS with the greatest carbonaceous residues of 10 wt.% obtained from PP and the lowest residues 4 wt% by LDPE respectively. Thus, the PS showed the lowest gaseous yield but the highest liquid yield. This is explained based on the polymer structure; the benzene ring in PS structure is very stable and decreases cracking reactions of PS to gaseous products.

Consequently, Renzini et al. [68], investigated the use of Zn-ZSM-11 and H-ZSM-11 zeolite catalysts over low density polyethylene (LDPE) in a fixed bed reactor at reaction temperature of 500 ^{o}C and reaction times of 20 and 60 minutes. The products obtained from the H-ZSM-11 catalyst in the range of gas/liquid/residues values are 39/57/4 wt.% and 63/31/7 wt.% for reaction times of 20 and 60 minutes respectively while the Zn-ZSM-

11 catalyst products range of gas/liquid/residues shows 17/82/1 wt.% and 40/55/5 wt.% respectively. The results showed that the H-ZSM-11 catalyst produced more gases due to greater Bronsted acid sites favoured by cracking reactions. Likewise, the Zn-ZSM-11 catalyst produced a higher proportion of C_6-C_9 aromatic hydrocarbon products in the liquid fraction due to the high concentration of Lewis acid sites favouring aromatization reaction because of the Zn exchange on the zeolite support. The author suggested that the selectivity of aromatic fraction in the liquid product could be increased to almost 100% based on experimental conditions such as higher temperature, longer reaction, smaller polymer/catalyst relationship, etc.

Furthermore, Pieralla et al. [69], analysed zeolite catalysts consisting of Zn/Mo-ZSM-11, Zn-MCM-41 and H-ZSM-11 over high density polyethylene (HDPE) at temperatures ranging between 410-500 ^{o}C. It was discovered that H-ZSM-11 yielded more gaseous products (>48 wt.%), Zn-ZSM-11 exhibited higher liquid aromatic hydrocarbon (> 57 wt.%) which were mainly of benzene, toluene, xylenes while Zn-MCM-41 showed a liquid hydrocarbon range of C_5-C_{16} products. The H-ZSM-11 catalyst resulted in a higher fraction of gaseous hydrocarbon (C_1-C_4). Lin and Yang [70] equally investigated five commercial catalysts (FCC-s1, ZSM-5, HUSY, amorphous silica-alumina-SAHA and Silicalite) for polypropylene (PP) degradation, the results indicated that the ZSM-5 gave the highest gaseous yield (about 90 wt.%) under temperature conditions of 400 ^{o}C and reaction time of 30 minutes.

Other authors such as Miskolczi et al. [71], investigated polyethylene and polystyrene over three catalysts consisting of ZSM-5, FCC and clinoptillolite in a batch reactor in a temperature range of 410-450 ^{o}C, it was discovered that the ZSM-5 produced the highest quantity of gaseous products while the polystyrene composed majorly of aromatic compounds (ethyl-benzene, styrene, toluene, and benzene) produced while the polyethylene composition had a linear, non-branched structure. The liquid obtained consisted of a wide range of hydrocarbons distributed within the C_5-C_{28} carbon number range depending on the cracking parameters. Hence, the product yield was majorly determined by the effect of cracking temperature and grain size of the catalyst but catalyst type was the determinant factor of gas yields.

Lopez et al. [22], carried out pyrolysis of three plastic waste streams over ZSM-5 zeolite catalyst at a temperature of 440 ^{o}C. The ZSM-5 zeolite was reported to be effective in the production of high C_3-C_4 gases and aromatic compound at low temperature of 440 ^{o}C from plastics packing waste under semi batch conditions.

Williams and Bagri [72], analysed hydrocarbon gases/oil obtained from polystyrene over pyrolysis and catalytic pyrolysis of ZSM-5 and Y-Zeolite in a fixed bed reactor. It was observed that an increase in the gas yield and a decrease in oil produced when the temperature, as well as the quantity of Y-zeolite catalyst in the catalytic bed, were increased; this equally led to coke deposition on the catalyst. The hydrocarbon gases obtained include: methane, ethane, ethane, propane, propene, butane and butene. The main product of the pyrolysis of PS was oil consisting mostly of styrene and aromatic hydrocarbons.

Zhou et al. [73], investigated low density polyethylene (LDPE) and polypropylene (PP) over a modified ZSM-5 zeolite catalyst, DelaZSM-5 which was compared with those of commercial catalyst USY, ZSM-5. It was discovered that modified DelaZSM-5 gave a higher gas yield, especially those of the LDPE waste yielded the most gaseous products. LDPE had higher catalytic degradation activity on the modified DeLaZSM-5 catalyst than PP due to the narrow pore structure of the DeLaZSM-5 zeolite catalyst that permitted LDPE molecules to enter the cavities having contact with the acid site of the zeolite but prevented PP due to the presence of side-chain methyl groups that increased the cross-section of the PP molecules.

Manos et al. [74], equally investigated high-density polyethylene over nano-crystalline HZSM-5 in a fluidised-bed at a temperature of 360 ^{o}C, the hydrocarbon yield produced with medium-pore zeolites were lighter than those obtained with large-pore zeolites as shown in the following order (lighter products) ZSM-5 < mordenite < β < Y < US-Y (heavier products), and for the bond saturation: (more alkenes) ZSM-5 < mordenite < β < Y < US-Y (more alkanes) respectively.

Shah et al. [75], conducted studies in a constructed pyrolytic reactor for converting plastic waste (polyethylene) at the relatively low temperatures of 250 ^{o}C and 275 ^{o}C over zeolite catalyst. The non-catalytic process products include: oil, wax, gas and char with values of 48.6, 40.7, 10.1 and 0.6% yield for the temperature of 275 ^{o}C. The introduction of zeolite catalyst at a temperature of 250 ^{o}C produced a product yield range of 47.98%, 35.43%, 16.09% and 0.50% for oil, gas, wax, and residue respectively. There was a slightly higher gaseous yield observed with a consequent decrease in oil, wax and char with the use of zeolite catalyst.

Bagri and Williams [76], equally investigated polyethylene using Y-zeolite and ZSM-5 in a fixed bed reactor, based on the different pore size, surface area and surface acidity of the two catalysts, the ZSM-5 catalyst produced higher concentrations of gases than the

Y-zeolite at increasing temperatures from 400 °C to 600 °C but Y-zeolite catalyst gave a higher concentration of aromatic hydrocarbons. The gaseous products were mainly alkanes, alkenes, methane, ethane, ethene, propane, propene and butane.

Table 2.6. Total aromatic content in the product oils from Y-zeolite and ZSM-5 catalytic pyrolysis of polyethylene (wt.%) [76].

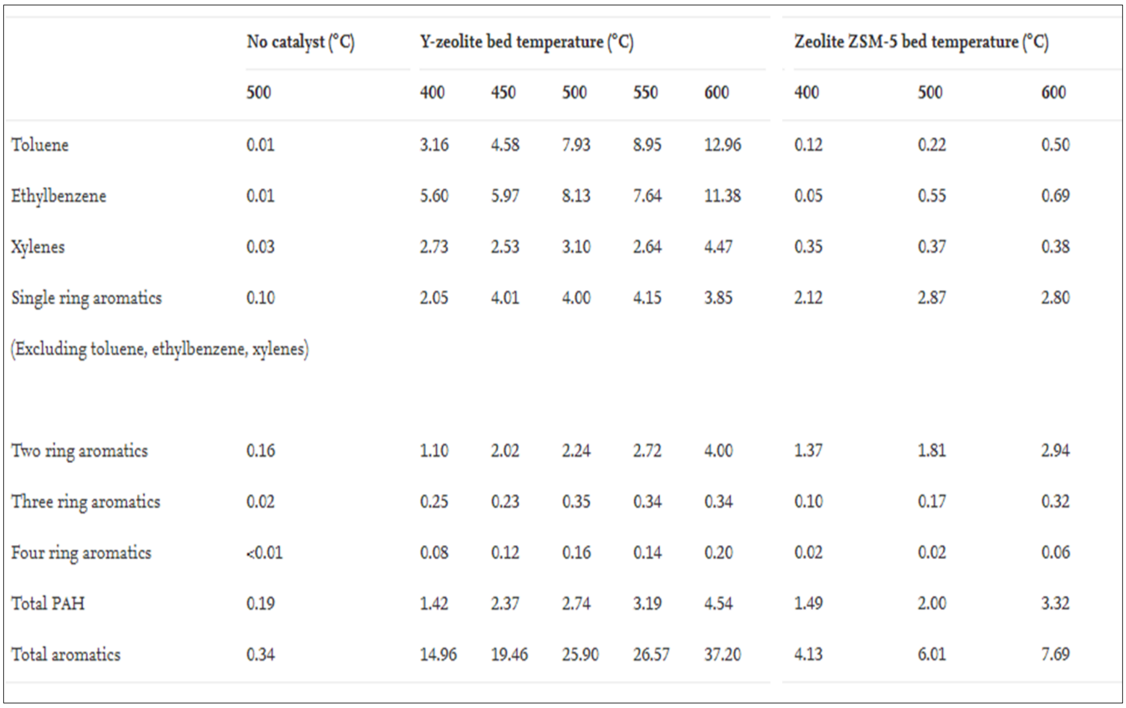

	No catalyst (°C)	Y-zeolite bed temperature (°C)					Zeolite ZSM-5 bed temperature (°C)		
	500	400	450	500	550	600	400	500	600
Toluene	0.01	3.16	4.58	7.93	8.95	12.96	0.12	0.22	0.50
Ethylbenzene	0.01	5.60	5.97	8.13	7.64	11.38	0.05	0.55	0.69
Xylenes	0.03	2.73	2.53	3.10	2.64	4.47	0.35	0.37	0.38
Single ring aromatics (Excluding toluene, ethylbenzene, xylenes)	0.10	2.05	4.01	4.00	4.15	3.85	2.12	2.87	2.80
Two ring aromatics	0.16	1.10	2.02	2.24	2.72	4.00	1.37	1.81	2.94
Three ring aromatics	0.02	0.25	0.23	0.35	0.34	0.34	0.10	0.17	0.32
Four ring aromatics	<0.01	0.08	0.12	0.16	0.14	0.20	0.02	0.02	0.06
Total PAH	0.19	1.42	2.37	2.74	3.19	4.54	1.49	2.00	3.32
Total aromatics	0.34	14.96	19.46	25.90	26.57	37.20	4.13	6.01	7.69

Comparing the total aromatic yield from the two catalysts, Y-zeolite produced 37.20 wt.% higher than 7.69 wt.% obtained for ZSM-5 as shown in Table 2.6. These differences in product yield and composition might be because the Y-zeolite exhibited a larger surface area and pore size than ZSM-5 catalyst. The higher pore size enables large molecules to enter the active sites of the catalyst for aromatization reactions leading to increases in aromatic compounds in oil produced notably single ring aromatics such as toluene, benzene and xylene, which are of high petrochemical value. In addition, the Y-zeolite catalyst had a lower silica:alumina (Si/Al ratio) of 11 compared to that of 50 for the ZSM-5 catalyst, it was reported that reducing the Si/Al ratio increases the relative surface concentration of aluminium. Thus, Y-zeolite with a lower Si/Al ratio and higher surface acidity than ZSM-5 catalyst produced a higher aromatic hydrocarbon due to the acidity of the catalyst that provided catalytic activity while the pore size regulates the shape selectivity. In addition, increase in temperature further led to an increase in aromatic concentration for the both catalysts.

In pyrolysis of plastic solid wastes (PSW), acid based zeolite catalysts (HZSM-5 and Y-zeolite) are reported to be more effective than the less acidic ones such as amorphous silica-alumina [32]. According to Sharuddin et al. [9], reviewed studies pointed out that the final end product of pyrolysis over zeolite catalysts reactivity is determined by the ratio of SiO_2/Al_2O_3, the yield of light alkanes and aromatic increases with a reduction of SiO_2/Al_2O_3 ratio. The author stated that the use of zeolite catalyst in plastics pyrolysis maximized the production of volatile hydrocarbons. Furthermore, as reviewed by many authors, zeolite catalysts are often used at relatively low temperatures for the pyrolysis-catalysis of plastic wastes [73, 75, 76].

2.2.3.3 Other catalysts

Other catalysts such as MCM-41 have also been investigated. MCM-41 is a mesoporous material described as having a large surface area of about 1000 m^2/g, pore diameter in a range ~ 2-10 nm larger than zeolites, Al_2O_3 and other oxide supports, promote mass transfer as well as uniform distribution of the catalyst particles within the porous structure [77, 78]. The highly ordered hexagonal porous structure of MCM-41 permits the incorporation of metals into the framework, thus improving both oxidizing and Lewis acidity properties [77]. Lucredio and Assaf [79], stated that the mesoporous MCM-41 support catalyst with very large surface area and orderly pore distribution, promote a greater increase of metal dispersions within the framework of the support catalyst. However, significant enhancement of oil composition with staged catalysts was reported in the literature [80]. For example, Devy et al. [38], studied high-density polyethylene using the staging of mesoporous MCM-41 over microporous zeolite (ZSM-5) catalyst in a two stage fixed bed reactor at a catalytic bed temperature of 500 ^oC for pyrolysis-catalysis of polyethylene plastics, agricultural wastes, etc. It was reported that the lighter hydrocarbon yield was high in the gasoline range of C_8-C_{12} ~ 97.72 wt.% with aromatic contents of 95.85 wt.%. Other authors equally reported improvement in product distributions by mixture of MCM-41 and HZSM-5 as well as individual catalysts [81-85].

Fluid catalytic cracking (FCC): the FCC process has been widely used in cracking crude petroleum in refineries and they are used to convert high boiling point, high molecular weight, denser fractions hydrocarbon petroleum, crude oil into further relevant and profitable products such as olefin gases, gasoline etc. FCC catalysts are reported to include zeolite, silica- alumina and clay. Zeolite Y was reported to be the principal zeolitic component in the FCC catalyst which enhances higher cracking activity, coke and gasoline selectivity, others zeolite catalysts mentioned as components in FCC include ZSM-5 and USY [86]. Some major commercial FCC catalysts are shown in Table 2.7.

Table 2.7. Illustration of dominant FCC catalysts [61].

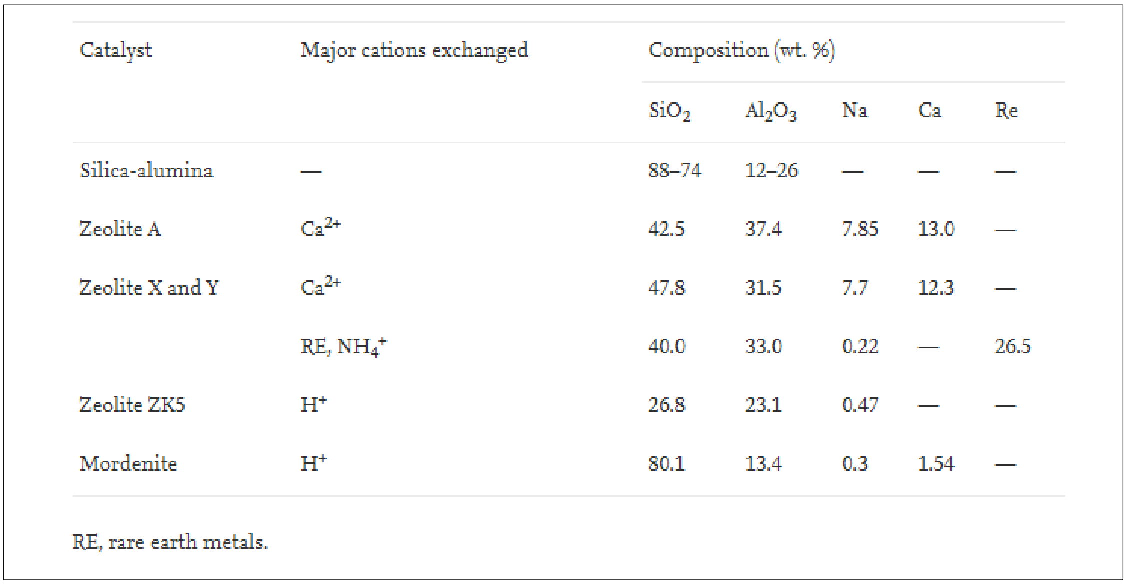

Catalyst	Major cations exchanged	Composition (wt. %)				
		SiO_2	Al_2O_3	Na	Ca	Re
Silica-alumina	—	88–74	12–26	—	—	—
Zeolite A	Ca^{2+}	42.5	37.4	7.85	13.0	—
Zeolite X and Y	Ca^{2+}	47.8	31.5	7.7	12.3	—
	RE, NH_4^+	40.0	33.0	0.22	—	26.5
Zeolite ZK5	H^+	26.8	23.1	0.47	—	—
Mordenite	H^+	80.1	13.4	0.3	1.54	—

RE, rare earth metals.

Activated carbon catalyst: The activated carbon is also called activated charcoal or activated coal which is made from charcoal, the carbon is formed to have low-volume pores that increase surface area applicable for chemical reaction (one gram of activated carbon has a surface area over 500 m^2/5,400 sq ft). According to Uemichi et al. [63], activated carbon impregnated with metals (such as Pt, Fe and Mo) were discovered to be an adequate catalyst for cracking polyethylene to aromatic hydrocarbon, see Figure 2.7. The major products were reported to be n-alkanes and aromatics with about 50-60% aromatic hydrocarbons.

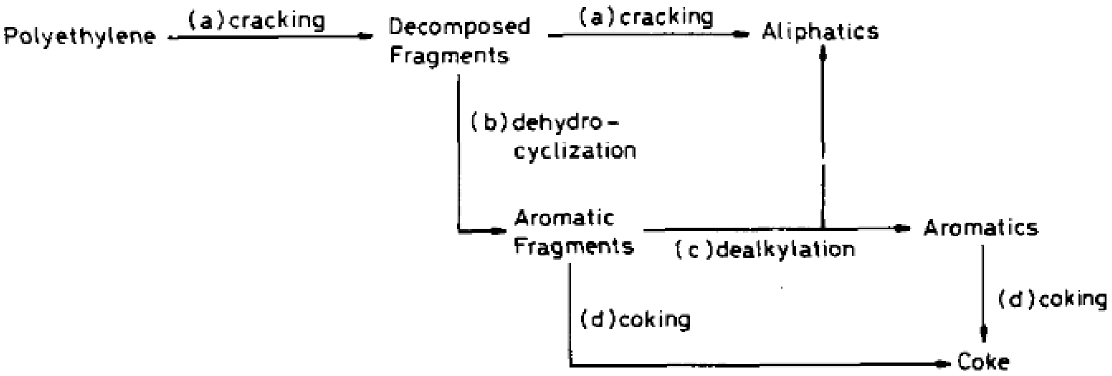

Figure 2.7. Polyethylene degradation reaction over metal-supported activated carbon catalysts adopted from [61].

Several other groups of catalysts have been investigated for the catalytic degradation of plastic wastes such as metal chloride, bentonites, red mud, etc. For example, Ivanova et al. [87], analysed a couple of metal chloride based catalysts for polyethylene at a cracking temperature of 370 °C, these include $MgCl_2.AlCl_3$, $NaAlCl_4$ and $AlCl_3$ with a high gaseous product yield of 88.2 wt%, 84.8wt % and 47.6 wt% respectively, while isobutane was the dominant product produced. In another study performed by Donaj et al. [88], they investigated a polyolefin mixture of high density polyethylene (HDPE), low density polyethylene (LDPE) and polypropylene (PP) in a fluidized quartz-bed reactor using a commercial Ziegler-Natta (Z-N):$TiCl_4/MgCl_2$ for catalytic pyrolysis for production of gaseous olefin monomers. The product yields in the ratio of gas/liquid/solid were 6.5/89.0/4.5 wt% and 54.3/41.9/3.8 wt% at the temperature of 500 °C and 650 °C respectively. Furthermore Adrados et al. [89], used red mud as pyrolysis catalyst for the investigation of packaging plastics waste which aided the aromatisation and cracking reactions leadings to high gaseous yields, aromatics rich in toluene and ethylbenzene. Faiad [90], investigated calcium bentonite for converting plastic waste to biofuel, the product yield obtained was gaseous products, which consisted of methane, ethane and propane leading to further conversion to biofuel.

2.3 Catalytic degradation of plastic wastes

Catalytic degradation/cracking involves the use of catalyst for the reduction of factors like temperature and residence time, eliminating unwanted materials and to increase the quality of product yields [91, 92]. Catalytic cracking is categorized into homogeneous or heterogeneous [46]. de Marco et al. [93], stated that homogenous catalysts are based on Lewis acids, the catalyst is usually mixed up with the feedstock during the reaction which makes it challenging to separate (an example of homogenous catalyst includes red mud, $AlCl_3$, $TiCl_4$, $NaAlCl_4$, $MgCl_2$), while heterogeneous catalysts are simple to recover from the reaction but have the problem of deactivation as a result of their entrance to the internal acids sites created by the massive molecules of the polymer. Examples of heterogeneous catalyst include conventional solid acid such as fluid catalyst cracking (FCC), nanocrystalline zeolites, silica alumina zeolites and aluminium pillared clays [94] and an illustration of the reactions pathway are shown in Figures 2.8 and 2.9, comparison of thermal and catalytic cracking shown in Table 2.8.

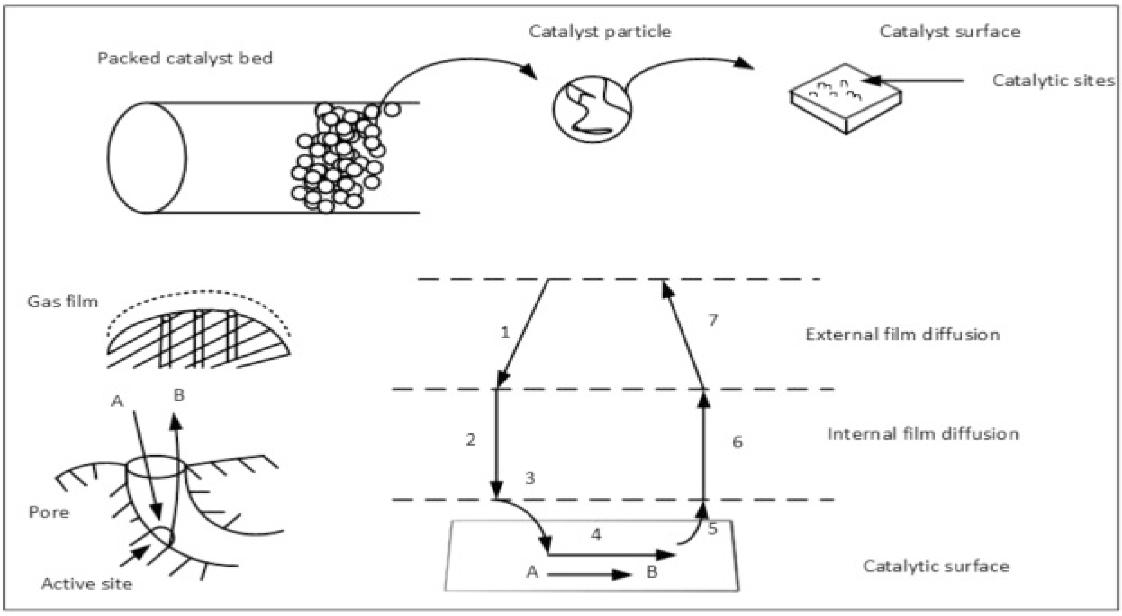

Figure 2.8. Illustration of reaction pathway by heterogeneous catalysts [32].

According to Serrano et al. [38], catalytic cracking involves a carbocation mechanism formed by protonation of the hydrocarbon on Bronsted acid sites producing carbonium ions or by abstraction of a hydride ion by Lewis acid site to create carbonium ions. Catalytic cracking usually involves diverse acid-catalysed reactions occurring at the acid sites such as cracking, isomerisation, oligomerisation, cyclization and aromatisation. Catalytic cracking usually occurs at lower temperatures with the end products having higher cyclic, branched and aromatic compounds, this is quite different from thermal cracking. Lewis acids or Bronsted acids and sometimes a combination of the two are contained in the catalyst usually used for cracking polyolefin. For catalytic cracking of plastic wastes, the major types of solid catalysts usually in use are silica-alumina, FCC catalyst, clays, mesoporous aluminosilicates (Al-MCM-41 and Al-SBA-15) and zeolites. Mordi et al. [95], analysed a couple of catalysts consisting of H-ZSM-5 zeolites, H-Theta-1 and H-mordenite in a batch reactor at a cracking temperature of 350 ^oC for catalytic reaction of polyethylene, it was discovered that H-ZSM-5 produced the lightest hydrocarbon less than C_{14}, the highest amount of aromatics (16.8%) and gaseous products (54%) as compared with H-modenite and H-Theta-1 catalyst having a product range between C_{11}-C_{19}, an aromatic yield of 3.4% and 1.4% while the gaseous yields were 43% and 38% respectively. Manos and Dwyer [74], investigated zeolite-based catalysts which include H-mordenite, Beta, USY, HY and HZSM-5 for catalytic cracking of high density polyethylene (HDPE) in a batch reactor at a temperature of 360 ^oC. The analyses showed the product yield range from C_3-C_{15} in the following order of (lighter products) HZSM-

5<H-mordenite<Beta<HY<USY (heavier products), and for the saturation bond includes the following order (more alkanes) USY>Y>Beta>H-mordenite> HZSM-5 (more alkene). Bagri and Williams [76], investigated polyethylene in a fixed bed reactor with Y-zeolite and ZSM-5 over a range of temperatures from 400 to 600 ^oC. There was a rise in aromatic yield as the temperature increased; Y-zeolite gave higher aromatic yield as compared to ZSM-5 (37.2% against 7.69% at 600 ^oC) which contained majorly toluene, ethylbenzene, xylenes and aromatic hydrocarbon with higher molecular weight majorly of naphthalene, phenanthrene, methylnaphthalene, methylphenanthrene. Zeaiter [25] investigated two catalysts HUSY and HBeta zeolites for cracking polyethylene using the direct induction heating method to supply energy, thereby reducing the reaction time for the process. There was an increased gas yield of both catalysts of more than 90%, with high amounts of olefins and aromatics which were mainly (1,2,4-Trimethylbenzene).

Lin and Yang [96], investigated post-consumer polymer PE/PP/PS/PVC over some zeolite catalysts (HZSM-5, HUSY, HMOR) and non-zeolite catalysts (SAHA, MCM-41) in a fluidised bed reactor under constant temperature and atmospheric pressure. There was a higher product yield of volatile hydrocarbons for the zeolite catalysts than non-zeolite catalysts. HSZM-5 produced an olefins range of C_3-C_5 with about 60 wt.% while HMOR, HUSY produced paraffin mainly of butane (C_4) and are prompt to deactivation as compared to HZSM-5. MCM-41 and SAHA produced an olefin-based range of product C_3-C_7 lower than those of zeolite catalysts. de Marco [93], carried out a study on three catalyst HZSM-5, $AlCl_3$ and red mud using a semi-batch non-stirred autoclave reactor at a temperature range of 400-600 ^oC. The liquid products were a mixture of C_5-C_{20} compounds with a high proportion of aromatics (>70 %), containing styrene (20-40%), toluene (9-15%) and ethylbenzene (7-16%) with a high gross calorific value (GCV) 40-43 MJ kg-1. HZSM-5 was reported to improve aromatic yields of lower molecular weight and gas production, $AlCl_3$ produced lighter liquids without any noticeable modification variation, while red mud products have higher liquid hydrocarbons with reduced viscosity from the plastic packaging waste, majorly polyolefin sample. Onwudili et al. [40], utilised a closed batch autoclave reactor to investigate the pyrolysis of carbon reinforced composite plastic (CRCP) waste at temperatures between 350 ^oC and 500 ^oC. The product mixture contained solid yield (72-77 wt.%) with a prevailing product of carbon fibre at a recovery of about 98% and char, liquid (22-25 wt.%) with about 15-20 wt.% of water in the liquid products and the oil yield contained monomers chemical feedstocks which are aniline, methyl aniline, o-toluidine, phenols and alkyl phenols for producing the resin and bisphenol-A preserving agents. The gaseous products (2-4 wt.%) chiefly carbon dioxide with calorific values of about 35MJ/m^3 at higher temperatures that can serve as fuel for the process was obtained. Muhammad et al. [19], investigated Zeolite HZSM-5 catalyst over real world post-consumer waste plastics, simulated mixed plastic and four other single polymer plastics using a two stage pyrolysis catalytic fixed bed reactor. A range of 81-97 wt.% of oil/wax was obtained, with the addition of catalyst, the oil/wax yield reduces to a range of 44-51 wt.% as the gas yield increased. The long carbon chain molecules in the composition of the oil yield which was about C_{16+} was reduced to hydrocarbon fuel range C_5-C_{15} and an increase in single ring aromatic hydrocarbon content was obtained such as benzene, toluene, ethylbenzene, xylenes, and styrene.

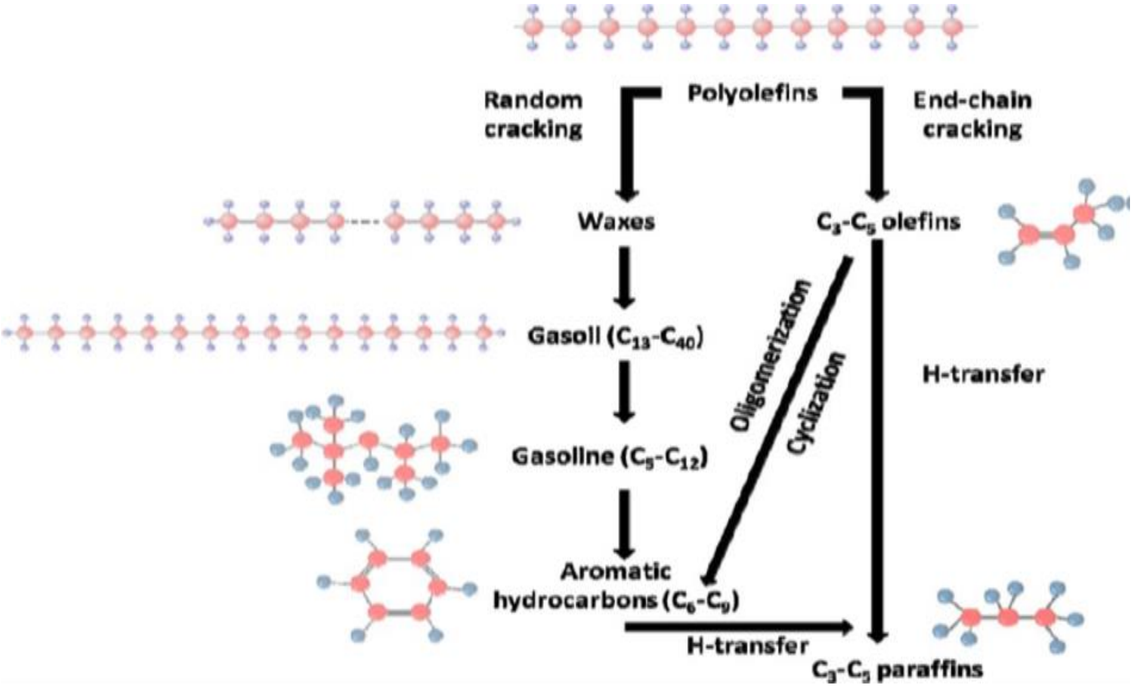

Figure 2.9. Catalytic cracking reaction pathway for polyolefins [38].

Table 2.8. Comparison on thermal and catalytic cracking characteristics [15].

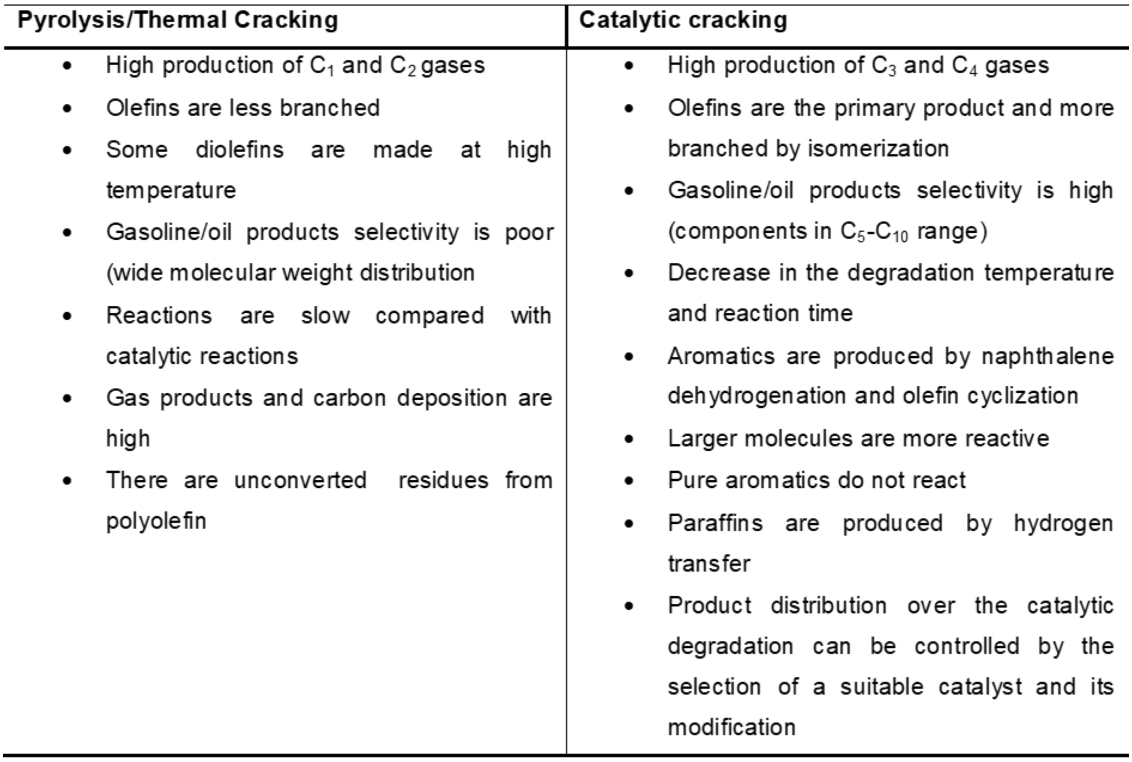

Pyrolysis/Thermal Cracking	**Catalytic cracking**
• High production of C_1 and C_2 gases • Olefins are less branched • Some diolefins are made at high temperature • Gasoline/oil products selectivity is poor (wide molecular weight distribution • Reactions are slow compared with catalytic reactions • Gas products and carbon deposition are high • There are unconverted residues from polyolefin	• High production of C_3 and C_4 gases • Olefins are the primary product and more branched by isomerization • Gasoline/oil products selectivity is high (components in C_5-C_{10} range) • Decrease in the degradation temperature and reaction time • Aromatics are produced by naphthalene dehydrogenation and olefin cyclization • Larger molecules are more reactive • Pure aromatics do not react • Paraffins are produced by hydrogen transfer • Product distribution over the catalytic degradation can be controlled by the selection of a suitable catalyst and its modification

2.3.1.1 Catalytic-pyrolysis of plastics waste to aromatic hydrocarbons

Converting waste plastics into chemical feedstocks for industry is a viable option which provides a solution for waste plastics disposal other than by landfill. Chemical feedstock recycling has been reported to entail higher catalytic cracking with higher selectivity greater than that of fuel energy. Polyolefin usually disintegrate to a very high degree for feedstocks generation [97]. Takuma et al. [98], investigated H-gallosilicate catalyst for the degradation of polyolefin (LDPE, HDPE and PP) in a fixed-bed reactor at a temperature range of 375-550 ^{o}C, gaseous products and liquid aromatic hydrocarbons with a total product yield between 64-69 wt% majorly of benzene, toluene and xylene (BTX) were obtained. The acidic gallosilicate was stated to be stable with little formation of coke on the surface of the catalyst. Uemichi et al. [97], analysed the use of H-Ga-silicate for the decomposition of polyethylene at temperatures ranging between 400-525 ^{o}C under atmospheric pressure and helium stream, there was a high product yield, greater than 70 wt% at 525 ^{o}C majorly of benzene, toluene and xylene (BTX). H-Ga-Silicate catalyst was compared with H-ZSM-5 and silica-alumina, H-Ga-silicate gave the highest yield of aromatic followed by H-ZSM-5 and the least was silica-alumina. It was stated that H-ZSM-5 had strong acidity characteristics that favour cracking and gaseous yield while H-Ga-silicate has a tendency for aromatisation. Aromatisation and cracking usually occur concurrently, but as the temperature increases, aromatisation overcomes cracking leading to a higher yield of aromatics.

Also, the use of acidic and basic catalysts such as calcium carbide (CaC_2), silica (SiO_2), alumina (Al_2O_3), zinc oxide (ZnO), magnesium oxide (MgO), and silica alumina (SiO_2-Al_2O_3) for conversion of waste plastic (low density polyethylene LDPE) were investigated, and the results indicated that the oxide containing catalysts are more suitable for selective conversion of LDPE into aromatic compounds [99]. Likewise, Kaminsky and Kim [4], utilised a fluidized bed reactor to carry out analyses on mixed plastics for the production of aromatic hydrocarbons which were mainly benzene, toluene, xylenes and styrene of about 30-40% yield. The reaction temperature was ranged between 685 ^oC and 738 ^oC which had a major impact on the production of benzene.

Aromatisation of aliphatic hydrocarbons, mainly of light alkanes, leads to production of higher value aromatic hydrocarbons, majorly of benzene, toluene and xylene (BTX) which are important feedstock for the petrochemical industry. Akhtar and Al-Khattaf [100], stated three procedures for aromatisation of light alkanes which includes conversion of alkanes into alkenes, further conversion of alkenes into higher alkenes and lastly alkenes to aromatic compounds. Kocal [101], equally highlighted three stages of conversion of paraffins and olefins to aromatic hydrocarbons which include dehydrogenation, oligomerization and aromatization reactions. Gnep et al. [102], investigated HZSM-5 supported platinum catalyst at atmospheric pressure and a reaction temperature of 530 ^oC for dehydrocyclodimerization conversion of propane to aromatic which occurred via a propene pathway. There was an increase in the rate of conversion of aliphatic and alicyclic C_6+ transition into aromatics but methane and ethane were also produced. Pt-HZSM-5 compared with HZSM-5 revealed platinum had been active for propene conversion to aromatic compounds. Other research has been conducted on optimisation of aliphatic hydrocarbon conversion into aromatics yield using bifunctional catalysts [100, 101, 103-105].

2.3.1.2 Effect of metals on catalytic-pyrolysis of plastics waste to aromatics, hydrogen and other gases

Metal catalysts have been extensively studied for optimisation of waste plastics into aromatic hydrocarbons. For example, Scott et al. [106], investigated iron-impregnated charcoal and also discovered that increase in aromatics was formed with iron content as high as 5%. Pierella et al. [69], examined pyrolysis of high density polylethylene (HDPE) over some zeolite catalysts H-ZSM-11, Mo-ZSM-11, Zn-ZSM-11 and Mo-MCM-41 in the temperature range 410-500 ^{o}C, it was discovered that Zn-Zeolite yielded more aromatic compounds (>57%) mainly of benzene, toulene, xylene (BTX) with selectivity of 47 wt.%. Huang et al. [94], suggested some supported catalysts such as SiO_2, Al_2O_3, MgO, TiO_2, activated carbon, clay, zirconia, zeolite with different metals that include Pt, Pd, Ir, Ru, Rh, Ni, Co, Fe, Mn, Mg, Ca, Mo, Ti, Zn, Al and metal alloys. It was reported that metal catalysts reduced the formation of n-alkanes and increased selectivity of aromatic compounds with a high octane number. Uemichi et al. [63], investigated bifunctional catalysts for decomposition of polyethylene using transition metals (Pt, Fe, Mo, Zn, Co, Ni and Cu) impregnated on activated carbon, the most effective were Pt, Fe and Mo (see Figure 2.10), dependent on the catalyst support such as Al_2O_3, SiO_2 -Al_2O_3 but activated carbon was the most effective. The Pt-based catalyst yielded benzene product while Fe and Mo based catalysts produced toluene respectively as the major constituent with about 45% aromatic yields corresponding to about 60% of the hydrocarbon produced. The inexpensive metal catalysts such as Ni, Fe, Co are used for industrial purposes such as ammonia production, liquid fuels from syngas and in some cases an Ni-based catalyst reacts in a similar way to that of Pt [94]. The same author also investigated Pt/C and Fe/C for catalytic decomposition of polypropylene (PP) in a fixed bed flow system, increased yield of aromatic compounds was observed as Pt was more active than Fe [107].

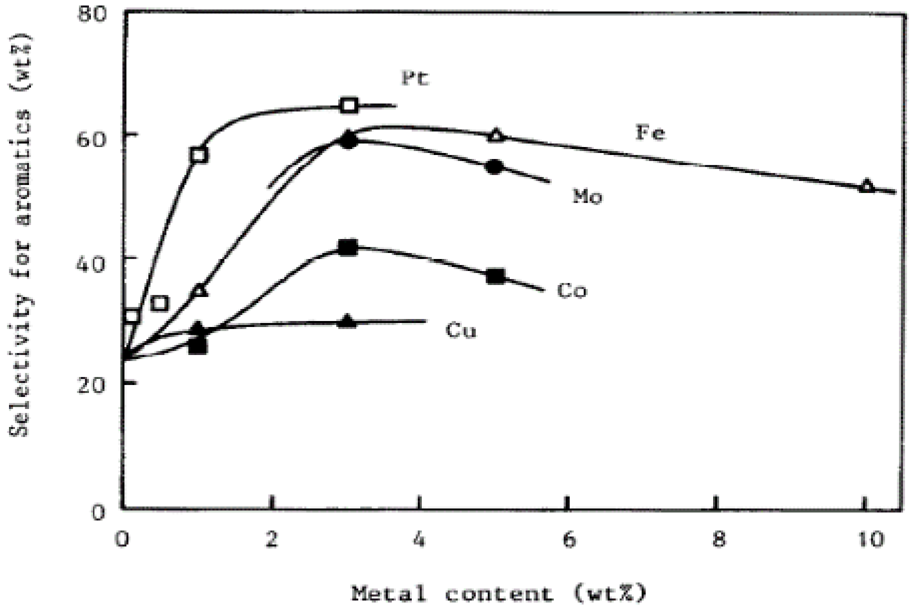

Figure 2.10. Effect of metal content on selectivity to aromatics [63].

Methane as well as hydrogen are important fuels which have been produced from waste plastics. For example Santiago-Maldonado et al. [108], produced methane by thermally degrading waste plastics in the presence of oxygen to produce CO_2 and CO which was reacted with hydrogen over an Ni/Mg catalyst on Al_2O_3 (Sabatier reaction). The Ni/Mg on Al_2O_3 catalysts proficiently converted $CO\text{-}CO_2/H_2$ to CH_4/H_2O at high temperature. The Sabatier process involves an exothermic reaction of carbon-dioxide with hydrogen at high temperatures and pressures in the presence of a nickel catalyst to produce methane. The Sabatier reaction is shown in Equation 2.1 as follows:

$CO_2 + 4H_2 + \text{catalyst} \rightarrow CH_4 + 2H_2O + \text{energy/heat}$ ($\Delta H = -165.0 \text{kJ/mol}$)……….. (2.1)

Furthermore, Bagri and Williams [76], investigated polyethylene using Y-zeolite and ZSM-5 in a fixed bed reactor, the gaseous products contained mainly alkanes and alkenes; hydrogen, methane, ethane, ethene, propane, propene and butane. The ZSM-5 catalyst produced higher concentrations of gases than the Y-zeolite at an increasing temperature from 400 ^{o}C to 600 ^{o}C. Several other authors also suggested production of gaseous products together with aromatic hydrocarbons from polyolefin plastic wastes [11, 22, 65, 67-75, 87-90].

2.4 Summary

Plastics contain long molecular compounds of carbon and hydrogen, which can be broken down into smaller molecular chains to generate fuel and other useful chemicals by thermochemical processing. Solid catalysts such as zeolite-type catalysts are known to degrade waste plastics by catalytic and thermal processes into liquid fuel and aromatic chemicals. The use of catalysts plays an important role in the pyrolysis-catalysis process of waste hydrocarbons. Noble metals have been investigated as they promote the catalytic process, but they are very expensive and are not effective for industrial processing of plastic wastes. The catalyst supports affect the process, and the most commonly used catalyst supports are zeolite, MCM-41 and alumina, among others. In most of the literature reviewed [15, 38, 109], zeolite catalysts such as HZSM-5 have been reported by many researchers to yield high gaseous products such as hydrogen and methane, while Y-zeolite has been reported to yield more aromatic hydrocarbons. The Y-zeolite catalyst, as investigated in this study, appeared to produce higher concentrations of aromatic hydrocarbons from plastic wastes due to the larger pore size, surface area and surface acidity as compared with ZSM-5.

Therefore, novel catalysts prepared from Ni, Mo, Fe, Ga, Ru and Co transition metals supported on Y-zeolite catalyst have been explored in the pyrolysis-catalysis of waste plastics for production of aromatic hydrocarbons and methane/hydrogen production.

2.5 Biomass as a fuel source conversion process

Biomass is universally known to have the potential to replace fossil fuel as an energy source and it is the only renewable energy resource that has the potential to be converted into multiple fuels such as gas, liquid and char-solid. Likewise the ease of production and marketing is also an advantage [110]. Biomass, as a source of energy, has received great interest, because it is a sustainable and renewable source of energy with several readily available feedstock from agricultural residues, forestry residues, municipal solid waste, demolition and construction activities, etc. Biomass is stated to be carbon neutral which aids in combating air pollution [111]. This is due to the fact that the same carbon dioxide taken from the atmosphere during photosynthesis is being returned back to the atmosphere when the biomass resource is used as fuel**.** Biomass resources, such as green plants, covert sunlight into energy through photosynthesis in the form of chemical bonds which when broken down into carbon, hydrogen and oxygen molecules via digestion, combustion or decomposition releases the stored chemical energy [112]. There are different types of biomass sources, these include: edible and non-edible sources. The edible sources are the starch-based biomass such as corn crops, cassava, and sugar cane bagasse etc. The non-edible sources are the lignocellulosic biomass such as wood, grass and agricultural waste, energy crops, etc., which are preferable because they do not compete with food resources [113]. Biomass resources may be classified into five categories [114, 115]: (i) virgin wood waste such as wood chips, sawdust, tree branches etc.; (ii) energy crops grown for the purpose of energy applications such as jatropha, pongamai, hybrid eucalyptus, napier grass and miscanthus; (iii) agricultural residues such as sugar cane bagasse, coconut shell, corn husks, palm kernel shells; (iv) municipal solid waste (MSW), animal wastes and food waste; (v) industrial wastes from the manufacturing industrial processes such as construction, demolition activities [114, 115].

2.5.1 Pyrolysis of biomass and components

Biomass is made of three major components which include: cellulose, hemicellulose and lignin. Biomass is stated to contain 40-50 wt.% of cellulose, 15-30 wt.% of hemicellulose and 15-30 wt.% of lignin [113, 116]. Consequently, Wu et al. [117] suggested that biomass samples are quite different due to the composition of the components of cellulose, hemicellulose and lignin. For example, wood bark was stated to contain larger amount of lignin ~ 43% but lower cellulose of about ~ 24%, while grass contain more of cellulose ~ 54% and a much lower lignin ~ 4% [118]. These biomass components, which consist of cellulose, hemicellulose, and lignin usually, influence the type of product that should be produced as well as determining the decomposition temperature and other pyrolysis conditions. It is reported that the chemical structure of cellulose contains the OH and C-O carboxyl functional group, hemicellulose is made of C=O carbonyl compounds while lignin is found with meth-oxyl-O-CH_3, C-O-C and C=C functional groups [117, 119]. The gaseous product released from pyrolysis of the biomass components such as CO and CO_2 was reported to originate from the decomposition and reforming of carboxyl (COO) and carbonyl (C=O) functional group, while H_2 resulted from secondary decomposition and reforming of aromatic C=C and C-H functional at high temperatures [120]. Likewise, other researchers confirmed that more CO was produced from cellulose pyrolysis due to the COC and C=O group, while more CO_2 was obtained from hemicellulose because of C=O and COOH, and lignin with more CH_4 mainly from the cracking of methoxy-O-CH_3 group. The H_2 produced was stated to be obtained mainly from the cracking reaction and deformation of C=C and CH group [121].

The thermal decomposition process of biomass components is an important factor that determines the proportion of each product fractions (gases, liquid and char) and its compositions. The pyrolysis process of biomass samples or the component mixture was stated to be divided into four (4) temperature categories: less than 220 °C as moisture evolution, between 220-315 °C as hemicellulose decomposition, 315-400 °C as the cellulose decomposition while greater than 400 °C involved lignin decomposition respectively [122]. The effect of temperature on biomass components indicating lignin with a higher degradation temperature than cellulose had equally been extensively studied [123-127]. According to Block et al. [124], hemicellulose decomposes between temperatures of 190-290 ^{o}C, cellulose decomposes at the range of 290-360 ^{o}C while lignin has a wider decomposition temperature between 360-500 ^{o}C. A similar tendency was observed by Yang et al. [119], who stated that lignin is a very stable component as it is an aromatic polymer with three dimensional linkage in an alkyl-benzene structure which is more difficult to decompose (at about 160-900 ^{o}C) compared to cellulose. However, cellulose is a polysaccharide with a linear chain of β ($1 \rightarrow 4$) linked to a D-glucose unit which decomposes at a range of temperature from 325-400 ^{o}C [126]. Burhenne [128], proposed that a higher activation energy will be needed to decompose lignin contained feedstock such as woody biomass, than feedstock (wheat straw) having more cellulose as well as feedstock such as rape straw with higher hemicellulose in it, as examined on TGA and fixed bed reactor.

The reaction schemes of cellulose degradation (Equation 2.2), hemicellulose degradation (Equation 2.3), and lignin degradation (Equation 2.4) showed significant yields of H_2 during biomass pyrolysis as shown below [129].

Cellulose degradation (2.2)

$$Cellulose \longrightarrow active\ cellulose \longrightarrow C_2H_4O_2 + C_2H_2O_2 + CH_3CHO + C_3H_6O + H_2 + CO_2 + CO + CH_4 + H_2O + 5 - Hydroxymethyl - furtural + char$$

$$Active\ cellulose \longrightarrow levoglucosan$$

$$Cellulose \longrightarrow Char + H_2O$$

Hemicellulose degradation (2.3)

$$Hemicellulose \longrightarrow Intermediate\ hemicellulose \longrightarrow H_2 + CO_2 + C0 + H_2O + CH_2O + CH_3OH + C_2H_5OH + char$$

$$Intermediate\ hemicellulose \longrightarrow Xylose$$

Lignin degradation (2.4)

$$Lignin \longrightarrow Para - coumaryl + Phenol + H_2 + CO_2 + CO + CH_4 + H_2O + C_3H_4O_2 + C_2H_4 + char$$

$$Lignin \longrightarrow C_{11}H_{12}O_4$$

The decomposition of cellulose and hemicellulose in biomass forms anhydro-sugars and highly oxygenated compounds while the depolymerisation of lignin, form oligomers and phenolic monomers. The degradation reaction of cellulose initially results in a partial depolymerisation leading to formation of an intermediary called active cellulose or anhydrocellulose [130]. Likewise, other authors equally reported that the primary components formed from cellulose and hemicellulose are hydrogen, methane, carbonyls, carboxylic acids, anhydro-sugars, and furans while lignin forms mono-aromatic, hydrogen, methane, phenols, guaiacols and its derivatives as well as secondary reactions of these primary components including xylenols, phenol, catechols, cresols, PAHs, coke and gases [131-133].

2.5.2 Influence of pyrolysis parameters on biomass

The process parameters affect the product distributions and composition of the products directly. Manipulating the process conditions implicates the yield and composition of the products by maximising the required products. The main parameters that directly influence the final product include: feedstock composition, temperature, heating rate, moisture content of sample, residence time, gasifying agent, catalyst, reactor design (detail discussion on reactor in section 2.2.2), etc. Many researchers have reported on the influence of process parameters. According to Waheed et al. [134], product yield from biomass pyrolysis usually relies upon important conditions such as temperature, heating rate, residence time, atmospheric pressure, particle size, feedstock type, reactor configuration, etc.

2.5.2.1 Feedstock composition

There are significant differences with different biomass feedstock materials due to the origin and environmental conditions such as the weather, soil type, etc. According to Monono et al. [135], the chemical composition of biomass and the product yields vary with different plant species, management practices and environment. Therefore, biomass samples differ in their chemical characteristics, physical properties and heating values. Proximate and ultimate analyses are preliminary classification of biomass samples on a dry basis and an ash-free basis. According to Vassilev et al. [136], the chemical composition of biomass is highly variable as determined by proximate, ultimate and ash analysis. The characteristics of the proximate and ultimate analysis data showed some irregularities due to different genetic types of inorganic matter; bulk ash yield and high variations of moisture in different biomass samples (see Table 2.9). The proximate analysis provides information relating to moisture content (MC), volatile matter (VM), fixed carbon (FC) and ash content, while the ultimate analysis gives information about the elemental composition of the feedstock sample. Table 2.9 shows proximate analysis of most biomass to have high volatile content and low ash content, while ultimate analysis shows that the biomass contains low nitrogen and sulphur content respectively, which makes the biomass samples suitable and desirable feedstock for pyrolysis and gasification processes. Biomass moisture content is also a very important factor which determines the heating value, the composition and the product yield [137]. High moisture content lowers the efficiency of the pyrolysis and gasification process. For example, fresh green plant/biomass usually contains more moisture, which requires drying before it can be pyrolysed or gasified. A range between 10 to 20 % of moisture content is suitable for optimum fuel processes and production from biomass wastes [129].

Likewise, other authors equally analysed the organic and inorganic composition content of biomass. The content of structural component (cellulose, hemicellulose and lignin) and extractive content in different types of biomass (93 varieties) on a dry-ash-free basis were reported [138]. Examples of the structural composition of seven different biomass are shown in Figure 2.11 and Table 2.10.

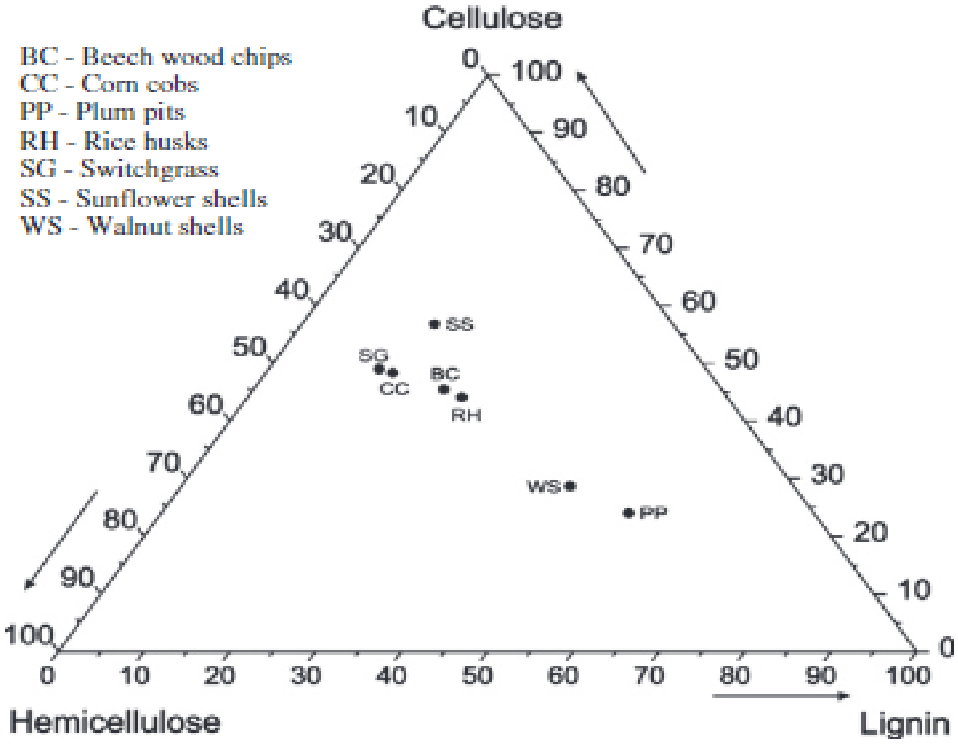

Figure 2.11. Structural composition of seven different biomass samples (wt.%), adapted from [138].

The chemical composition suitability of different biomass for pyrolysis and gasification of these biomass samples have been investigated by many researchers. For example, gasification of hazelnut shells in a pilot scale downdraft gasifier was conducted, a full mass balance including composition of the gas produced, as well as the tar production rate as a function of feed rate has been reported [139]. Other studies equally reviewed different biomass gasification. Kirubakaran et al. [140], reviewed studies on the effect of biomass size, structure, temperature, heating rate, composition, ash and environment. Auto gasification of biomass into gaseous fuel by bio-oxygen and catalyst ash for production of hydrogen and CO was reported. Likewise, the organic composition in combination with mineral matter of biomass, is suggested to play a major role in determining pyrolysis product distribution and product properties [141].

Table 2.9. Chemical composition of different biomass samples based on proximate and ultimate analysis (wt.%) adapted from [136].

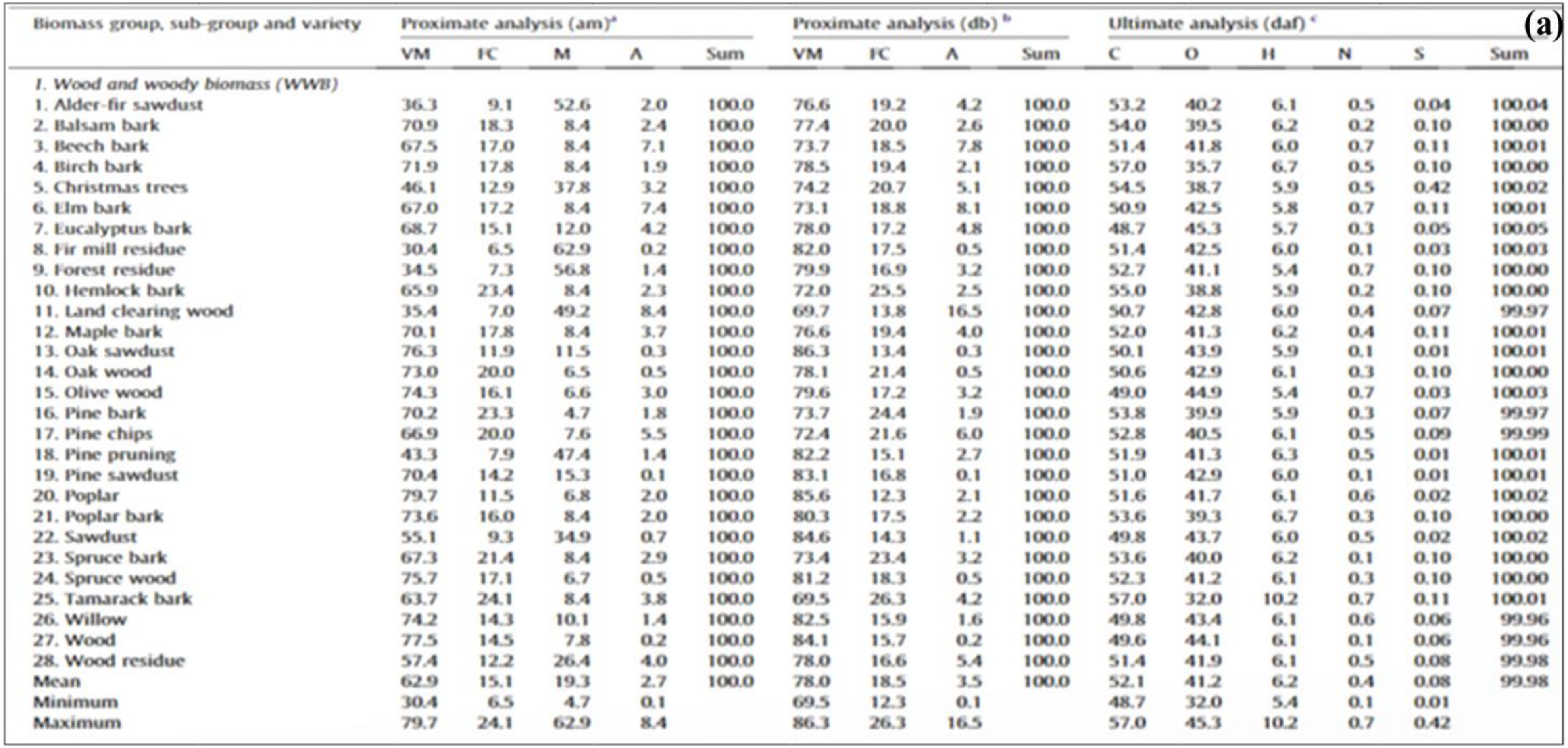

(a)

Biomass group, sub-group and variety	Proximate analysis (am)[a]					Proximate analysis (db)[b]				Ultimate analysis (daf)[c]					
	VM	FC	M	A	Sum	VM	FC	A	Sum	C	O	H	N	S	Sum
I. Wood and woody biomass (WWB)															
1. Alder-fir sawdust	36.3	9.1	52.6	2.0	100.0	76.6	19.2	4.2	100.0	53.2	40.2	6.1	0.5	0.04	100.04
2. Balsam bark	70.9	18.3	8.4	2.4	100.0	77.4	20.0	2.6	100.0	54.0	39.5	6.2	0.2	0.10	100.00
3. Beech bark	67.5	17.0	8.4	7.1	100.0	73.7	18.5	7.8	100.0	51.4	41.8	6.0	0.7	0.11	100.01
4. Birch bark	71.9	17.8	8.4	1.9	100.0	78.5	19.4	2.1	100.0	57.0	35.7	6.7	0.5	0.10	100.00
5. Christmas trees	46.1	12.9	37.8	3.2	100.0	74.2	20.7	5.1	100.0	54.5	38.7	5.9	0.5	0.42	100.02
6. Elm bark	67.0	17.2	8.4	7.4	100.0	73.1	18.8	8.1	100.0	50.9	42.5	5.8	0.7	0.11	100.01
7. Eucalyptus bark	68.7	15.1	12.0	4.2	100.0	78.0	17.2	4.8	100.0	48.7	45.3	5.7	0.3	0.05	100.05
8. Fir mill residue	30.4	6.5	62.9	0.2	100.0	82.0	17.5	0.5	100.0	51.4	42.5	6.0	0.1	0.03	100.03
9. Forest residue	34.5	7.3	56.8	1.4	100.0	79.9	16.9	3.2	100.0	52.7	41.1	5.4	0.7	0.10	100.00
10. Hemlock bark	65.9	23.4	8.4	2.3	100.0	72.0	25.5	2.5	100.0	55.0	38.8	5.9	0.2	0.10	100.00
11. Land clearing wood	35.4	7.0	49.2	8.4	100.0	69.7	13.8	16.5	100.0	50.7	42.8	6.0	0.4	0.07	99.97
12. Maple bark	70.1	17.8	8.4	3.7	100.0	76.6	19.4	4.0	100.0	52.0	41.3	6.2	0.4	0.11	100.01
13. Oak sawdust	76.3	11.9	11.5	0.3	100.0	86.3	13.4	0.3	100.0	50.1	43.9	5.9	0.1	0.01	100.01
14. Oak wood	73.0	20.0	6.5	0.5	100.0	78.1	21.4	0.5	100.0	50.6	42.9	6.1	0.3	0.10	100.00
15. Olive wood	74.3	16.1	6.6	3.0	100.0	79.6	17.2	3.2	100.0	49.0	44.9	5.4	0.7	0.03	100.03
16. Pine bark	70.2	23.3	4.7	1.8	100.0	73.7	24.4	1.9	100.0	53.8	39.9	5.9	0.3	0.07	99.97
17. Pine chips	66.9	20.0	7.6	5.5	100.0	72.4	21.6	6.0	100.0	52.8	40.5	6.1	0.5	0.09	99.99
18. Pine pruning	43.3	7.9	47.4	1.4	100.0	82.2	15.1	2.7	100.0	51.9	41.3	6.3	0.5	0.01	100.01
19. Pine sawdust	70.4	14.2	15.3	0.1	100.0	83.1	16.8	0.1	100.0	51.0	42.9	6.0	0.1	0.01	100.01
20. Poplar	79.7	11.5	6.8	2.0	100.0	85.6	12.3	2.1	100.0	51.6	41.7	6.1	0.6	0.02	100.02
21. Poplar bark	73.6	16.0	8.4	2.0	100.0	80.3	17.5	2.2	100.0	53.6	39.3	6.7	0.3	0.10	100.00
22. Sawdust	55.1	9.3	34.9	0.7	100.0	84.6	14.3	1.1	100.0	49.8	43.7	6.0	0.5	0.02	100.02
23. Spruce bark	67.3	21.4	8.4	2.9	100.0	73.4	23.4	3.2	100.0	53.6	40.0	6.2	0.1	0.10	100.00
24. Spruce wood	75.7	17.1	6.7	0.5	100.0	81.2	18.3	0.5	100.0	52.3	41.2	6.1	0.3	0.10	100.00
25. Tamarack bark	63.7	24.1	8.4	3.8	100.0	69.5	26.3	4.2	100.0	57.0	32.0	10.2	0.7	0.11	100.01
26. Willow	74.2	14.3	10.1	1.4	100.0	82.5	15.9	1.6	100.0	49.8	43.4	6.1	0.6	0.06	99.96
27. Wood	77.5	14.5	7.8	0.2	100.0	84.1	15.7	0.2	100.0	49.6	44.1	6.1	0.1	0.06	99.96
28. Wood residue	57.4	12.2	26.4	4.0	100.0	78.0	16.6	5.4	100.0	51.4	41.9	6.1	0.5	0.08	99.98
Mean	62.9	15.1	19.3	2.7	100.0	78.0	18.5	3.5	100.0	52.1	41.2	6.2	0.4	0.08	99.98
Minimum	30.4	6.5	4.7	0.1		69.5	12.3	0.1		48.7	32.0	5.4	0.1	0.01	
Maximum	79.7	24.1	62.9	8.4		86.3	26.3	16.5		57.0	45.3	10.2	0.7	0.42	

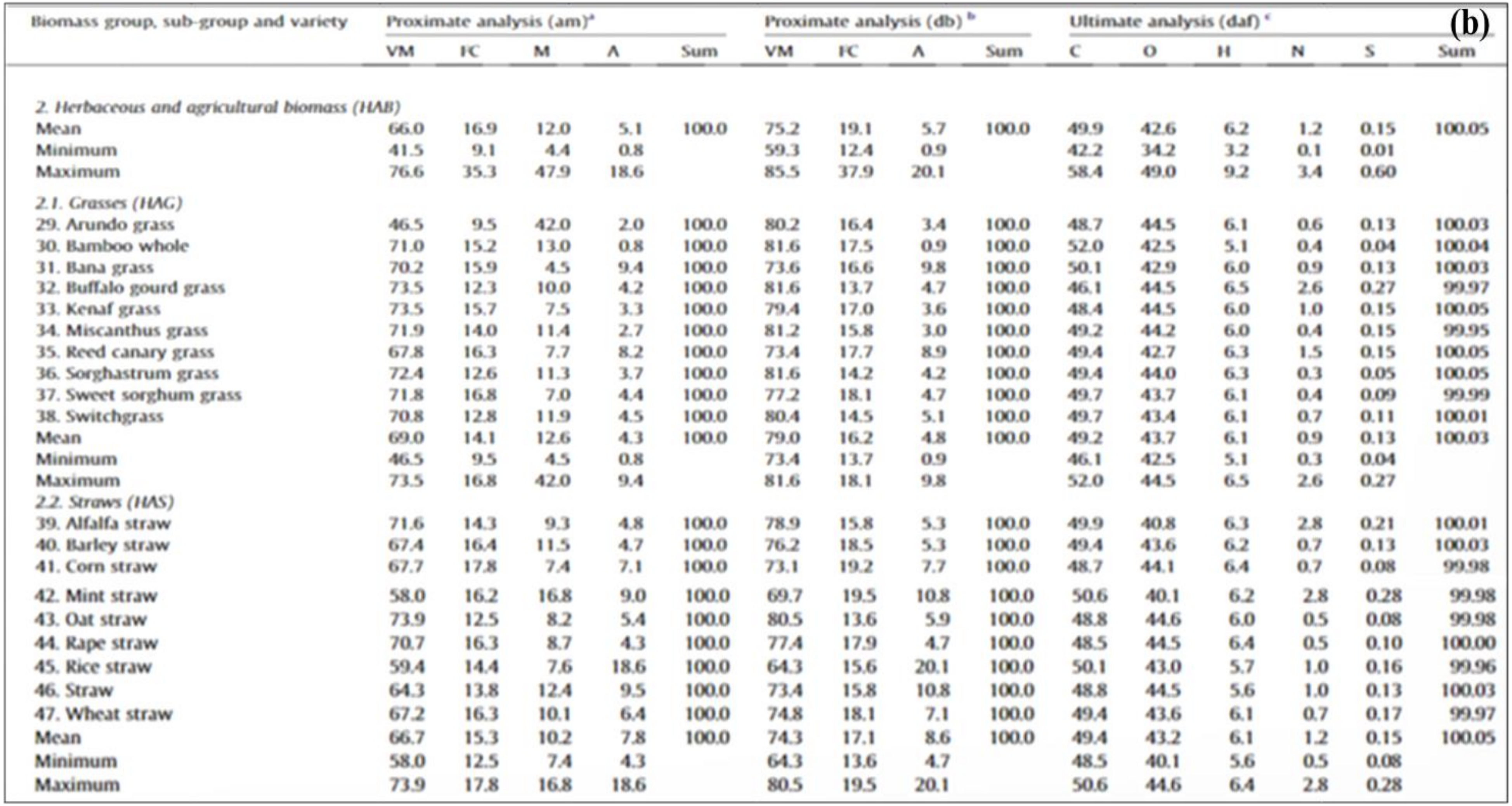

(b)

Biomass group, sub-group and variety	Proximate analysis (am)[a]					Proximate analysis (db)[b]				Ultimate analysis (daf)[c]					
	VM	FC	M	A	Sum	VM	FC	A	Sum	C	O	H	N	S	Sum
2. Herbaceous and agricultural biomass (HAB)															
Mean	66.0	16.9	12.0	5.1	100.0	75.2	19.1	5.7	100.0	49.9	42.6	6.2	1.2	0.15	100.05
Minimum	41.5	9.1	4.4	0.8		59.3	12.4	0.9		42.2	34.2	3.2	0.1	0.01	
Maximum	76.6	35.3	47.9	18.6		85.5	37.9	20.1		58.4	49.0	9.2	3.4	0.60	
2.1. Grasses (HAG)															
29. Arundo grass	46.5	9.5	42.0	2.0	100.0	80.2	16.4	3.4	100.0	48.7	44.5	6.1	0.6	0.13	100.03
30. Bamboo whole	71.0	15.2	13.0	0.8	100.0	81.6	17.5	0.9	100.0	52.0	42.5	5.1	0.4	0.04	100.04
31. Bana grass	70.2	15.9	4.5	9.4	100.0	73.6	16.6	9.8	100.0	50.1	42.9	6.0	0.9	0.13	100.03
32. Buffalo gourd grass	73.5	12.3	10.0	4.2	100.0	81.6	13.7	4.7	100.0	46.1	44.5	6.5	2.6	0.27	99.97
33. Kenaf grass	73.5	15.7	7.5	3.3	100.0	79.4	17.0	3.6	100.0	48.4	44.5	6.0	1.0	0.15	100.05
34. Miscanthus grass	71.9	14.0	11.4	2.7	100.0	81.2	15.8	3.0	100.0	49.2	44.2	6.0	0.4	0.15	99.95
35. Reed canary grass	67.8	16.3	7.7	8.2	100.0	73.4	17.7	8.9	100.0	49.4	42.7	6.3	1.5	0.15	100.05
36. Sorghastrum grass	72.4	12.6	11.3	3.7	100.0	81.6	14.2	4.2	100.0	49.4	44.0	6.3	0.3	0.05	100.05
37. Sweet sorghum grass	71.8	16.8	7.0	4.4	100.0	77.2	18.1	4.7	100.0	49.7	43.7	6.1	0.4	0.09	99.99
38. Switchgrass	70.8	12.8	11.9	4.5	100.0	80.4	14.5	5.1	100.0	49.7	43.4	6.1	0.7	0.11	100.01
Mean	69.0	14.1	12.6	4.3	100.0	79.0	16.2	4.8	100.0	49.2	43.7	6.1	0.9	0.13	100.03
Minimum	46.5	9.5	4.5	0.8		73.4	13.7	0.9		46.1	42.5	5.1	0.3	0.04	
Maximum	73.5	16.8	42.0	9.4		81.6	18.1	9.8		52.0	44.5	6.5	2.6	0.27	
2.2. Straws (HAS)															
39. Alfalfa straw	71.6	14.3	9.3	4.8	100.0	78.9	15.8	5.3	100.0	49.9	40.8	6.3	2.8	0.21	100.01
40. Barley straw	67.4	16.4	11.5	4.7	100.0	76.2	18.5	5.3	100.0	49.4	43.6	6.2	0.7	0.13	100.03
41. Corn straw	67.7	17.8	7.4	7.1	100.0	73.1	19.2	7.7	100.0	48.7	44.1	6.4	0.7	0.08	99.98
42. Mint straw	58.0	16.2	16.8	9.0	100.0	69.7	19.5	10.8	100.0	50.6	40.1	6.2	2.8	0.28	99.98
43. Oat straw	73.9	12.5	8.2	5.4	100.0	80.5	13.6	5.9	100.0	48.8	44.6	6.0	0.5	0.08	99.98
44. Rape straw	70.7	16.3	8.7	4.3	100.0	77.4	17.9	4.7	100.0	48.5	44.5	6.4	0.5	0.10	100.00
45. Rice straw	59.4	14.4	7.6	18.6	100.0	64.3	15.6	20.1	100.0	50.1	43.0	5.7	1.0	0.16	99.96
46. Straw	64.3	13.8	12.4	9.5	100.0	73.4	15.8	10.8	100.0	48.8	44.5	5.6	1.0	0.13	100.03
47. Wheat straw	67.2	16.3	10.1	6.4	100.0	74.8	18.1	7.1	100.0	49.4	43.6	6.1	0.7	0.17	99.97
Mean	66.7	15.3	10.2	7.8	100.0	74.3	17.1	8.6	100.0	49.4	43.2	6.1	1.2	0.15	100.05
Minimum	58.0	12.5	7.4	4.3		64.3	13.6	4.7		48.5	40.1	5.6	0.5	0.08	
Maximum	73.9	17.8	16.8	18.6		80.5	19.5	20.1		50.6	44.6	6.4	2.8	0.28	

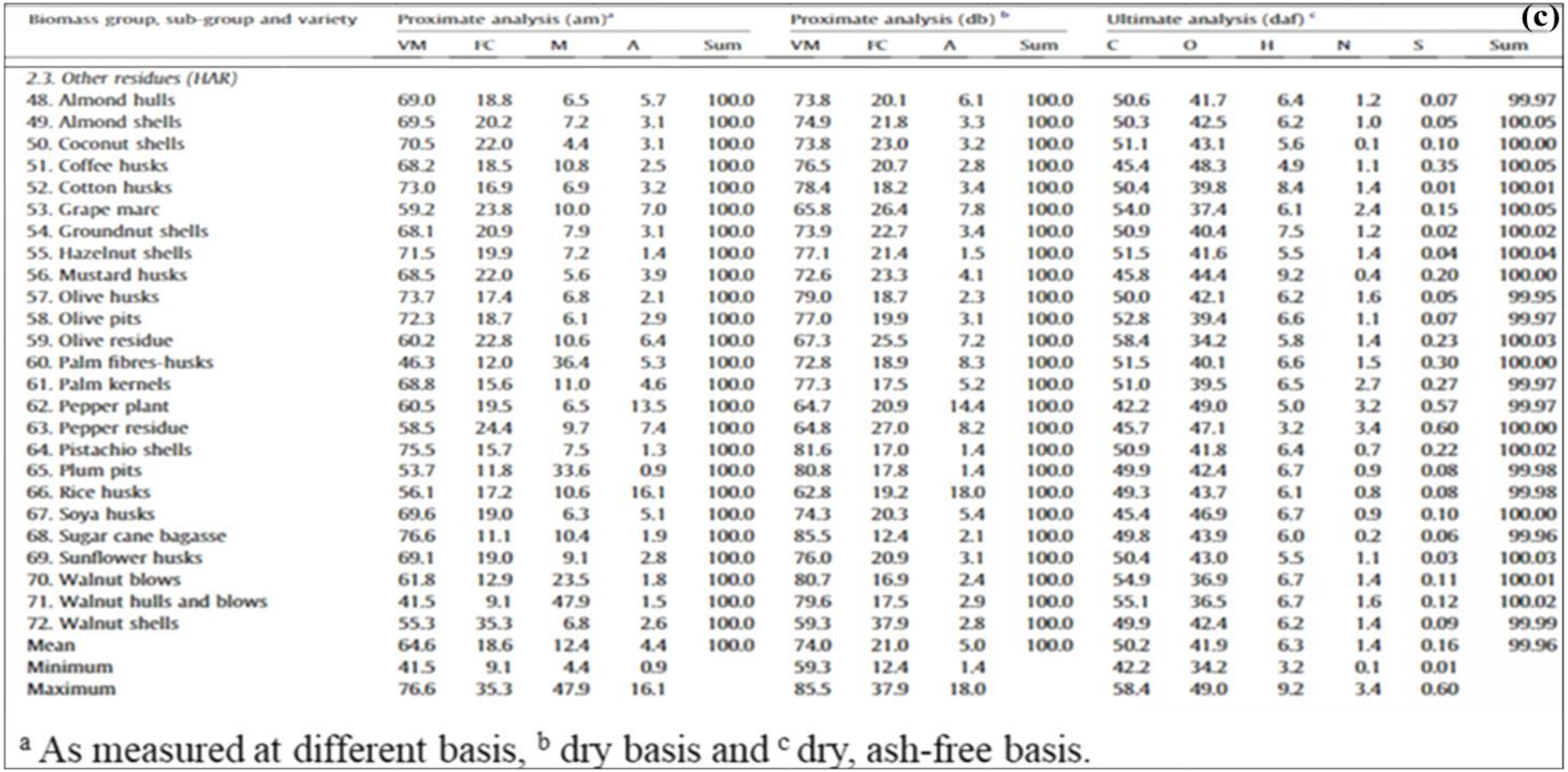

(c)

Biomass group, sub-group and variety	Proximate analysis (am)[a]					Proximate analysis (db)[b]				Ultimate analysis (daf)[c]					
	VM	FC	M	A	Sum	VM	FC	A	Sum	C	O	H	N	S	Sum
2.3. Other residues (HAR)															
48. Almond hulls	69.0	18.8	6.5	5.7	100.0	73.8	20.1	6.1	100.0	50.6	41.7	6.4	1.2	0.07	99.97
49. Almond shells	69.5	20.2	7.2	3.1	100.0	74.9	21.8	3.3	100.0	50.3	42.5	6.2	1.0	0.05	100.05
50. Coconut shells	70.5	22.0	4.4	3.1	100.0	73.8	23.0	3.2	100.0	51.1	43.1	5.6	0.1	0.10	100.00
51. Coffee husks	68.2	18.5	10.8	2.5	100.0	76.5	20.7	2.8	100.0	45.4	48.3	4.9	1.1	0.35	100.05
52. Cotton husks	73.0	16.9	6.9	3.2	100.0	78.4	18.2	3.4	100.0	50.4	39.8	8.4	1.4	0.01	100.01
53. Grape marc	59.2	23.8	10.0	7.0	100.0	65.8	26.4	7.8	100.0	54.0	37.4	6.1	2.4	0.15	100.05
54. Groundnut shells	68.1	20.9	7.9	3.1	100.0	73.9	22.7	3.4	100.0	50.9	40.4	7.5	1.2	0.02	100.02
55. Hazelnut shells	71.5	19.9	7.2	1.4	100.0	77.1	21.4	1.5	100.0	51.5	41.6	5.5	1.4	0.04	100.04
56. Mustard husks	68.5	22.0	5.6	3.9	100.0	72.6	23.3	4.1	100.0	45.8	44.4	9.2	0.4	0.20	100.00
57. Olive husks	73.7	17.4	6.8	2.1	100.0	79.0	18.7	2.3	100.0	50.0	42.1	6.2	1.6	0.05	99.95
58. Olive pits	72.3	18.7	6.1	2.9	100.0	77.0	19.9	3.1	100.0	52.8	39.4	6.6	1.1	0.07	99.97
59. Olive residue	60.2	22.8	10.6	6.4	100.0	67.3	25.5	7.2	100.0	58.4	34.2	5.8	1.4	0.23	100.03
60. Palm fibres-husks	46.3	12.0	36.4	5.3	100.0	72.8	18.9	8.3	100.0	51.5	40.1	6.6	1.5	0.30	100.00
61. Palm kernels	68.8	15.6	11.0	4.6	100.0	77.3	17.5	5.2	100.0	51.0	39.5	6.5	2.7	0.27	99.97
62. Pepper plant	60.5	19.5	6.5	13.5	100.0	64.7	20.9	14.4	100.0	42.2	49.0	5.0	3.2	0.57	99.97
63. Pepper residue	58.5	24.4	9.7	7.4	100.0	64.8	27.0	8.2	100.0	45.7	47.1	3.2	3.4	0.60	100.00
64. Pistachio shells	75.5	15.7	7.5	1.3	100.0	81.6	17.0	1.4	100.0	50.9	41.8	6.4	0.7	0.22	100.02
65. Plum pits	53.7	11.8	33.6	0.9	100.0	80.8	17.8	1.4	100.0	49.9	42.4	6.7	0.9	0.08	99.98
66. Rice husks	56.1	17.2	10.6	16.1	100.0	62.8	19.2	18.0	100.0	49.3	43.7	6.1	0.8	0.08	99.98
67. Soya husks	69.6	19.0	6.3	5.1	100.0	74.3	20.3	5.4	100.0	45.4	46.9	6.7	0.9	0.10	100.00
68. Sugar cane bagasse	76.6	11.1	10.4	1.9	100.0	85.5	12.4	2.1	100.0	49.8	43.9	6.0	0.2	0.06	99.96
69. Sunflower husks	69.1	19.0	9.1	2.8	100.0	76.0	20.9	3.1	100.0	50.4	43.0	5.5	1.1	0.03	100.03
70. Walnut blows	61.8	12.9	23.5	1.8	100.0	80.7	16.9	2.4	100.0	54.9	36.9	6.7	1.4	0.11	100.01
71. Walnut hulls and blows	41.5	9.1	47.9	1.5	100.0	79.6	17.5	2.9	100.0	55.1	36.5	6.7	1.6	0.12	100.02
72. Walnut shells	55.3	35.3	6.8	2.6	100.0	59.3	37.9	2.8	100.0	49.9	42.4	6.2	1.4	0.09	99.99
Mean	64.6	18.6	12.4	4.4	100.0	74.0	21.0	5.0	100.0	50.2	41.9	6.3	1.4	0.16	99.96
Minimum	41.5	9.1	4.4	0.9		59.3	12.4	1.4		42.2	34.2	3.2	0.1	0.01	
Maximum	76.6	35.3	47.9	16.1		85.5	37.9	18.0		58.4	49.0	9.2	3.4	0.60	

[a] As measured at different basis, [b] dry basis and [c] dry, ash-free basis.

Table 2.10. Composition of some biomass samples, adapted from [137].

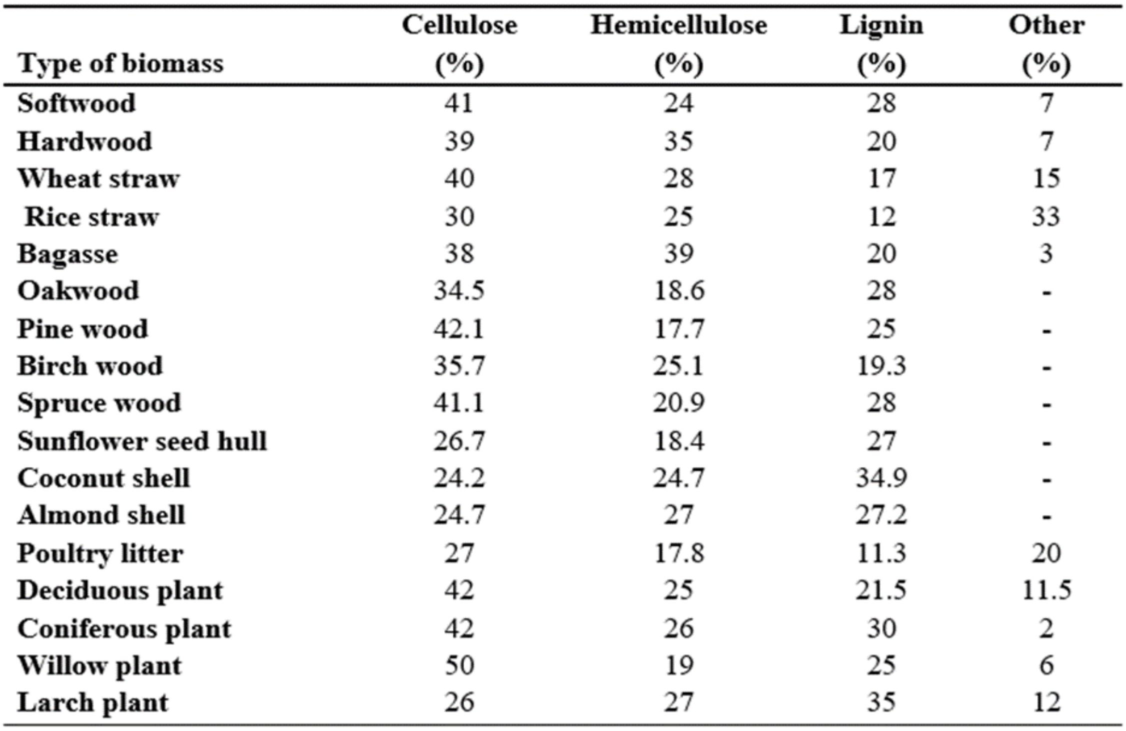

Type of biomass	Cellulose (%)	Hemicellulose (%)	Lignin (%)	Other (%)
Softwood	41	24	28	7
Hardwood	39	35	20	7
Wheat straw	40	28	17	15
Rice straw	30	25	12	33
Bagasse	38	39	20	3
Oakwood	34.5	18.6	28	-
Pine wood	42.1	17.7	25	-
Birch wood	35.7	25.1	19.3	-
Spruce wood	41.1	20.9	28	-
Sunflower seed hull	26.7	18.4	27	-
Coconut shell	24.2	24.7	34.9	-
Almond shell	24.7	27	27.2	-
Poultry litter	27	17.8	11.3	20
Deciduous plant	42	25	21.5	11.5
Coniferous plant	42	26	30	2
Willow plant	50	19	25	6
Larch plant	26	27	35	12

2.5.2.2 Influence of Temperature

Temperature is a very important factor in pyrolysis and gasification of biomass with respect to the final composition of the gases and product distribution. Many researchers have investigated the effect of temperature on product yield and distribution, reporting that hydrogen concentration, as well as total gas yield, increases with increase in gasification temperature [137, 142-146]. Likewise, the carbon conversion efficiency was enhanced with the increase in temperature. Most of the reactions shown in equations 2.2-2.12 are favoured at high temperature. It has also been reported that a high temperature was favoured in most of the reactions leading to hydrogen production [134]. The water gas shift reaction (equation 2.9) is slightly exothermic with enthalpy of -41 kJ mol^{-1} favoured by medium to high temperature (~ 600 – 800 ^{o}C), while steam methane reforming (equation 2.10) an endothermic reaction with the enthalpy + 206 kJ mol^{-1}, requires a much higher temperature (~ 700 – 1100 ^{o}C), and these are the two main reactions used in industry for the production of hydrogen. Waheed et al. [147], stated that the increase in hydrogen production with increased gasification temperature linked to the various endothermic reactions result in water gas reactions, steam methane reaction and the Boudouard reaction were favoured at high temperature. It has been suggested that a gasification temperature up to 800 ^{o}C is required in order to obtain higher production of hydrogen [134].

In the study performed by Xiao et al. [148], it was stated that reaction temperature is the most crucial for the overall biomass gasification, the influence of temperatures ranging from 540 to 639 ^oC was studied on catalytic gasification of livestock manure compost in a two-stage fluidized bed. It was reported that a higher temperature favours hydrogen production and gas yield.

Yan et al. [149], investigated the influence of temperature (600 to 850 ^oC) and steam on the production of hydrogen yield and syngas gas from biomass in a fixed-bed reactor. The results showed that the high gasification temperature led to higher gas yield and carbon conversion efficiency. The various reactions involved in the process include pyrolysis, tar reforming and water gas shift reactions, Boudouard reaction, methanation and steam methane reforming reactions. This trend was explained such that higher temperature favours the release of more unconverted volatiles and benefits all the endothermic reactions as well as favouring cracking and reforming of tar. At a temperature range of 600 to 700 ^oC, H_2 and CO concentration compared to higher temperatures, due to water gas shift reaction, was suggested to be the dominant reaction. An increase in the temperature resulted in a decrease in heating value of the product gas due to higher concentrations of CO and H_2 with a corresponding decrease in the CH_4 in the product gas. In the temperature range of 800 to 850 ^oC, there was a greater increase in H_2 and CO concentration alongside the decrease in CO_2 and CH_4 which was due to the water gas reaction, Boudouard reaction and steam methane reforming reactions [149]. Likewise, Luo et al.[150], equally investigated hydrogen yield and syngas on the catalytic steam gasification effect of temperature from 600 to 900 ^oC from biomass sample in a fixed bed reactor. The results showed that the higher gasification temperature improved carbon conversion efficiency and more so, for hydrogen production as the H_2 content increases from 25.2 % to 51.5 %, with CO_2 increasing while CO decreased due to water-gas shift reactions. CH_4 and C_{2+} gases decreased as the temperature increased respectively.

Similarly, Franco et al. [151], studied the effect of steam gasification temperature from 700 – 900 ^oC on three forestry biomass samples (softwood - pine, Eucalyptus globulus and hardwood - holm-oak) in a fluidised bed reactor. The results showed that gas yield and hydrogen yield increased, and there was higher energy and carbon conversion efficiency at an optimum temperature of 830 ^oC. The higher gas yield, hydrogen yield and corresponding decrease in liquid and char yield with respect to increase in temperature suggest that the initial pyrolysis step, endothermic char gasification reaction, steam methane reforming, the cracking of heavier hydrocarbon and tar reactions were implicated in producing more gases. At the temperatures between 750 and 850 ^{o}C, variation in gas yield existed for the three biomass samples but at 900 ^{o}C there was no significant variation of gas yield for all the biomass samples investigated. This difference relates to char reactivity of the different content of cellulose and lignin in the various biomass samples, favoured by higher temperatures due to char gasification as it is an endothermic reaction. As the temperature increased from 800 to 900 ^{o}C, there was an increase in hydrogen concentration with a consequent decrease in hydrocarbon gases (CnHm), and CO, due to water gas, Boudouard reaction and water-gas shift reactions as well as a slight decrease in CH_4 and CO_2 which was associated with steam methane reforming and Boudouard reactions favoured at higher temperatures respectively. Other workers equally investigated the influence of temperature from 800 to 950 ^{o}C on pine sawdust in a continuous feeding fixed-bed reactor, it was observed that hydrogen yield increased from 49.97 to 79.91 g H_2/kg biomass, as the reactions of H_2 production are an endothermic process, hence reaction temperatures greatly influence the yield of H_2 produced [152].

2.5.2.3 Gasifying agent

Gasifying agent is an important factor in gasification processes as the composition of product yield and the quantity produced is influenced by the type of gasifying agent. The composition of individual gases and the total gas yield are dependent on the gasifying agent employed. The most common gasifying agents include: steam, air, nitrogen and oxygen as used in the gasification procedures. The influence of air as a gasifying agent for biomass sample had been reported because of the cost effectiveness for large scale industrial processes, but the low production of hydrogen yield makes it less attractive. Likewise, the combination of steam and oxygen in gasification have proved to enhance more hydrogen production in terms of the amount produced but the high cost of pure oxygen makes it less economically feasible. However, the use of steam in the gasification processes has resulted in greater hydrogen production in the product yield. For example, the effect of different types of gasifying agents such as air, pure steam and a mixture of steam-oxygen in biomass gasification on product distribution have been conducted in a fluidized bed reactor, the result showed that the steam gasifying agent favours hydrogen production more as compared to air and steam-oxygen [153]. Likewise, the use of steam and dry (CO_2) gasification of biomass processing with pyrolysis-catalysis into fuel and useful chemicals has been suggested to be effective [154-157]. According to Lv et al.[158], who investigated the influence of air and oxygen/steam as gasifying agents in a downdraft gasifier, for the oxygen/steam gasification; the concentration of H_2 and CO ranges from 63.27-72.56% while the use of pure air produces an H_2 and CO yield of 52.19-63.13% for the biomass gasification respectively. The ratio of H_2/CO for oxygen/steam biomass gasification observed to be 0.70-0.90, which is lower than that of biomass air gasification with 1.06-1.27, confirmed that the oxygen/steam gasification in a downdraft gasifier is an effective process due to the low energy consumption for hydrogen production.

Similarly, Lucas et al.[145], equally studied the influence of air and steam gasification of densified biofuel using high temperature in a fixed bed up-draft gasifier. The use of steam as a gasifying agent was observed to enhance hydrogen production more than air gasification. The effect of the feed gas (air or mixture of air/steam) showed that an increase in the lower heating value was due to an increase in the molar fraction of the combustible gases (H_2, CO CH_4, and CxHy), caused by the pyrolysis process and cracking of hydrocarbons due to the application of high temperature. The results equally showed that the use of steam in the feed gas decreased the process temperature sharply as the gasification temperature does not respond to the feed gas composition.

Kalinci et al. [143], also explained that biomass can be gasified using different gasifying agents depending on the desired product gas composition and energy considerations. The use of air as gasifying agent is an exothermic process that produced low heating value gas (LHV 5-6 MJ/Nm^3) rich in CO with a corresponding relatively small amount of H_2 yield and higher production of hydrocarbon gases. In the case of steam gasification, the gas produced was rich in H_2 and CO with a medium heating value (LHV 12-13 MJ/Nm^3) due to endothermic reaction being favoured at high temperatures.

The same tendency was observed by Gonzalez et al. [144], who investigated the influence of different gasifying agents such as air and air/steam for hydrogen production from gasification of biomass (olive waste) over $ZnCl_2$ and dolomite catalysts in a laboratory reactor at atmospheric pressure over a temperature range of 700-900 ^oC using a steam/biomass ratio of 1.2 w/w. It was reported that the use of air as gasifying agent at an optimum condition of 900 ^oC temperature showed an H_2, CO concentration of 4.73, 6.95 moles/kg of biomass (olive oil waste) while steam/air gasification produced an H_2, CO yield of 32.59, 10.4 moles/kg of biomass (olive oil waste). This clearly confirmed that steam as a gasfying agent showed better improvement on the yield of H_2. Other authors have also highlighted the effect of gasifying agents [137, 159].

2.5.2.4 Steam to biomass ratio

Steam to biomass ratio (SBR) has been referred to as the number of moles steam fed per mole of biomass which has as strong an effect as temperature on product gas and energy input. Low values of SBR leads to production of solid carbon and methane formation. As more steam is introduced, reforming of CO and H_2 species occurred. For SBR greater than 1 (> 1), lead to carbons and CH_4 moles reduction to very small values while H_2 and CO_2 increase [143]. An optimum value of steam to biomass ratio is recommended for enhanced hydrogen production, as excess steam in the gasification process reduces temperature and favours tar production. Several researchers have reported studies on steam to biomass ratio [137, 146]. Inayat et al. [142], conducted biomass gasification kinetic modelling studies on the effect of parameters such as steam/biomass ratio on hydrogen production, the results showed that the yield of H_2 increased as the steam/biomass ratio increased but CO and CH_4 decreased in the product gas due to methane reforming and water gas shift reactions being highly dependent on the steam feed. The maximum hydrogen efficiency occurred at the steam/biomass ratio of 2.0 due to the minimum consumption of energy at a temperature of 800 K.

Luo et al. [150], investigated the effect of steam from 0 to 2.8 on the catalytic steam gasification of biomass in a fixed bed reactor on hydrogen yield. The results indicate that introduction of steam contributes to hydrogen yield, gas yield, carbon conversion efficiency but excessive steam input degrades fuel gas quality and decreases hydrogen content as maximum production of 52.7 % was obtained at a steam rate of 2.10. It was reported that the steam atmosphere and the use of a catalyst enhances the char gasification and the reforming reactions leading to production of lighter gases such as H_2, CO and CO_2. Likewise, the influence of steam was reported as an adequate amount of steam was introduced into the pyrolysis process which greatly improved hydrogen yield as well as the carbon conversion efficiency, but excessive increase in steam led to a decrease in hydrogen yield and the carbon conversion efficiency [149].

Franco et al. [151], conducted studies on steam to biomass ratio from 0.4 to 0.85 w/w varied by changing the biomass feed rate while the steam flow rate kept constant and vice versa on three different forestry biomass samples. It was reported that an optimum steam/biomass ratio of 0.6-0.7 w/w was observed to produce higher energy and carbon conversion, greater gas yield as well as improvement in H_2 yield. The water-gas shift reaction was dominant at temperatures up to 830 ^{o}C while in the range 830 - 900 ^{o}C water gas and Boudouard reactions were the dominant reactions.

In another study by Xiao et al. [148], they analysed, in a two-stage fluidised bed, the gasification of characteristics of livestock manure, introduction of steam into the process led to improvement in gas quality and hydrogen yield as steam reforming and water-gas shift reactions were favoured.

Additionally, Gao et al. [152], performed biomass steam gasification in an up-draft gasifier with steam biomass ratio ranging from 1.05 to 2.53 at a temperature of 850 ^{o}C. An optimum steam to biomass ratio of (2.05) gave high hydrogen production while higher steam/biomass ratio did not favour hydrogen yield, because excess steam consumes more heat in the process of the reaction leading to product gas separation from steam condensation and dryness.

2.5.2.5 Effect of pressure

Pressure is a temperature dependant factor in a closed-system, pyrolysis and gasification process, which has an influence on product yields and distribution. Therefore, the effect of temperature has been the focus, and then keeping the reactor pressure at atmospheric pressure as investigated by many researchers. For example, Hanoka et al. [160], investigated the effect of reaction parameters such as reaction pressure, reaction temperature and molar ratio of CaO to carbon in woody biomass steam gasification on hydrogen production. Gas conversion and H_2 yield were observed to depend majorly on the reaction pressure and exhibited maximum value at 0.6 MPa, therefore as reaction temperature increases, H_2 yield increased.

Basile et al. [161], investigated the influence of pressure (from 0.1 to 4 MPa) on the heat of biomass pyrolysis for four different energy crops (corn stalks, poplar, switchgrass Alam and switchgrass Trailblazer). The result showed that an increase in the operating pressure shows lower heat demand and the final char yield increases. It was suggested that an endothermic reaction of the decomposition process occurred for volatile formation and exothermic vapour-solid interactions that resulted in secondary formation of char.

Gamero et al. [162], studied the cellulose pyrolysis process using a bench scale high pressure thermobalance for evaluating the influence of pressure, particle size, sweep gas flow and initial weight of sample. It was observed that an increase of pressure led to a decrease in temperature at which pyrolysis took place and an increase in char as well as promotion of CH_4 and CO_2 formation while H_2 yield was negligible at high pressure respectively. It was also shown that the higher the pressure, the higher the porosity, the lower the pore size, the higher the occurrence of alkanes and carbonyl components in the char produced.

Wang and Kinoshia [163], highlighted both the advantages and disadvantages on the effect of pressure as examined in a kinetic model for biomass gasification. It was reported that the advantage of increased pressure is the higher reaction rate due to increased partial pressure of each species, and longer residence time due to reduced volumetric flow. Likewise, the disadvantages of increased pressure are higher production of carbon and methane with lower yields of H_2 and CO, due to a shift in equilibrium.

Other researchers have investigated the influence of pressure on biomass gasification [137, 143, 164] and suggested atmospheric pressure is preferable [165].

2.5.2.6 Residence Time

Residence time is influenced by temperature. Wang and Kinoshia [163], reported that residence time is a function of the height of the gasifier, equivalence ratio and moisture in the reactants, hence as temperature increases, residence time decreases slightly, CO and H_2 increases while CH_4 and CO_2 decreases as temperature increases. Therefore, the residence time required to achieve about 90% carbon conversion efficiency decreases drastically as temperature increases. Likewise, De Lasa et al. [166], stated that the influence of residence time is significant to the amount and composition of the produced tars, as the fraction of oxygen-containing compounds tends to decrease by increasing residence time. In the study performed by Yang et al. [167], pyrolysis of palm oil shell wastes in a fixed-bed reactor to study the effect of residence time varied from 7.5 to 26 seconds, showed significant influence on enhancement of H_2 and CO_2 yields. Total gas yield increased first to a maximum of 0.42 m^3/kg at 14 s and decreased slightly with increase in residence time. The composition of the gases such as H_2 and CO increased to a maximum of 117.22 ml/g at 9 s and then decreased, CO_2 increased, CH_4 and C_2H_4 decreased with increase in residence time. The results obtained were reported to vary differently from other authors suggesting that the differences might be due to operating conditions and the physical-chemical characterisations of the sample.

In the work by Xianwen et al. [168], who investigated the effect of pyrolysis parameters such as temperature and particle size on fast pyrolysis of biomass in a circulating fluidized bed (CFB) reactor, it was observed that at longer residence time and higher temperature contributes to secondary reactions which decreases the liquid yield as well as having an important effect on the enhancement of pyrolysis gas composition and the bio-oil yield.

Font et al. [169], conducted an investigation into a sand fluidized bed reactor and pyroprobe 100 pyrolyser on fast pyrolysis of almond shells for gaseous hydrocarbon production. The effect of residence time varied from 1 to 3 s alongside a temperature range from 745 to 950 ^{o}C. The investigation showed that the highest gas yield of about 85-90% was obtained at a maximum temperature of 890 ^{o}C and residence time of 2.3 s with an increase up to 1.5% H_2 yield. In the total gas yield, gas composition of H_2, CO, CO_2, CH_4 and C_2H_4 were reported to increase but decreases in C_2H_2, C_3H_6 and C_4 fractions as residence time increased.

Scott et al. [170], investigated fast pyrolysis of cellulose and wood in two reactors; a fluid bed and a transport reactor with a temperature range from 450-900 ^{o}C and residence time varied from 50-900 ms and 300-1500 ms. The results showed that the product range was 95-100% of the feeds, such that the gas yield increases with a corresponding liquid and char reduction as the results were compared at a constant vapour residence of 500 ms (0.5 s). Other authors have studied the effect of residence time as an important factor on product yields and distribution [171].

2.5.2.7 Influence of heating rate

Heating rate is considered a function of temperature and residence time [129]. Many researchers have investigated the influence of heating rate [168, 171-173]. Sikarwar et al.[137], highlighted the influence of heating rate such that a faster heating rate results in greater production of gas and a decrease in tar production while a slower heating rate showed reduction in gas yield and an increase in tar production. This influence of slower heating rate linked to higher production of char is due to recombination of the lower-volatility hydrocarbons on the surface of the char particles. In another study by Gonzalez et al. [174], they conducted pyrolysis of cherry stones under temperatures between 300-800 ^{o}C and heating rates from 5-20 K min^{-1}. It was reported that as the heating rate increased, an increase in gas yield with a decrease of the char and oil yields had been observed. Similarly, Uddin et al. [129], conducted reviews on the effects of pyrolysis parameters on hydrogen production from biomass. Slow heating rates were reported to produce more char, lower production of total gas from biomass decomposition and a lesser amount of liquids at 450-550 ^{o}C compared with fast heating rates due to secondary reactions of volatiles being active at lower temperatures.

Efika et al. [175], also investigated the influence of heating rates from 5 to 350 ^{o}C min^{-1} on product yields in the pyrolysis of wood and biomass components (cellulose, hemicellulose and lignin) at a temperature of 800 ^oC. The result showed that the gas yield increased as the heating rate increased alongside an increase in aromatics due to rapid devolatilization degradation and cracking of primary pyrolysis vapours. Secondary cracking of volatiles, linked to an increase in gas yield with high caloric values, was observed from the samples.

Likewise, Zuo et al. [176], studied slow pyrolysis of wood in a vertical tubular furnace at various heating rates for the evolution of gaseous products from biomass pyrolysis of Fir wood impregnated with phosphoric acid. The effect of the heating rate on the evolved gases (H_2, CO, CO_2 and CH_4) showed that increasing the heating rate from 1 to 6 ^oC min^{-1} enhanced the production of gaseous products H_2 and CH_4 as a result of secondary reactions.

In addition, Sensoz and Can [177], investigated the influence of temperature and heating rate on the product yields from pyrolysis of Pine, the yield of volatiles increased with heating rate as the higher heating rate investigated results in maximum oil yield due to the decrease in the mass transfer limitations. Furthermore, a fast heating rate promoted the heat transfer between the hot walls of the reactor and the particles as it prevents secondary degradation reaction of organic compounds due to primary vapour rapid removal from the reactor. It was also added that either low heating rates combined with large amounts of the sample or with significant limitations to the volatiles escape, leading to relatively higher production of char due to active mass loss.

2.5.2.8 Influence of catalyst for pyrolysis-gasification of biomass

Catalyst is a very important pyrolysis parameter that provides an alternative reaction pathway with a lower activation energy than the non-catalysed mechanism. It reduces the thermal heat and mass transfer resistance providing an alternative lower-energy pathway for the reaction to progress [137]. According to Xiao et al. [148], the presence of catalyst in the steam gasification process significantly increases total gas yield, improves gas quality and eliminates tar content; as the two-stage fluidized bed gasification was observed to have better catalytic utilisation which enhances steam reforming and water-gas shift reaction. In another study, the effect of catalyst on cotton stalk pyrolysis gasification was investigated and the result showed a higher hydrogen composition of 39.4 vol.% as compared with the absence of catalyst with a yield of 22.4 vol.%, as well as reduction in CO and CH_4 [178].

Biomass pyrolysis-gasification catalysts can be classified into primary and secondary (guard bed) catalysts. The primary catalysts are mixed directly with the biomass either by physical addition, dry, or by wet impregnation unto the biomass [179]. These types of catalysts cannot be recovered and reused due to the nature of homogenous mix with the biomass. The secondary catalysts are put in a different segment of the reactor downstream, the pyrolytic biomass volatiles from the top section of the reactor passes over the catalyst for reforming [179]. These types of catalysts are recovered and reused; hence, parameters such as temperature and heating rate are varied independent of the main section of the feedstock as well as steam injection for improvement of H_2 production and tar reduction.

The criteria for selection of catalysts for appropriate performance and appropriate products selection are outlined such that the catalysts must be effective in tar removal, capable of methane reforming for hydrogen-syngas production, resistant to coke deposition and deactivation as a result of sintering and carbon fouling, able to regenerate, strong and inexpensive catalysts [180]. Likewise, the catalyst composition is divided into three primary components: (1) the active catalytic phase or the metal site; (2) promoter that increases activity and stability; and (3) the support with high surface area that promotes dispersion of the active phase [180]. Anis and Zainal [181], reviewed studies on the different types of tar cracking catalysts which are divided into four: 1. Ni-based catalysts, 2. Alkali metal catalysts, 3. Dolomite catalysts, and 4. Novel metal catalysts. The catalysts are further classified into six groups such as nickel-based catalysts, non-nickel metal catalysts, alkali metal catalysts, basic catalysts, acid catalysts and activated carbon catalysts.

2.5.2.8.1 Nickel-based catalysts

Nickel-based catalysts are among the most common catalysts for hydrogen/syngas production and tar reduction, which are cost effective compared to other metal-based catalysts. Nickel based catalysts have been extensively used in the petrochemical industry and for tar reforming in biomass. Uddin et al. [129], reviewed studies on Ni-based catalysts as having a strong catalytic effect that improves total gas content as well as enhancement of hydrogen production of up to 90%, also confirmed hydrogen production has been improved by increasing temperature due to tar reduction up to more than 99% due to nickel-based catalysts. From their studies they pointed out that, the effect of Ni-based catalysts on gas composition and tar reduction using a catalytic bed reactor resulted in more than 99% efficiency of tar elimination by Ni-based catalysts. The results also showed that as temperature increases, hydrogen formation increases with a corresponding decrease in CH_4 and C_2H_4 components, suggesting that the tar reduction in the presence of Ni-based catalysts was prevalent in chemical kinetics. In the study by another author who investigated three different catalysts; alkaline metal oxides, dolomite and Ni-based catalysts for the ability to promote gasification reformation reactions, Ni-based catalysts were observed to be effective for conversion of lighter hydrocarbon [137].

Yang and Chen [179], highlighted the influence of nickel-based catalysts employed for steam reforming of hydrocarbon and methane with the use of temperatures above > 740 ^oC, observed increase in hydrogen and carbon monoxide as well as elimination of tar hydrocarbon and methane content. Nickel-based catalysts were reported to nearly decompose all the tar completely alongside ammonia decomposition as secondary catalysts [182].

Additionally, the use of a support for the catalysts performed an important role in tar conversion and hydrogen production from biomass gasification. Alumina (Al_2O_3) is the most regularly used support for Ni-based catalysts. Anis and Zainal [181], highlighted parameters such as acidity, surface area, electronic and pore structure of the support does affect the activity of the catalyst. For example, Ni/Al_2O_3 at high temperatures ~ 900 ^oC resulted in about 100% tar elimination, as Ni is the active site of the catalyst while the support gives durability, high surface area and coking resistance. The $Ni\text{-}Al_2O_3$ catalyst was suggested to promote steam reforming and tar cracking concurrently.

Similarly, Sutton et al. [183], conducted an investigation on nickel supported catalysts for gasification of brown peat in a test rig gasifier under pyrolysis, a temperature range of 25-550 ^oC at 5 $^oC/min^{-1}$ and a secondary catalytic reforming reactor temperature at 800 ^oC. The alumina-supported nickel catalysts investigated gave the highest activities as the conversion of hydrocarbon increased to (90.3-92.2%), the syngas ratio was 1.81:1, an increased HHV by a factor of 5.3 and a complete elimination of methane from the gas stream as compared with other supported nickel catalysts Ni/MOR1, Ni/SiO_2, Ni/TiO_2 and Ni/ZrO_2.

In another observation by Simell and Bredenberg [184], catalytic purification of tarry fuel gas in an industrial-scale peat-fired up-draft gasification at temperature 900 ^oC was conducted. The result shows that the nickel catalyst (Ni on Al_2O_3) completely degraded tar and light hydrocarbons into H_2 and CO. The order of the catalysts tested on tar reduction includes, nickel catalyst (Ni on Al_2O_3) > dolomite> activated alumina catalyst > silica-alumina catalyst > silicon carbide (inert).

Likewise, Yang et al. [167], conducted studies in a fixed bed reactor in the presence of Ni-based and (γ-Al_2O_3, Fe_2O_3 and La/Al_2O_3) catalysts on pyrolysis of palm oil wastes in the temperature range of 500 °C to 900 °C for enhanced hydrogen rich gas production. The results showed that the Ni-based catalyst had the strongest effect on H_2 production with the maximum H_2 yield of 29.78 g/kg. An addition of 5 wt.% nickel led to improvement of total gas yield as well as gas quality enhancement even at a lower temperature (600 – 700 °C).

Promoters in a catalyst increase activity and/or stability of that catalyst. Nickel catalysts through the addition of promoters have been studied [182]. According to Yang and Cheng [179], the effect of the addition of promoters to nickel alumina catalyst as magnesium was added to the Ni/Al_2O_3 catalyst, increased the physical strength of the catalyst and resistance to attrition. However, the gas yield was lower by 14% and an increase in char yield was observed as well as a corresponding decrease in H_2 and CO yield respectively. In the study conducted by Dou et al. [185], they equally investigated five different catalysts (CaO, SiO_2, Al_2O_3, CuMn and NiMo) and the effect of promoter metals as well as the highest surface area in the NiMo catalyst exhibited the greatest activity on tar removal as compared with other catalysts. Several Ni-based catalysts have been investigated as well as the influence of promoters. For example, Ni in Cu/Ni/γ-Al_2O_3 catalysts was reported to enhance gaseous product yield as well as acetic acid reduction during ethanol gasification [129].

2.5.2.8.2 Mineral based catalysts and other catalysts

Dolomite has been used as catalyst in biomass gasification, which can increase hydrogen and CO yield as well as tar reduction due to water-gas shift reaction and tar conversion reactions. According to Yang and Chen [179], dolomite has the general formula $MgCO_3.CaCO_3$ as magnesium ore-mineral with a general chemical composition containing 30 wt.% CaO, 21 wt.% MgO and 45 wt.% CO_2. It is a cheap, disposable catalyst, which can be used as primary catalyst or as a secondary catalyst for reforming. It can also be used as support for Ni-based catalysts. Xu et al. [182], conducted review studies on calcine dolomite catalyst (MgO-CaO) obtained by the decomposition of dolomite at high temperatures from 800 to 900 °C as secondary catalysts for tar reduction in the product gas. This was due to an increase in surface area and oxide contents on the surface of the calcined dolomite that made it more active than the un-calcined dolomite for tar decomposition. Using calcined dolomites as secondary catalysts was suggested to increase the H_2 content and H_2/CO ratio in the product gas due to cracking and reforming of the tars. In addition, Corella et al. [159], experimentally studied calcined dolomite (CaO.MgO) in a fluidised bed reactor for biomass gasification both as primary catalysts (mixed with feedstock; in-bed) and secondary catalysts (downstream in gasifier). The result showed that downstream-dolomite catalyst had slightly higher chemical effectiveness for tar removal and H_2, CO_2 yield than in-bed-dolomite catalysts. The down side of dolomite catalyst is that they are not stable and release CO_2 when decomposed at high temperature. The calcined dolomite is suggested to be a soft and fragile material as it can easily be eroded, limiting its use [182].

Another mineral catalyst is olivine, which has also been investigated by many researchers. For example, Hu et al. [165], conducted steam gasification of apricot stones in a fixed bed reactor using olivine and dolomites as downstream catalysts. The calcination of the catalysts causes elimination of (Mg, Fe) SiO_3 phase and the formation of Fe_2O_3 for olivine as well as the removal of CO_2 and formation of CaO-MgO for dolomite. The results showed that calcined dolomite produced a higher H_2 yield of 130.9 g H_2/kg compared to calcined olivine with 67.7 g H_2/kg biomass. The calcined dolomite is reported to be brittle as compared with the calcined olivine, which kept its mechanical strength after calcination and reaction. A similar trend was observed by Rapagna et al. [186], who studied steam gasification of biomass in a fluidised bed reactor using calcined dolomite and calcined olivine. The results showed that the olivine activity is comparable to calcined dolomite. Another author pointed out that olivine as catalyst in a fluidized-bed presented an optimum gasification temperature slightly above 800 ^{o}C. Likewise, olivine can equally be used as support for Ni-based catalysts, as investigated by different authors [182, 187].

With the same tendency, alkali metal and alkaline-earth metal catalysts have been investigated for biomass pyrolysis-gasification. The metals such as potassium (K) are often added directly to the biomass and cannot be recovered but increase the ash content of the biomass char. For example, Sueyasu et al. [188], conducted a study on potassium (K) loaded cedar wood biomass in a two-stage reactor for pyrolysis at temperatures of 500-600 ^{o}C and steam reforming at 600-700 ^{o}C. The potassium (K) catalyst resulted in increased concentration of H_2 yield and reduction of heavy tar to about 20 m/m^3.

Zeolite catalysts are crystalline aluminosilicates with microporous structure having a large surface area, pore size and surface acidity. They are known to be effective for pyrolysis-gasification of biomass materials and likewise used as support for Ni-based catalysts. Buchireddy et al. [189], investigated catalytic removal of tar over zeolites (Zeolite Y-ZY, ZY-5.2, ZY-30 and ZY-80) and nickel supported zeolite catalysts (Ni/ZY-

5.2, Ni/ZY-30, Ni/ZY-80, Ni/Si-Al and Ni/chabazite), and emphasised Y-zeolite (ZY) had better catalytic activity due to its larger pore size compared to ZSM-5. The ZY-5.2 with more acidity had greater conversion compared with ZY-80, as increase in acidity increases the catalytic activity of the zeolite catalysts. Additionally, nickel impregnation on the zeolite catalysts (nickel supported Y-zeolite) significantly enhanced the activity with naphthalene removal > 99 % due to the steam reforming ability of the nickel metal.

Another important catalyst researched for hydrogen and syngas production from pyrolysis-gasification of biomass is MCM-41 catalyst. Wu et al. [190], investigated nickel/MCM-41 using a fixed bed two stage reactor for the pyrolysis-gasification of wood sawdust at 550 ^{o}C pyrolysis temperature and at 800 ^{o}C catalytic bed temperature. It was reported that the gas yield increased from 38.9 to 62.8 wt.% and an increase from 5.7 to 18.0 mmol/g of hydrogen yield was observed. In another study, an increase in hydrogen and CO production was reported with increasing temperatures from 400 to 600 ^{o}C in a study conducted with lignocellulosic biomass from beech wood in a two stage fixed bed reactor using mesoporous Al-MCM-41 over microporous zeolite HZSM-5 in a staged catalyst system [80].

2.5.3 Summary

It has been shown from the different literature reviewed, that thermochemical conversion of biomass seems to be an attractive option. The production of hydrogen and syngas from biomass equally depends on various process conditions and factors.

There are significant differences in biomass feedstock materials due to the origin and environmental conditions such as the weather and soil type. Biomass samples differ in chemical characteristics, physical properties as well as the heating values. The knowledge of the influence of lignin content in the mixtures of the biomass components on hydrogen and syngas production as a main controlling factor is key. Therefore, an understanding of the production of hydrogen and syngas from different agricultural biomass samples and the main components through pyrolysis-catalytic steam reforming will aid the optimisation of industrial scale-up processes as an alternative non-fossil fuel source and to ensure availability of feedstock material at all times.

Temperature is the most significant parameter in the pyrolysis-gasification due to other parameters such as residence time and heating rate are dependent on temperature. An increase in temperature results in an increase in overall gas yield and hence, increase in hydrogen/syngas yield. The influence of gasifying agent and steam ratio has key impact on product yield and composition, as an increase in hydrogen production was reported when steam was introduced into the process but excess steam had no effect.

Similarly, the use of catalyst plays the most prominent role in the pyrolysis-gasification of biomass as it reduces temperature requirement, appropriate product selection and optimisation. Hydrogen production using nickel-based catalysts for catalytic steam reforming at high temperature has been explored. Likewise, there is need for further evaluation of other metals such as cobalt, molybdenum, cerium, etc., for high catalytic activity in the process.

2.5.4 Hydrogen and syngas production from pyrolysis-catalytic gasification of biomass in a two-stage fixed bed reactor

Hydrogen is an energy carrier which is predicted to be in high demand in the future since it possesses high energy density (122 kJ kg^{-1}), this is approximately 2.75 times more than hydrocarbon fuels. Also, the combustion of hydrogen does not generate any harmful emission as only water is produced [191, 192]. Hydrogen is mainly (~95%) produced from fossil fuel coal, natural gas, and crude oil [191]. Therefore, there has been increasing interest in producing hydrogen from alternative, sustainable sources such as biomass.

One such route for hydrogen production from biomass is the two-stage pyrolysis-catalytic steam reforming process. The process mimics the natural gas catalytic steam reforming process, but the first stage pyrolysis produces a suite of hydrocarbon gases for subsequent reforming, rather than the hydrocarbons found in natural gas (mostly methane) [134, 150, 193]. Equations (2.5-2.12) show the main reactions taking place during pyrolysis and the catalytic steam reforming/gasification process [155, 194]. Pyrolysis thermally degrades the biomass to produce a range of hydrocarbons and carbonaceous species (Equation 2.5). Catalytic steam reforming of the hydrocarbons, oxygenated hydrocarbons and tar produced from pyrolysis is the main process for hydrogen enriched syngas (H_2 and CO) production (Equations 2.6 and 2.7). However, many other reactions will occur in the catalytic steam reforming reactor, including, catalytic cracking of tar, dry (CO_2) reforming of hydrocarbons and oxygenated hydrocarbons, water gas shift reaction, char gasification, etc. (Equations 2.6-2.12). The two-stage pyrolysis-catalytic steam reforming reactor system has been used to effectively produce high yield hydrogen syngas. The two-stage reaction system, as described earlier, has advantages over a single stage reactor where the biomass and catalyst are mixed together, in that there is more effective separate control of the process conditions of the pyrolysis and catalyst stages, e.g. temperature, steam input etc. [190].

$$Biomass \rightarrow gases\ (H_2 + CO + CO_2 + CH_4 + H_20) + tar\ + char \qquad (2.5)$$

Tar cracking and reforming: $tar + H_2O \rightarrow CO + CO_2 + H_2 + CH_4 + C_{2+}$ (2.6)

Tar steam reforming: $C_nH_m + nH_2O \leftrightarrow 2nH_2 + nCO$ (2.7)

Hydrocarbon dry (CO_2) reforming: $C_nH_m + CO_2 \leftrightarrow H_2 + CO$ (2.8)

Water-gas shift reaction: $H_2O + CO \leftrightarrow H_2 + CO_2$ (2.9)

Methane steam reforming: $CH_4 + H_2O \leftrightarrow CO + 3H_2$ (2.10)

Boudouard reaction: $C + CO_2 \leftrightarrow 2CO$ (2.11)

Char steam gasification: $C + H_2O \leftrightarrow CO + H_2$ (2.12)

Several different catalysts and catalyst support materials have been investigated in the production of hydrogen-rich syngas from the catalytic steam reforming of biomass. Platinum, palladium and rhodium metal-based catalysts have been shown to be effective for enhancing the production of hydrogen from the catalytic steam reforming/gasification of biomass [195-197]. However, such noble metal catalysts tend to be expensive. Lower cost transition metals such as nickel have been used as the preferred nickel-based catalysts used in the commercial natural gas catalytic steam reforming process for industrial scale hydrogen production. Therefore, nickel-based catalysts have also been investigated for the pyrolysis-catalytic steam reforming of biomass for hydrogen production and have been shown to be effective [190, 198]. Different support materials for the nickel metal have also been investigated to maximise the production of hydrogen, for example, Al_2O_3, SiO_2, dolomite, zeolites and MCM-41 [190, 199-202]. Alumina (Al_2O_3) is a common support material used for hydrogen production via catalytic steam reforming due to its chemical and physical stability, high mechanical resistance and high nickel particle dispersion throughout the Al_2O_3 material [203]. High volumetric concentrations of hydrogen can be achieved through the pyrolysis-catalytic steam reforming of biomass at more than 50 vol.% [190].

The two-stage pyrolysis-catalytic steam reforming process for biomass involves the evolution of hydrocarbons from the biomass during the pyrolysis process, which then become subsequently reformed in the catalytic steam reactor. Biomass is composed of mainly cellulose, hemicellulose and lignin, and it has been suggested that pyrolysis of biomass can be considered as the superposition of these three main components [119].

Each of the components thermally decompose to produce different inorganic and hydrocarbon gases and higher molecular weight chemical vapours that enter the catalytic steam reforming process. The volatile thermal degradation products from the pyrolysis of cellulose include: CO, CO_2, H_2, levoglucosan, aldehydes, ketones, organic acids etc. [119, 204]. Specific compounds produced from the pyrolysis of cellulose have been identified by Quan et al. [205] and include, light oxygenated species, such as, 6-acetyl-β-D-mannose, 1, 4:3, 6-dianhydro-a-D-glucopyranose, 3-methyl-1, 2-cyclopentanedione and 5-methyl-furfural. Hemicellulose pyrolysis produces CO, CO_2, H_2, C_1- C_2 hydrocarbons, organic acids and aldehydes, specific compounds include mainly, 2-methyliminoperhydro-1,3-oxazine, tetrahydropyridazine-3,6-dione, furfural and levoglucosenone [205]. Lignin pyrolysis produces mainly, CO, C_1 – C_2 hydrocarbons, phenols, organic acids, alcohols and ketones [119, 204], with specific compounds identified as methylphenol, creosol, 2-methoxy-4-vinylphenol and phenanthrene [205].

2.6 Co-pyrolysis of biomass and plastic wastes for hydrogen/syngas production

Due to the low yield of hydrogen, syngas and biofuel from biomass gasification, it is suggested to incorporate high hydrogen-rich feedstock such as plastics in the catalytic pyrolysis, thus modifying the reaction by substituting decarboxylation and decarbonylation with dehydration [113]. In addition, the high demand and production of plastics for different uses such as household utensils, packaging, building and construction, etc., had led to generation of plastic wastes in abundance and increased quantity. It has been reported by the World Bank that, the global plastics waste found in municipal solid waste (MSW) produced in different countries is estimated to be about 8-12% and may increase to 9-13% by 2025 [206]. Therefore, co-pyrolysis of these plastic wastes with biomass components produce a higher yield of hydrogen and syngas as well as bio-oil, than biomass solely [113]. The use of these plastic wastes in co-pyrolysis with biomass provide an alternative avenue for waste disposal management rather than by landfill. In co-pyrolysis of biomass and plastic wastes, a higher quantity of wastes are used up as feedstock leading to significant reduction of these wastes in the environment, therefore preserving land use, cost reduction of waste treatment as well as remediation of environmental problems. Furthermore, co-pyrolysis of biomass and plastic wastes proffer several advantages over biomass solely such as reduced cost compared to independently running both biomass and plastics waste systems. If pyrolysis of biomass and plastic (or waste tire) occurs independently or separately, more energy is usually required and the cost for gas or oil production will significantly increase. Co-pyrolysis produces more homogeneous gas or oil compared to blending of the two separate products together. Aside from the addition of plastics to lignocellulosic biomass, other advantages includes increase in the heating value of the fuel produced since plastics have a high heating value up to 40 MJ/kg [2]. A schematic diagram of the lignocellulosic biomass with plastics waste (or waste tires) in the co-pyrolysis system showing the feedstock as well as sample preparation unit, the co-pyrolysis unit and the condensation unit are illustrated in Figure 2.12.

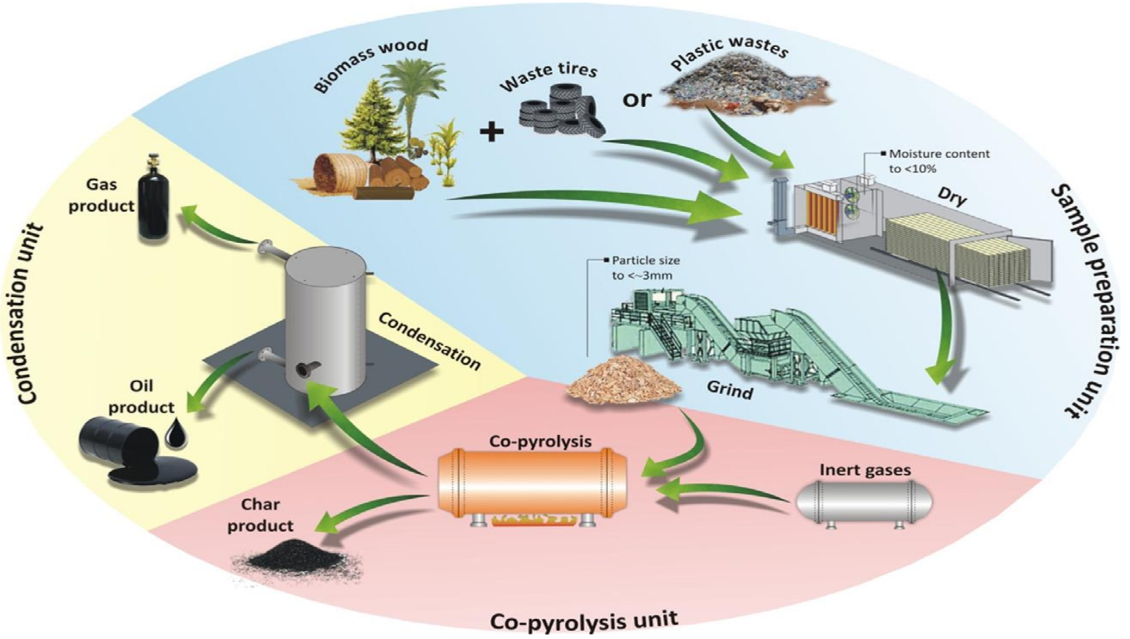

Figure 2.12. The schematic diagram of lignocellulosic biomass and polymers in the co-pyrolysis system [110].

Apart from the high yield of hydrogen and syngas as observed in this study, an increase in the petrochemical products such as aromatic selectivity and minimal formation of coke on the catalyst in co-pyrolysis of biomass with hydrogen-enriched feedstock (plastics) as a novel and suitable option have been reported [113]. Many researchers have suggested that one of the main reasons and the most important of adding plastics to biomass in a co-pyrolysis blend is to improve the oil yield and quality [207-210]. Improvement of the heating value of the bio oil, higher heating value (HHV) of the pyrolysis oil been observed [208]. The high oxygen content in bio-oil from co-pyrolysis of biomass and plastic was reduced. For example, the co-feeding of oxygen-rich biomass with hydrogen-rich polymers resulted in a positive approach for improving the quality and quantity of bio-oil, especially the H/O ratio [211], as well as product gases such as hydrogen and syngas yield.

According to Zhang et al. [212], the petrochemical yield increases to about 43.9% with LOSA-1 catalyst more than twice compared with the yield without catalyst. The highest aromatic yield (55.3%) was produced by PS while the highest olefin yield (13%) was produced by PE with more benzene, naphthalene and the derivatives in a catalytic co-pyrolysis with black liquor lignin conducted in a fluidized bed reactor. Likewise, Xue et al. [213], studied co-pyrolysis of biomass components (cellulose, xylan and lignin) with polyethylene (PE) in a tandem micro-pyrolyzer using HZSM-5 catalyst, an increase in aromatic hydrocarbons yield was observed, suggesting that the Diels-Alder reaction, hydrocarbon pool mechanism and hydrogen transfer reactions are the dominant reactions with significant synergy between biomass and PE. The same tendency was observed by Dorado et al. [214], who suggested the Diels-Alder reaction mechanism as furan-derived compounds from biomass react with olefins derived from plastics leading to an increase in aromatic hydrocarbon production in the presence of H-ZSM-5 catalyst. Also, Brebu and Nistor [215], investigated the co-pyrolysis of various lignins with polycarbonate plastics and observed that the interaction of the components was more pronounced at high temperatures, leading to an increase in oil yield.

Similarly, Ojha and Vinu [211], conducted experiments on co-pyrolysis of cellulose and polypropylene in a Pyroprobe reactor (PP) for production of high quality biofuel, aromatic hydrocarbons increased with pyrolysis temperature while the char yield decreased. The heating value (range from 36-41MJkg^{-1}), and the products were significantly enhanced when the PP was blended with cellulose; deoxygenation promoted via decarboxylation and decarbonylation reactions. The increase in reaction temperature equally promoted a synergistic effect in the catalytic co-pyrolysis blend of cellulose and thermoplastics over HY and HZSM-5 catalysts [216]. In another investigation of co-pyrolysis of black liquor lignin with plastics (PE, PS and PP) showed that aromatic and olefin yields increased with increasing temperatures of 450-650 ^{o}C [212].

2.6.1 Summary

There are various types of catalysts for reforming and cracking of hydrocarbon polymers such as waste plastics as well as biomass. The different types of catalysts on reforming includes noble metals catalysts, alkali metals base catalysts while the cracking catalysts majorly includes the acidic catalysts such as zeolites (Y-zeolites with micropores and

ZSM-5 with mesopores), alumina and silica-alumina with mesopores [64]. Bifunctional catalysts, as used in this study, have been investigated by many researchers [217]. According to Huang et al. [64], a bifunctional catalyst is made up of two sections, the acidic support which provides the cracking and isomerisation function while the metal supplies the other function such as dehydrogenation/hydrogenation. Different support catalysts with nickel loading have also been investigated by many researchers, amongst the very common ones including, but not limited to, Al_2O_3, MgO, zeolites [201, 218]. Furthermore, dolomite, olivine and CeO_2 have been support for nickel catalysts and the nickel on mesopores catalyst MCM-41 was reported to improve hydrogen production [190].

There has been much concentration of research work in the direction of bio oil (liquid) up-grade with plastics waste in co-pyrolysis with biomass [209, 210]. However, there has not been much data available on the aspect of biogas production as well as the optimisation process for syngas and hydrogen production from co-pyrolysis-gasification of biomass components with plastic wastes.

To the best of the author’s knowledge, there is no, or limited research on co-pyrolysis of biomass components with plastics waste for syngas and hydrogen production. The use of novel prepared catalysts with different metals (nickel, cobalt and molebdenum) impregnated on mesoporous support of MCM-41 for the catalytic co-pyrolysis-gasification of biomass components (lignin & cellulose) with plastic wastes (HDPE and PS) blend, for enhanced production of hydrogen and syngas yield were conducted. In addition, optimisation of the syngas and hydrogen production by adjusting operating parameters such as steam ratio and catalytic temperature were equally investigated.

References

1. Patni, N., et al., *Alternate Strategies for Conversion of Waste Plastic to Fuels.* ISRN Renewable Energy, 2013. 2013: p. 1-7.
2. Panda, A.K., R.K. Singh, and D.K. Mishra, *Thermolysis of waste plastics to liquid fuelA suitable method for plastic waste management and manufacture of value added products—A world prospective.* Renewable and Sustainable Energy Reviews, 2010. 14(1): p. 233-248.
3. Al-Salem, S., P. Lettieri, and J. Baeyens, *Recycling and recovery routes of plastic solid waste (PSW): A review.* Waste Management, 2009. 29(10): p. 2625-2643.
4. Kaminsky, W. and J.-S. Kim, *Pyrolysis of mixed plastics into aromatics.* Journal of Analytical and Applied Pyrolysis, 1999. 51(1): p. 127-134.
5. Baeyens, J., A. Brems, and R. Dewil, *Recovery and recycling of post-consumer waste materials. Part 2. Target wastes (glass beverage bottles, plastics, scrap metal and steel cans, end-of-life tyres, batteries and household hazardous waste).* International Journal of Sustainable Engineering, 2010. 3(4): p. 232-245.
6. Achilas et al, *Recent Advances in the Chemical Recycling of Polymers (PP, PS, LDPE, HDPE, PVC, PC, Nylon, PMMA),.* 2015.
7. Williams, P.T. and A.J. Brindle, *Temperature selective condensation of tyre pyrolysis oils to maximise the recovery of single ring aromatic compounds.* Fuel, 2003. 82(9): p. 1023-1031.
8. Brems, A., et al., *Gasification of plastic waste as waste-to-energy or waste-to-syngas recovery route.* Natural Science, 2013. 05(06): p. 695-704.
9. Sharuddin, S.D.A., et al., *A review on pyrolysis of plastic wastes.* 2016. 115: p. 308-326.
10. Abnisa, F. and W.M.A. Wan Daud, *A review on co-pyrolysis of biomass: An optional technique to obtain a high-grade pyrolysis oil.* Energy Conversion and Management, 2014. 87: p. 71-85.
11. Uddin, M.A., et al., *Thermal and catalytic degradation of structurally different types of polyethylene into fuel oil.* Polymer Degradation and Stability, 1997. 56(1): p. 37-44.
12. Demirbas, A., *Pyrolysis of municipal plastic wastes for recovery of gasoline-range hydrocarbons.* Journal of Analytical and Applied Pyrolysis, 2004. 72(1): p. 97-102.
13. Kiran, N., et al., *Recyling of plastic wastes via pyrolysis.* 2000. 29(4): p. 273-283.
14. Angyal, A., N. Miskolczi, and L. Bartha, *Petrochemical feedstock by thermal cracking of plastic waste.* Journal of Analytical and Applied Pyrolysis, 2007. 79(1): p. 409-414.
15. Kumar, S., A.K. Panda, and R.K. Singh, *A review on tertiary recycling of high-density polyethylene to fuel.* Resources Conservation and Recycling, 2011. 55(11): p. 893-910.
16. Lopez, A., et al., *Influence of time and temperature on pyrolysis of plastic wastes in a semi-batch reactor.* 2011. 173(1): p. 62-71.

17. Marcilla, A., et al., *Study of the catalytic pyrolysis behaviour of polyethylene–polypropylene mixtures.* 2005. 74(1-2): p. 387-392.

18. Chin, B.L.F., et al., *Kinetic studies of co-pyrolysis of rubber seed shell with high density polyethylene.* 2014. 87: p. 746-753.

19. Muhammad, C., J.A. Onwudili, and P.T. Williams, *Thermal Degradation of Real-World Waste Plastics and Simulated Mixed Plastics in a Two-Stage Pyrolysis-Catalysis Reactor for Fuel Production.* Energy & Fuels, 2015. 29(4): p. 2601-2609.

20. Acomb, J.C., C.F. Wu, and P.T. Williams, *Effect of growth temperature and feedstock:catalyst ratio on the production of carbon nanotubes and hydrogen from the pyrolysis of waste plastics.* Journal of Analytical and Applied Pyrolysis, 2015. 113: p. 231-238.

21. del Remedio Hernandez, M., et al., *Effect of the temperature in the nature and extension of the primary and secondary reactions in the thermal and HZSM-5 catalytic pyrolysis of HDPE.* 2007. 317(2): p. 183-194.

22. Lopez, A., et al., *Pyrolysis of municipal plastic wastes II: Influence of raw material composition under catalytic conditions.* Waste Manag, 2011. 31(9-10): p. 1973-83.

23. Gao, F. *Pyrolysis of waste plastics into fuels*. 2010; Available from: https://ir.canterbury.ac.nz/handle/10092/4303.

24. Acomb, J.C., M.A. Nahil, and P.T. Williams, *Thermal processing of plastics from waste electrical and electronic equipment for hydrogen production.* Journal of Analytical and Applied Pyrolysis, 2013. 103: p. 320-327.

25. Zeaiter, J., *A process study on the pyrolysis of waste polyethylene.* Fuel, 2014. 133: p. 276-282.

26. Kayacan, I. and Ö. Doğan, *Pyrolysis of low and high density polyethylene. Part I: non-isothermal pyrolysis kinetics.* Energy Sources, Part A, 2008. 30(5): p. 385-391.

27. Encinar, J. and J.J.F.P.T. González, *Pyrolysis of synthetic polymers and plastic wastes. Kinetic study.* 2008. 89(7): p. 678-686.

28. FakhrHoseini, S.M. and M.J.J.o.C. Dastanian, *Predicting pyrolysis products of PE, PP, and PET using NRTL activity coefficient model.* 2013. 2013.

29. Mastral, F., et al., *Pyrolysis of high-density polyethylene in a fluidised bed reactor. Influence of the temperature and residence time.* 2002. 63(1): p. 1-15.

30. Ludlow-Palafox, C., H.A.J.I. Chase, and e.c. research, *Microwave-induced pyrolysis of plastic wastes.* 2001. 40(22): p. 4749-4756.

31. Scheirs, J. and W. Kaminsky, *Feedstock recycling and pyrolysis of waste plastics*. John Willy & Sons, Ltd. 2006.

32. Al-Salem, S., et al., *A review on thermal and catalytic pyrolysis of plastic solid waste (PSW).* 2017. 197: p. 177-198.

33. Bhaskar, T., et al., *Pyrolysis studies of PP/PE/PS/PVC/HIPS-Br plastics mixed with PET and dehalogenation (Br, Cl) of the liquid products.* 2004. 72(1): p. 27-33.

34. Murata, K., K. Sato, and Y. Sakata, *Effect of pressure on thermal degradation of polyethylene.* Journal of Analytical and Applied Pyrolysis, 2004. 71(2): p. 569-589.

35. Ismadji, S., et al., *Activated carbon from char obtained from vacuum pyrolysis of teak sawdust: pore structure development and characterization.* 2005. 96(12): p. 1364-1369.

36. Paradela, F., et al., *Study of the co-pyrolysis of biomass and plastic wastes.* 2009. 11(1): p. 115-122.

37. He, M., et al., *Syngas production from catalytic gasification of waste polyethylene: Influence of temperature on gas yield and composition.* 2009. 34(3): p. 1342-1348.

38. Serrano, D., J. Aguado, and J. Escola, *Developing advanced catalysts for the conversion of polyolefinic waste plastics into fuels and chemicals.* ACS Catalysis, 2012. 2(9): p. 1924-1941.

39. Fogler, H.S., *Elements of Chemical Reaction Engineering*. 3rd ed. ed. 2000, New Jersey: Prentice Hall International.

40. Onwudili, J.A., N. Insura, and P.T. Williams, *Autoclave pyrolysis of carbon reinforced composite plastic waste for carbon fibre and chemicals recovery.* Journal of the Energy Institute, 2013. 86(4): p. 227-232.

41. Van Grieken, R., et al., *Thermal and catalytic cracking of polyethylene under mild conditions.* Journal of Analytical and Applied Pyrolysis, 2001. 58: p. 127-142.

42. Manos, G., et al., *Catalytic cracking of polyethylene over clay catalysts. Comparison with an ultrastable Y zeolite.* Industrial & engineering chemistry research, 2001. 40(10): p. 2220-2225.

43. Essential chemical industry online and U.o. York *Chemical reactors*. 2015. 2015.

44. Westerhout, R., J. Kuipers, and W. Van Swaaij, *Experimental determination of the yield of pyrolysis products of polyethene and polypropene. Influence of reaction conditions.* Industrial & engineering chemistry research, 1998. 37(3): p. 841-847.

45. Lee, K.-H. and S.C. Oh, *Thermal and catalytic degradation of pyrolytic waxy oil in a plug flow reactor.* Journal of Analytical and Applied Pyrolysis, 2012. 93: p. 19-23.

46. Lin, H.-T., et al., *Hydrocarbon fuels produced by catalytic pyrolysis of hospital plastic wastes in a fluidizing cracking process.* Fuel Processing Technology, 2010. 91(11): p. 1355-1363.

47. Kaminsky, W., M. Predel, and A. Sadiki, *Feedstock recycling of polymers by pyrolysis in a fluidised bed.* Polymer Degradation and Stability, 2004. 85(3): p. 1045-1050.

48. Williams, P.T. and A.J. Brindle, *Fluidised bed catalytic pyrolysis of scrap tyres: Influence of catalyst: tyre ratio and catalyst temperature.* Waste Management & Research, 2002. 20(6): p. 546-555.

49. Murata, K., et al., *Basic study on a continuous flow reactor for thermal degradation of polymers.* Journal of Analytical and Applied Pyrolysis, 2002. 65(1): p. 71-90.

50. Uppal, A., W. Ray, and A. Poore, *The classification of the dynamic behavior of continuous stirred tank reactors—influence of reactor residence time.* Chemical Engineering Science, 1976. 31(3): p. 205-214.

51. Serrano, D., et al., *Conversion of low density polyethylene into petrochemical feedstocks using a continuous screw kiln reactor.* Journal of Analytical and Applied Pyrolysis, 2001. 58: p. 789-801.

52. Fantozzi, F., et al., *Rotary Kiln Slow Pyrolysis for Syngas and Char Production From Biomass and Waste—Part I: Working Envelope of the Reactor.* Journal of Engineering for Gas Turbines and Power, 2007. 129(4): p. 901-907.

53. Serrano, D., et al., *Performance of a continuous screw kiln reactor for the thermal and catalytic conversion of polyethylene–lubricating oil base mixtures.* Applied Catalysis B: Environmental, 2003. 44(2): p. 95-105.

54. Hall, W.J., et al., *Thermal processing of toxic flame-retarded polymers using a waste fluidized catalytic cracker (FCC) catalyst.* 2008. 22(3): p. 1691-1697.

55. Hall, W.J., P.T.J.J.o.a. Williams, and a. pyrolysis, *Removal of organobromine compounds from the pyrolysis oils of flame retarded plastics using zeolite catalysts.* 2008. 81(2): p. 139-147.

56. Wu, C. and P.T. Williams, *Pyrolysis–gasification of post-consumer municipal solid plastic waste for hydrogen production.* International Journal of Hydrogen Energy, 2010. 35(3): p. 949-957.

57. Marcilla, A., A. Gómez-Siurana, and F. Valdés, *Catalytic pyrolysis of LDPE over H-beta and HZSM-5 zeolites in dynamic conditions: study of the evolution of the process.* Journal of Analytical and Applied Pyrolysis, 2007. 79(1): p. 433-442.

58. Uemichi, Y., et al., *Conversion of polyethylene into gasoline-range fuels by two-stage catalytic degradation using silica-alumina and HZSM-5 zeolite.* Industrial & engineering chemistry research, 1999. 38(2): p. 385-390.

59. Kunwar, B., et al., *Plastics to fuel: a review.* Renewable and Sustainable Energy Reviews, 2016. 54: p. 421-428.

60. Miskolczi, N., et al., *Fuels by pyrolysis of waste plastics from agricultural and packaging sectors in a pilot scale reactor.* Fuel Processing Technology, 2009. 90(7): p. 1032-1040.

61. Buekens, A. and H. Huang, *Catalytic plastics cracking for recovery of gasoline-range hydrocarbons from municipal plastic wastes.* Resources, Conservation and Recycling, 1998. 23(3): p. 163-181.

62. Rahimpour, M.R., M. Jafari, and D. Iranshahi, *Progress in catalytic naphtha reforming process: A review.* Applied Energy, 2013. 109: p. 79-93.

63. Uemichi, Y., Y. Makino, and T. Kanazuka, *Degradation of polyethylene to aromatic hydrocarbons over metal-supported activated carbon catalysts.* Journal of Analytical and Applied Pyrolysis, 1989. 14(4): p. 331-344.

64. Huang, C., A. Gujar, and M. Rodgers, *Methods of producing liquid hydrocarbon fuels from solid plastic wastes*. 2015, Google Patents.

65. Wang, S., G.Q. Lu, and G.J. Millar, *Carbon Dioxide Reforming of Methane To Produce Synthesis Gas over Metal-Supported Catalysts: State of the Art.* Energy & Fuels, 1996. 10(4): p. 896-904.

66. Aguado, J., D. Serrano, and J. Escola, *Fuels from waste plastics by thermal and catalytic processes: a review.* Industrial & engineering chemistry research, 2008. 47(21): p. 7982-7992.

67. Lerici, L.C., M.S. Renzini, and L.B. Pierella, *Chemical Catalyzed Recycling of Polymers: Catalytic Conversion of PE, PP and PS into Fuels and Chemicals over HY.* Procedia Materials Science, 2015. 8: p. 297-303.

68. Renzini, M.S., U. Sedran, and L.B. Pierella, *H-ZSM-11 and Zn-ZSM-11 zeolites and their applications in the catalytic transformation of LDPE.* Journal of Analytical and Applied Pyrolysis, 2009. 86(1): p. 215-220.

69. Pierella, L.B., S. Renzini, and O.A. Anunziata, *Catalytic degradation of high density polyethylene over microporous and mesoporous materials.* Microporous and Mesoporous Materials, 2005. 81(1-3): p. 155-159.

70. Lin, Y.H. and M.H. Yang, *Chemical catalysed recycling of polypropylene over a spent FCC catalyst and various commercial cracking catalysts using TGA.* Thermochimica Acta, 2008. 470(1-2): p. 52-59.

71. Miskolczi, N., L. Bartha, and G. Deák, *Thermal degradation of polyethylene and polystyrene from the packaging industry over different catalysts into fuel-like feed stocks.* Polymer Degradation and Stability, 2006. 91(3): p. 517-526.

72. Williams, P.T. and R. Bagri, *Hydrocarbon gases and oils from the recycling of polystyrene waste by catalytic pyrolysis.* international journal of energy research, 2004. 28(1): p. 31-44.

73. Zhou, Q., et al., *Catalytic degradation of low-density polyethylene and polypropylene using modified ZSM-5 zeolites.* Polymer Degradation and Stability, 2004. 84(3): p. 493-497.

74. Manos, G., A. Garforth, and J. Dwyer, *Catalytic degradation of high-density polyethylene over different zeolitic structures.* Industrial & engineering chemistry research, 2000. 39(5): p. 1198-1202.

75. Shah, S.H., et al., *Low temperature conversion of plastic waste into light hydrocarbons.* Journal of Hazardous Materials, 2010. 179(1-3): p. 15-20.

76. Bagri, R. and P.T. Williams, *Catalytic pyrolysis of polyethylene.* Journal of Analytical and Applied Pyrolysis, 2002. 63(1): p. 29-41.

77. Todorova, S., et al., *Metal states in cobalt-and cobalt–vanadium-modified MCM-41 mesoporous silica catalysts and their activity in selective hydrocarbons oxidation.* Microporous and Mesoporous Materials, 2008. 113(1-3): p. 22-30.

78. Szegedi, A., et al., *Cobalt-containing mesoporous silicas—Preparation, characterization and catalytic activity in toluene hydrogenation.* Applied Catalysis A: General, 2008. 338(1-2): p. 44-51.

79. Lucredio, A.F. and E.M. Assaf, *Cobalt catalysts prepared from hydrotalcite precursors and tested in methane steam reforming.* Journal of power sources, 2006. 159(1): p. 667-672.

80. Ratnasari, D.K., et al., *Two-stage ex-situ catalytic pyrolysis of lignocellulose for the production of gasoline-range chemicals.* 2018. 134: p. 454-464.

81. Lin, Y.-H., et al., *Catalytic degradation of high density polyethylene over mesoporous and microporous catalysts in a fluidised-bed reactor.* 2004. 86(1): p. 121-128.

82. Aguado, J., et al., *Feedstock recycling of polyethylene in a two-step thermo-catalytic reaction system.* 2007. 79(1-2): p. 415-423.

83. Aguado, J., et al., *Catalytic conversion of polyolefins into liquid fuels over MCM-41: comparison with ZSM-5 and amorphous SiO2− Al2O3.* 1997. 11(6): p. 1225-1231.

84. Aguado, J., et al., *Influence of the operating variables on the catalytic conversion of a polyolefin mixture over HMCM-41 and nanosized HZSM-5.* 2001. 40(24): p. 5696-5704.

85. Garcia, R., et al., *Catalytic cracking of HDPE over hybrid zeolitic–mesoporous materials.* 2005. 74(1-2): p. 379-386.

86. Degnan Jr, T.F., *Applications of zeolites in petroleum refining.* Topics in Catalysis, 2000. 13(4): p. 349-356.

87. Ivanova, S., et al., *Selective catalytic degradation of polyolefins.* Progress in polymer science, 1990. 15(2): p. 193-215.

88. Donaj, P.J., et al., *Pyrolysis of polyolefins for increasing the yield of monomers' recovery.* Waste Manag, 2012. 32(5): p. 840-6.

89. Adrados, A., et al., *Pyrolysis of plastic packaging waste: A comparison of plastic residuals from material recovery facilities with simulated plastic waste.* Waste Manag, 2012. 32(5): p. 826-32.

90. Faiad, A.A.H. *Student finds new way of turning plastic into biofuel*. 2012.

91. Insura, N., *Thermal and Catalytic Pyrolysis of waste Plastics for recovery of fuel and Higher Value products*. 2011, University of Leeds.

92. Vasile, C., et al., *Feedstock recycling from the printed circuit boards of used computers.* Energy & Fuels, 2008. 22(3): p. 1658-1665.

93. de Marco, I., et al., *Pyrolysis of the rejects of a waste packaging separation and classification plant.* Journal of Analytical and Applied Pyrolysis, 2009. 85(1): p. 384-391.

94. Huang, C., A. Gujar, and M. Rodgers, *Methods of Producing Liquid Hydrocarbon Fuels from Solid Plastic Wastes*. 2012, Google Patents.

95. Mordi, R.C., R. Fields, and J. Dwyer, *Thermolysis of low density polyethylene catalysed by zeolites.* Journal of Analytical and Applied Pyrolysis, 1994. 29(1): p. 45-55.

96. Lin, Y.-H. and M.-H. Yang, *Catalytic reactions of post-consumer polymer waste over fluidised cracking catalysts for producing hydrocarbons.* Journal of Molecular Catalysis A: Chemical, 2005. 231(1): p. 113-122.

97. Uemichi, Y., K. Takuma, and A. Ayame, *Chemical recycling of poly (ethylene) by catalytic degradation into aromatic hydrocarbons using H-Ga-silicate.* Chem. Commun., 1998(18): p. 1975-1976.

98. Takuma, K., et al., *Production of aromatic hydrocarbons by catalytic degradation of polyolefins over H-gallosilicate.* Industrial & engineering chemistry research, 2001. 40(4): p. 1076-1082.

99. Shah, J., et al., *Catalytic pyrolysis of LDPE leads to valuable resource recovery and reduction of waste problems.* Energy Conversion and Management, 2010. 51(12): p. 2791-2801.

100. Akhtar, M.N. and S.S. Al-Khattaf, *Catalytic Aromatization of Alkanes.* Catalysts in Petroleum Refining & Petrochemicals, 2010.

101. Kocal, J.A., *Process for producing aromatic compounds from C2-C6 aliphatic hydrocarbons*. 1988, Google Patents.

102. Gnep, N., et al., *Conversion of light alkanes into aromatic hydrocarbons: 1-dehydrocyclodimerization of propane on PtHZSM-5 catalysts.* Applied catalysis, 1987. 35(1): p. 93-108.

103. Guisnet, M., et al., *Conversion of light alkanes into aromatic hydrocarbons: VI. Aromatization of C2-C4 alkanes on H-ZSM-5—reaction mechanisms.* Applied Catalysis A: General, 1992. 87(2): p. 255-270.

104. Guisnet, M., N. Gnep, and F. Alario, *Aromatization of short chain alkanes on zeolite catalysts.* Applied Catalysis A: General, 1992. 89(1): p. 1-30.

105. Tian, M., et al., *Methane and propane co-conversion study over zinc, molybdenum and gallium modified HZSM-5 catalysts using time-of-flight mass-spectrometry.* Chemical Physics Letters, 2014. 592: p. 36-40.

106. Scott, D., et al., *Fast pyrolysis of plastic wastes.* Energy & Fuels, 1990. 4(4): p. 407-411.

107. Uemichi, Y., Y. Makino, and T. Kanazuka, *Degradation of polypropylene to aromatic hydrocarbons over Pt-and Fe-containing activated carbon catalysts.* Journal of Analytical and Applied Pyrolysis, 1989. 16(3): p. 229-238.

108. Santiago-Maldonado, E., et al. *Creating Methane from Plastic: Recycling at a Lunar Outpost*. in *48th AIAA Aerospace Sciences Meeting Including the New Horizons Forum and Aerospace Expostion*. 2010.

109. Park, D., et al., *Catalytic degradation of polyethylene over solid acid catalysts.* Polymer Degradation and Stability, 1999. 65(2): p. 193-198.

110. Abnisa, F. and W.M.A.W. Daud, *A review on co-pyrolysis of biomass: an optional technique to obtain a high-grade pyrolysis oil.* Energy Conversion and Management, 2014. 87: p. 71-85.

111. Kirkels, A.F. and G.P. Verbong, *Biomass gasification: Still promising? A 30-year global overview.* Renewable and Sustainable Energy Reviews, 2011. 15(1): p. 471-481.

112. McKendry, P., *Energy production from biomass (part 1): overview of biomass.* Bioresource Technology, 2002. 83: p. 37-46.

113. Zhang, X., et al., *Catalytic co-pyrolysis of lignocellulosic biomass with polymers: a critical review.* Green Chemistry, 2016. 18(15): p. 4145-4169.

114. Jansen, R.A., *Second generation biofuels and biomass: essential guide for investors, scientists and decision makers*. 2012: John Wiley & Sons.

115. Anis Atikah Ahmad, et al., *Assessing the gasification performanceofbiomass:Areview on biomassgasification processconditions,optimization and economicevaluation.* Renewable and Sustainable Energy Reviews 2016. 53: p. 1333–1347.

116. Alonso, D.M., S.G. Wettstein, and J.A. Dumesic, *Bimetallic catalysts for upgrading of biomass to fuels and chemicals.* Chemical Society Reviews, 2012. 41(24): p. 8075-8098.

117. Wu, C., et al., *Pyrolysis/gasification of cellulose, hemicellulose and lignin for hydrogen production in the presence of various nickel-based catalysts.* Fuel, 2013. 106: p. 697-706.

118. Carole Couhert , Jean-Michel Commandre, and S. Salvador, *Is it possible to predict gas yields of any biomass after rapid pyrolysis at high temperature from its composition in cellulose, hemicellulose and lignin?* Fuel Processing Technology, 2009. 88: p. 408-417.

119. Yang, H., et al., *Characteristics of hemicellulose, cellulose and lignin pyrolysis.* Fuel, 2007. 86(12): p. 1781-1788.

120. Kan, T., V. Strezov, and T.J. Evans, *Lignocellulosic biomass pyrolysis: A review of product properties and effects of pyrolysis parameters.* Renewable and Sustainable Energy Reviews, 2016. 57: p. 1126-1140.

121. Qu, T., et al., *Experimental study of biomass pyrolysis based on three major components: hemicellulose, cellulose, and lignin.* Industrial & engineering chemistry research, 2011. 50(18): p. 10424-10433.

122. Yang, H., et al., *In-depth investigation of biomass pyrolysis based on three major components: hemicellulose, cellulose and lignin.* 2006. 20(1): p. 388-393.

123. Akubo, K., M.A. Nahil, and P.T.J.J.o.t.E.I. Williams, *Pyrolysis-catalytic steam reforming of agricultural biomass wastes and biomass components for production of hydrogen/syngas.* 2018.

124. Block, C., et al., *Co-pyrogasification of Plastics and Biomass, a Review.* Waste and Biomass Valorization, 2018: p. 1-27.

125. Liu, Q., et al., *Interactions of biomass components during pyrolysis: A TG-FTIR study.* Journal of Analytical and Applied Pyrolysis, 2011. 90(2): p. 213-218.

126. Williams, P.T. and S. Besler, *The influence of temperature and heating rate on the slow pyrolysis of biomass.* Renewable Energy, 1996. 7(3): p. 233-250.

127. Jin, W., et al., *Evaluation of the co-pyrolysis of lignin with plastic polymers by TG-FTIR and Py-GC/MS.* 2016. 133: p. 65-74.

128. Burhenne, L., et al., *The effect of the biomass components lignin, cellulose and hemicellulose on TGA and fixed bed pyrolysis.* Journal of Analytical and Applied Pyrolysis, 2013. 101: p. 177-184.

129. Uddin, M.N., W.W. Daud, and H.F. Abbas, *Effects of pyrolysis parameters on hydrogen formations from biomass: a review.* RSC Advances, 2014. 4(21): p. 10467-10490.

130. Collarda François-Xavier and B. Joël, *A review on pyrolysis of biomass constituents: Mechanisms and composition of the products obtained from the conversion of cellulose, hemicelluloses and lignin.* Renewable and Sustainable Energy Reviews 2014. 38: p. 594-608.

131. Palma, C.F.J.A.E., *Modelling of tar formation and evolution for biomass gasification: A review.* 2013. 111: p. 129-141.

132. Hosoya, T., et al., *Pyrolysis gasification reactivities of primary tar and char fractions from cellulose and lignin as studied with a closed ampoule reactor.* 2008. 83(1): p. 71-77.

133. Asmadi, M., et al., *Gas-and solid/liquid-phase reactions during pyrolysis of softwood and hardwood lignins.* 2011. 92(2): p. 417-425.

134. Waheed, Q.M. and P.T. Williams, *Hydrogen production from High temperature pyrolysis/steam reforming of waste biomass: rice husk, sugar cane bagasse, and wheat straw.* Energy & Fuels, 2013. 27(11): p. 6695-6704.

135. Monono, E.M., et al., *Variability in biomass yield, chemical composition, and ethanol potential of individual and mixed herbaceous biomass species grown in North Dakota.* 2013. 41: p. 331-339.

136. Vassilev, S.V., et al., *An overview of the chemical composition of biomass.* 2010. 89(5): p. 913-933.

137. Sikarwar, V.S., et al., *An overview of advances in biomass gasification.* 2016. 9(10): p. 2939-2977.

138. Vassilev, S.V., et al., *An overview of the organic and inorganic phase composition of biomass.* 2012. 94: p. 1-33.

139. Dogru, M., et al., *Gasification of hazelnut shells in a downdraft gasifier.* 2002. 27(5): p. 415-427.

140. Kirubakaran, V., et al., *A review on gasification of biomass.* 2009. 13(1): p. 179-186.

141. Raveendran, K., A. Ganesh, and K.C.J.F. Khilar, *Influence of mineral matter on biomass pyrolysis characteristics.* 1995. 74(12): p. 1812-1822.

142. Inayat, A., et al., *Effect of process parameters on hydrogen production and efficiency in biomass gasification using modelling approach.* 2010. 10(24): p. 3183-3190.

143. Kalinci, Y., A. Hepbasli, and I.J.I.j.o.h.e. Dincer, *Biomass-based hydrogen production: a review and analysis.* 2009. 34(21): p. 8799-8817.

144. González, J., et al., *Investigation on the reactions influencing biomass air and air/steam gasification for hydrogen production.* 2008. 89(8): p. 764-772.

145. Lucas, C., et al., *High-temperature air and steam gasification of densified biofuels.* 2004. 27(6): p. 563-575.

146. Parthasarathy, P. and K.S.J.R.e. Narayanan, *Hydrogen production from steam gasification of biomass: influence of process parameters on hydrogen yield–a review.* 2014. 66: p. 570-579.

147. Waheed, Q.M., C. Wu, and P.T. Williams, *Hydrogen production from high temperature steam catalytic gasification of bio-char.* Journal of the Energy Institute, 2016. 89(2): p. 222-230.

148. Xiao, X., et al., *Catalytic steam gasification of biomass in fluidized bed at low temperature: conversion from livestock manure compost to hydrogen-rich syngas.* 2010. 34(10): p. 1505-1512.

149. Yan, F., et al., *Hydrogen-rich gas production by steam gasification of char from biomass fast pyrolysis in a fixed-bed reactor: Influence of temperature and steam on hydrogen yield and syngas composition.* 2010. 101(14): p. 5633-5637.

150. Luo, S., et al., *Hydrogen-rich gas from catalytic steam gasification of biomass in a fixed bed reactor: Influence of temperature and steam on gasification performance.* 2009. 34(5): p. 2191-2194.

151. Franco, C., et al., *The study of reactions influencing the biomass steam gasification process☆.* 2003. 82(7): p. 835-842.

152. Gao, N., A. Li, and C.J.B.t. Quan, *A novel reforming method for hydrogen production from biomass steam gasification.* 2009. 100(18): p. 4271-4277.

153. Gil, J., et al., *Biomass gasification in atmospheric and bubbling fluidized bed: effect of the type of gasifying agent on the product distribution.* 1999. 17(5): p. 389-403.

154. Saad, J.M. and P.T.J.W.m. Williams, *Catalytic dry reforming of waste plastics from different waste treatment plants for production of synthesis gases.* 2016. 58: p. 214-220.

155. Dong, L., et al., *Promoting hydrogen production and minimizing catalyst deactivation from the pyrolysis-catalytic steam reforming of biomass on nanosized NiZnAlOx catalysts.* 2017. 188: p. 610-620.

156. Guana Guoqing, et al., *Catalytic steam reforming of biomass tar: Prospects and challenges.* Renewable and Sustainable Energy Reviews 2016. 58: p. 450-461.

157. Chen, F., et al., *Catalytic steam reforming of volatiles released via pyrolysis of wood sawdust for hydrogen-rich gas production on Fe–Zn/Al2O3 nanocatalysts.* 2015. 158: p. 999-1005.

158. Lv, P., et al., *Hydrogen-rich gas production from biomass air and oxygen/steam gasification in a downdraft gasifier.* 2007. 32(13): p. 2173-2185.

159. Corella, J., et al., *Biomass gasification in fluidized bed: where to locate the dolomite to improve gasification?* 1999. 13(6): p. 1122-1127.

160. Hanaoka, T., et al., *Hydrogen production from woody biomass by steam gasification using a CO2 sorbent.* 2005. 28(1): p. 63-68.

161. Basile, L., et al., *Influence of pressure on the heat of biomass pyrolysis.* 2014. 137: p. 277-284.

162. Puig-Gamero, M., et al., *Pyrolysis process using a bench scale high pressure thermobalance.* 2017. 167: p. 345-354.

163. Wang, Y. and C.J.S.e. Kinoshita, *Kinetic model of biomass gasification.* 1993. 51(1): p. 19-25.

164. Knight, R.A.J.B. and Bioenergy, *Experience with raw gas analysis from pressurized gasification of biomass.* 2000. 18(1): p. 67-77.

165. Hu, G., et al., *Steam gasification of apricot stones with olivine and dolomite as downstream catalysts.* 2006. 87(5): p. 375-382.

166. De Lasa, H., et al., *Catalytic steam gasification of biomass: catalysts, thermodynamics and kinetics.* 2011. 111(9): p. 5404-5433.

167. Yang, H., et al., *Pyrolysis of palm oil wastes for enhanced production of hydrogen rich gases.* 2006. 87(10): p. 935-942.

168. Xianwen, D., et al., *The fast pyrolysis of biomass in CFB reactor.* 2000. 14(3): p. 552-557.

169. Font, R., et al., *Gaseous hydrocarbons from flash pyrolysis of almond shells.* 1988. 27(7): p. 1143-1149.

170. Scott, D.S., et al., *The role of temperature in the fast pyrolysis of cellulose and wood.* 1988. 27(1): p. 8-15.

171. Demirbas, A. and G.J.E.s. Arin, *An overview of biomass pyrolysis.* 2002. 24(5): p. 471-482.

172. Miranda, R., et al., *Pyrolysis of textile wastes: I. Kinetics and yields.* 2007. 80(2): p. 489-495.

173. Zanzi, R., et al., *Rapid pyrolysis of agricultural residues at high temperature.* 2002. 23(5): p. 357-366.

174. González, J.F., et al., *Pyrolysis of cherry stones: energy uses of the different fractions and kinetic study.* 2003. 67(1): p. 165-190.

175. Efika, C.E., J.A. Onwudili, and P.T.J.W.M. Williams, *Influence of heating rates on the products of high-temperature pyrolysis of waste wood pellets and biomass model compounds.* 2018. 76: p. 497-506.

176. Zuo, S., et al., *Evolution of gaseous products from biomass pyrolysis in the presence of phosphoric acid.* 2012. 95: p. 236-240.

177. Şensöz, S. and M.J.E.S. Can, *Pyrolysis of pine (Pinus brutia Ten.) chips: 1. Effect of pyrolysis temperature and heating rate on the product yields.* 2002. 24(4): p. 347-355.

178. Mohamed A. Hamad, et al., *Hydrogen rich gas production from catalytic gasification of biomass.* Renewable Energy 2016. 85: p. 1290-1300.

179. Yang, H. and H. Chen, *Biomass gasification for synthetic liquid fuel production*, in *Gasification for Synthetic Fuel Production*. 2015, Elsevier. p. 241-275.

180. Sutton, D., B. Kelleher, and J.R.J.F.p.t. Ross, *Review of literature on catalysts for biomass gasification.* 2001. 73(3): p. 155-173.

181. Anis, S., Z.J.R. Zainal, and s.e. reviews, *Tar reduction in biomass producer gas via mechanical, catalytic and thermal methods: A review.* 2011. 15(5): p. 2355-2377.

182. Xu, C.C., et al., *Recent advances in catalysts for hot-gas removal of tar and NH3 from biomass gasification.* 2010. 89(8): p. 1784-1795.

183. Sutton, D., et al., *Investigation of nickel supported catalysts for the upgrading of brown peat derived gasification products.* 2001. 80(2): p. 111-116.

184. Simell, P.A. and J.-s.J.F. Bredenberg, *Catalytic purification of tarry fuel gas.* 1990. 69(10): p. 1219-1225.

185. Dou, B., et al., *Removal of tar component over cracking catalysts from high temperature fuel gas.* 2008. 49(8): p. 2247-2253.

186. Rapagnà, S., et al., *Steam-gasification of biomass in a fluidised-bed of olivine particles.* 2000. 19(3): p. 187-197.

187. Courson, C., et al., *Development of Ni catalysts for gas production from biomass gasification. Reactivity in steam-and dry-reforming.* 2000. 63(2-4): p. 427-437.

188. Sueyasu, T., et al., *Simultaneous steam reforming of tar and steam gasification of char from the pyrolysis of potassium-loaded woody biomass.* 2011. 26(1): p. 199-208.

189. Buchireddy, P.R., et al., *Biomass gasification: catalytic removal of tars over zeolites and nickel supported zeolites.* 2010. 24(4): p. 2707-2715.

190. Wu, C., et al., *Hydrogen production from biomass gasification with Ni/MCM-41 catalysts: influence of Ni content.* Applied Catalysis B: Environmental, 2011. 108: p. 6-13.

191. Balat, H. and E. Kırtay, *Hydrogen from biomass–present scenario and future prospects.* International Journal of Hydrogen Energy, 2010. 35(14): p. 7416-7426.

192. Zhang, B., et al., *Hydrogen-rich gas production from wet biomass steam gasification with CaO/MgO.* International Journal of Hydrogen Energy, 2015. 40(29): p. 8816-8823.

193. Luo, S., et al., *Hydrogen-rich gas from catalytic steam gasification of biomass in a fixed bed reactor: Influence of particle size on gasification performance.* 2009. 34(3): p. 1260-1264.

194. Zhao, M., N.H. Florin, and A.T. Harris, *Mesoporous supported cobalt catalysts for enhanced hydrogen production during cellulose decomposition.* Applied Catalysis B: Environmental, 2010. 97(1-2): p. 142-150.

195. Barati, M., et al., *Hydrogen production via supercritical water gasification of bagasse using unpromoted and zinc promoted Ru/γ-Al2O3 nanocatalysts.* 2014. 123: p. 140-148.

196. Nishikawa, J., et al., *Promoting effect of Pt addition to Ni/CeO2/Al2O3 catalyst for steam gasification of biomass.* 2008. 9(2): p. 195-201.

197. Profeti, L.P., E.A. Ticianelli, and E.M.J.I.J.o.H.E. Assaf, *Production of hydrogen via steam reforming of biofuels on Ni/CeO2–Al2O3 catalysts promoted by noble metals.* 2009. 34(12): p. 5049-5060.

198. Kimura, T., et al., *Development of Ni catalysts for tar removal by steam gasification of biomass.* Applied Catalysis B: Environmental, 2006. 68(3): p. 160-170.

199. Efika, C.E., et al., *Syngas production from pyrolysis–catalytic steam reforming of waste biomass in a continuous screw kiln reactor.* 2012. 95: p. 87-94.

200. Cao, J.-P., et al., *Catalytic reforming of volatiles and nitrogen compounds from sewage sludge pyrolysis to clean hydrogen and synthetic gas over a nickel catalyst.* 2014. 123: p. 34-40.

201. Inaba, M., et al., *Hydrogen production by gasification of cellulose over Ni catalysts supported on zeolites.* Energy & Fuels, 2006. 20(2): p. 432-438.

202. Qari M.K. Waheed, Chunfei Wu, and P.T. Williams, *Pyrolysis/reforming of rice husks with a Niedolomite catalyst:Influence of process conditions on syngas and hydrogen yield.* Journal of the Energy Institute 2016. 89: p. 657-667.

203. Wu Chunfei and W.P. T, *Nickel-based catalysts for tar reduction in biomass gasification.* Biofuels 2011. 2(4): p. 451-464

204. Williams, P.T. and S. Besler, *The pyrolysis of rice husks in a thermogravimetric analyser and static batch reactor.* Fuel, 1993. 72(2): p. 151-159.

205. Quana Cui, Gao Ningbo, and S. Qingbin, *Pyrolysis of biomass components in a TGA and a fixed-bed reactor: Thermochemical behaviors, kinetics, and product characterization.* Journal of Analytical and Applied Pyrolysis 2016. 121: p. 84-92.

206. Wong, S., et al., *Current state and future prospects of plastic waste as source of fuel: A review.* Renewable and Sustainable Energy Reviews, 2015. 50: p. 1167-1180.

207. Zhang, H., et al., *Catalytic co-pyrolysis of biomass and different plastics (polyethylene, polypropylene, and polystyrene) to improve hydrocarbon yield in a fluidized-bed reactor.* Energy & Fuels, 2014. 28(3): p. 1940-1947.

208. Xue, Y., et al., *Fast pyrolysis of biomass and waste plastic in a fluidized bed reactor.* 2015. 156: p. 40-46.

209. Dorado, C., C.A. Mullen, and A.A.J.A.C.B.E. Boateng, *Origin of carbon in aromatic and olefin products derived from HZSM-5 catalyzed co-pyrolysis of cellulose and plastics via isotopic labeling.* 2015. 162: p. 338-345.

210. Li, J., et al., *Maximizing carbon efficiency of petrochemical production from catalytic co-pyrolysis of biomass and plastics using gallium-containing MFI zeolites.* 2015. 172: p. 154-164.

211. Ojha, D.K. and R.J.R.A. Vinu, *Fast co-pyrolysis of cellulose and polypropylene using Py-GC/MS and Py-FT-IR.* 2015. 5(82): p. 66861-66870.

212. Zhang, H., et al., *Catalytic pyrolysis of black-liquor lignin by co-feeding with different plastics in a fluidized bed reactor.* 2015. 192: p. 68-74.

213. Xue, Y., A. Kelkar, and X.J.F. Bai, *Catalytic co-pyrolysis of biomass and polyethylene in a tandem micropyrolyzer.* 2016. 166: p. 227-236.

214. Dorado, C., et al., *H-ZSM5 catalyzed co-pyrolysis of biomass and plastics.* 2013. 2(2): p. 301-311.

215. Brebu, M., M.J.C.C. Nistor, and TECHNOLOGY, *Co-pyrolysis of various lignins with polycarbonate.* 2014. 48(1-2): p. 69-74.

216. Kim, B.-S., et al., *Catalytic copyrolysis of cellulose and thermoplastics over HZSM-5 and HY.* 2016. 4(3): p. 1354-1363.

217. Zhang, Y., et al., *Fe–Ni–MCM-41 Catalysts for Hydrogen-Rich Syngas Production from Waste Plastics by Pyrolysis–Catalytic Steam Reforming.* 2017. 31(8): p. 8497-8504.

218. Wu, C. and P.T. Williams, *Hydrogen production by steam gasification of polypropylene with various nickel catalysts.* Applied Catalysis B: Environmental, 2009. 87(3-4): p. 152-161.

Chapter 3

Materials and Methodology

3.1 Introduction

This chapter describes and discusses in detail the materials, the experimental reactors and analytical techniques used in the research.

3.2 Materials

3.2.1 Virgin and waste plastics

The olefin plastics sample used as feedstock for conducting the experiments was virgin high-density polyethylene (HPDE) with a particle size of ~5 mm diameter, in the form of pellets. It was obtained from BP chemicals, Grangemouth, UK.

Figure 3.1. Plastic samples (from left to right: HDPE-virgin, PP, HDPE-waste and PS)

Polyethylene (PE) plastics are known to be semi-crystalline thermoplastic materials that belong to the olefin group with properties such as higher impact strength, good resistance to organic solvents, and resistance to stain and wear. PE is one of the most common and popular plastics in the world, characterised by densities between 0.918 – 0.965 g/cm^3 with versatile usage such as in electrical insulators, packaging, domestic wares, tubing, squeeze bottles, cold water tanks, among others [1]. Polyethylenes are generally classified into high, medium and low-density polyethylene (HDPE, MDPE and LDPE). The chemical formula for polyethylene is $(C_2H_4)n$. Polyethylene plastics have some similar properties to Polypropylene (PP) such as semi-rigidity, good fatigue, good chemical resistance, and heat resistance, among others. However, there are some differences between HDPE and PP, such as PP has better temperature resistance, which is why they are safe to use in microwaves, and as food storage bowls, but have lower densities of about 0.91 g/cm^3 compared to HDPE.

Polypropylene (PP) plastic is a thermoplastic produced by chain-growth polymerisation from the propylene monomer. It is non-polar, semi-crystalline and belongs to the group of polyolefins. The chemical formula for polypropylene is $(C_3H_6)n$. PP are used in a variety of applications such as packaging, industries such as automotive industry, textiles and others. There are two main types of polypropylene: homopolymers and copolymers. The homopolymer polypropylene is the general-purpose grade while copolymer is further divided into block and random copolymer polypropylene which are incorporated with ethylene (5% to 15% for block and 1% to 7% for random copolymer). In addition, PP plastic has high resistance to electricity which is useful for electronic components and have good properties for living hinges.

Polystyrene (PS) plastic is a transparent thermoplastic that exists as both solid plastics and rigid foam material. It is an aromatic hydrocarbon polymer made from styrene monomer. Polystyrene chemical formula is $(C_8H_8)n$ with densities between 0.96 – 1.04 g/cm^3. There are three major types of polystyrene, which include polystyrene foam, regular polystyrene plastics and polystyrene film. Polystyrene foam is further divided into expanded polystyrene (EPS) known as the common types of polystyrene (such as styrofoam) and extruded polystyrene (XPS) with wide use in applications such as architectural building models. Furthermore, it is widely used to make home and appliance insulation, lightweight protective packaging, automobile parts, in the food service and packaging industries as rigid trays and containers, foam bowls, cups, plates, cutleries and disposable eating utensils, among others.

There are seven (7) most common plastics with each having an identification code as designated by the Society of Plastics Industry (SPI) known as SPI code or number [2, 3]. These include:

i. Polyethylene terephthalate (PET), with SPI of 1. Common uses of PET are cooking oil/water bottles, peanut butter container, medicine jars, clothing, rope, carpet etc.

ii. High Density Polyethylene (HDPE), with SPI of 2. Common uses of HDPE are found in food storage and packaging such as beverages, yoghurt & milk containers, detergent/shampoo/conditional/soap & bleach containers, etc.

iii. Polyvinyl chloride (PVC) with SPI of 3. One of the most common uses of this is in plumbing pipes, plastic pipes, furniture and tiles are made of PVC.

iv. Low Density Polyethylene (LDPE) with SPI of 4. Also used in food storage containers such as grocery bag, disposable cutleries/cups/plates, dustbin & product carrying bags, plastic film, etc.

v. Polypropylene (PP) with SPI of 5. These are also used for making drinking straws, bottle caps, food containers, syrup and prescription bottles, etc.

vi. Polystyrene (PS) with SPI of 6. Uses include disposable coffee cups, plastics cutlery, food boxes.

Others miscellaneous types of plastic designated as SPI no.7 such as polycarbonates, polylactide. There are used in compact disc, medical storage containers, baby bottle, etc.,

3.2.2 Biomass samples and biomass components

Six different biomass samples from agricultural wastes were selected and investigated. These included rice husk, sugarcane bagasse, coconut shell, wheat straw, cotton stalk and palm kernel shell. In addition, the three main biomass components (also known as model compounds) which include cellulose, hemicellulose (xylan) and lignin were equally investigated in this study. The biomass sample wastes such as rice husk and sugarcane bagasse were obtained from Pakistan, coconut shell and palm kernel shell from Ghana, wheat straw from the United States, while cotton stalk was obtained from Syria. The biomass components were obtained from Sigma-Aldrich, UK Ltd. The biomass components were in powder form, with particles of about 1mm as shown in Figure 3.2, while the six biomass samples were ground into small sizes of about 212 microns, with irregular shapes as shown in Figure 3.3.

Figure 3.2. Biomass components (from left to right: cellulose, xylan (hemicellulose) and lignin kraft).

Figure 3.3. Biomass samples (from left to right: Rice husk, coconut shell, sugarcane, palm kernel shell, cotton stalk and wheat straw).

3.2.3 Proximate and Elemental analysis

Elemental analysis (also known as CHNS–O analysis) was carried out for the waste/pure plastics, biomass samples, and biomass components samples to determine carbon (C), hydrogen (H), nitrogen (N) and sulphur (S) content in feedstock. The elemental analyser used was a Thermo EA2000 (Figure 3.5), with a boat inside the analyser into which about 2 to 3mg weights of samples were placed for the analysis. High-density polyethylene (HDPE) and polystyrene (PS) plastic wastes were analysed. Likewise, the six different agricultural waste biomass samples were investigated, consisting of coconut shell, rice husk, sugarcane bagasse, cotton stalk, wheat straw and palm kernel shell. The three main biomass components, cellulose, hemicellulose (xylan) and lignin were equally analysed. High carbon contents (greater than 80 wt.%) were observed in plastic wastes as compared with biomass samples which were slightly above 40 wt.%. The lignin biomass component had the highest carbon content of ~ 60 wt.% as shown in Table 3.1. The nitrogen contents were detected in all the samples except xylan. Sulphur content of all the biomass and plastic samples were not detected except that of lignin with an amount of about 1.2 wt.%. This high sulphur content from lignin kraft used in this study is based on the extraction process. According to Nasrullah et al. [4], there are two main types of lignin based on extraction; the sulphur lignin and sulphur-free lignin. The sulphur-containing lignin is produced by commercial chemical pulping processes (paper and pulp industries), which includes the kraft lignin and lignosulfonates while the sulphur-free lignin includes soda or alkaline lignin and organosolv lignin produced by bioethanol production processes [4, 5]. Oxygen contents were determined by the difference in weight percent of the composition of the feedstock. Biomass samples had high oxygen contents above 40 wt.% compared to plastic wastes which were < 10 wt.%. The individual feedstock compositions contributed immensely to product distribution, as each type of sample determined the type of product yield.

Table 3.1. Elemental analysis of biomass samples, biomass components and plastic wastes.

Elemental analysis **Feedstock**	**C** **wt.%**	**H** **wt.%**	**N** **wt.%**	**S^a** **wt.%**	**O^b** **wt.%**
Coconut shell	48.32	5.26	0.29	nd	46.14
Sugarcane	44.34	5.92	0.57	nd	49.17
Cotton stalk	43.10	6.24	1.59	nd	49.07
Palm kernel shell	50.11	6.24	1.50	nd	42.16
Wheat straw	40.58	4.84	0.74	nd	53.84
Rice Husk	37.60	5.26	1.69	nd	55.45
Lignin	60.08	5.48	1.10	1.20	32.14
Cellulose	41.61	5.63	0.11	nd	52.64
Xylan	42.01	6.01	nd	nd	51.98
HDPE (waste)	81.78	10.59	0.54	nd	7.08
PS (waste)	90.49	6.87	0.52	nd	2.11

^{a}nd= not detected, b= calculated by difference.

Table 3.2. Proximate analysis of biomass samples and biomass components.

Proximate analysis **Feedstock**	**Moisture** **wt.%**	**Volatile** **wt.%**	**Fixed carbon** **wt.%**	**Ash** **wt.%**
Cellulose	4.74	84.16	9.85	1.25
Lignin	3.39	57.54	34.06	5.01
Xylan	3.33	82.18	12.15	2.34
Coconut shell	7.16	68.58	22.00	2.26
Cotton stalk	7.33	69.54	19.47	3.67
Palm kernel shell	6.70	67.52	22.13	3.65
Rice Husk	8.02	61.43	12.53	18.02
Sugarcane	5.33	83.39	7.79	3.49
Wheat straw	5.19	64.24	15.60	14.97

[a]nd= not detected, b= calculated by difference.

Also, proximate analysis using a thermogravimetric (TGA) analyser for all the samples were conducted as shown in Table 3.2. The proximate analysis was carried out to measure the moisture, ash and volatile content of each feedstock while the fixed carbon was determined by the difference in the weight percent. An example of a TGA thermogram from proximate analysis of coconut shell shown in Figure 3.4. The highest fixed carbon was exhibited by lignin both for biomass samples and components. Lignin alone showed a significant amount of sulphur content while others were negligible. Among all the biomass samples analysed, rice husk exhibited the highest ash content, and the lowest ash content was shown by cellulose. Reveendran et al. [6] equally carried out pyrolysis studies of different biomass samples and stated that the presence of ash content in biomass seems to have an influence on the pyrolysis characteristics and the product distribution. The high carbon content and fixed carbon found in lignin as well as high ash content in rice husk and low ash content in cellulose have been reported by other researchers [7]. According to Yang et al. [8], the production of volatile matter from biomass is the summation of the individual contributions from the three main biomass components, and also the yield of volatiles, gases and chars from pyrolysis were found to be proportional to the three major components in the biomass sample [8].

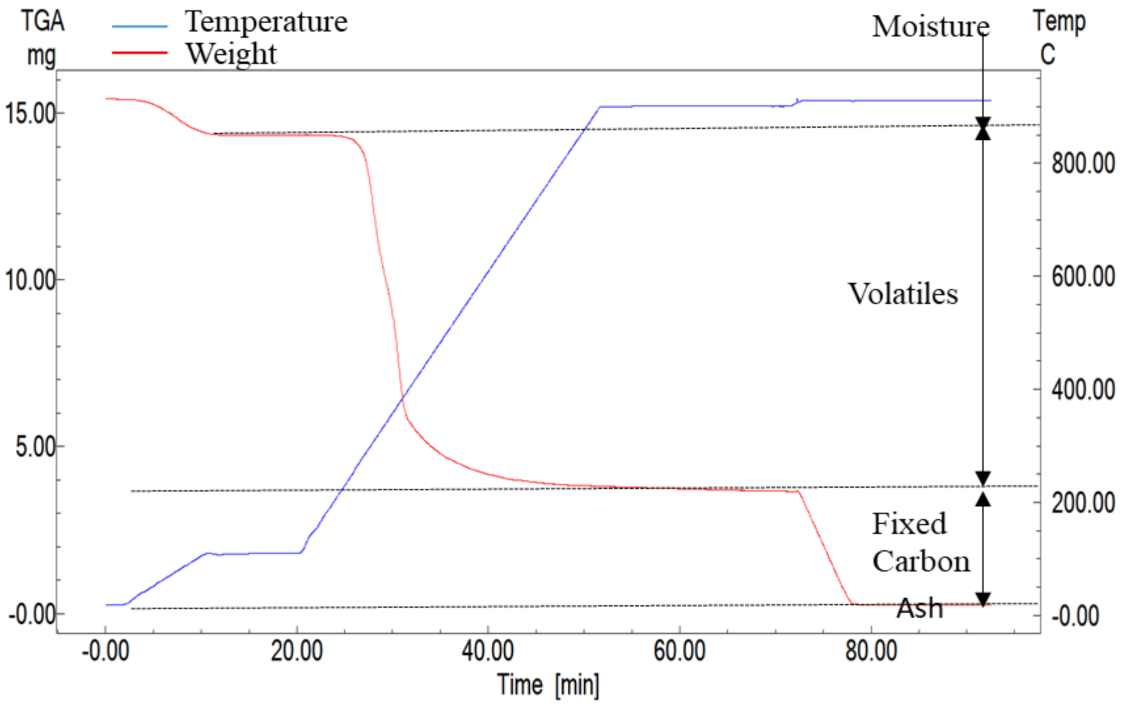

Figure 3.4. An example of proximate analysis TGA thermogram of coconut shell.

Figure 3.5. Illustration of the Elemental Analyser (CHNS-O).

3.2.4 Catalyst development and preparation

3.2.4.1 Metals on Y-zeolite catalysts

In this section, Y-zeolite commercial catalyst was investigated. The Zeolite Y (or Y-zeolite) catalyst was in pellet form of approximate size, 1mm by 5 mm. The Y type zeolites belong to the faujasite family, which consists of a cage like structure with pores, comprised of 12- membered rings. The Y-zeolite catalyst was obtained from Nankai University Catalyst Co. Ltd, Tianjin, PR China. Also, the incorporation of different transition metals impregnated on Y-zeolite was further explored for the production of higher grade fuels and chemicals through the pyrolysis-catalysis of high density polyethylene in a two-stage fixed bed reactor. The transition metals investigated included; nickel (Ni), iron (Fe), molybdenum (Mo), ruthenium (Ru), gallium (Ga) and cobalt (Co).

The transition metals were impregnated on the commercial Y-zeolite catalyst at 1 wt.% and 5 wt.% metal concentrations. The procedure for the preparation of the catalysts involved; aqueous solutions of the different metals prepared from $Ni(NO_3)_2{\cdot}6H_2O$, $Fe(NO_3)_3{\cdot}9H_2O$, RuO_2, $Ga(NO_3)_3{\cdot}H_2O$, $(NH_4)6Mo_7O_{24}{\cdot}4H_2O$, and $Co(NO_3)_2{\cdot}6H_2O$ via dissolution in 20 ml of deionised water with heating and stirring at a temperature of 45 ^oC. The Y-zeolite catalyst support was further added and then heated to 90 ^oC. Furthermore, the metals/Y-zeolite mixtures were left to mix for 1hr until they formed semi-solid slurries. Each slurry was dried overnight in an oven at 105 ^oC, calcined at a temperature of 500 ^oC for 3 hours and then sieved to obtain a uniform size of about 50-212 µm. These metal catalysts were used for all the experiments conducted in chapter four.

3.2.4.2 10% Ni/Al_2O_3

The catalyst used in conducting the catalytic steam reforming experiments of the six agricultural biomass waste samples as well as the three main components of biomass was a 10 wt.% $NiAl_2O_3$ as investigated in a two-stage fixed bed reactor. The catalyst was prepared by an incipient wetness impregnation method. The preparation process involved an aqueous solution of $Ni(NO_3)_2{\cdot}6H_2O$ in 20 ml of deionised water, which was stirred while heating at 45 ^oC. The alumina (Al_2O_3) support was added to the mixture, which was continuously stirred and then heated to 90 ^oC, and left for 1 hour until a semi-solid slurry was formed. The precursor slurry was dried overnight at 105 ^oC and the catalyst was calcined under an air atmosphere at a temperature of 750 ^oC for 3 hours. The catalyst was ground and then sieved to particle sizes of 50-212 µm. This nickel alumina catalyst was used for all the experiments conducted in chapter five.

3.2.4.3 Metals on MCM-41

In this section, a commercial mesoporous MCM-41 catalyst obtained from Nankai University Catalyst Co. Ltd, Tianjin, PR China, was used in conducting the catalytic steam reforming of volatiles from co-pyrolysis of biomass components with plastic wastes. The catalysts were prepared by an incipient wetness method. The metals were impregnated on the MCM-41 support to produce 10 wt.% of Ni/Co/Mo(MCM-41). Aqueous solutions of $Ni(NO_3)_2{\cdot}6H_2O$, $Co(NO_3)_2{\cdot}6H_2O$ and $(NH_4)6Mo_7O_{24}{\cdot}4H_2O$ in 20 ml of deionised water were prepared and stirred continuously under heat. The MCM-41 support was added to the mixture and was stirred, heated to 90 ^oC and left for about an hour until it formed a semi-solid slurry mixture. The precursor slurry was then dried in an oven at 105 ^oC overnight until all of the excess water was evaporated. The prepared catalysts were equally calcined in a calcination under an air atmosphere at a temperature of 750 ^oC with a heating rate of 20 ^oC for three (3) hours. The catalysts were ground and sieved to particle sizes of 50 – 212 µm. The prepared fresh catalysts were additionally reduced under 95% of nitrogen with a 5% balance of hydrogen. Some of the experiments conducted in chapter 6 were done using these metal/MCM-41 catalysts.

3.2.4.4 Different support catalysts

Furthermore, 10% nickel metal was impregnated on different catalyst supports such as Al_2O_3, Y-zeolite and dolomite, respectively. An aqueous solution of $Ni(NO_3)_2{\cdot}6H_2O$ in 20 ml of deionised water was prepared and stirred under heat of 45 ^oC. The different Al_2O_3, Y-zeolite and dolomite supports were added to each mixture and stirred with heat of 90 ^oC and left for an hour until it formed a semi-solid slurry. The slurry was dried overnight at 105 ^oC in an oven until all of the excess water was evaporated. The prepared fresh catalysts were equally calcined under an air atmosphere at a temperature of 750 ^oC with a heating rate of 20 ^oC for three 3 hours. The catalysts were ground and sieved to a particle sizes of 50-212 µm. Additional, the prepared catalysts were reduced under 95% of nitrogen with a 5% balance of hydrogen. These catalysts were equally used for some of the experiments conducted in chapter six.

3.3 Experimental Reactor System

Two different two-stage fixed bed reactors were used in this project, the first was for pyrolysis and pyrolysis-catalysis of plastics. The second reactor was incorporated with a steam injection point attached to the reactor and was used for pyrolysis/co-pyrolysis-catalytic steam reforming of biomass samples, biomass components and plastic wastes as well as mixtures.

3.3.1 Operation and description of the two-stage fixed-bed reactor

The first reactor was a two-stage fixed bed reactor used for the pyrolysis and catalytic experiments of plastic samples. The reactor was made of stainless steel of total length 50 cm and 2 cm internal diameter, (see Figures 3.6 and 3.7). Pyrolysis of the plastic sample was conducted in the first section of the reactor and involved 2 g of the plastic sample held in place by a stainless steel crucible, thermally heated to a temperature of 600 ^{o}C at a heating rate of 10 ^{o}C min^{-1} and held at 600 ^{o}C for 30 minutes. The evolved volatiles from pyrolysis of the plastic sample was passed directly to the second stage catalytic bed containing 4 g of catalyst supported by quartz wool at the base, which had been previously preheated and maintained at the catalytic bed temperature of 600 ^{o}C with a heating rate of 20 ^{o}C min^{-1}. However, in the case of only pyrolysis experiment, quartz sand was used at the catalytic bed at the same temperature of 600 ^{o}C and heating rate of 20 ^{o}C min^{-1}. Nitrogen at a flow rate of 100 ml min^{-1} was introduced into the process and was used as the carrier gas to purge product gases from the reactor into the condensation unit. Two different thermocouples were used to measure the temperatures in each section of the reactor. The procedure for the experiment was to first heat the second stage catalyst reactor to 600 ^{o}C at a heating rate of 20 ^{o}C min^{-1}. Once the catalyst reactor temperature was reached and maintained at that level, the pyrolysis reactor containing the feedstock was then heated to 600 ^{o}C at a heating rate of 10 ^{o}C min^{-1}. A three condenser system cooled in dry-ice (solid CO_2) was used to collect the liquid-oil produced while the non-condensable gases were collected in a 25 litres Tedlar™ sample gas bag before GC analysis. Experiments were repeated for accuracy as well as mass balances of above 90 wt.% with negligible differences between the repeated experiments. The results were the average of the repeated experiments using this two-stage reactor.

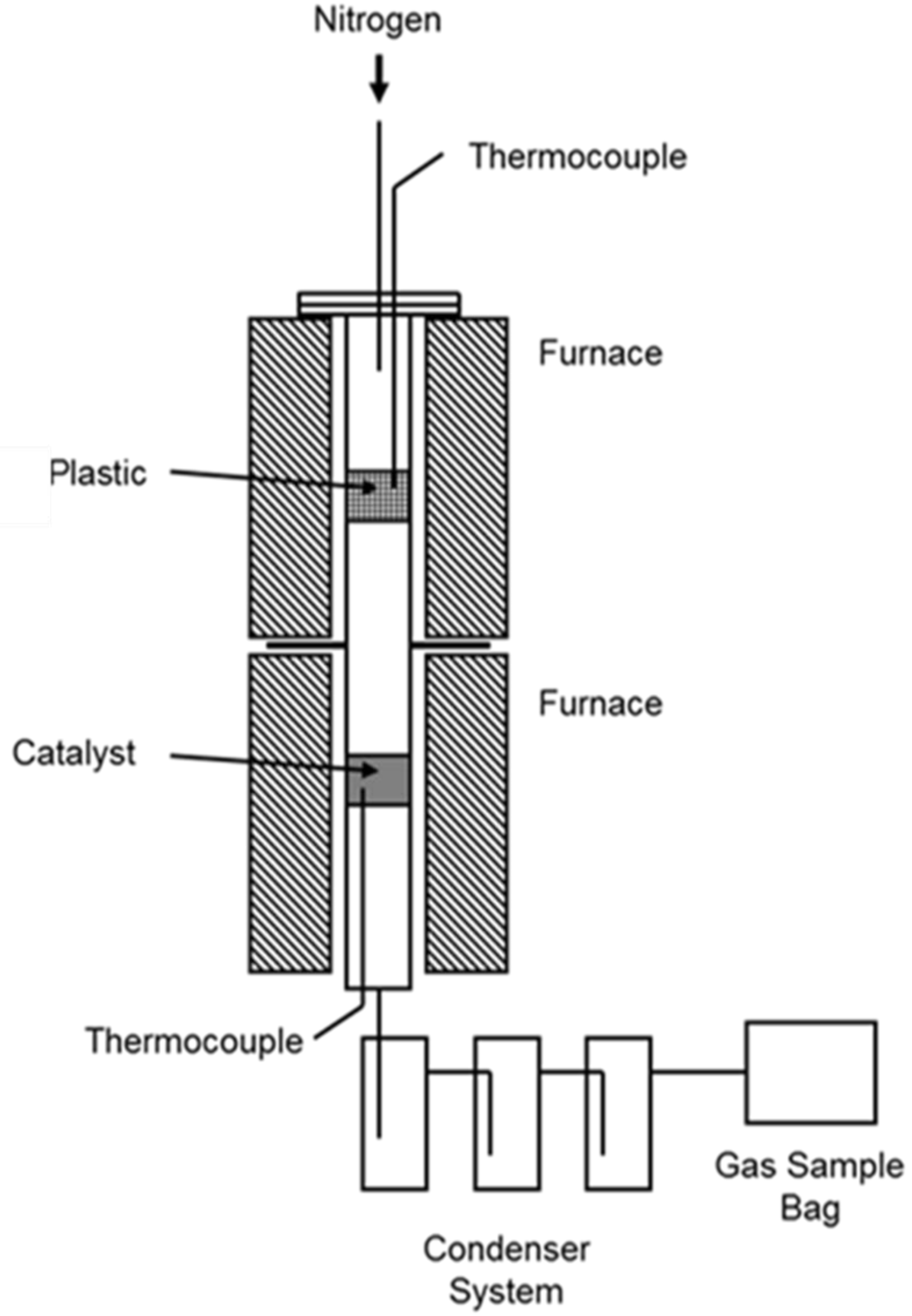

Figure 3.6. Illustration of the two-stage fixed bed reaction system.

Figure 3.7. Experimental set up of the two-stage fixed bed reactor system (photograph).

The second reactor was also a two-stage fixed bed reactor system operated with a steam injection point as shown in Figures 3.8 and 3.9 for pyrolysis/co-pyrolysis-catalytic steam reforming of biomass samples, biomass components and mixtures of biomass components with plastic wastes. This second reactor was modified for biomass feedstock experiments. The reactor was constructed of stainless steel of length 60 cm, internal diameter 2.5 m and heated externally using two separate 1.2 kW electrically-heated and controlled tube furnaces. Pyrolysis of the feedstock took place in the first stage reactor where the 2 g of feedstock was stationed in a crucible boat in the centre of the pyrolysis reactor. The second stage was a catalytic steam reforming reactor containing 1.0 g of catalyst supported by quartz wool. Furthermore, uncatalysed experiments were also carried out for comparison with the catalysed steam reforming experiments, where clean quartz sand was used in place of the catalyst in the second section of the reactor. The pyrolysis temperature was 550 ^{o}C with a heating rate of 20 ^{o}C min^{-1} from ambient to 550 ^{o}C. The volatiles from the feedstock (biomass samples, biomass components and biomass components with plastic wastes blend) pyrolysis were passed to the second section (stage) which was previously preheated to catalytic bed temperature of 750 ^{o}C at a heating rate of 40 ^{o}C min^{-1}, ready to react with the volatiles. However, in the case of pyrolysis experiments, quartz sand was used at the catalytic bed at the same temperature of 750 ^{o}C and heating rate of 40 ^{o}C min^{-1}. Water was injected at a flow rate of 5.7 g h^{-1} into the second stage catalyst bed reactor to produce steam for catalytic steam reforming. Nitrogen was introduced and was used as the carrier gas at a flow rate of 200 ml min^{-1}. Two thermocouples were used to monitor and control the temperatures of the biomass pyrolysis and catalytic bed. The experimental procedure was to first heat the second stage catalyst reactor to 750 ^{o}C at a heating rate of 40 ^{o}C min^{-1} and once the catalyst reactor temperature had stabilised, the pyrolysis reactor containing the feedstock was then heated to 550 ^{o}C at a heating rate of 20 ^{o}C min^{-1}, with the injection of water into the second stage reactor for catalytic steam reforming of the evolved volatiles. The condenser system used to collect liquids produced consisted of air-cooled and solid dry-ice (CO_2) cooled condensers. After the condenser system, all of the non-condensable gases were collected in a 25 litres Tedlar gas sample bag. The experiments conducted in this two-stage fixed bed reactor were repeated for accuracy as well as a mass balances of above 90 wt.% with negligible differences between the repeated experiments, and the results were the average of the repeated experiments.

Figure 3.8. Two-stage fixed bed reactor system with steam injection system, experimental set up (photograph).

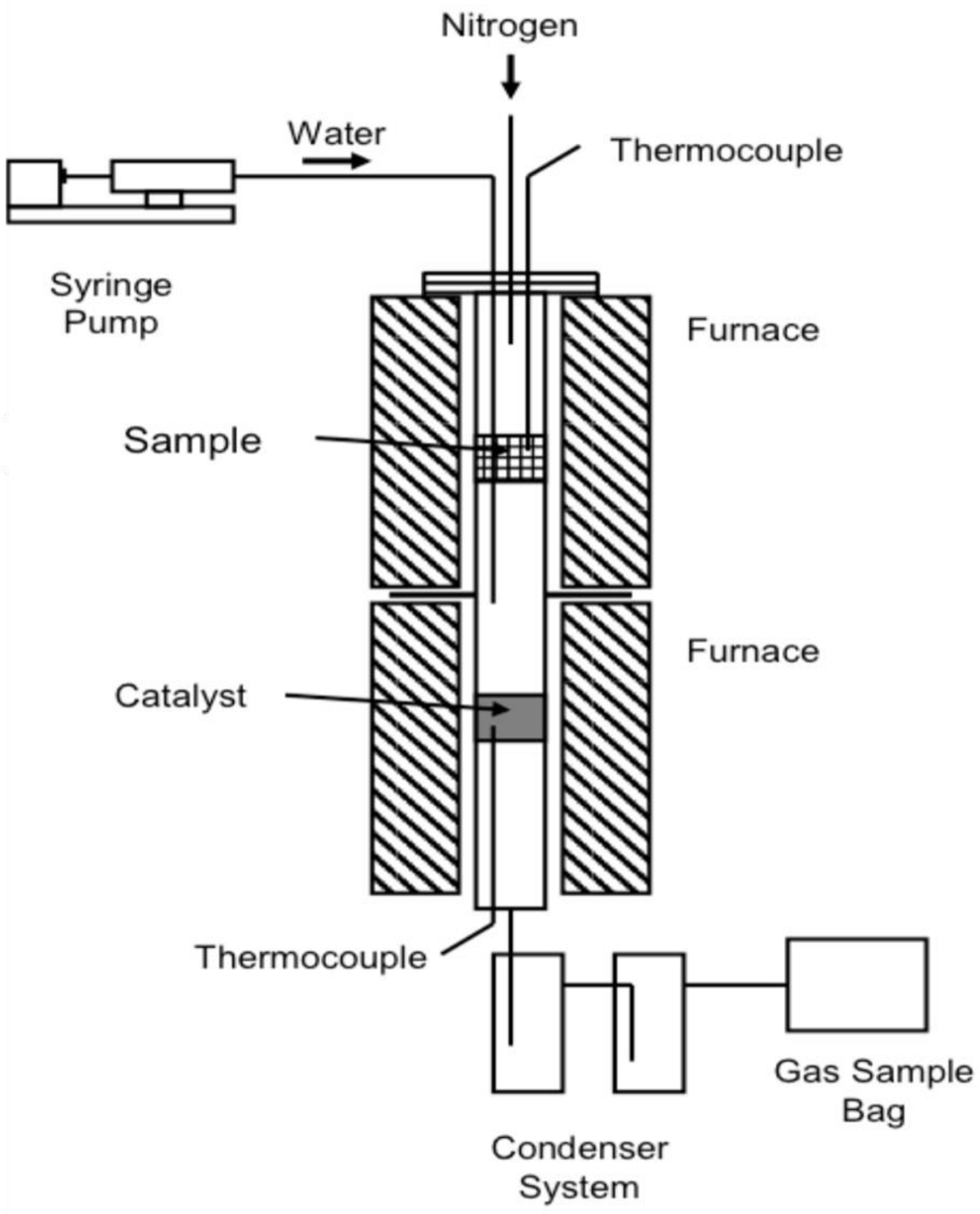

Figure 3.9. Schematic diagram of a two-stage fixed bed reactor system with steam injection system.

3.3.2 Start up and validation of products by pyrolysis-catalysis in the two-stage fixed-bed reactor

All the reactors were designed and constructed within the Energy Research Institute in the School of Chemical and Processing Engineering, University of Leeds. The first reactor was newly set up for the purpose of these research experiments, therefore, validation had to be carried out to ensure accuracy of the experimental results. But, the second reactor had been used by previous PhD research students and was well-validated. Several experiments were conducted to validate and to optimise the reactor plus the condenser system. Repeated experiments were also conducted to validate and to determine accuracy of the obtained results as well as the most appropriate conditions and suitable operating parameters for the pyrolysis-catalysis process in the two-stage fixed bed reactors. For the experiments conducted, the results are shown in Table 3.3, in relation to product yields and mass balances obtained from the pyrolysis-catalysis of the two stage fixed bed reactor over Y-zeolite catalyst. The same conditions were used for all experiments conducted; the reaction temperature was set at 600 ^{o}C for both pyrolysis and catalytic bed temperature, and 2 g of virgin HDPE plastic sample and 1g of catalyst was used. The experiments were repeated in order to show reliability of the results and stability of the reactor system. All the experimental results showed consistency of product yields and mass balances obtained, as well as reproducibility of results which were all within a close range in the repeated experiments.

Table 3.3. Reproducibility analysis of product yields and mass balances for pyrolysis-catalysis of HDPE with catalyst in a two-stage fixed bed reactor.

	Exp 1	**Exp 2**	**Exp 3**	**Exp 4**	**Exp 5**	**Mean**	**Std. dev.**	**Rel. std. dev.**
Gas yield (wt.%)	55.67	56.02	55.85	55.80	55.88	55.84	0.13	0.23
Liquid yield (wt.%)	38.50	38.50	39.00	38.63	38.53	38.63	0.21	0.55
Char (wt.%)	5.00	5.00	5.00	5.00	5.00	5.00	0.00	0.00
Mass bal. (wt.%)	99.17	99.52	99.35	99.30	99.38	99.34	0.13	0.13

In the repeatability of the pyrolysis-catalysis/ pyrolysis-gasification in a two-stage reactor, the gas injection for all experiments are usually repeated about three times to check the consistency of the results. The results of all the products yields consisting of gas yields, liquid yields, char and the mass balances had standard deviations and relative standard deviations below 10% of the mean value, which are an acceptable and reliable.

3.4 Characterisation of materials and analysis of products

3.4.1 Material analysis

3.4.1.1 TGA

Thermo-gravimetric analysis (TGA) was used to characterise plastic wastes and biomass samples for the determination of thermal degradation. TGA and DTG curves of the waste samples were plotted as output of the analysis. The TGA curve denotes the percentage weight loss of the samples analysed with increasing temperature while the DTG curves are the differential of TGA showing inflection point of any change in the physical and chemical properties as a result of the thermal effects. For example, Figure 3.10a shows a TGA curve for individual virgin plastic (PP and HDPE), Figure 3.10b shows TGA-DTG curves for high-density polyethylene (HDPE). The degradation temperature of HDPE and PP is between the range of 450 and 500 ^{o}C, with HDPE having slightly higher temperature as shown in Figure 3.10a.

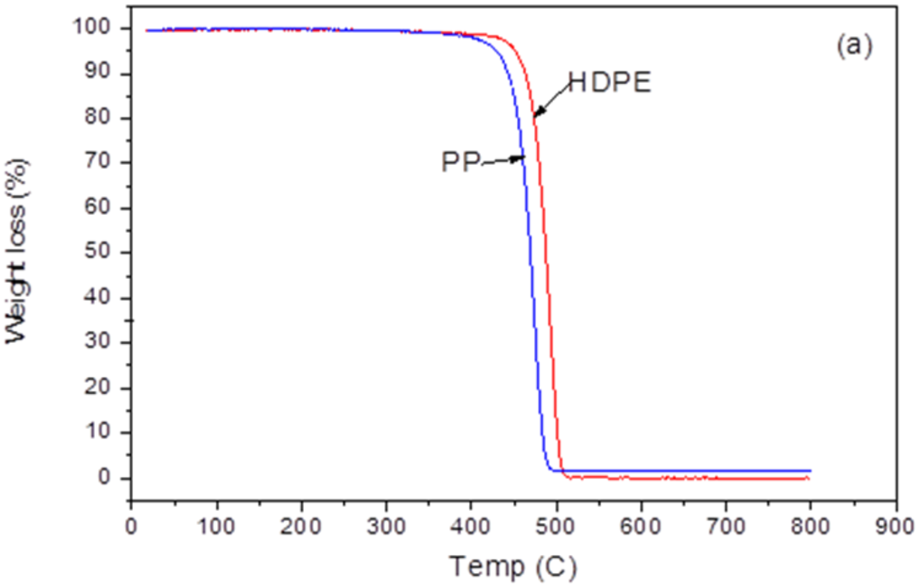

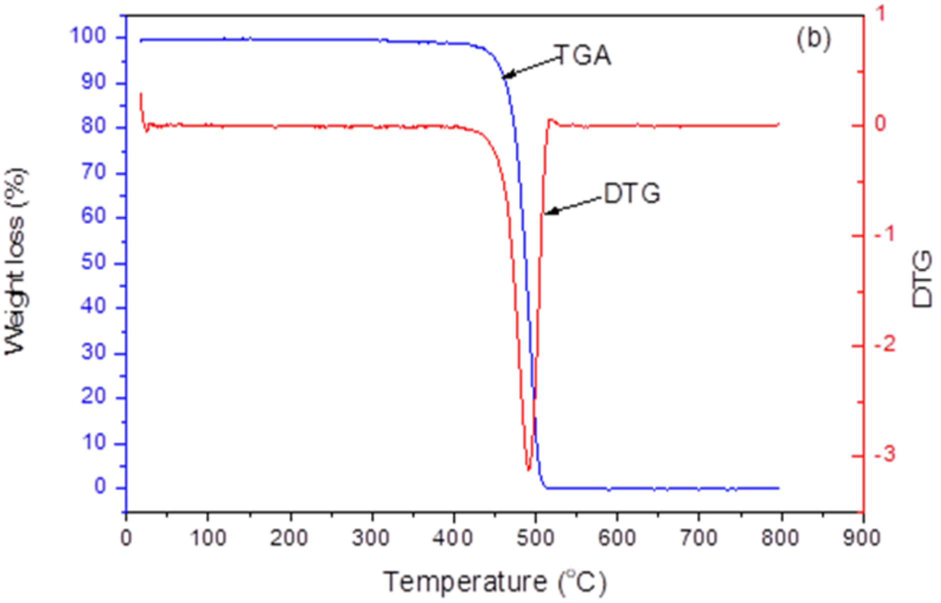

Figure 3.10. Illustration of thermogravimetric analysis for (a) individual plastic, (b) TGA-DTG curves for HDPE.

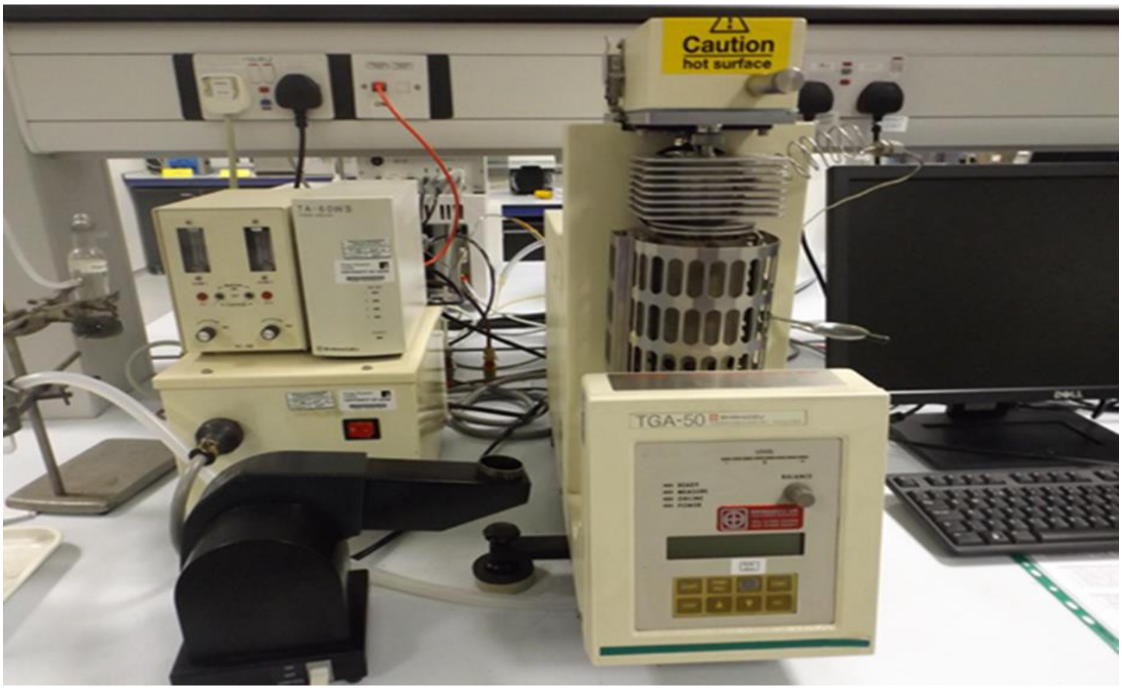

Figure 3.11. Illustration of the thermogravimetric analysis instrument.

3.4.2 Catalyst analysis (fresh and reacted)

3.4.2.1 TGA-TPO

Temperature programmed oxidation (TGA-TPO) experiments were conducted using a thermogravimetric analyser (TGA) 50 Shimadzu instrument (Figure 3.11). Controlled oxidation of the carbon deposited on the used catalysts after reaction was carried out to determine the amount and type of carbon deposited. The TPO analysis is used to determine the weight loss data of used catalysts which by calculation subsequently gave the mass of carbon deposit. Sample weights of between 25-30 mg of the reacted catalysts were placed in an alumina crucible inside the thermogravimetric analysis machine for analysis. The samples were heated from room temperature to a final temperature of 800 ^oC, at a heating rate of 15 $^oC\ min^{-1}$. Air was used as the oxidising agent at a flow rate of 50 ml min^{-1}.

The pyrolysis-catalysis processes usually form carbon deposits on the catalyst which might deactivate the catalyst, depending on the type of carbon, and the TGA-TPO process oxides the carbon in relation to the temperature of oxidation. The oxidation of the carbon occurred over a temperature range of 400-650 ^oC. It has been reported that carbon oxidation occurring in the lower temperature range of 450-550 ^oC is mainly ascribed to amorphous type carbon and oxidation in the temperature range of 550-650 ^oC is ascribed to filamentous type carbon [30]. The amorphous type carbons are more problematic for catalyst activity in that the coke encapsulates the metal particles, reducing catalyst activity. Filamentous carbons grow away from the catalyst surface and have less of an effect on the catalyst activity. An example of a TGA-TPO thermogram for Y-zeolite catalyst is shown in Figure 3.12.

The amount of carbon deposited on the catalyst is usually calculated using Equation (3.1)

$$W = \frac{(W_1 - W_2)}{W_1} X\ 100\ (wt.\%) \qquad 3.1$$

Where W is the amount of carbon deposited on the catalyst in wt.%,

W_1 is the initial weight of the catalyst after the loss of moisture (water) and

W_2 is the final weight of the catalyst after oxidation.

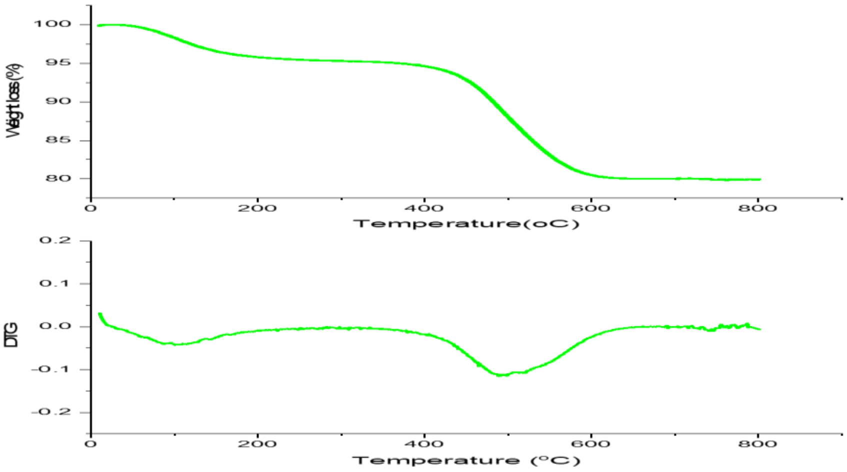

Figure 3.12. TGA-TPO and DTG-TPO thermograms of Y-zeolite catalyst at 700 °C.

3.4.2.2 Brunauer-Emmett-Teller (BET) surface area and porosity analysis

The surface area, pore size and pore volume of fresh catalysts were obtained using a Quantrachrome NOVA 2200e instrument as shown Figure 3.13. The analysis was carried out by weighing about 1-2 g of each sample in a sample tube and then degassed under vacuum for about 2-3 hours at a temperature of 200 °C, in order to remove and to clear the surface of the pores of the catalyst from previous physical adsorption materials, impurities and moisture. After the degassing process, the sample was reweighed and then transferred to the analysis chamber insulated with an isothermal jacket and placed under nitrogen atmosphere. The total time for the analysis was 6-8 hours and usually carried out overnight. A full Isotherm analysis was conducted on the catalysts for the determination of the porous properties. The porosity properties such as BET surface area, pore size and pore volume were determined by measuring the amounts of nitrogen adsorption and desorption from the adsorbent sample surface at equilibrium vapour pressure by the static volumetric method. Nitrogen adsorption at the boiling temperature of 77K remains the most widely used method to determine catalyst surface area and its porous texture characterisation. The nitrogen adsorbed volume against its relative pressure is the determination of the adsorption isotherm while adsorbate desorption is the opposite of the adsorption except for mesopores where evaporation usually occurs at lower pressures. Table 3.4 shows the surface area and porosity of the prepared metal Y-zeolite catalysts. The Y-zeolite catalyst had a BET surface area of 421 m^2g^{-1}, and impregnation with the metals produced, in most cases, a small decrease in surface area. Pierella et al. [9], also reported a small decrease in the surface of ZSM-5 zeolite catalyst when metal promoters, including Mo and Zn, were incorporated into the catalyst. The increase in pore size with increasing metal loading might be due to selective closing of the smaller pores, although there is a loss of pore volume and surface area, the average pore diameter increases because the only pore remaining for physisorption are the larger one, see Table 3.4.

Table 3.4. BET surface area and porosity of prepared metal-Y-zeolite catalysts.

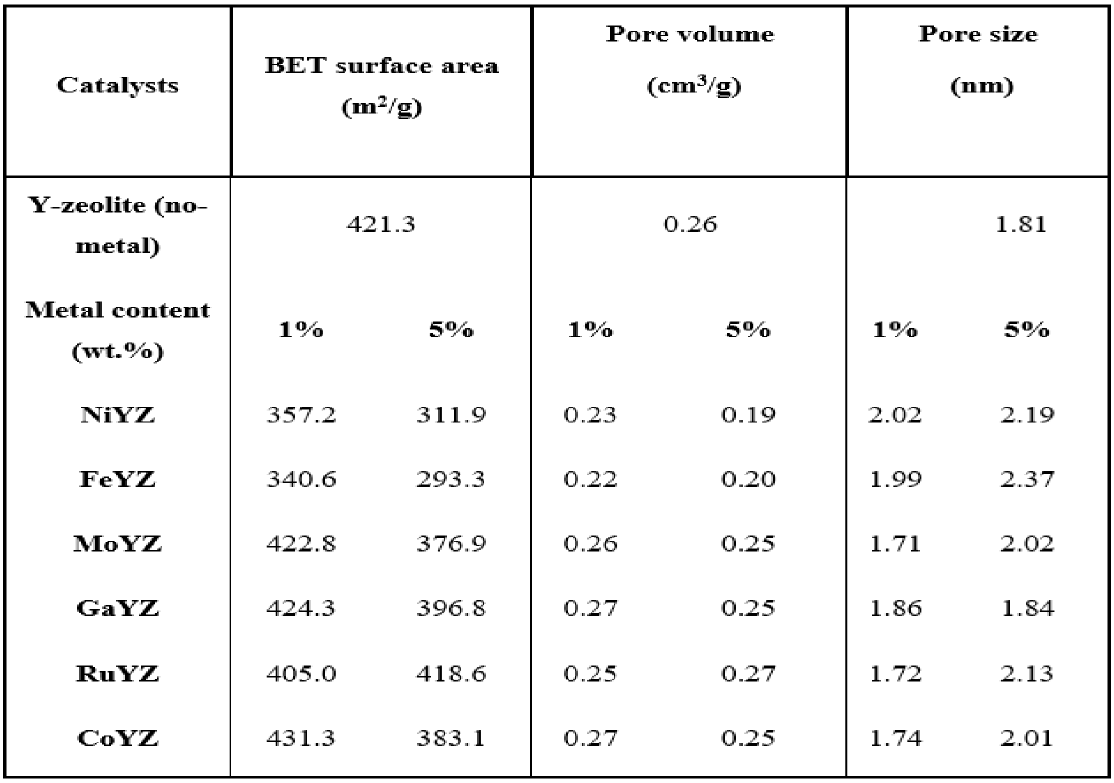

Catalysts	**BET surface area (m^2/g)**		**Pore volume (cm^3/g)**		**Pore size (nm)**	
Y-zeolite (no-metal)	421.3		0.26		1.81	
Metal content (wt.%)	**1%**	**5%**	**1%**	**5%**	**1%**	**5%**
NiYZ	357.2	311.9	0.23	0.19	2.02	2.19
FeYZ	340.6	293.3	0.22	0.20	1.99	2.37
MoYZ	422.8	376.9	0.26	0.25	1.71	2.02
GaYZ	424.3	396.8	0.27	0.25	1.86	1.84
RuYZ	405.0	418.6	0.25	0.27	1.72	2.13
CoYZ	431.3	383.1	0.27	0.25	1.74	2.01

Figure 3.13. BET surface area and pore size NOVA 2200e instrument.

3.4.2.3 Scanning electron microscopy (SEM)

Scanning electron microscopy (SEM) was used to produce images of the fresh and the reacted catalysts as well as biomass components and samples. These images helped to identify the types of carbon deposited on the catalysts. Two different microscopic techniques were used for the characterisation of the catalysts and the biomass feedstock. One was a high resolution scanning electron microscope Hitachi SU8230 while the other was a Field Electron Gun Scanning Electron Microscopy (FEGSEM) LEO 1530 coupled with an energy dispersive X-ray spectrometer (EDXS). The SEM analysis was conducted in order to further gain an understanding of the samples, in addition to other characterisation techniques. For example, TGA-TPO shows the type and amount of carbon deposited on the catalyst during reaction such as amorphous and filamentous carbons. Therefore, the results of SEM images may be compared with the results of TGA-TPO and DTG-TPO. The EDXS was used to characterise the elemental composition of the samples. The specimen was prepared in the form of powder, and an adhesive carbon tape was used to fix the sample on a flat aluminium stub. The prepared samples were coated with iridium/platinum. Examples of SEM images of the biomass samples are shown in Figure 3.14 and the analyser is shown in Figure 3.15.

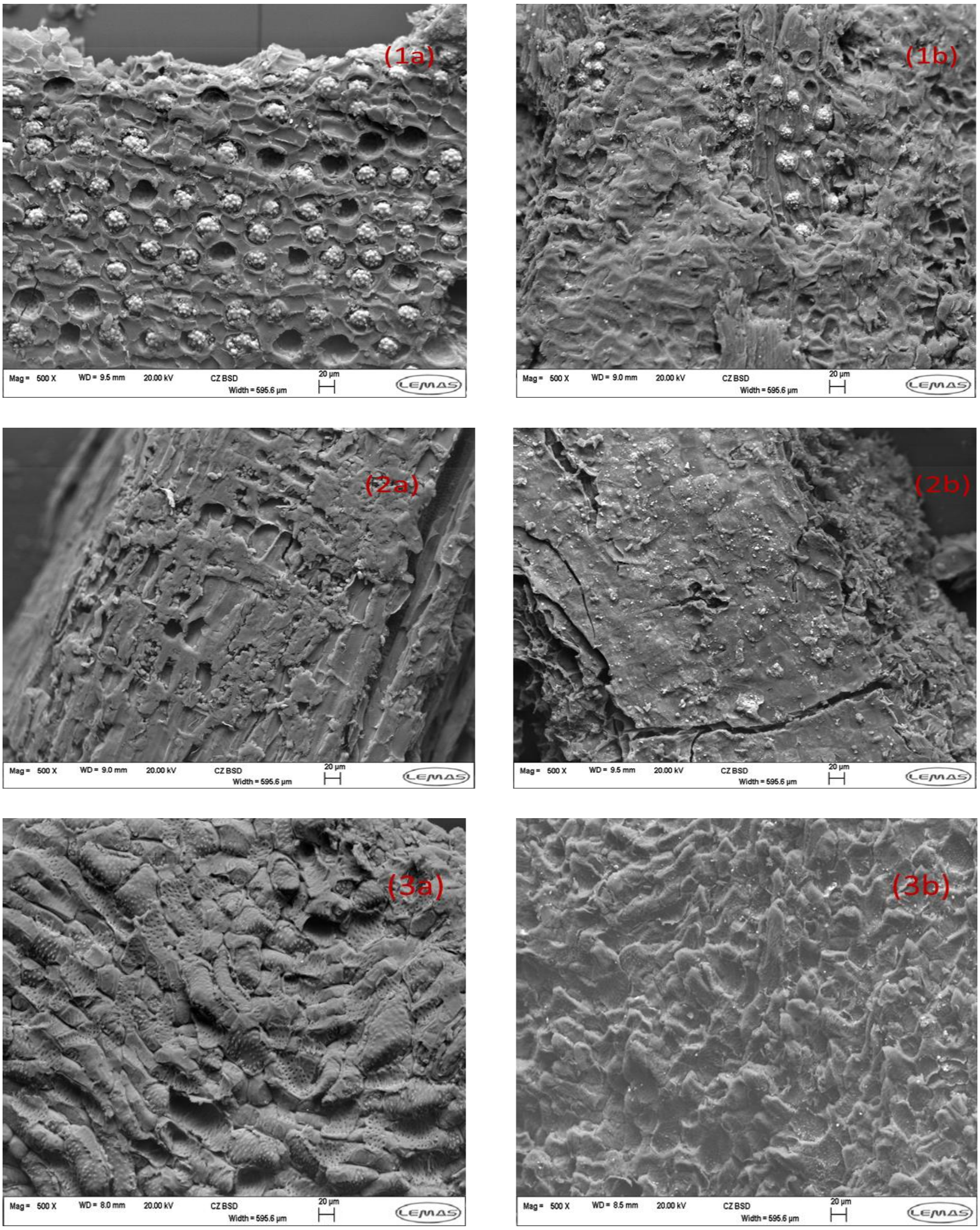

Figure 3.14. Scanning electron microscope images of (1a) Palm kernel shell sample (1b) Palm kernel shell char, (2a) Cotton stalk sample (2b) Cotton stalk char and (3a) Coconut shell sample (3b) Coconut shell char.

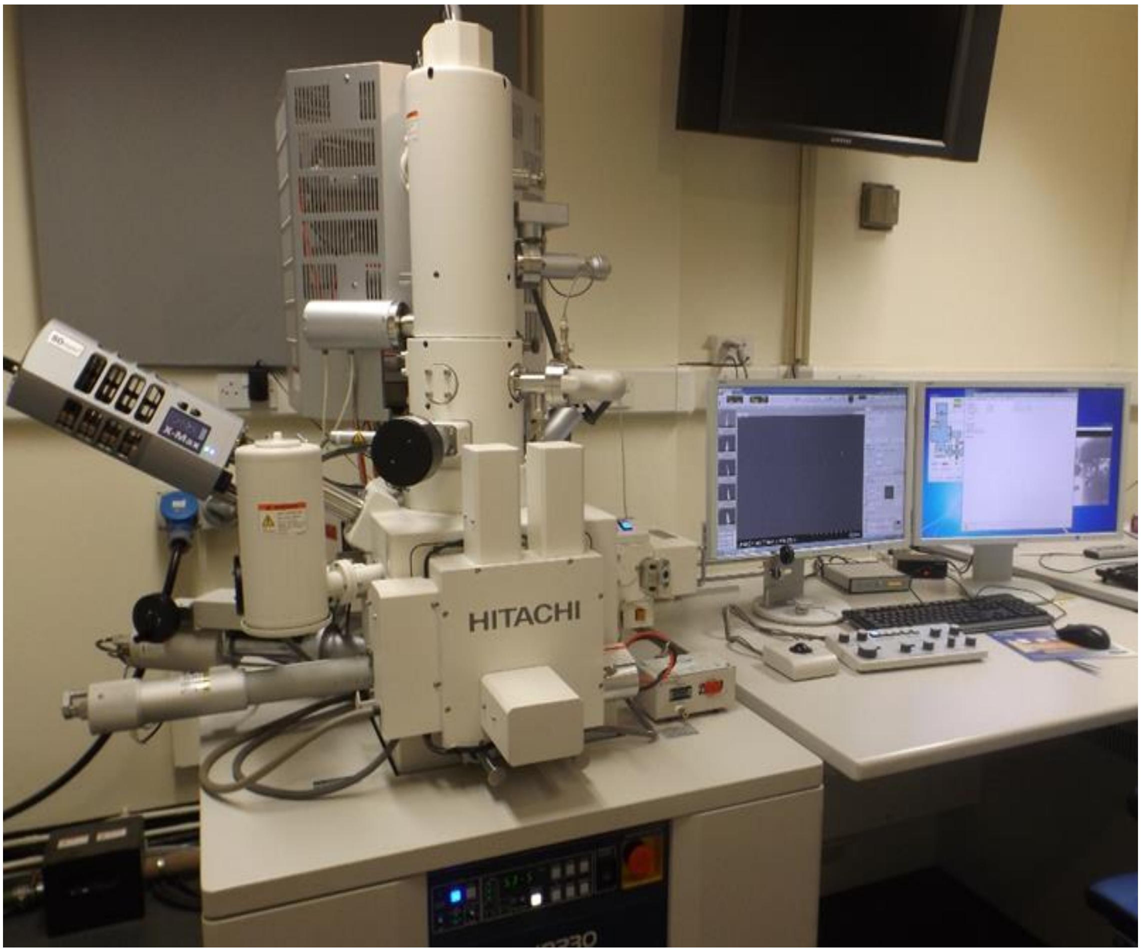

Figure 3.15. Scanning electron microscopy (SEM) Hitachi SU8230.

3.4.2.4 X-ray diffraction (XRD) analysis

X-ray diffraction analysis was conducted for both the fresh and reacted catalysts using a D8 Bruker (Figure 3.17) diffractometer using Cu-ka radiation X-ray source with a Vantec position sensitive detector. The XRD analysis was used in characterising the main chemical compounds, identifying crystalline structures and crystallite sizes. The specimen was prepared by placing the powdered sample on a specimen holder surface. The angle 2 theta (2θ) was varied from 10 to 80 degrees. DIFFRACplus software was used to record the data while HighScore Plus software was used to identify the produced spectra. An example of XRD spectrum of reduced 10%NiAl_2O_3 catalyst is shown in Figure 3.16.

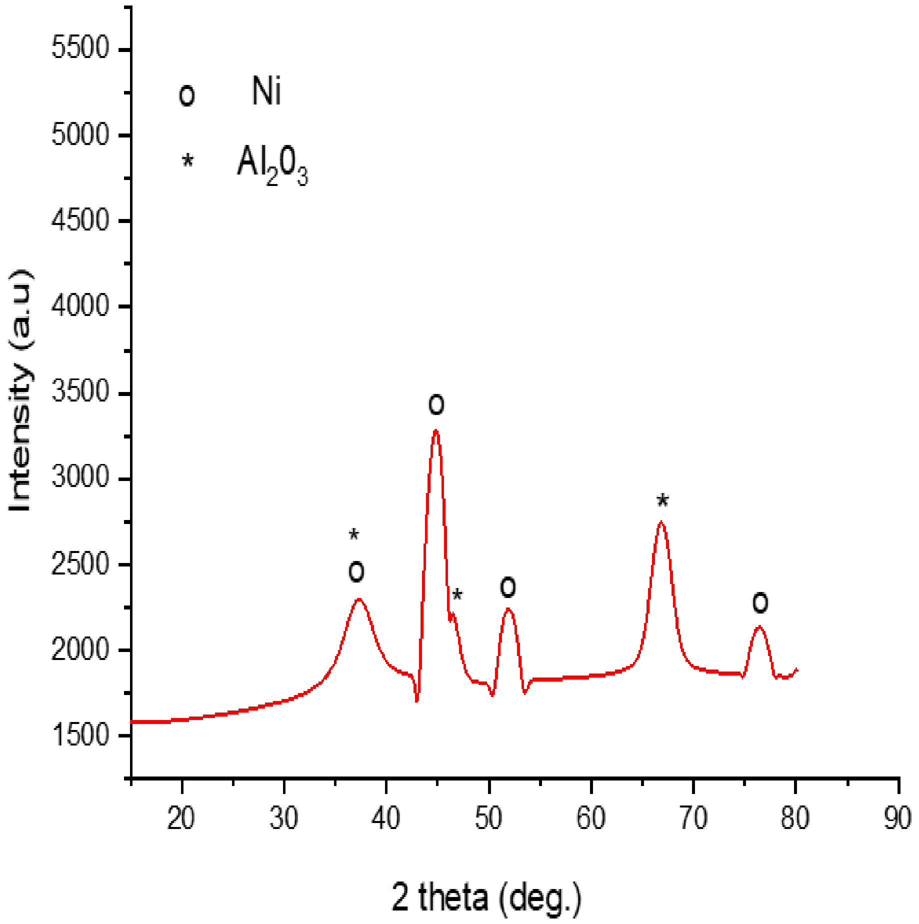

Figure 3.16. Example of an XRD spectrum of reduced 10%$NiAl_2O_3$ catalyst.

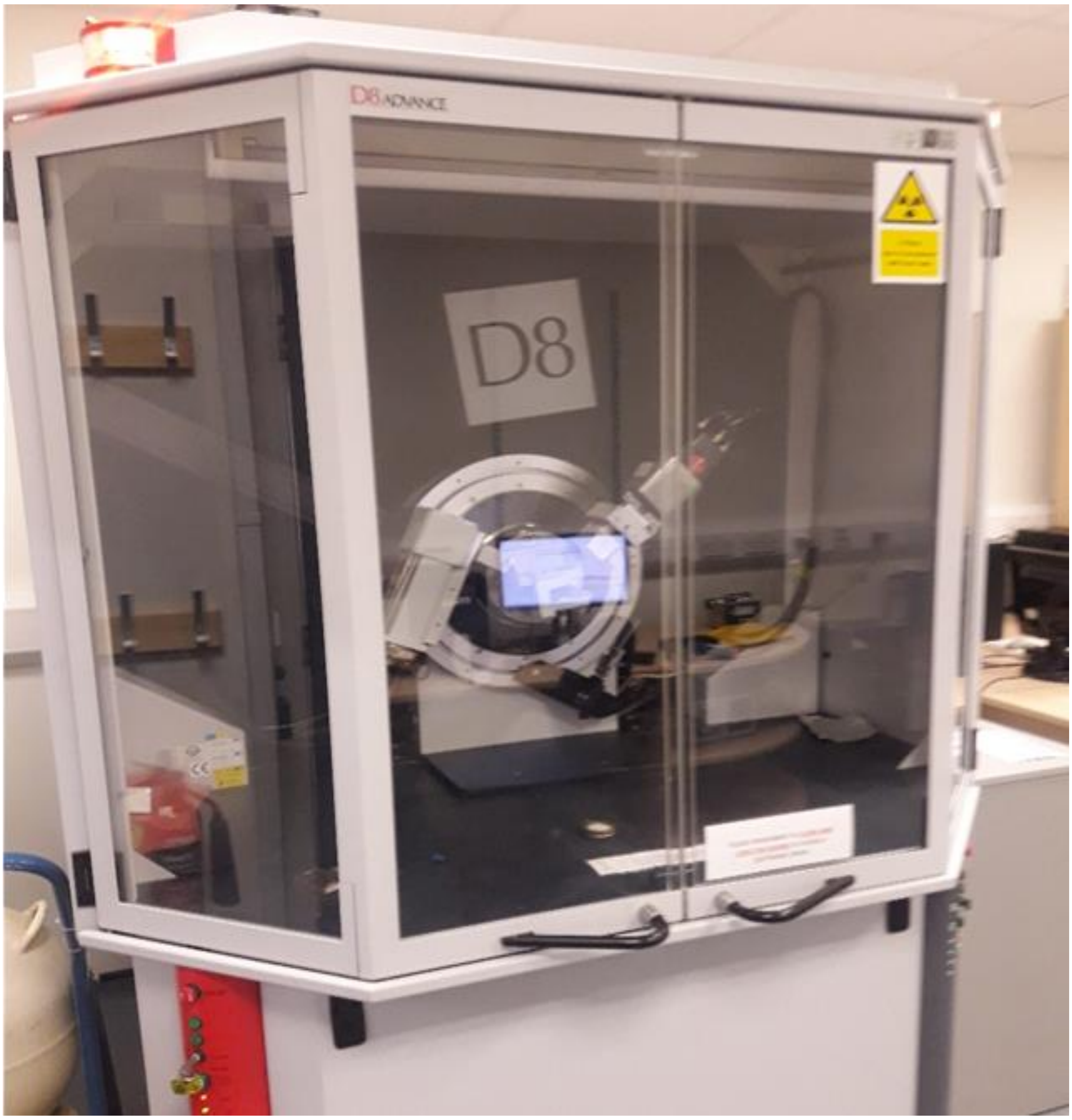

Figure 3.17. The Bruker D8 X-Ray diffraction Instrument.

3.5 Product analysis and calculations

3.5.1 Gaseous product analysis by gas chromatography (GC)

The produced gases collected from the process of pyrolysis-catalysis and the co-pyrolysis-gasification with catalysis experiments were analysed offline by packed column gas chromatography. The Tedlar sample gas bag was used to collect the produced gases and taken for gas analyses immediately after every experiment to avoid decomposition. Packed column gas chromatography was used to analyse the gases; hydrocarbon gases of C_1 to C_4 were analysed by a Varian CP 3380 gas chromatograph with a flame ionisation detector (FID), 2m x 2mm GC column, 80-100 mesh size Hayesep packed column and nitrogen as the carrier gas. The permanent gases, including hydrogen (H_2), nitrogen (N_2), oxygen (O_2) and carbon monoxide (CO), were analysed using a different Varian CP 3380 chromatography (GC) with a thermal conductivity detector (TCD), 2m x 2mm GC column, 60-80 mesh molecular sieve size Hayesep packed column with argon as the carrier gas. Carbon dioxide (CO_2) was analysed with adifferent Varian CP 3380 gas chromatograph with a thermal conductivity detector (TCD), 2m long x 2mm diameter GC column, 80-100 mesh molecular sieve size and argon was used as the carrier gas, the GC is shown in Figure 3.18.

Figure 3.18. Gas chromatograph for gas analysis.

3.5.1.1 Calibration of gas chromatographs

Standard gases were used for calibration of the GC equipment in order to ensure accuracy of results obtained from the analysis. The standard permanent gases used contained 1 vol. % of each gas (H_2, O_2, CO, CO_2) with a balance of nitrogen of about 96 vol.%. The hydrocarbon standard for the alkane gases contained 1 vol. % of each gas (methane, ethane, propane and butane) while the hydrocarbon standard for alkene gases contained 1 vol.% of each gas (ethylene, propene, butene and butadiene) with a balance of nitrogen respectively. The calibration was carried out by injecting 1ml of each standard gases into the respective GCs. Tables 3.5 and 3.6 show the repeatability of peak areas corresponding to each type of gas for the standard gases injected. Gases were identified based on the retention time indicated for each type of gas on the software, which was in turn used as reference for all the experimental gases obtained. In addition, the response factor was obtained based on the standard gases as used in an excel spreadsheet for all the calculations. Examples of GC- chromatograms of standard gas peaks are shown in Figure 3.19.

Table 3.5. Repeatability of peak area values for standard gases (permanent gases).

Perm Gases	**Exp 1**	**Exp 2**	**Exp 3**	**Exp 4**	**Exp 5**	**Mean**	**Rel. Std. dev.**
H_2	489445	489657	489710	489869	489617	489660	0.03
O_2	59526	59132	59033	58737	59205	59127	0.48
N_2	3886549	3890769	3891824	3894989	3889978	3890822	0.08
CO	41055	41118	41133	41180	41106	41118	0.11
CO_2	11778	11793	11797	11808	11790	11793	0.09

*****Peak area measured in mvolt per unit time as shown in Figure 3.19.

Table 3.6. Repeatability of peak area values for standard gases (hydrocarbon gases).

Hydrocarbon gases	**Exp 1**	**Exp 2**	**Exp 3**	**Exp 4**	**Exp 5**	**Mean**	**Rel. Std. dev.**
Methane	750776	750921	750849	750830	750862	750848	0.01
Ethene	1470029	1458455	1464242	1465689	1463157	1464314	0.29
Ethane	1436383	1435246	1435815	1435957	1435708	1435822	0.03
propene	2114871	2100543	2107707	2109498	2106364	2107797	0.25
Propane	2127444	2125958	2126701	2126887	2126562	2126710	0.03
Butene & Butadiene	5171640	5117903	5144772	5151489	5139734	5145107	0.38
Butane	2842177	2837393	2839785	2840383	2839337	2839815	0.06

*****Peak area measured in mvolt per unit time as shown in Figure 3.19.

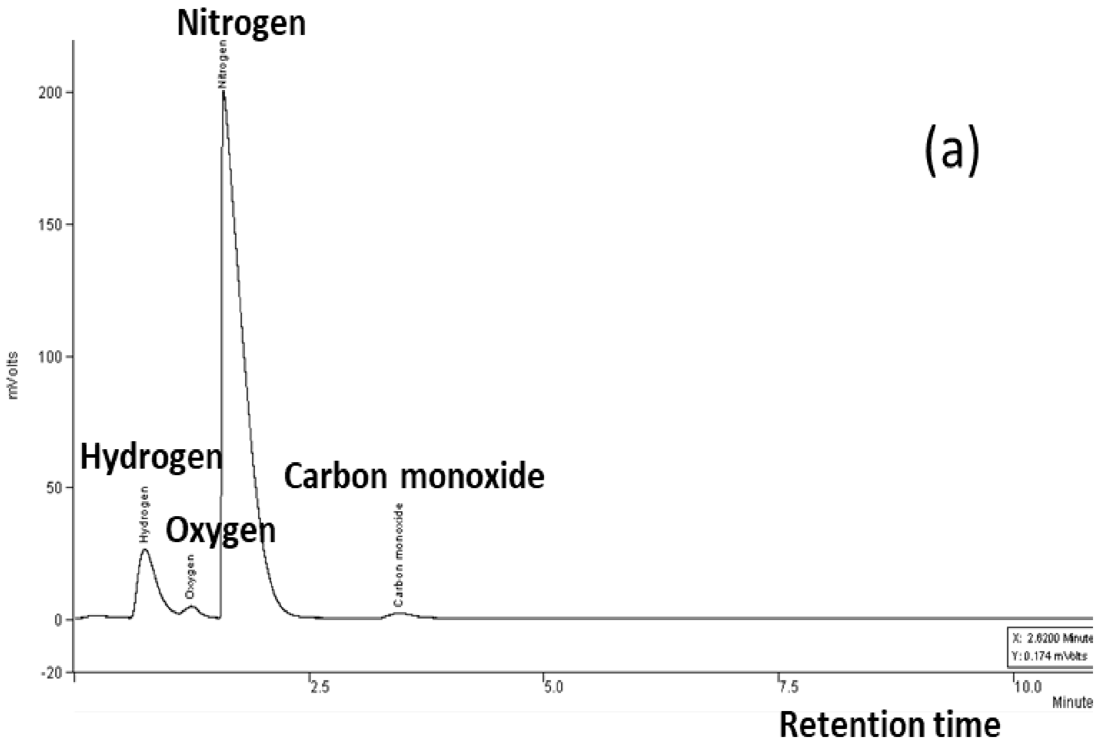
Nitrogen
(a)
mVolts
200
150
100
50
0
-20
Hydrogen
Oxygen
Carbon monoxide
X: 2.6200 Minute
Y: 0.174 mVolts
2.5
5.0
7.5
10.0
Minute
Retention time

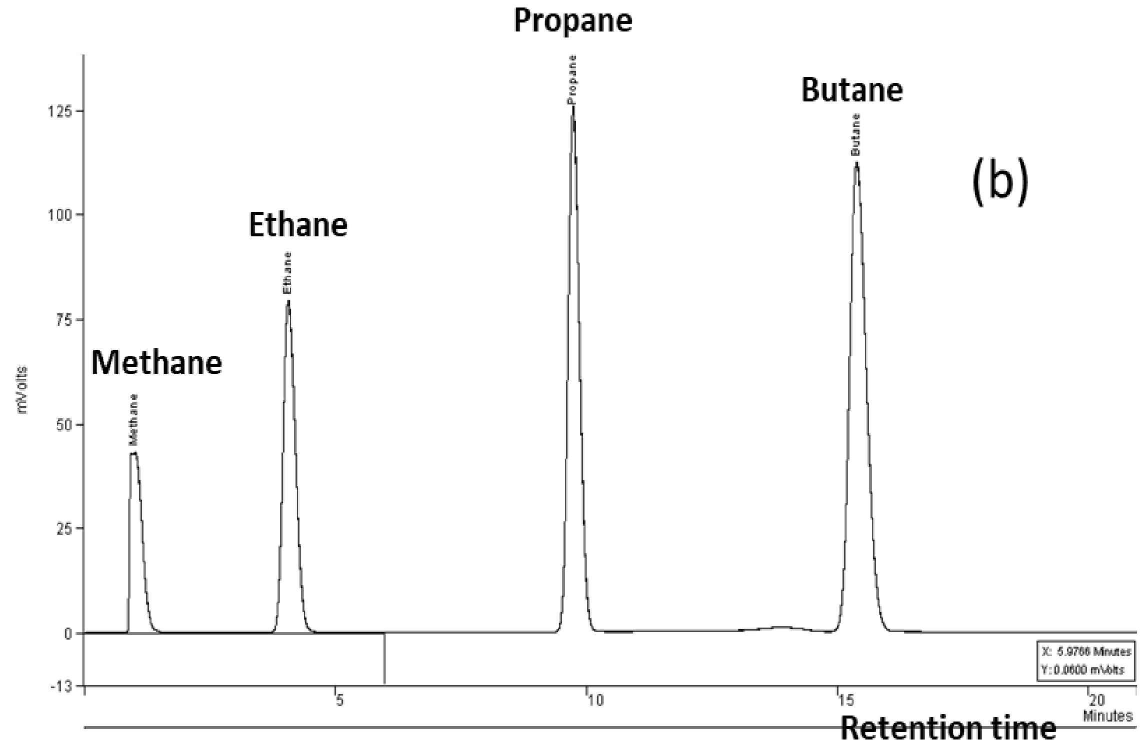
Propane
Butane
(b)
Ethane
Methane
mVolts
125
100
75
50
25
0
-13
X: 5.9766 Minutes
Y: 0.0600 mVolts
5
10
15
20
Minutes
Retention time

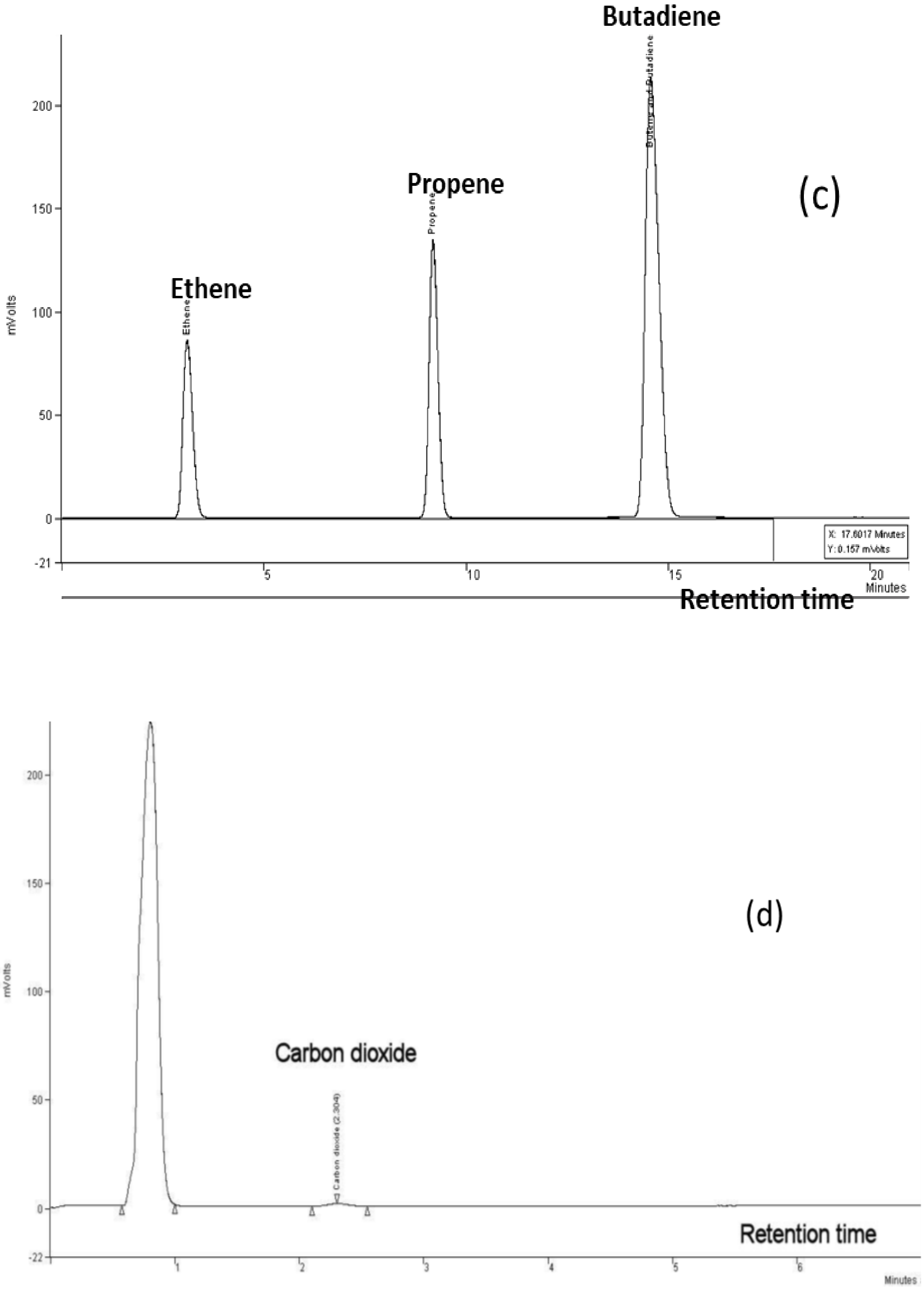

Figure 3.19. GC response peaks for standard gas (a) Permanent gases (H_2, O_2, N_2 & CO); (b) Alkane hydrocarbons; (C) Alkene hydrocarbons; (d) Carbon dioxide (CO_2), chromatogram.

3.5.2 Gas concentration calculations

As the response factor and peak area of the standard gases was established, 1ml of the product gases from the experiments were obtained from the process of the pyrolysis/co-pyrolysis-gasification of plastics, biomass components etc. were analysed by GC. Peak areas relating to each obtained gas in the product yield were calculated by Varian Star software. The produced gases were injected into the GC three times (x3) to ensure reliable and accurate results. The gas concentration from the pyrolysis-gasification process were calculated respectively. The gas concentration is thus calculated in Equation (3.2).

$$\boldsymbol{C_{sample}} = \frac{\boldsymbol{C_{standard}\ X\ P_{sample}}}{\boldsymbol{P_{standard}}} \qquad 3.2$$

Where:

C_{sample} = is the concentration volume (vol.%) of sample gas

$C_{standard}$ = is the concentration volume (vol.%) of standard gas

P_{sample} = is the peak area of sample gas obtained from GC

$P_{standard}$ = is the peak area of standard gas obtained from GC

The reproducibility and repeatability of results from the GC-TCD and GC-FID are shown in Tables 3.5 and 3.6.

An Excel spreadsheet designed and embedded with all the formulas for the purpose of calculating the product yield, mass balance and composition of the gases was prepared. Since each sample gas was injected three times in the various GCs, the calculated concentrations of all the gases were averaged and normalised to obtain the final value of concentration of the product gases.

The response factor for the standard gas was calculated and then used to calculate the concentration volume percent of all the sample gases analysed as shown in the Equation (3.4).

$$\boldsymbol{Response\ factor\ (RF)} = \frac{\textbf{peak area of standard gas}}{\boldsymbol{Conc.\ volume\ of\ standard\ gas\ (vol.\%)}} = \frac{\boldsymbol{P_{standard}}}{\boldsymbol{C_{standard}}} \qquad 3.3$$

$$\boldsymbol{Conc.volume\ of\ sample\ gas\ Y(vol.\%)} = \frac{\boldsymbol{Peak\ area\ of\ analysedgas}}{\boldsymbol{Response\ factor\ (RF)}} =$$

$$\boldsymbol{C_{sample}} = \frac{\boldsymbol{C_{standard}\ X\ P_{sample}}}{\boldsymbol{P_{standard}}} \qquad 3.4$$

Nitrogen was used as the carrier gas for the process of pyrolysis-catalysis/gasification experiments. Therefore, the total volume of nitrogen gas injected into the pyrolysis-catalysis/gasification process is calculated as follows:

$$\boldsymbol{Total\ volume\ of\ nitrogen = flow\ rate\ of\ nitrogen\ (ml/min) x\ total\ time\ (min)} \qquad 3.5$$

As the total volume of nitrogen and the concentration of nitrogen in the product gas mixture are known, therefore, the total volume of gas can be calculated using the following formula:

$$\textbf{Total gas volume (litres)} = \frac{\textbf{100}}{\textbf{nitrogen conc.(vol.\%)}} \boldsymbol{X} \frac{\boldsymbol{total\ nitrogen\ vol.(ml)}}{\textbf{1000}} \qquad 3.6$$

Since the concentration of each gas is known, the number of moles of each gas can be calculated as shown in the following Equation (3.7).

$$\textbf{Number of moles of gas Y} = \frac{\textbf{Conc.of Gas Y (vol.\%)}(\boldsymbol{C_{sample}})}{\textbf{100}} \boldsymbol{X} \frac{\boldsymbol{Total\ volume\ (litre)}}{\textbf{22.4}} \qquad 3.7$$

Also, since the number of moles of each gas have been calculated, therefore the weight of each produced individual gas is calculated as follows:

$$\boldsymbol{Weight\ of\ gas\ Y = Molecular\ weight\ of\ gas\ Y\ (ml/min) x\ moles\ of\ gas\ (min)} \qquad 3.8$$

Then, the total weight of the gases can be calculated by adding the number of grams of each individual gas together.

The nitrogen-free gas composition can be calculated:

$$\boldsymbol{N_2}\textbf{free gas conc. (vol.\%)} = \frac{\textbf{Gas Y conc.(vol.\%)}(\boldsymbol{C_{sample}})}{\textbf{total gas vol.\%}-\boldsymbol{N_2}\textbf{ conc.(vol.\%)}} \boldsymbol{X}\ \textbf{100} \qquad 3.9$$

Since the total amount of gas (grams) is known, therefore, the gas yield can be calculated using the formula:

$$\textbf{Gas yield (wt.\%)} = \frac{\textbf{Total amount of gas (grams)}}{\textbf{Amount of biomass (grams)}} \boldsymbol{X}\ \textbf{100} \qquad 3.10$$

The mass balance for pyrolysis can be calculated using the following formula

$$\textbf{Mass balance (wt.\%)} = \frac{\textbf{Gas (g)+Oil (g)+Solid (g)}}{\textbf{Biomass (g)}} \boldsymbol{X}\ \textbf{100} \qquad 3.11$$

While the mass balance for the pyrolysis/gasification is calculated as shown in the equation:

$$\textbf{Mass balance (wt.\%)} = \frac{\textbf{Gas (g)+Oil (g)+Solid (g)}}{\textbf{(Biomass+injected steam)(g)}} \boldsymbol{X}\ \mathbf{100} \qquad 3.12$$

Therefore, the product yield with respect to the feedstock/samples only are calculated as follows:

$$\textbf{Gas yield (wt.\%)} = \frac{\textbf{Total amount of gas (grams)}}{\textbf{Amount of biomass (grams)}} \boldsymbol{X}\ \mathbf{100} \qquad 3.13$$

$$\textbf{Oil yield (wt.\%)} = \frac{\textbf{Total amount of oil (grams)}}{\textbf{Amount of biomass (grams)}} \boldsymbol{X}\ \mathbf{100} \qquad 3.14$$

$$\textbf{Solid yield (wt.\%)} = \frac{\textbf{Total amount of solid (grams)}}{\textbf{Amount of biomass (grams)}} \boldsymbol{X}\ \mathbf{100} \qquad 3.15$$

The product yield with respect to the feedstock/sample plus the injected water are calculated as follows:

$$\textbf{Gas yield (wt.\%)} = \frac{\textbf{Total amount of gas (grams)}}{\textbf{(Amount of biomass+Injected steams) (grams)}} \boldsymbol{X}\ \mathbf{100} \qquad 3.16$$

$$\textbf{Solid yield (wt.\%)} = \frac{\textbf{Total amount of solid (grams)}}{\textbf{(Amount of biomass+Injected steams) (grams)}} \boldsymbol{X}\ \mathbf{100} \qquad 3.17$$

3.5.2 Oil/liquid products analysis by GC-MS

The condensed liquid fraction from the process of pyrolysis-catalysis of plastics was collected in the three-condenser system. The liquid/oil was extracted using dicloromethane (DCM) as organic solvent from the condenser into a storage bottle and kept in the fridge prior to analysis. The oil sample was prepared using 10 ml of DCM to an approximate 10,000 ppm concentration. The oil produced was analysed using a Varian 430 liquid gas chromatograph (GC) with a flame ionisation detector (FID), equipped with split/splitless injection port having injection volume of 2µL and hydrogen (H_2) was used as the carrier gas at a constant flow rate of 1 ml/min. The gas chromatograph oven was programmed with a temperature rise from 40 to 310 ^{o}C at a heating rate of 5 ^{o}C/min. The analysis was performed on a ZB-1 capillary column with dimensions of 30 m length x 0.53 mm internal diameter and 0.5 µm thickness. The varian 430 gas chromatograph (GC) was used to investigate the produced oil for aromatic and aliphatic hydrocarbons, and the boiling point distribution ranges for the determination of simulated distillation of the oil (ASTM standard 2887).

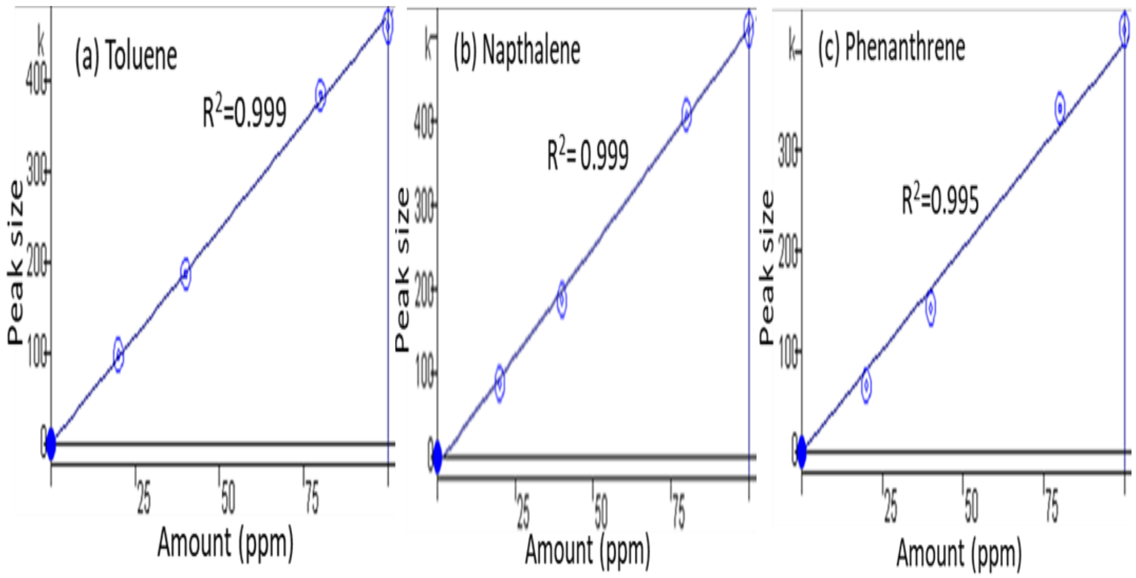

Figure 3.20. Calibration curves for some standard aromatic hydrocarbons and PAHs injected into the GC-MS.

The GC system was calibrated with aromatic and polycyclic aromatic hydrocarbon (PAH) standards, shown in Figures 3.20 and 3.21. In order to confirm the presence of aromatic components in the oil, relative retention indices and another GC/mass spectrometry (GC-MS) as shown in Figure 3.23 was employed. The GC-MS was a Varian CP-3800 GC coupled to a Varian Saturn 2200 GC-MS instrument equipped with DB-5 capillary column of 30 m length x 0.25 µm internal diameter.

Examples of some standard aromatic calibration curves with coefficient of determination (R^2) value close to 1 are shown in Figure 3.20. The R^2 is a key output of regression analysis as R^2 of 1 signifies that the dependent variable can be predicted without error from the independent variable while R^2 of 0 means that the dependent variables cannot be predicted from the independent variable.

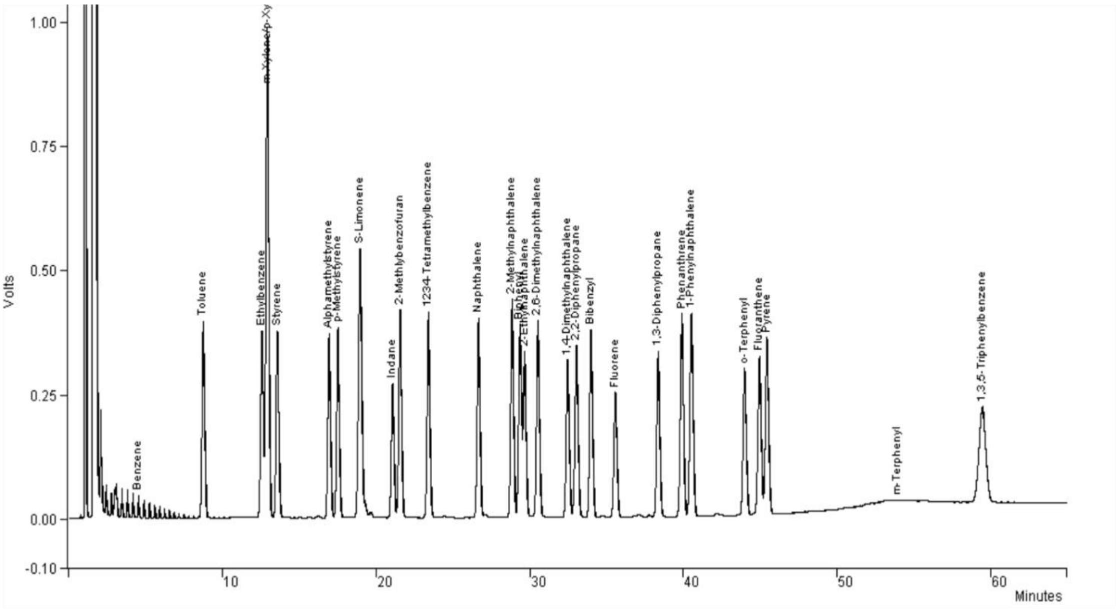

Figure 3.21. Example of Peak response for standard aromatic and PAH injected in GC-MS chromatogram.

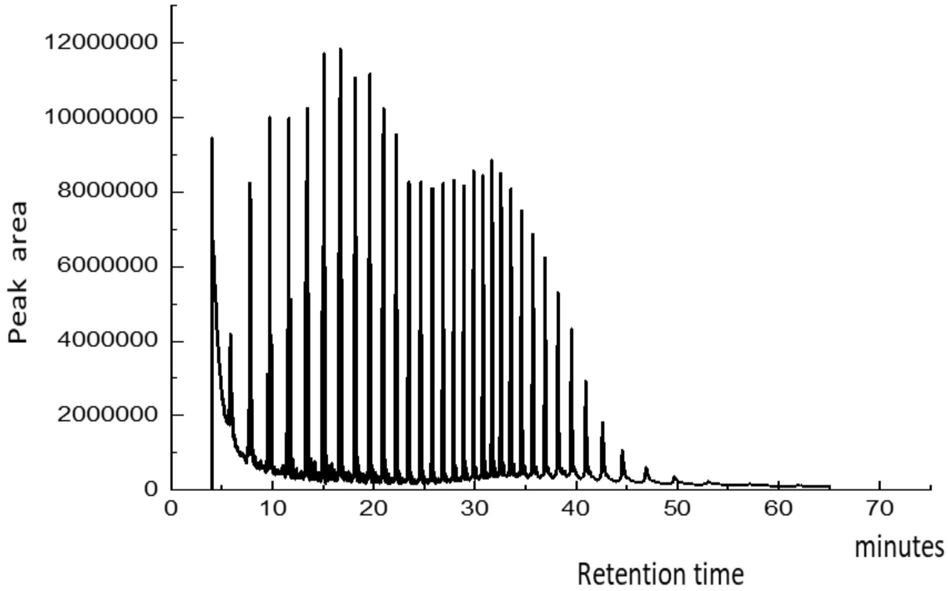

Figure 3.22. An example of GC-MS chromatogram for pyrolysis of HDPE.

The oil analyses results were quantified using the calibration line. The installed NIST 2008 spectral searches were used for identification of some unknown compounds in some cases. The results were presented in peak area alongside the retention time of the compounds, an example of the GC-MS chromatogram of HDPE oil sample at a cracking temperature of 600 ^{o}C is shown in Figure 3.22 as well as the schematic diagram of a typical GC-MS system, see Figure 3.23.

Figure 3.23. Gas chromatograph-mass spectrometer (GC-MS) for oil analysis.

References

1. Hamad, K., M. Kaseem, and F. Deri, *Recycling of waste from polymer materials: An overview of the recent works.* Polymer Degradation and Stability, 2013. 98(12): p. 2801-2812.
2. Ryedale *Different types of plastics and their classification* 2012.
3. Reuseit. *The 7 Most Common Plastics and How They are Typically Used*. 2016; Available from: http://www.reuseit.com/product-materials/learn-more-the-7-most-common-plastics-and-how-they-are-typically-used.htm.
4. Nasrullah, A., et al., *9 - Comprehensive approach on the structure, production, processing, and application of lignin*, in *Lignocellulosic Fibre and Biomass-Based Composite Materials*, M. Jawaid, P. Md Tahir, and N. Saba, Editors. 2017, Woodhead Publishing. p. 165-178.
5. Carvajal, J.C., Á. Gómez, and C.A.J.B.t. Cardona, *Comparison of lignin extraction processes: Economic and environmental assessment.* 2016. 214: p. 468-476.
6. K. Raveendran, Anuradda Ganesh, and K.C. Khilar, *Pyrolysis characteristics of biomass and biomass components* Fuel Processing Technology 1996. 75(987-998).
7. Shen, J., et al., *The prediction of elemental composition of biomass based on proximate analysis.* 2010. 51(5): p. 983-987.
8. Yang, H., et al., *In-depth investigation of biomass pyrolysis based on three major components: hemicellulose, cellulose and lignin.* 2006. 20(1): p. 388-393.
9. Pierella, L.B., S. Renzini, and O.A. Anunziata, *Catalytic degradation of high density polyethylene over microporous and mesoporous materials.* Microporous and Mesoporous Materials, 2005. 81(1-3): p. 155-159.

Chapter 4

Aromatic Fuel Oils Produced from the Pyrolysis-Catalysis of Polyethylene Plastic with Metal-Impregnated Zeolite Catalysts

4.1 Introduction

In this Chapter, pyrolysis-catalysis of high-density polyethylene (HPDE) was carried out in a fixed-bed two-stage reactor for the production of upgraded aromatic pyrolysis oils and high hydrogen yields. The plastics sample used as feedstock for the experiments was virgin high-density polyethylene (HPDE) of ~5 mm diameter particle sizes in the form of pellets. Pyrolysis of the HDPE took place at 600 °C in the first stage of the reactor system and the evolved pyrolysis gases were passed to the second stage catalytic reactor, which had been pre-heated to 600 °C at a heating rate of 10 °C min^{-1} and held at 600 °C for 30 minutes. Furthermore, the catalytic bed temperatures were varied from 600 to 900 ^{o}C to determine the effect of temperature on gas composition and aromatic oil yield. The experiments were conducted with and without catalysts. The catalysts investigated were Y-zeolite with transition metal promoters with 1 wt.% and 5 wt.% metal loading of Ni, Fe, Mo, Ga, Ru and Co impregnated on Y-zeolite to determine the influence on aromatic fuel composition. The non-condensable gases were analysed immediately after each experiment using packed column gas chromatographs (GC) while the oils produced were analysed using a Varian 430 liquid gas GC with FID. Brunauer-Emmet-Teller (BET) nitrogen adsorption analysis was conducted for the determination of surface area, pore size and pore volume of the fresh catalysts using a NOVA 2200e instrument. The used catalysts were analysed by temperature programmed oxidation (TPO) using a Shimadzu 50 thermogravimetric instrument. Likewise, the reacted catalysts were also examined using scanning electron microscopy (SEM) using a Hitachi SU8230 SEM instrument.

4.2 Effect of temperature on product yield

Reaction temperature is considered one of the most influencing pyrolysis conditions that affect product yields and distributions. Temperature is also known to affect both the quality and quantity of the pyrolysis products, affecting the cracking reactions thus modifying the gaseous yield and liquid oil produced, but it appears to have little effect on the quantity of solid carbon-char produced as observed [1-4].

Experiments were conducted without and with catalyst. In the experiment without catalyst, quartz sand was used on the catalytic bed at a reaction temperature of 600 °C while the experiments carried out with catalyst were studied over a temperature range of 600, 700, 800 and 900 °C. This was to show the effect of temperature and to determine the best temperature condition for aromatic chemical oil and hydrogen yield. As shown in Table 4.1 and Figure 4.1, comparing experimental results with catalyst and without catalyst, slightly more gaseous and liquid yields were produced with the use of Y-zeolite catalyst at the same temperature of 600 °C with the same pyrolysis conditions respectively. In the absence of catalyst at 600 °C, the total gas yield produced was approximately 21.09 wt.% and the liquid yield was about 69 wt.% compared with the use of catalyst (Y-zeolite), the total gas yield increased to 22.49 wt.% while the liquid yield increased to 71 wt.%. Similar studies in the presence of zeolite catalysts and as temperatures were increased suggest that gas yields increase with a consequent decrease in oil yields produced from polyethylene pyrolysis [5-9]. It was also reported that Y-zeolite catalyst as investigated in this study had a larger pore size and a higher surface area compared to ZSM-5 catalyst. Pore size is a very important factor for determining the size of the molecules that can enter and leave the active sites of the catalyst for cracking and aromatization reactions.

Table 4.1. Mass balance, product yield and gas composition for pyrolysis-catalytic of HDPE over quartz sand (no catalyst) and Y-zeolite catalyst, (HDPE-2 g, catalyst-1 g).

	No catalyst/600 °C	**600 °C**	**700 °C**	**800 °C**	**900 °C**
Product yield (wt.%)					
Gas	21.09	22.49	59.48	62.43	46.80
Liquid	69.00	71.00	44.50	37.50	40.50
Catalyst carbon	0.00	4.50	5.00	7.00	10.00
Mass balance	90.09	97.99	108.98	106.93	97.30
Gas composition (vol.%)					
H_2	4.95	25.40	25.28	27.86	41.05
CH_4	19.39	20.44	24.51	32.44	41.44
C_2	47.02	26.60	31.74	32.55	17.03
C_3	22.60	23.24	14.78	5.12	0.28
C_4	6.05	4.32	3.68	2.03	0.21

Furthermore, as shown in Table 4.1 and Figure 4.1, experiments were conducted in the presence of Y-zeolite catalyst at different catalytic bed temperatures from 600 to 900 ^{o}C. At a temperature of 700 ^{o}C, the gas yield drastically increased to 59.58 wt.% (more than double the yield produced without and with catalyst at the temperature of 600 ^{o}C) while the liquid yield decreased to 44.50 wt.%. Hernandez et al. [10], stated that pyrolysis temperature and volatiles residence time affect both the primary and secondary reactions, and were therefore suggested as the most influential factors. Al-Salem et al. [11], also highlighted that temperature controls the major role of plastic decomposition, such as the cracking reactions where the van der Waals force between the molecules collapse due to the increase of the vibration of the molecules on the surface, which results in the breaking of the carbon chain in the plastics [2]. Another researcher [12], reported that at higher temperatures, the impact of polymer type, product concentration and residence time on product distribution were insignificant compared to the influence of temperature. Likewise, the range of temperature studied in another work [13], showed that at a higher temperatures the major product obtained were gases, but below 700 ^{o}C solids were the main product in the product yield [13].

Subsequently in this study, the total gaseous yield increased while the liquid yield decreased with increasing temperature up to 800 ^{o}C. At 900 ^{o}C, the liquid yield started to increase again while the total gas yield started to decrease, which might be as a result of deactivation of the catalyst at this high temperature whereby the volatiles were no longer going into gaseous state but remaining in the liquid state and then undergoing secondary reaction of cyclisation (particularly polycyclic aromatic hydrocarbons) as the temperatures increased. Additionally, there was a continuous increase of carbon deposition on the catalyst which might have led to it deactivation as the temperature increased from 600 to 900 ^{o}C as observed. This is shown in Table 4.1 and Figure 4.1. The initial increase in gas yields with increase in temperature, suggests there was a dominance of cracking reactions in which heavier hydrocarbons were broken down to lighter components, with a corresponding decrease in liquid yields. Liu et al. [14], similarly highlighted the effect of temperature while varying catalytic bed temperatures from 500 to 800 ^{o}C, and reported an increase in gas yields up to 700 ^{o}C with a corresponding reduction in liquid yields, but at 800 ^{o}C the gas yield decreased. Likewise, Lopez et al. [2], investigated influence of temperature on pyrolysis plastic wastes in a semi-batch reactor and reported that the gas yield increased while the liquid yield decreased as the pyrolysis temperature increased from 460 to 600 ^{o}C. In addition, the char formation was due to secondary repolymerisation reactions between the polymers in the products. Aguado et al. [15], also analysed effects of temperatures and catalysts on polyethylene, and their results show that the yield of gaseous products increases in the presence of catalytic reforming over HZSM-5. It was suggested that temperatures determined the conversion values in the thermal reactor while the catalytic step determined the extent of the reforming reactions to generate the final products. High temperatures resulted in gas production as the heavy hydrocarbons molecules break down to form lighter hydrocarbon molecules, and as the temperature increases further, there is higher amount of energy leading to secondary reactions with an oil product decreasing with a consequent increase in the gas phase product [11]. The effect of temperature was studied on the composition of products from the pyrolysis of polyethylene and polypropylene in a fluidized bed reactor [8]. The production of a high yield of hydrocarbon gases and char with a decrease in the oil yield was observed as the temperature was increased due to secondary reactions, thermal cracking, isomerisation and aromatization reactions [8, 16]. Mastral et al. [17], thermally degraded HDPE in a fluidised bed reactor, and they reported that the highest gas yield was obtained at a temperature of 780 ^{o}C at about 86.4 wt.% while oil yield was 9.6 wt.%. It was reported that hydrogen and methane yield increased at temperatures above 800 ^{o}C, as also obtained in this work. According to Hernandez et al. [18], the total gas yield increased as the temperature was increased from 400 to 700 ^{o}C after which there was a decrease in gas yield due to deactivation of the catalytic activity of the HUSY catalyst for the degradation of HDPE in a fluidised bed reactor. Furthermore, HDPE is stated to start degrading at a temperatures above 325 ^{o}C while at about 467 ^{o}C and higher temperatures, complete degradation usually occurs [19], producing a gaseous yield, liquid and an insignificant amount of char. However, heating rates were said to control the speed of the degradation process and the rate of reaction as most of the pyrolytic reactors are designed on the basis of temperature range that falls within the range of the various plastics used as feedstock [11]. It is consistent with this study, as one of the advantages of the fixed bed reactor as investigated is the precise temperature control in the reactor. Xiao et al. [20], equally suggested an advantage of a two-stage reactor is having better catalytic utilization and improve reforming reactions to some degree.

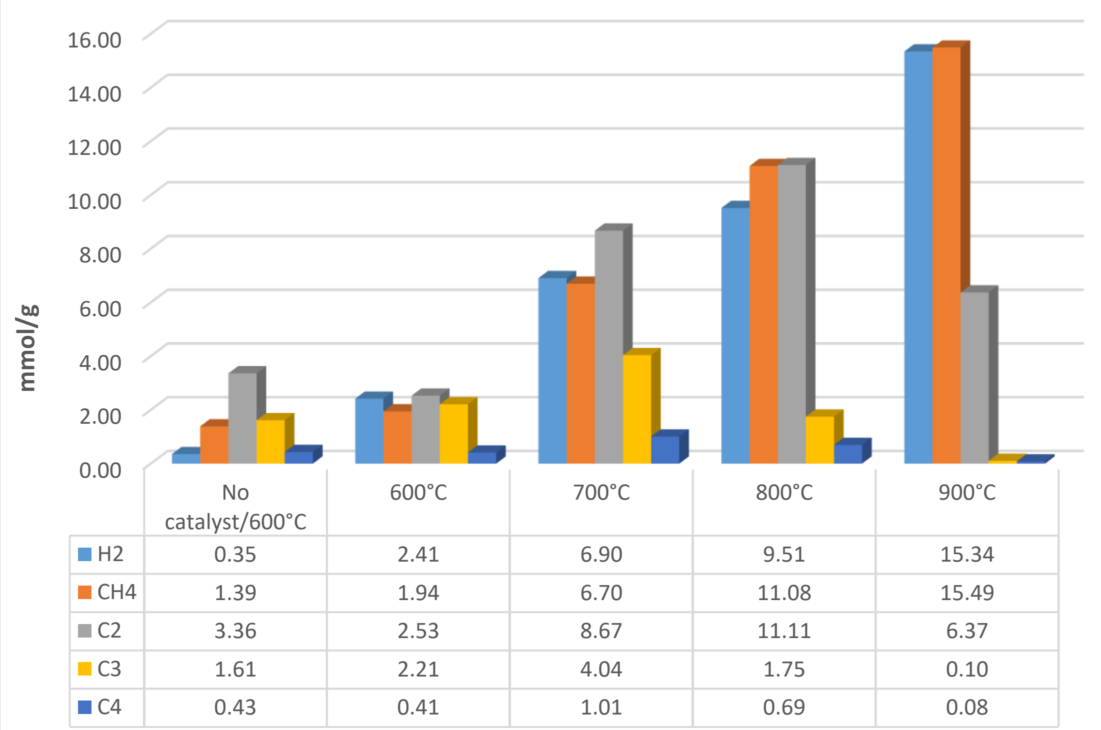

	No catalyst/600°C	600°C	700°C	800°C	900°C
🟦 H2	0.35	2.41	6.90	9.51	15.34
🟧 CH4	1.39	1.94	6.70	11.08	15.49
▨ C2	3.36	2.53	8.67	11.11	6.37
🟨 C3	1.61	2.21	4.04	1.75	0.10
🟦 C4	0.43	0.41	1.01	0.69	0.08

Figure 4.1. Hydrocarbon gas yield for pyrolysis-catalysis of HDPE over sand (no catalyst) and Y-zeolite catalyst at difference temperatures.

4.2.1 The effect of temperature on gas composition

Table 4.1 and Figure 4.1 show the gas composition without and with catalyst for the pyrolysis of HDPE. Quartz sand was used in the experiment without catalyst, and in other experiments Y-zeolite catalyst was used in the second stage of the fixed-bed reactor. There was a remarkable rise in gas yield with the addition of Y-zeolite catalyst to the second stage of the fixed bed reactor. In particular, an increase in hydrogen production was more dominant at the bed temperature of 600 °C when catalyst was introduced into the system. The yield of hydrogen in the absence of catalyst was just 0.35 mmol/g (4.95 vol.%) but increased to 2.41 mmol/g (25.40 vol.%) by introduction of Y-zeolite catalyst into the pyrolysis system at the temperature of 600 °C. Also, hydrogen and methane continuously increased as the temperature was increased, throughout the entire temperature range studied. Hydrogen increased to 15.34 mmol/g (41.05 vol.%) while methane increased to 15.49 mmol/g (41.44 vol.%) at catalytic temperature of 900 °C.

Another author reported that the yield of methane considerably increases above 700 °C due to contribution from secondary reactions [18]. The major gases produced were C_2 (mainly ethene) in the absence of catalyst at 600 °C. Also, all the C_2-C_4 gases produced decreased with the introduction of Y-zeolite catalyst and continued to decrease throughout the entire temperature range studied (600-900 °C), while hydrogen and methane continuously increased as temperature increased. Cracking of heavier hydrocarbons to lighter components can be observed with the increase in temperature, as shown in results in Figure 4.2. Also, catalytic reforming by Y-zeolite is evident in the gas compositions obtained, since the difference in results from the absence and presence of catalyst at 600 ^{o}C is pronounced, especially on hydrogen yield. Furthermore, the composition of gaseous product identified from the pyrolysis of individual plastics and the mixture of plastic in a fixed bed reactor at a temperature of 700 ^{o}C includes H_2, CH_4, C_2-C_4, CO_2 and CO respectively [21]. Singh and Ruj [7], reported that the gaseous product increases as temperature increases and the composition of the main gases obtained includes methane, ethane, propane and n-butane in addition to H_2, CO and CO_2 yield. Hernandaz et al. [10], investigated the effect of temperature and HZSM-5 catalyst on HDPE using a flash coil pyrolyzer and fluidised bed reactor, and reported that the influence of catalyst was more prominent in the primary cracking reactions as shown by an increase of the volatile compounds with degradation temperature and the yield of C_3-C_5 hydrocarbons were favoured in the presence of HZSM-5 catalyst. It was also stated that the olefin and paraffin yields depend on the extension of secondary reactions as well as temperature of the process. From literature and as observed in this study, it can be suggested that as temperature increases in addition to the cracking reactions enabled by the Y-zeolite catalyst analysed, production of hydrogen increases and C_2-C_4 gases decrease respectively.

4.2.2 Effect of temperature on oil composition

Analysis was carried out on the oil product obtained from pyrolysis-catalysis of HDPE over Y-zeolite at different temperatures, by gas chromatograph-mass spectrometry (GC-MS). Results are shown in Table 4.2 and Figure 4.2. The composition of oil produced at the reaction temperatures of 600, 700, 800 and 900 ^{o}C showed that there was a remarkable increase in aromatic yield, while aliphatic hydrocarbon yield decreased with increase in temperature over the Y-zeolite catalyst. At a reaction temperature of 600 ^{o}C, aliphatic yield was 47.56% while aromatic yield was 52.44% (peak area %). At the temperature of 700 ^{o}C, aromatic yield increased to 83.12% (an increment of about 31%) with a corresponding decrease in aliphatic compounds 16.88%. Furthermore, aromatic compounds increased to 96.94% (an increment of about 13.82%) and aliphatics decreased to 3.06% at 800 ^{o}C. At a final temperature of 900 ^{o}C, aromatic yield increased to 98.27% while aliphatic compounds decreased to 1.73%. This might be attributed to cracking reactions which occurred as temperatures increased. The heavier hydrocarbon molecules which were cracked were subsequently converted to aromatic compounds by ring action. In addition, cracking of primary decomposition products is proposed to account for aromatic formation, while aliphatic hydrocarbons (a class of products from primary decomposition of polyethylene) naturally evolved into light gases and aromatics at increasing pyrolysis temperatures [4]. Catalytic cracking, along with secondary reactions, cyclisation and aromatisation reactions have been suggested as reasons for increased aromatic hydrocarbon production at this temperature [22]. Lopez et al. reported that at a low temperature of 460 ^{o}C, a highly viscous liquid yield with a high content of long chain hydrocarbons was obtained while, at the highest tested temperature, a lower fraction of liquid yield with high aromatic content was produced. This was attributed to the strong cracking of the C-C bonds between the heavy hydrocarbon molecules, leading to lighter hydrocarbons with shorter carbon chains at high temperatures [2].

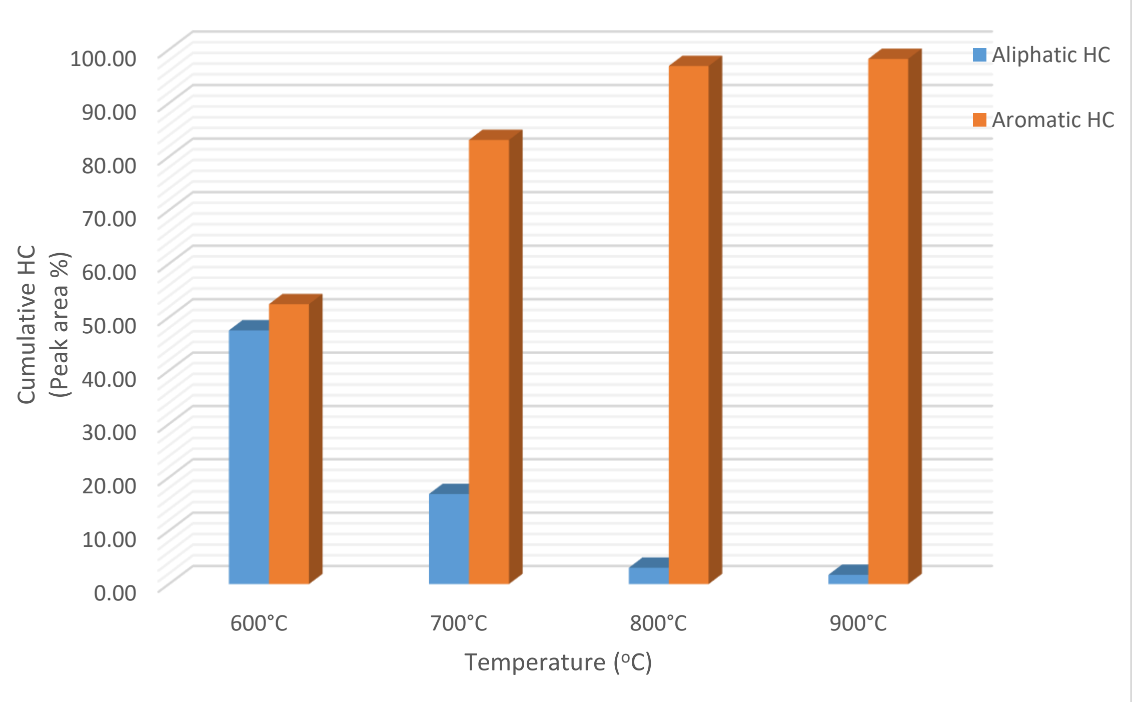

Figure 4.2. Hydrocarbon composition of oils produced from pyrolysis-catalysis of HDPE over Y-zeolite at different temperatures.

Figure 4.3 shows the yield of aromatic ring compounds in oils produced from the pyrolysis-catalysis of HDPE over Y-zeolite at increasing temperatures. Single ring (1R) aromatic hydrocarbons appeared to be dominant at lower temperatures (600 – 700 °C) while double ring (2R) aromatic compounds dominated as temperatures increased from 700 to 900 °C. Likewise, three and four ring (3R and 4R) aromatic hydrocarbons have been reported to increase with temperature [8, 22]. This was attributed to cyclisation and aromatisation reactions. According to Xue et al [23], PE-derived olefins and alkanes undergo further cracking through carbocationic intermediates, which are activated by Lewis and Bronsted sites of catalysts. Hence, light olefins were further subjected to oligomerization, cyclisation and aromatization for the formation of aromatics [23]. Thus, aromatic hydrocarbons are produced as a result of secondary reactions at higher temperatures [10, 24]. In another study, formation of aromatics in the pyrolysis of polyolefin was reported to have occurred by the Diel-Alder reaction, followed by dehydrogenation [8, 25].

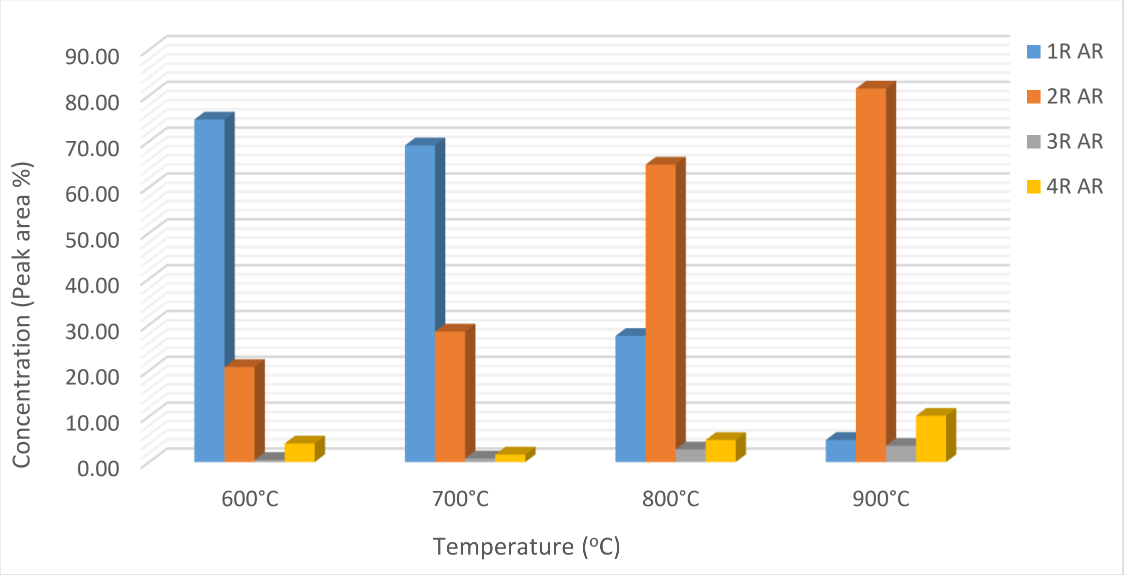

Figure 4.3. Composition of aromatic hydrocarbons in oils produced from pyrolysis-catalysis of HDPE over Y-zeolite at different temperatures.

Table 4.2 shows the aromatic and aliphatic hydrocarbon composition produced from the pyrolysis-catalysis of HDPE. The individual hydrocarbon composition at 600 ^{o}C indicates toluene is the dominant product up to 700 ^{o}C while naphthalene was the major product from 800 ^{o}C to 900 ^{o}C. Other aromatic compounds produced included ethylbenzene, O and P-xylene, styrene, methylstyrene, 2-methyl and 2-ethylnaphthalene, 2,6 and 1,4-dimethylnaphthalene, phenanthrene, pyrene and M and P-terphenyl. In the case of hydrocarbon composition of the aliphatic compounds produced in the oil, the results indicate between C_8-C_{34} were obtained with the reaction temperatures of 600-900 ^{o}C. Singh and Ruj [7], analysed the effect of temperature and time on municipal plastic waste and reported that the volume of oil increased as the temperature was increased from 450 to 550 ^{o}C. A further increase in temperature to 600 ^{o}C showed no increase in the oil volume, but there was increase in the density of the oil with formation of more aromatic hydrocarbons. It has further been suggested that an increase in temperature lowers the residence time of volatiles in a reactor, thereby reducing the proportion of cracking reactions which can occur. This results in production of heavier hydrocarbons molecules, including high carbon chain molecules and aromatics in the oil fraction. [11].

Table 4.2. Aliphatic and aromatic hydrocarbons produced at different temperatures.

Aliphatic compounds					
Retention Time (RT)	**Compound Name**	**Area percent (%)**	**Area percent (%)**	**Area percent (%)**	**Area percent (%)**
		600°C	**700°C**	**800°C**	**900°C**
4.276	N-OCTANE C_8	14.86			
7.979	N-DECANE C_{10}		6.36		
9.924	N- UNDECANE C_{11}	7.85	8.36		
11.797	N- DODECANE C_{12}	6.42	7.27		
13.573	N-TRIDECANE C_{13}	6.22	5.97		
15.248	N-TETRADECANE C_{14}	6.47	5.99		
16.83	N-PENTADECANE C_{15}	6.71	5.83		0.35
18.323	N-HEXADECANE C_{16}	7.04	5.64		0.75
19.752	N- HEPTADECANE C_{17}				1.10
19.749	PRISTANE C_{19}	6.40	4.43		1.74
21.099	PHYTANE C_{20}	4.87	4.00		
22.383	N- NONADECANCE C_{19}	4.90	4.46		2.23
23.605	N- EICOSANE C_{20}	4.12	4.44		2.37
24.774	N-HENEICOSANE C_{21}	3.23	3.53		2.35
25.894	N- DOCOSANE C_{22}	2.68	3.23	1.45	2.79
26.967	N- TRICOSANE C_{23}	2.15	2.95	2.85	3.83
28	N- TETRACOSANE C_{24}	2.19	2.99	5.13	5.84
28.992	N-PENTACOSANE C_{25}	2.10	3.24	10.44	7.15
29.944	N- HEXACOSANE C_{26}	2.30	3.24	10.22	8.29
30.864	N- HEPTACOSANE C_{27}	2.36	4.53	13.26	12.26
31.752	N- OCTACOSANE C_{28}	2.18	3.89	12.44	9.83
32.627	N- NONACOSANE C_{29}	1.93	3.45	13.26	11.27
33.612	N-TRIACONTANE C_{30}	1.47	2.77	11.75	10.03
34.692	N- HENTRIACONTANE C_{31}	0.43	2.25	9.24	8.40
35.821	N- DOTRIACONTANE C_{32}	0.68	1.16	5.22	5.39
37.031	N- TRITRIACONTANE C_{33}	0.44		3.02	3.40
38.303	N- TETRATRIACONTANE C_{34}			1.71	0.61
Total (%)		100.00	100.00	100.00	100.00

Aromatic compounds					
Retention Time (RT)	**Compound Name**	**Area percent (%)**	**Area percent (%)**	**Area percent (%)**	**Area percent (%)**
		600°C	**700°C**	**800°C**	**900°C**
4. 764	TOLUENE	36.30	48.94	23.79	4.63
8.621	ETHYLBENZENE	5.25	6.50	1.37	0.11
9.116	P-XYLENE	21.53	8.74	1.50	0.08
10.327	STYRENE	0.00	4.34	9.37	4.82
10.338	0-XYLENE	11.66	4.90	0.86	0.00
17.355	P-METHYLSTYRENE	0.00	0.50	0.42	0.02
27.189	NAPHTHALENE	8.22	16.09	49.84	75.16
31.038	2-METHYLNAPHTHALENE	8.15	5.41	4.56	1.37
33.912	2-ETHYLNAPHTHALENE	0.96	1.22	0.56	0.13
34.281	2,6 DIMETHYLNAPHTHALENE	1.72	0.49	0.11	0.01
35.133	1,4 DIMETHYLNAPHTHALENE	1.69	0.45	0.04	0.00
43.43	PHENANTHRENE	0.46	0.79	2.67	3.41
45.272	O-TERPHENYL	0.00	0.00	0.00	0.01
49.7	PYRENE	4.05	1.65	4.81	10.10
50.334	M-TERPHENYL	0.00	0.00	0.06	0.09
51.003	P-TERPHENYL	0.00	0.00	0.03	0.05
Total (%)		100.00	100.00	100.00	0.00

4.3 Product yields and gas compositions in relation to Y-zeolite-metal catalysts

The product yields obtained from pyrolysis-catalysis of high-density polyethylene over the Y-zeolite catalyst at pyrolysis and catalytic temperatures of 600 °C, using Y-zeolite catalyst impregnated with Ni, Mo, Fe, Ga, Ru and Co metals are shown in Table 4.3. Products included gases, liquids, and carbons deposited on the catalyst; no pyrolysis residue or char was produced in these experiments. Pyrolysis of the HDPE without a catalyst, but with a substitute of quartz sand of similar particle size, produced a mainly liquid product of ~70 wt.% and a gas yield of 21 wt.%. Introduction of the Y-zeolite catalyst into the second stage produced a significant increase in gas yield to 36 wt.% and a corresponding decrease in oil yield. In addition, there was deposition of carbon on the catalyst. Addition of the metal promoter to the Y-zeolite showed only a small difference in oil and gas yield compared to the non-metal containing Y-zeolite, however, there was a marked increase in the deposition of carbon on the metal-Y-zeolite catalyst. Uemichi et al. [26], also reported an increase in carbon deposits on metal catalysts compared to metal free catalysts for the thermal degradation of polyethylene. In addition, Guisnet et al. [27], reported that the deactivation of catalyst occurred faster with the introduction of Pt metal on zeolite catalyst due to the formation of carbon deposits on the metal catalyst compared to metal-free catalyst. The degradation reaction of polyethylene over metals impregnated on activated carbon was suggested as shown in the following Equations 4.1 and 4.2 [26].

$$C_nH_{2n+2} \xrightarrow{(A)} C_nH_{2n-6} + 8H^* \ (n \geq 6) \tag{4.1}$$

$$8\,H^* \xrightarrow{(B)} 4H_2 \tag{4.2}$$

Where C_nH_{2n+2} and H* are stated to be the saturated fragment and the hydrogen atom on the catalyst surface, (A) is stated to be the metal catalyst step, while (B) is the dehydrogenation reaction step. This reaction mechanism also seems to be applicable to the formation of aromatic hydrocarbons and hydrogen from the degradation of polyethylene over transition metals impregnated on Y-zeolite catalyst, as analysed in this study.

Table 4.3. Product yields and mass balances for pyrolysis of HDPE, over Y-zeolite and metal/Y-zeolite catalysts, (HDPE-2 g, catalyst-4 g).

	Pyro.(no catalyst)	**Y-zeo (no metal)**	**NiYZ**		**MoYZ**		**FeYZ**		**GaYZ**		**RuYZ**		**CoYZ**	
			1%	**5%**	**1%**	**5%**	**1%**	**5%**	**1%**	**5%**	**1%**	**5%**	**1%**	**5%**
Product yield (wt.%)														
Gas	21	36	36	36	38	36	33	38	37	37	42	31	36	40
Liquid	69	45	36	43	31	35	40	30	36	29	34	43	36	30
Catalyst carbon	0	10	22	18	24	20	14	22	18	24	18	20	22	26
Mass balance	90	91	94	97	93	91	87	90	91	90	94	94	93	96
Gas composition (vol.%)														
H_2	5	33	52	66	48	60	36	45	38	54	31	39	47	68
CH_4	19	24	18	28	18	12	25	18	23	16	26	8	18	12
C_2	47	18	11	1	13	10	18	12	17	11	18	21	12	5
C_3	23	22	16	3	18	12	17	17	20	15	21	27	19	9
C_4	6	3	3	3	4	5	4	7	3	4	3	4	4	6

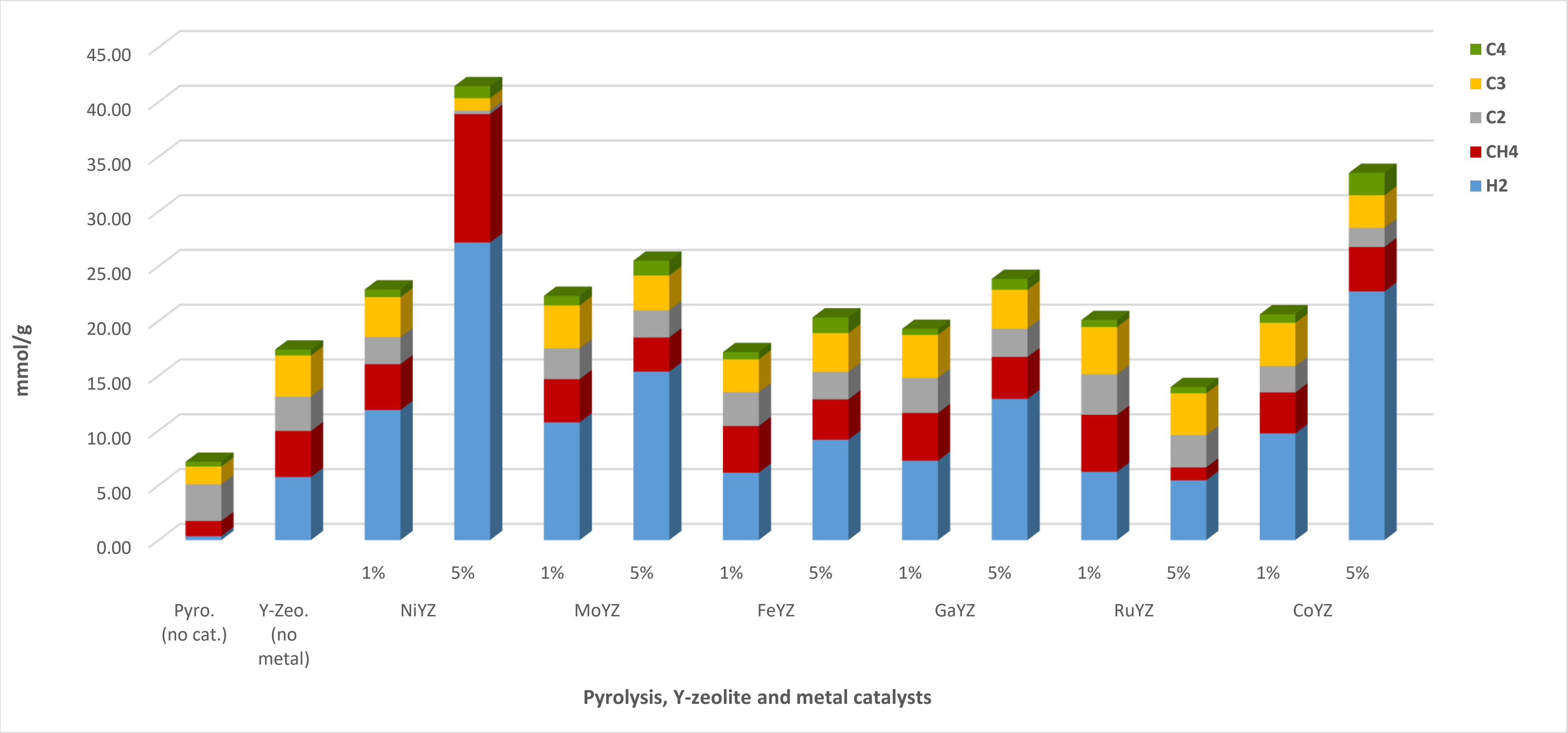

Figure 4.4. Hydrocarbon gas compositions for pyrolysis of HDPE, over Y-zeolite and metal/Y-zeolite catalyst at a temperature of 600 ^{o}C.

4.3.1 Effect of metal catalysts on gas composition

Table 4.3 and Figure 4.4 also show the composition of the gas product (as vol.%) derived from the pyrolysis-catalysis of the HDPE with the metal impregnated Y-zeolite catalysts. The main gases produced in the absence of catalyst were methane, ethane, ethene, propane and propene together with lower concentrations of C_4 hydrocarbons. However, in the presence of the Y-zeolite, there were significantly higher concentrations of hydrogen produced and lower $C_2 – C_4$ hydrocarbon concentrations. The influence of metal addition to the Y-zeolite was to further enhance the concentration of hydrogen in the product gas and higher concentrations of metal addition further increased hydrogen concentrations in the product gases. For example, the Ni-Y-zeolite resulted in a product gas with 52 vol.% hydrogen content at a metal loading of 1 wt.%, which further increased to 66 vol.% of hydrogen as the metal concentration was increased to 5 wt.% Ni. Similarly, the Co-Y-zeolite catalyst produced a hydrogen content in the gas product of 47 vol.% at 1 wt.% metal loading and increased to 68 vol.% hydrogen at a 5 wt.% cobalt loading. The order of the metal impregnated catalysts in terms of hydrogen vol.% in the product gas at 5 wt.% metal loading was Co>Ni>Mo>Ga>Fe>Ru. The increase in hydrogen content of the product gases resulted in a consequent decrease in C_1-C_4 hydrocarbons.

According to Guisnet et al. [27], the bifunctional catalyst-GaH-ZSM-5 investigated for aromatisation of propane showed that the gallium active species catalyse the dehydrogenation of propane into propene, naphthenes into aromatics and probably the cyclisation steps by dehydrogenating C_6-C_9 alkenes into dienes. Acid sites catalysed the oligomerisation of light alkenes and the cyclisation C_6-C_9 alkenes. Cracking of propane through carbonium ion intermediates and hydrogen transfer reactions also occurred on the acid sites. Therefore, the bifunctional process might be limited by dehydrogenation on gallium species, by cyclisation and oligomerisation on the zeolite acid sites or by diffusion steps. It was also mentioned that propene conversion on GaH-ZSM-5 leads to the production of one mole of aromatic hydrocarbons accompanied by 1.8 moles of hydrogen [27]. Similarly, it was observed that the substrate could enter the channel of the large pore size of the Y-zeolite, making the reaction proceed to form smaller products such as benzenes, tetralins and indans, in addition to gaseous products [28]. Therefore, it is suggested that bifuntional catalysts are very active for the production of aromatics and hydrogen from alkanes as shown in equation 4.3.

Aromatization process

$$C_3H_6 \xrightarrow{Ga} C_3H_6 \xrightarrow{H^+} \boxed{\begin{matrix} C_6 - C_8 \\ Alkenes \end{matrix}} \xrightarrow{H^+,Ga} \boxed{\begin{matrix} C_6 - C_6 \\ Dienes \end{matrix}} \xrightarrow{H^+} \boxed{\begin{matrix} C_6 - C_8 \\ Naphthenes \end{matrix}} \xrightarrow{Ga} \boxed{\begin{matrix} C_6 - C_8 \\ Aromatics \end{matrix}}$$

Secondary Reactions

On Acid Sites: - $C_3H_8 \xrightarrow{H^+} C_2H_4 + CH_4(C_3H_6 + H_2)$

-Hydrogen Transfer

$$\begin{matrix} C_6 - C_8 \\ Naphthenes \end{matrix} + \begin{matrix} C_2 - C_4 \\ Alkenes \end{matrix} \rightarrow \begin{matrix} C_6 - C_8 \\ Aromatics \end{matrix} + \begin{matrix} C_2 - C_4 \\ Alkanes \end{matrix}$$

4.3

In light of the above and via Equation 4.3, it is hereby suggested that the formation of gaseous products might be due to the higher production of hydrogen by the metal/Y-zeolite catalysts as compared with no metal/catalyst, in the pyrolysis process investigated in this study.

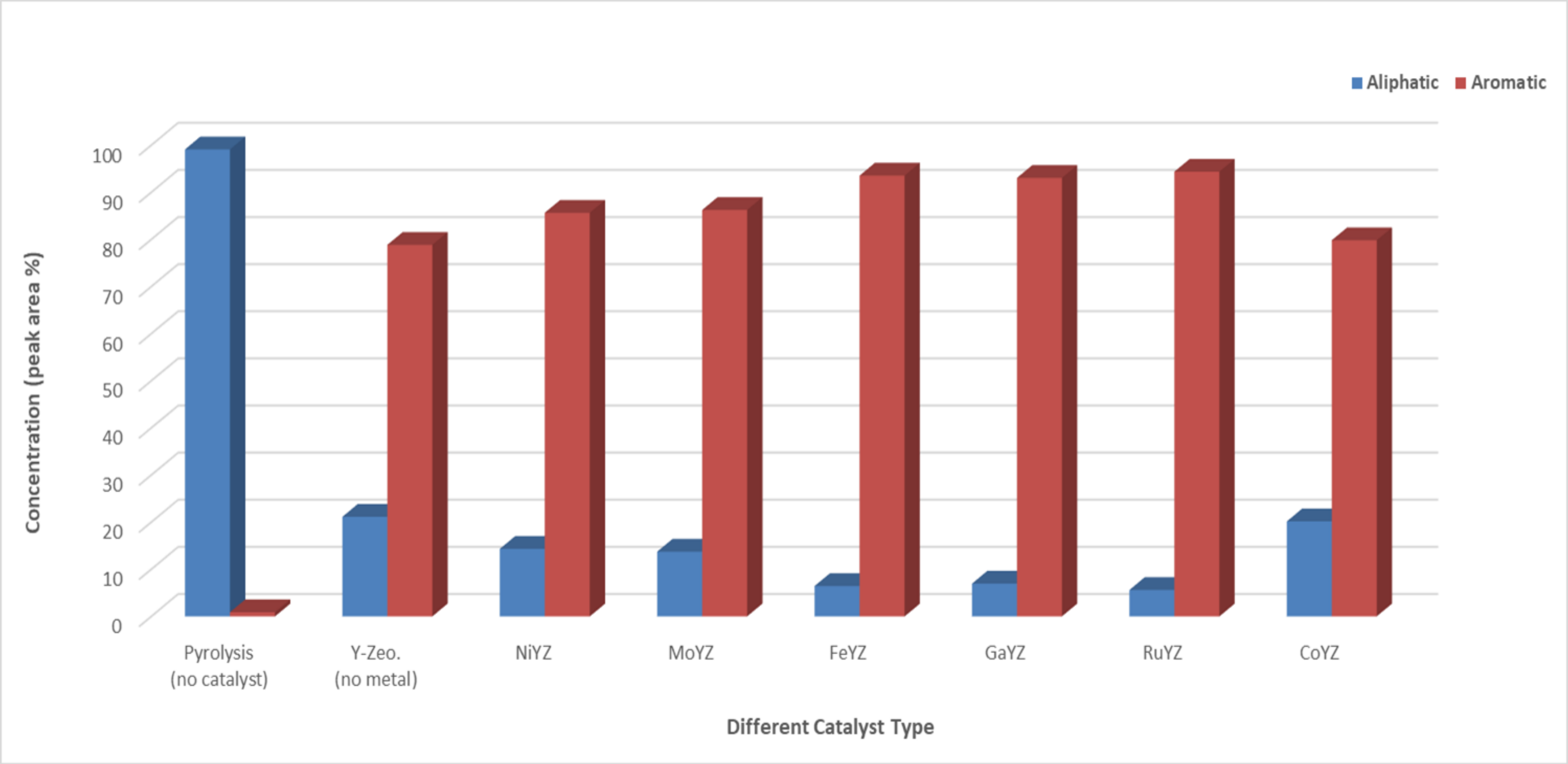

Figure 4.5. Hydrocarbon composition of oils produced from pyrolysis-catalysis of HDPE, over Y-zeolite catalyst and with 1 wt.% metal/Y-zeolite catalysts at a temperature of 600 ^{o}C.

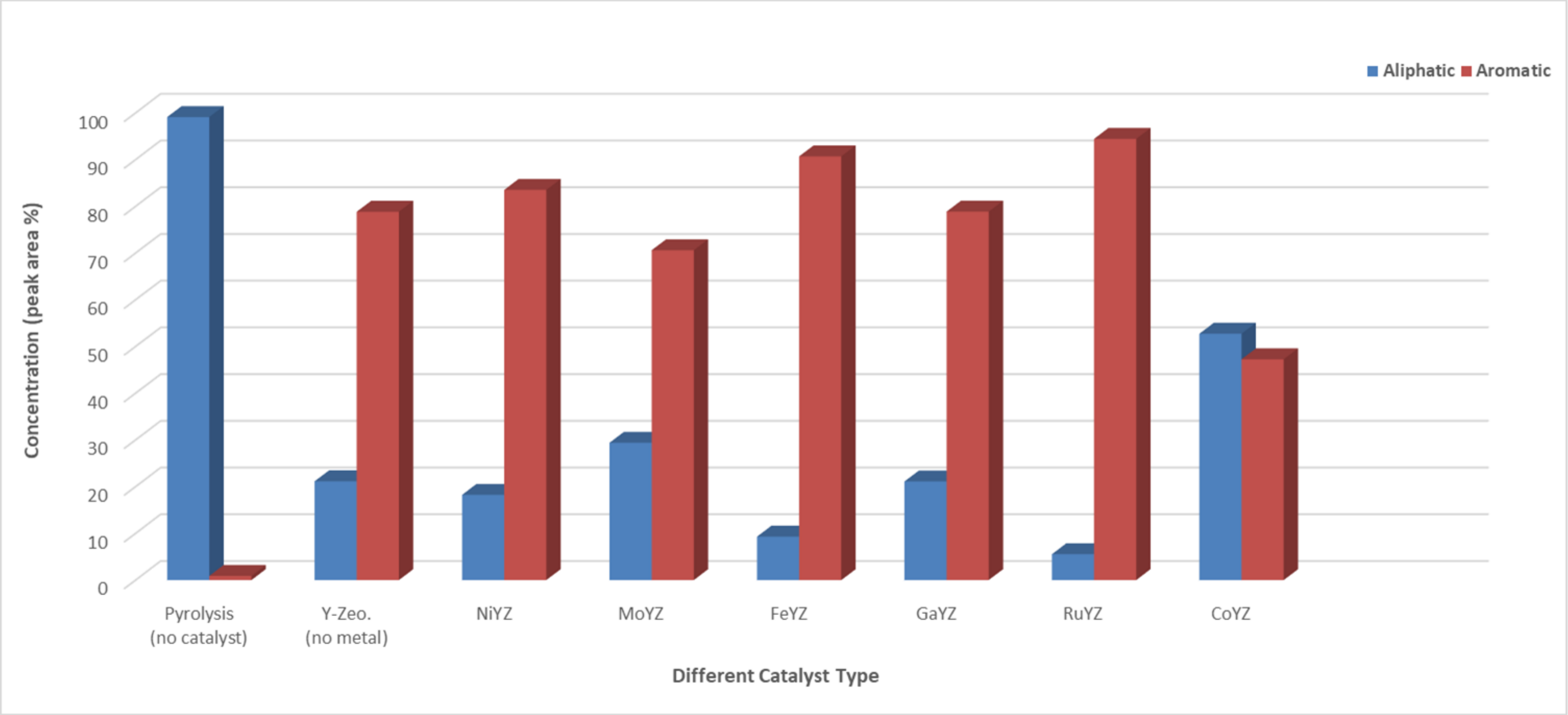

Figure 4.6. Hydrocarbon composition of oils produced from pyrolysis-catalysis of HDPE, over Y-zeolite catalyst and with 5 wt.% metal/Y-zeolite catalysts at a temperature of 600 °C.

4.3.2 Effect of metal catalysts on oil composition

Figures 4.5 and 4.6 show the aliphatic and aromatic hydrocarbon contents of oils produced from pyrolysis-catalysis of high-density polyethylene over the prepared metal-Y-zeolite catalysts in relation to metal loading concentrations of 1 wt.% and 5 wt.%. Compared to the non-catalysed pyrolysis, there was a marked change in product oil chemistry with the introduction of the catalyst. Non-catalytic pyrolysis produced a mainly aliphatic product >99% of the oil composition. Therefore, the yield of oil which was 69 wt.% was almost entirely aliphatic in composition (Table 4.3). However, introduction of the Y-zeolite to the pyrolysis-catalysis process, although reducing oil yield to 45 wt.% (Table 4.3), produced an oil product with an aromatic hydrocarbon content of ~80% (Figure 4.5 & 4.6). Also, the addition of a 1 wt.% metal concentration to the Y-zeolite resulted in a decrease in the product oil yield, but an increase in aromatic hydrocarbon content of the product oil and a consequent decrease in aliphatic hydrocarbon content. For some particular metals, the aromatic content increased markedly. For example, the aromatic content of the product oil for the 1 wt.% Ga-Y-zeolite was 93.1%, for the 1 wt.% Fe-Y-zeolite it was 93.5%, and for the 1 wt.% Ru-Y-zeolite the aromatic content reached 94.4% (percentages calculated as GC peak area). The addition of 5 wt.% of cobalt to the Y-zeolite produced no effect on the aromatic hydrocarbon content of the product oil compared to the non-metal zeolite catalyst. It should also be noted that the Co-Y-zeolite also produced the highest deposition of carbon on the catalyst during reaction.

Serrano et al. [29] have reviewed different types of solid acid catalysts (such as zeolites) and their influence on the process of catalytic pyrolysis of waste plastics (polyolefin plastics) for the production of fuels and chemicals. They also suggested a mechanism for the catalytic pyrolysis process through a carbocation catalytic cracking mechanism to produce carbenium ions via Lewis acid site reactions or carbonium ions via protonation of hydrocarbons on Bronsted acid sites. Subsequent isomerisation, oligomerisation, cyclisation, aromatisation and cracking reactions occur on the catalyst to produce an aromatic-rich product oil. This is in contrast to non-catalytic pyrolysis where the polymer degradation process produces a mainly aliphatic hydrocarbon product slate consisting of alkanes, alkenes and alkadienes [16, 30-32]. The mechanism involves initial random scission of the C ─ C bonds in the linear polymer structure to produce hydrocarbon fragments which stabilise to produce alkanes and alkenes through carbon-carbon double bond stabilisation [11, 29-31].

Other researchers have reported the increase in aromatic content through the use of catalytic pyrolysis. For example, Auxilio et al. [33], used a two-stage pyrolysis-catalysis reactor system with continuous feeding of the plastic for the processing of virgin plastics and mixed plastic wastes. The catalysts used were five different zeolite catalysts and clay-based catalysts in powder or pellet form. They reported that a high acidity clay-based catalyst in pellet form produced the highest yield of gasoline range ($C_5 - C_{11}$) oil product with 22 wt.% aromatic content for the processing of high-density polyethylene. Silva et al. [34] developed a novel HZSM-12 zeolite catalyst for the catalytic pyrolysis of high density polyethylene. The non-catalytic pyrolysis of the plastic produced a heavy molecular weight range hydrocarbon product mainly consisting of $C_8 - C_{22}$ hydrocarbons whereas catalytic pyrolysis produced mainly $C_3 - C_7$ hydrocarbons. Almustapha et al. [35], investigated a sulphated zirconia catalyst for the catalytic pyrolysis of high density polyethylene in a fixed bed reactor. The product oil contained hydrocarbons with a molecular weight range of $C_7 - C_{12}$ hydrocarbons with an aromatic content of 58 wt.%.

It has been shown that the zeolite supporting material in addition to the presence of metals influences the production of aromatic hydrocarbons. For example, Huang et al. [36], described the application of transition metals supported on zeolite or silica-alumina catalyst as bifunctional catalysts with two functions, whereby the acidic support provides the cracking and isomerisation function while the metals provide the hydrogenation or aromatisation function. Fricke et al. [37], have suggested that introduction of a transition metal (gallium) into zeolites favours dehydrogenation activity and increases selectivity of aromatic hydrocarbons in the processing of hydrocarbons. Chang et al. [38], studied the reactions of hexane over Ga-ZSM-5 zeolite and reported that gallium provides the active site for cracking, oligomerization and cyclization of aliphatic hydrocarbons while the major factor influencing the performance of Ga-supported catalysts is the dispersion of gallium rather than its oxidation state [38]. Other researchers have investigated metal impregnated catalysts on different support materials such as activated carbon, silica-alumina, and zeolites for the thermal degradation of polyethylene for the production of aromatic hydrocarbons [13, 36]. Scott et al. [13], investigated iron impregnated on charcoal for the fast pyrolysis-catalysis of polyethylene and other plastics, and found that high yields of aromatic compounds were produced. Uemichi et al. [26], also studied the use of transition metals as catalysts for the degradation of polyethylene over different supported catalysts such as activated carbon, Al_2O_3 and SiO_2-Al_2O_3. They reported that activated carbon gave the highest yield of aromatic hydrocarbons compared to Al_2O_3 and

SiO_2-Al_2O_3 supported transition metals, including Pt, Fe, Mo, Zn, Co, Ni and Cu, Pt, Fe, and Mo were reported to be the most effective. Later work by the same group [39] showed that for catalytic pyrolysis of polypropylene, Pt produced more aromatic hydrocarbon yield than Fe on activated carbon as the catalyst support [39]. The literature suggests that the increased yields of aromatic compounds with certain transition metal-Y-zeolite catalysts used in this work is due to the dual activity of the Y-zeolite which induces cracking and isomerisation and that the metals enhance dehydrogenation and aromatisation reactions.

The addition of increased metal content at 5 wt.% in the Y-zeolite catalysts produced a decrease in aromatic hydrocarbon concentration in the product oil (Figure 4.6). The decrease in aromatic content was small for the Ni-, Fe- and Ru-Y-zeolite catalysts, but was more significant for the Mo-, Ga- and Co-Y-zeolites. For example, the 5 wt.% Mo-Y-zeolite catalyst showed a reduction in aromatic hydrocarbon content from 86.3% for the 1 wt.% catalyst to 70.6% at 5 wt.% metal content. Also, for the cobalt Y-zeolite catalyst at 5 wt.% addition, the aromatic hydrocarbon content of the product oil fell to only 47.3 wt.%. The 5 wt.% Co-Y-zeolite catalyst also produced the lowest oil yield and the highest deposition of carbon onto the catalyst at 26 wt.% (Table 4.3).

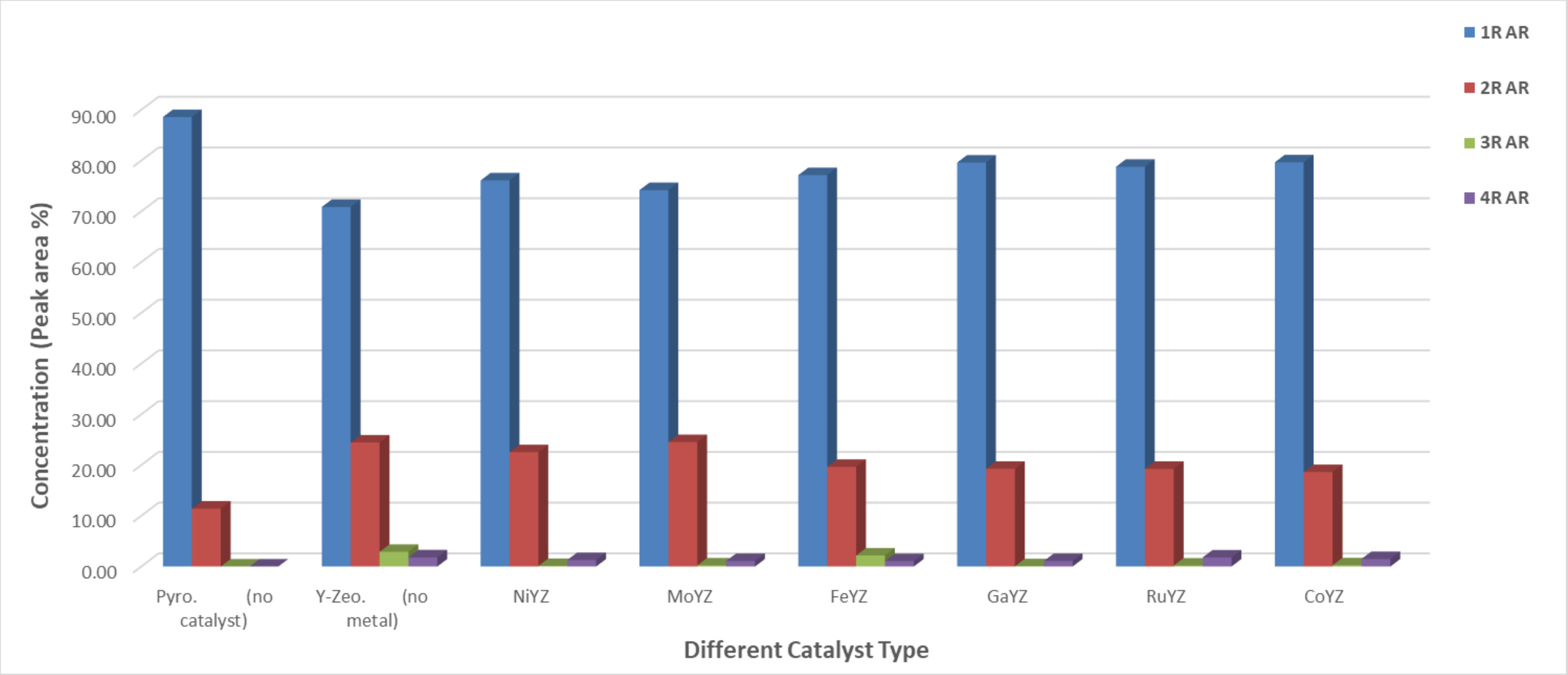

Figure 4.7. Hydrocarbon compositions of oils produced from pyrolysis of HDPE, over Y-zeolite and 1 wt.% metals/Y-Zeolite catalysts, (1R = single ring; 2R = two ring; 3R = three ring; 4R = four ring aromatic hydrocarbons).

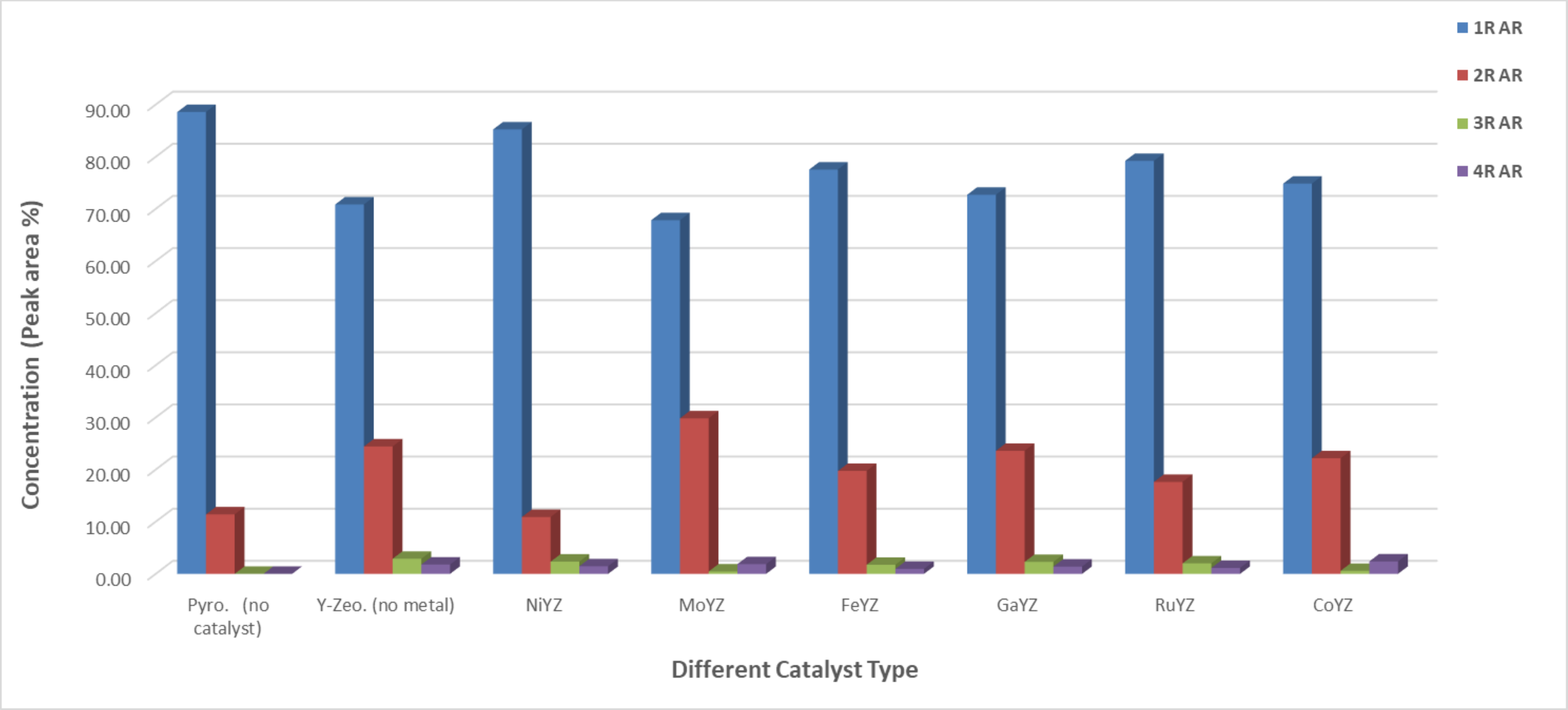

Figure 4.8. Hydrocarbon compositions of oils produced from pyrolysis of HDPE, over Y-zeolite and 5 wt.% metals/Y-Zeolite catalysts, (1R = single ring; 2R = two ring; 3R = three ring; 4R = four ring aromatic hydrocarbons).

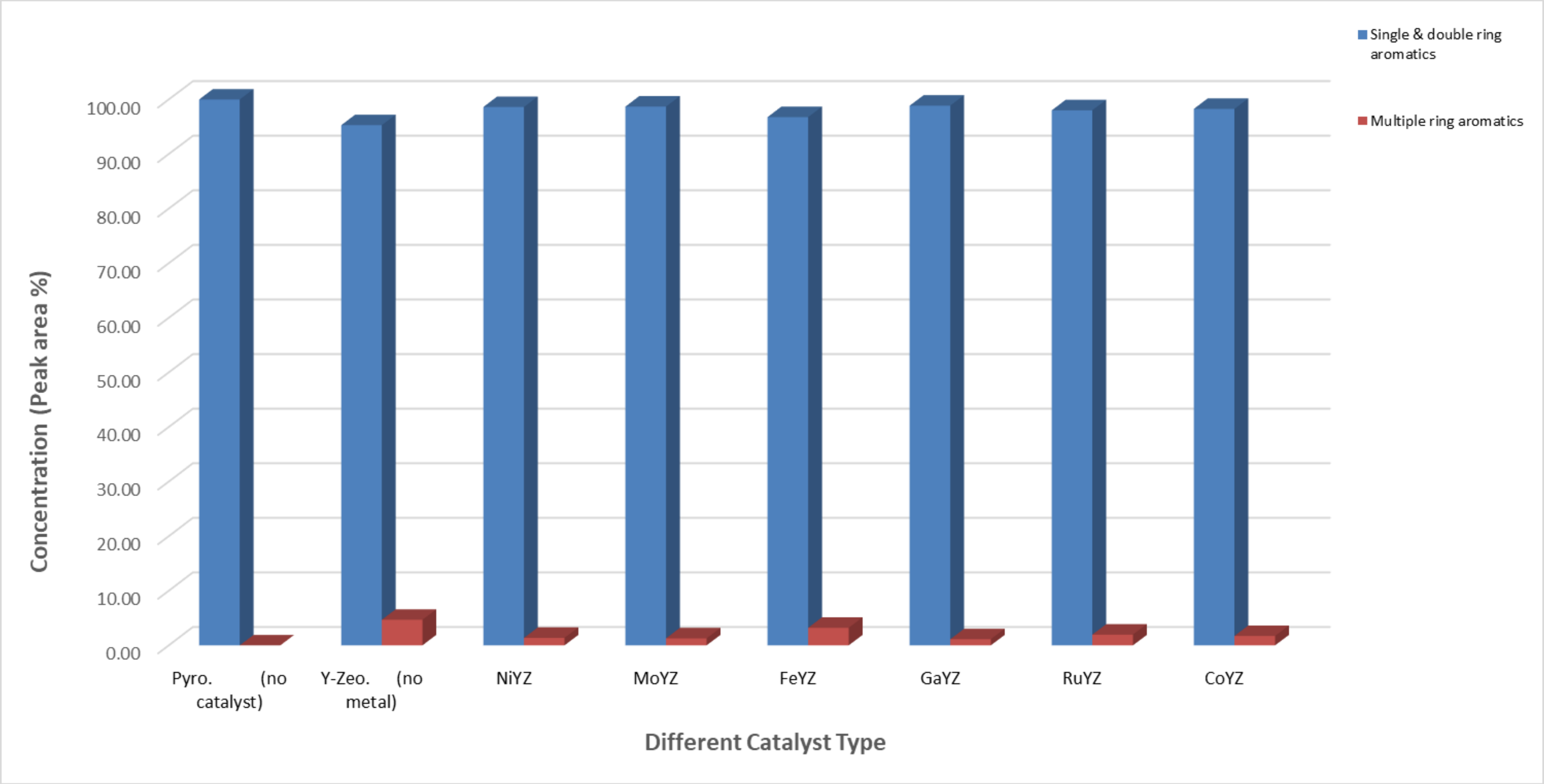

Figure 4.9. Hydrocarbon aromatic ring compositions of oils produced from pyrolysis of HDPE, over Y-zeolite and 1 wt.% metals/Y-zeolite catalysts.

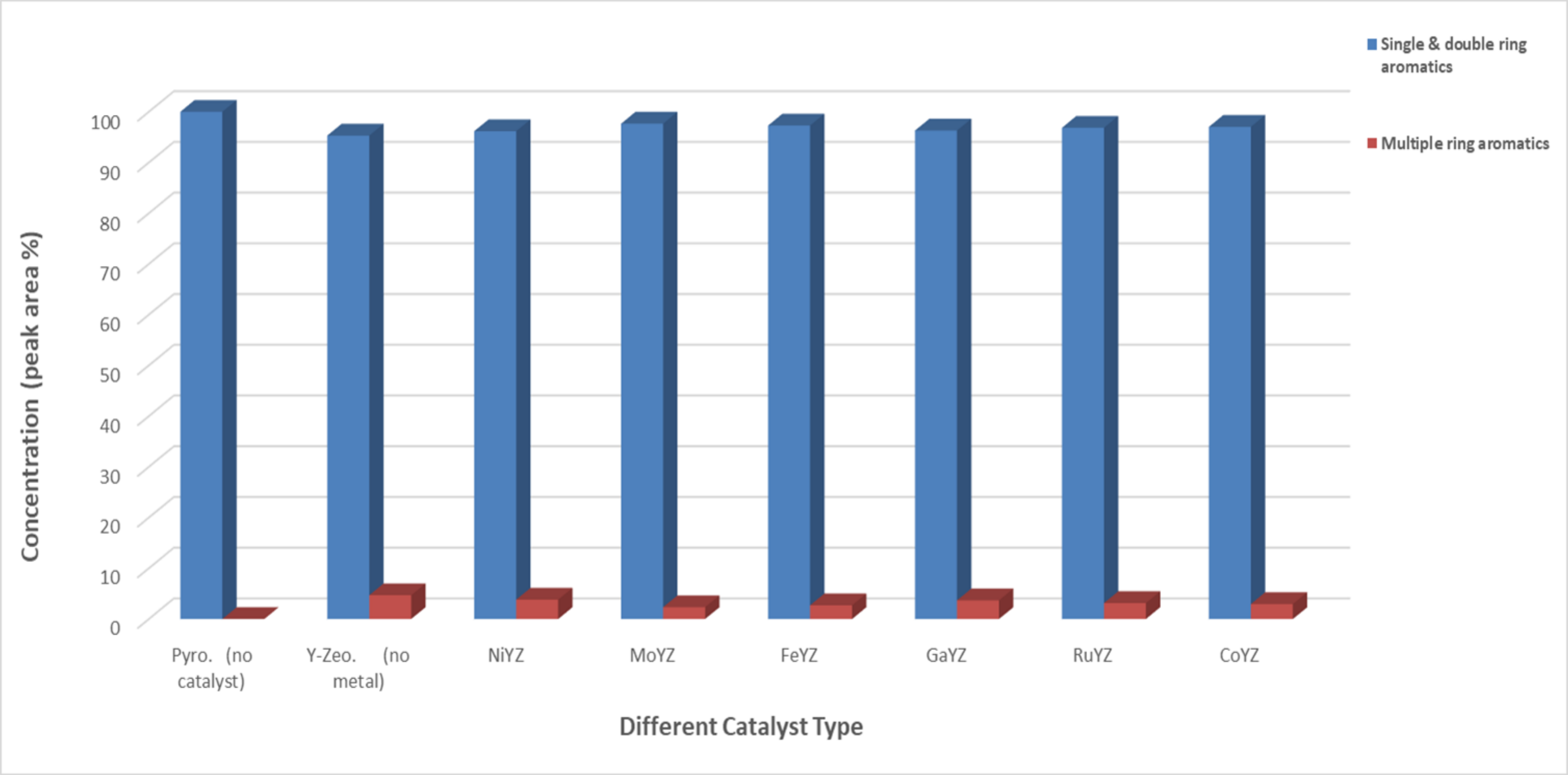

Figure 4.10. Hydrocarbon aromatic ring compositions of oils produced from pyrolysis of HDPE, over Y-zeolite and 5 wt.% metals/Y-zeolite catalysts.

Figures 4.7-4.10 show the distribution of single and 2-ring aromatic hydrocarbons and larger polycyclic aromatic compounds in the product oil. The results show that most of the aromatic hydrocarbons are single and 2-ring aromatic hydrocarbons. The Y-zeolite with no metal addition produced a product oil with 95.3% 1-2 ring aromatic hydrocarbon content and with the addition of the metal promoters this increased to 97-98%. The single ring aromatic hydrocarbons were mostly toluene, ethylbenzene and xylene and the 2-ring aromatic hydrocarbons were naphthalene and alkylated naphthalenes. The higher molecular weight >3-ring polycyclic aromatic hydrocarbons were mostly 3-ring phenanthrene and 4-ring pyrene and alkylated derivatives. Increasing the metal content to 5 wt.% resulted in only a small decrease of ~1% in 1-2 ring aromatic hydrocarbon content. The Y-zeolite catalyst produced higher concentration of multiple ring hydrocarbons but there was a reduction by the metal-Y-zeolite catalysts with a corresponding increase in single ring hydrocarbons. For example, Y-zeolite catalyst produced about 4.69% of multiple ring aromatic hydrocarbons but was reduced to 1.37 % using 1 wt.% Ni-Y-zeolite catalyst. Matsui et al. [28], in their investigation of the reactions of polycyclic aromatic hydrocarbons over nickel-zeolite reported an increased yield of single and two ring aromatic hydrocarbons. Many authors have reported increase in single and double ring contents of aromatic hydrocarbons with a corresponding decrease in aliphatic yields with addition of zeolite catalysts [6, 8, 40]. Consequently, as observed in this study, the metal/Y-zeolite catalysts have been used to enhance single and double ring aromatics production, which are important chemicals in the petrochemical industry.

4.4 Characterisation of catalysts

4.4.1 Catalyst characterisation in relation to catalyst temperature

The thermal and catalytic degradation of HDPE produces a wide range of aliphatic hydrocarbon gases, oils and waxes, and polymer fragments from light gases up to heavy molecular weight species when hydrocarbons volatiles pass over the metals/Y-zeolite catalyst. The volatiles/pyrolysis gases are cracked and solid carbons are deposited on the catalyst. The decomposition of plastics to form solid carbon and gas products has been illustrated via the reaction in equations [41].

$$\text{Thermal cracking: } pC_nH_x \rightarrow qC_mH_y + rH,$$

$$\text{Carbon formation:} \quad C_nH_x \rightarrow nC + x/2H_2$$

In the process of the pyrolysis-catalysis of the plastics, the polyalkene HDPE plastic was initially degraded into smaller organic compounds, and then subsequently dehydrogenated to produce carbon products and gaseous products. Likewise, as the catalyst temperatures increased, the heavy hydrocarbons decomposed into light hydrocarbons, providing more carbon for deposition on the catalysts [42]. This is consistent with the results in Table 4.1, as C_2-C_4 gaseous products and the liquid fraction decreased as temperature increases from 600 ^oC to 900 ^oC.

Claridge et al. [43], stated that there are two possible mechanisms for carbon formation: the Boudouard reaction and the catalytic methane (hydrocarbon) decomposition reaction. Using an electron micrograph, two types of carbon were identified on the nickel catalyst; tubular carbon filaments (whisker carbon) with a co-axial channel, and the other form of carbon was encapsulated carbon shown on the micrograph.

Alberton et al.[44], evaluated carbon deposition on Ni/Al_2O_3 and reported the routes for carbon formation on the catalyst as: Boudouard reaction, methane decomposition and polymerization of ethane, with the latter originating from ethanol dehydration over Al_2O_3 acidic sites. It was also reported that the direct deactivation of the catalysts occurs mostly by covering active phases/sites of the catalyst with encapsulating carbon. However, carbon may be deposited on catalysts without deactivation in a mechanism that includes: carbon deposition over metal surface, migration of carbon containing species to the bulk phase of metal, saturation of these species and condensation of carbon.

The carbon produced from the process of pyrolysis-catalysis of HDPE can encapsulate the active metal sites of the catalyst, which results in catalyst deactivation. Likewise, the conversion efficiency of the plastics in the catalytic reforming process could decrease due to the deactivation of the catalyst depending on the type of carbon deposited and the amount of carbon deposited. There are different types of carbon which may form on the catalyst, including encapsulating carbons, which lead to catalyst deactivation, and/or filamentous-type carbons, which have a lesser influence on the deactivation of the catalyst. Therefore, the properties of the deposited carbons on the catalyst were determined by a series of analyses: TGA-TPO was used to identify the type of carbon deposited, and SEM was used to characterise the morphology of the carbon deposition.

The thermogravimetric analysis-temperature programmed oxidation (TGA-TPO) analysis was carried out to determine the weight loss data of the used catalyst (Y-zeolite) which by calculation subsequently gave the mass of carbon deposited on the catalyst. Figure 4.11a shows the weight loss percentage against temperature and the derivative curve (DTG-TPO). The TGA-TPO results show between 15-20% carbons deposited on the reacted catalyst at reaction temperatures of 600 to 800 ^{o}C. The derivative thermogram (DTG-TPO) results of the reacted Y-zeolite in Figure 4.11b Shows two main oxidation peaks between 0 and 200 ^{o}C which is suggested to be moisture loss, and at 400 and 600 ^{o}C as well as a smaller peak above 600 ^{o}C. This indicates that there are two different types of carbon deposited on the Y-zeolite catalyst during the process of pyrolysis-catalysis of HDPE at different temperatures from 600-800 ^{o}C. There were amorphous carbons which were oxidised between temperatures of 400 and 600 ^{o}C, and at temperatures above 600 ^{o}C the oxidation weight loss can be attributed to filamentous carbons which were deposited on the catalyst [45, 46]. As shown in Table 4.1, the solid carbon deposition increased as temperature increased, corresponding with reductions in oil yield. It could be suggested that as the solid carbon increased on the catalysts it caused deactivation of the catalyst at higher temperatures.

Scanning electron microscopy (SEM) images were also used to analyse the reacted catalysts at difference temperatures. These images aided identification of the types of carbon deposited on the catalyst. Figure 4.12 shows images taken at different temperatures with carbon deposits. They indicate that the deposits are mostly amorphous carbon and filamentous carbon and these were more visible at 900 ^{o}C.

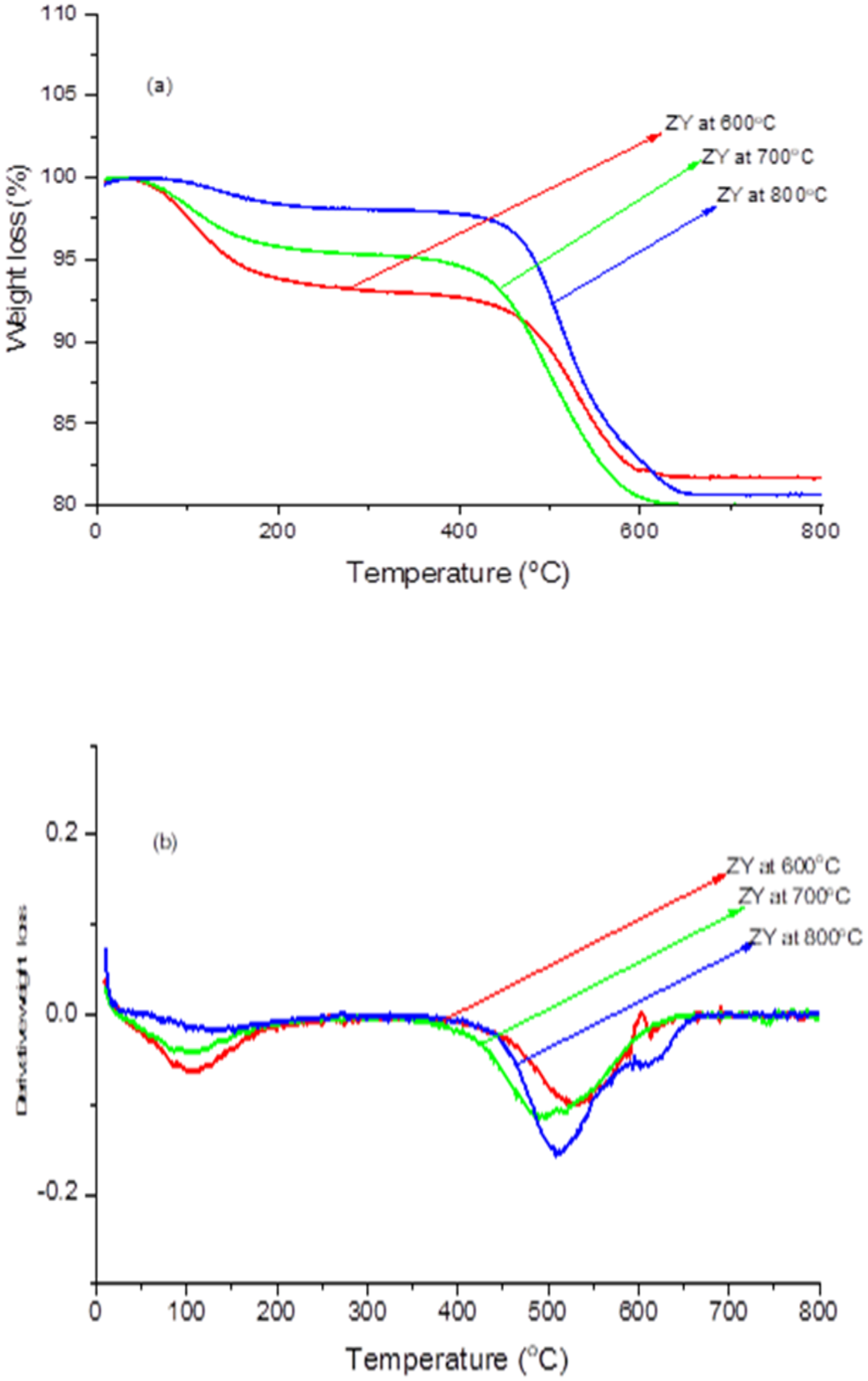

Figure 4.11. TGA-TPO and DTG-TPO results of reacted Y-zeolite at different temperatures.

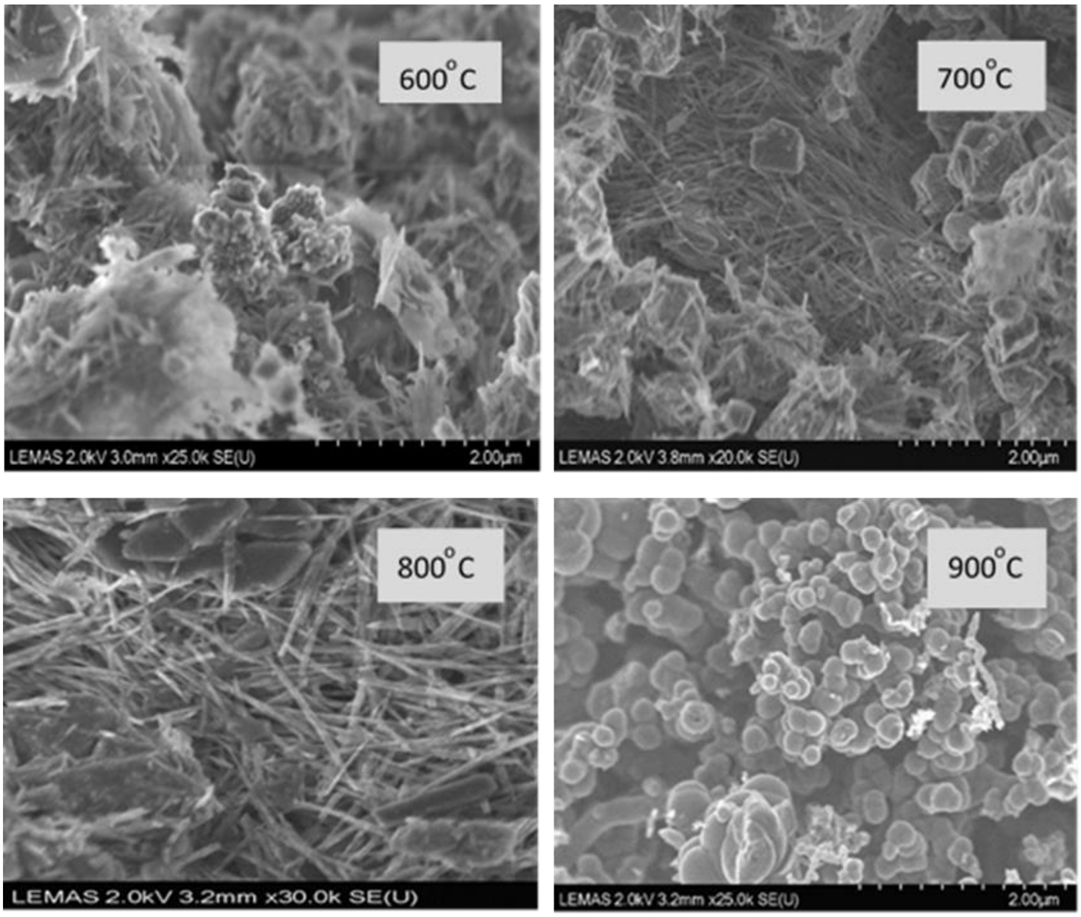

Figure 4.12. Scanning electron microscope images of Y-zeolite catalyst at different temperatures after pyrolysis-catalysis of the HDPE.

4.4.2 Catalyst characterisation with metal impregnated Y-zeolite catalysts.

Thermogravimetric analysis-temperature programmed oxidation (TGA-TPO) was used for the determination of the amount of carbon deposited on the reacted metal-Y-zeolite catalysts. The pyrolysis-catalysis processes can form carbon deposits on the catalyst, and the TGA-TPO process oxides the carbon in relation to the temperature of oxidation. Figure 4.13a shows the TGA-TPO thermograms for the used 1 wt.% metal loaded Y-zeolite catalysts and Figure 4.13b shows the TGA-TPO thermograms for the 5 wt.% metal catalysts after pyrolysis-catalysis of the HDPE. The TGA-TPO weight loss data showed that between 14-22 wt.% carbon was deposited on the 1% metal-Y-zeolite catalyst while for the 5 wt.% metal-Y-zeolite catalysts the range of carbon deposition was between 18-26 wt.% (data also shown in Table 4.3), also see Figure 4.14. This indicates that as the percentage of metal loading on the catalyst was increased from 1 wt.% to 5 wt.%, the more carbon was deposited on the catalyst indicating an increase in catalysed cracking reactions. Oxidation of the carbon occurred over a temperature range of 400 to 650 °C. It has been reported that carbon oxidation occurring in the lower temperature range of 450 - 550 °C is mainly ascribed to amorphous type carbon and oxidation in the temperature range of 550 - 650 °C is ascribed to filamentous type carbon [45]. The amorphous type carbons are more problematic for catalyst activity in that they encapsulate the metal particles, reducing catalyst activity. Filamentous carbons grow away from the catalyst surface and have lesser of an effect on catalyst activity.

In their study, Fang et al. [47], found no oxidation peak at temperatures below 400 ^{o}C (which are attributed to amorphous carbon and are highly reactive and easily oxidized from the surface of the nickel catalyst analysed), while the large peak at about 600 ^{o}C was attributed to more graphitic filamentous carbon which are more stable and are oxidized at higher temperatures.

Zhang et al. [46], highlighted that the SEM results showed that the carbon deposited (filamentous carbons) were relatively long, straight and of regular shape and the TEM analysis confirmed that the filamentous carbons were multi-walled carbon nanotubes (MWCNTs).

Wu and Williams [45], investigated SEM analysis on the reacted Ni-Mg-Al catalyst and showed that the catalyst particles were cracked, and a layer carbon seemed to have been deposited on the surface of the catalyst. This was suggested to be layered carbons. The layered carbons consisted of metal carbides or carbonaceous species or monoatomic carbons formed initially, followed by the formation of filamentous carbons on top of the layered carbons after the steam gasification of hydrocarbons from the pyrolysis-catalysis of plastics.

Li et al. [48], demonstrated that the type of carbon formed depends on the chemical structures of the hydrocarbon precursors. It was found that aromatic molecules favour the growth of single walled nanotube while aliphatic molecules tend towards the formation of multi-walled nanotubes or non-tubular carbon structures as investigated by SEM and TEM as well as other analysers. They also pointed out that the formation of different types of carbon (SWNTs or MWNTs) does not mainly depend on carbon precursors but also on other growth conditions such as catalyst, temperature and gas flow rate.

Zhang et al. [49], investigated SEM micrographs of the carbon formed on the reacted nickel-stainless-steel mesh catalyst, and reported that the diameters of filamentous carbons formed at a catalysis temperature at 700 ^{o}C were smaller than the filamentous carbons formed at higher catalysis temperatures. The TEM analysis indicated the presence of MWCNTs as the type of carbon deposited on the nickel-stainless-steel mesh catalyst and the amount of MWCNTs was compared to solid fibre filamentous carbons and amorphous carbons. Conclusively, the electron microscopy (SEM and TEM) examination of carbon revealed that the carbon consisted mainly of filamentous carbons, which consisted of a high proportion (approx. 40%) MWCNTs.

The quality of CNT was influenced by process conditions; the optimal conditions for the production of high yields of CNT was estimated at 800 ^{o}C catalytic temperature and plastic-to-catalyst ratio of 1:2. At these conditions the filamentous/CNT type carbons yields were more than 0.3g for each gram of plastic feedstock [49].

Kumar and Ando [50], reported an increase in diameters of CNTs with an increase in reaction temperature, with pure hydrocarbon as feedstock in a process using chemical vapour deposition. Likewise, carbon formation in the presence of different catalysts was suggested to be linked to hydrocarbon decomposition reactions and the carbon deposition on the surface of the catalyst was enhanced by lower steam presence, because the carbon-steam reaction would be depressed [46].

In addition, in another study, the selective removal of amorphous type carbons using steam to increase CNTs production has been reported. Higher reduction of amorphous carbons from 15.4 to 2.4 wt.% was observed compared to the reduction of graphitic (filamentous) carbons with the addition of steam to the pyrolysis reforming of a HDPE sample [51].

In a similar tendency, lower magnification SEM results for carbon deposited on a catalyst showed that there might be surface break-up of the Ni-Mg-Al catalyst during steam pyrolysis-gasification of plastics sample and this surface break-up of the reacted catalyst was suggested to be linked to filamentous type carbon as shown in the high magnifications of the SEM [52].

Studies have shown that some of the types of carbon formed on catalysts during pyrolysis-catalytic gasification of plastics to obtain hydrogen and other useful products have been graphitic carbons are suggested to be carbon nanotubes (CNTs) and regarded as a valuable by-product instead of being discarded as unwanted coke [53]. According to research [54], CNTs have special physical and chemical properties that enable their use in many applications. For example, bulk CNTs have been used for automotive parts, sporting goods and rechargeable batteries. Multi-walled carbon nanotubes (MWCNTs) can be added into paint, to reduce biofouling and are used for multi-functional coating materials. MWCNTs have been extensively used in lithium ion batteries for improvement of electrical and mechanical properties. In addition, CNTs can also be used in biosensors and medical devices due to their chemical and dimensional compatibility with biomolecules.

The deposition of carbon onto the Y-zeolite catalysts will have significant impact on the efficiency of the pyrolysis-catalytic processing of the plastic. The carbon will block the pores of the Y-zeolite and also cover the acidic active sites of the Y-zeolite and the metal active sites of the added promoter metals. Thereby, the reactions of the pyrolysis gases produced from the pyrolysis of the plastic over the catalyst will be reduced, leading to lower content of aromatic hydrocarbons in the product oil. For example, the Co-Y-zeolite with the highest carbon deposition on the catalyst produced an oil with a lower aromatic hydrocarbon content. Scanning electron microscopy (SEM) imaging was used to characterise the reacted metal-Y-zeolite catalysts. These images give an identification of the types of carbon deposited on the reacted catalyst. Figures 4.15 and 4.16 show the SEM images of the Y-zeolite and the metals/Y-zeolite catalysts at 1 wt.% and 5 wt.% loading. Noticeable on the SEM micrographs were the filamentous type deposits of carbon on the catalyst surface, particularly at the 5 wt.% metal loading.

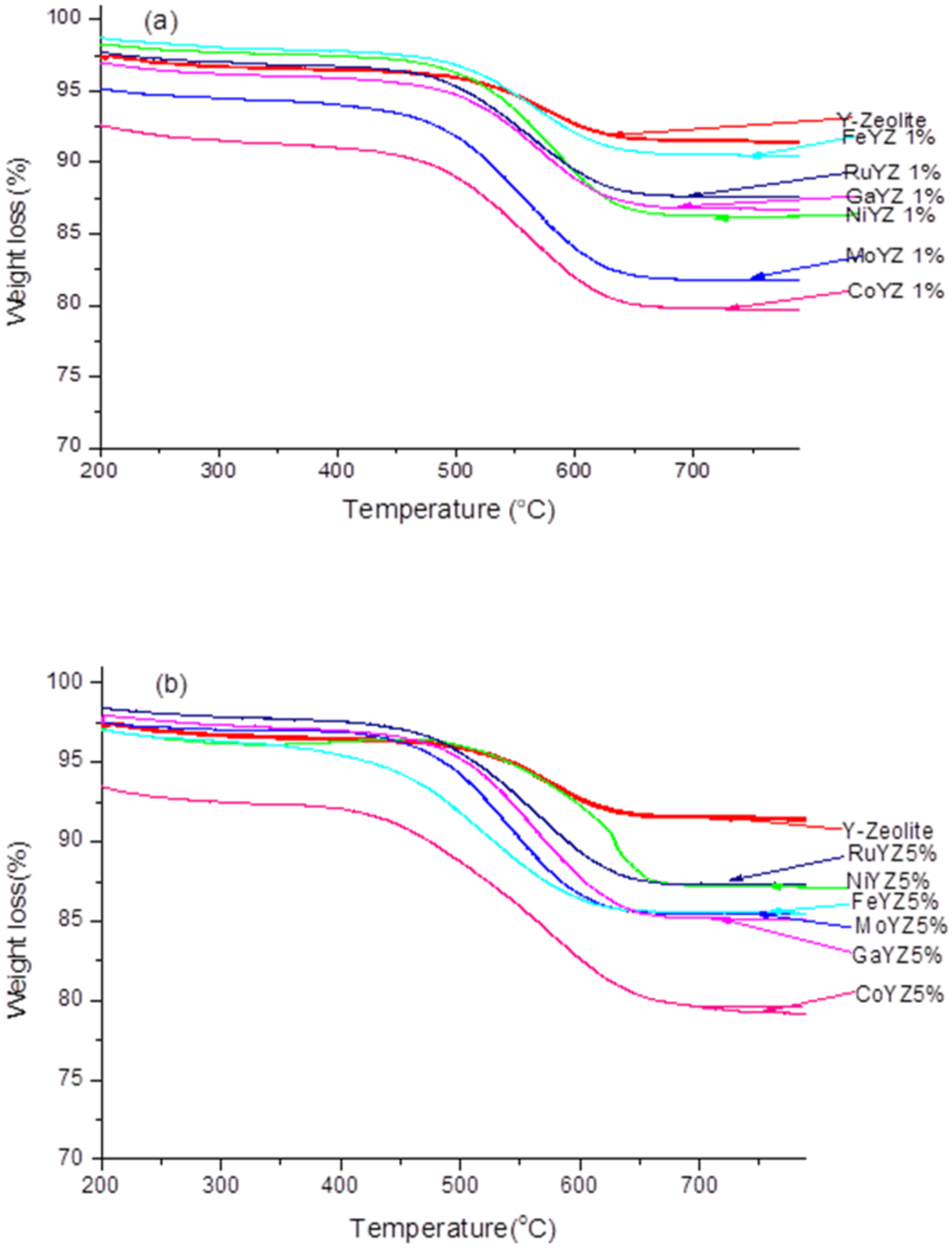

Figure 4.13. TGA-TPO thermograms after pyrolysis-catalysis of the HDPE results for the used catalysts (a) 1% and (b) 5% metal loaded Y-zeolite catalysts.

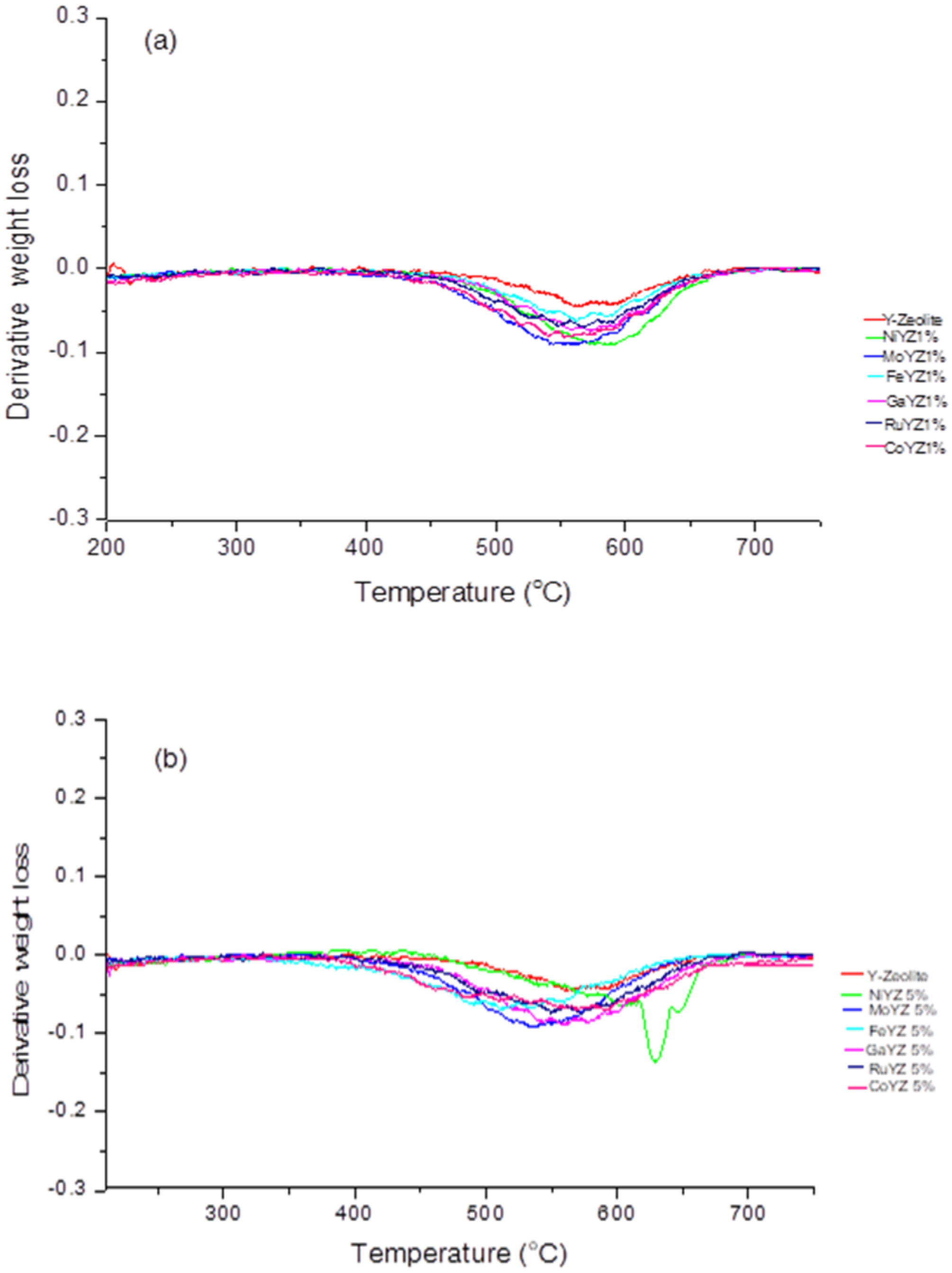

Figure 4.14. DTG-TPO thermograms after pyrolysis-catalysis of the HDPE results for the used catalysts (a) 1% and (b) 5% metal loaded Y-zeolite catalysts.

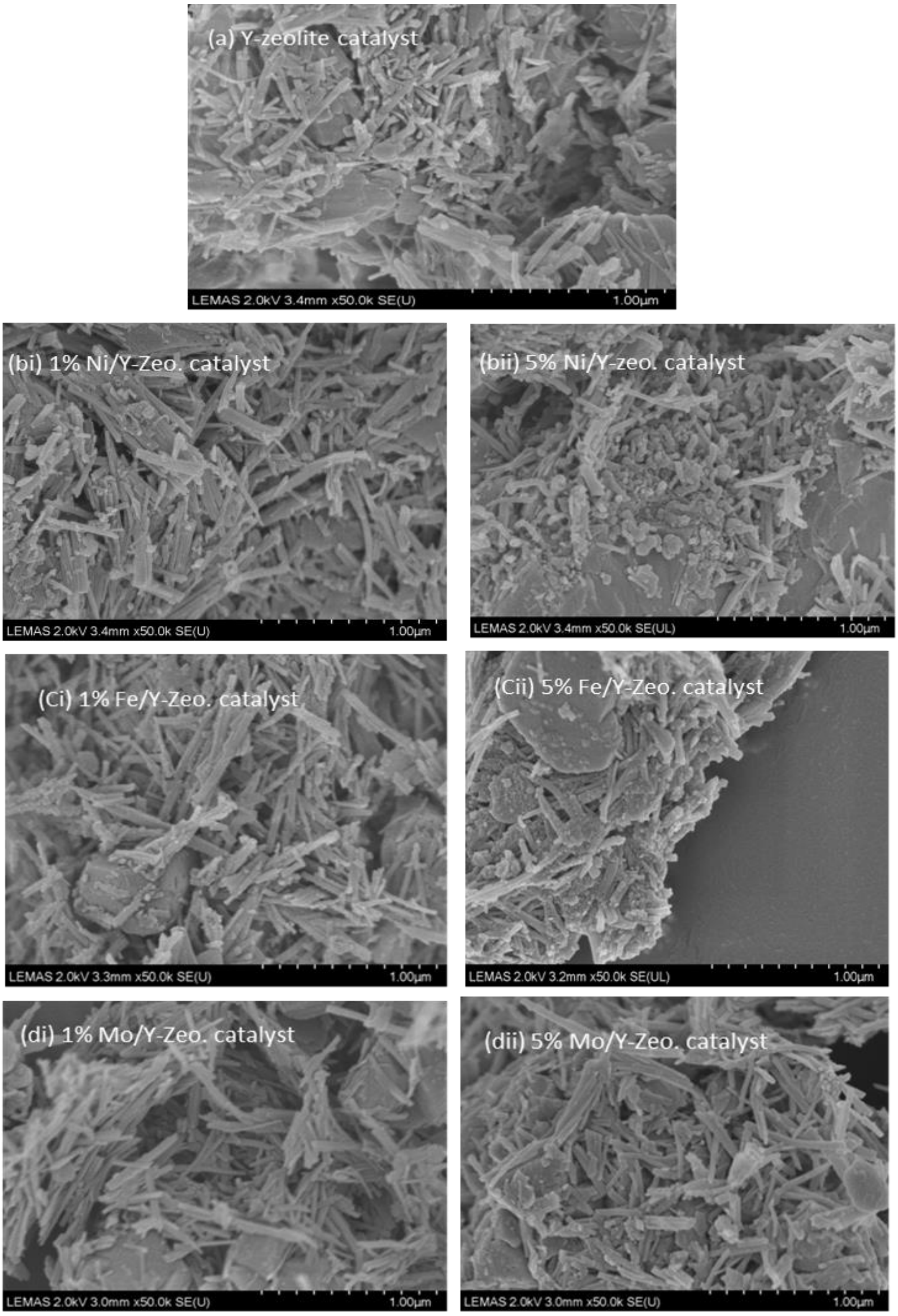

Figure 4.15. Scanning electron microscope images of the Y-zeolite, 1 wt% metal/Y-zeolite and the 5 wt.% metal/Y-zeolite catalysts after pyrolysis-catalysis of the HDPE.

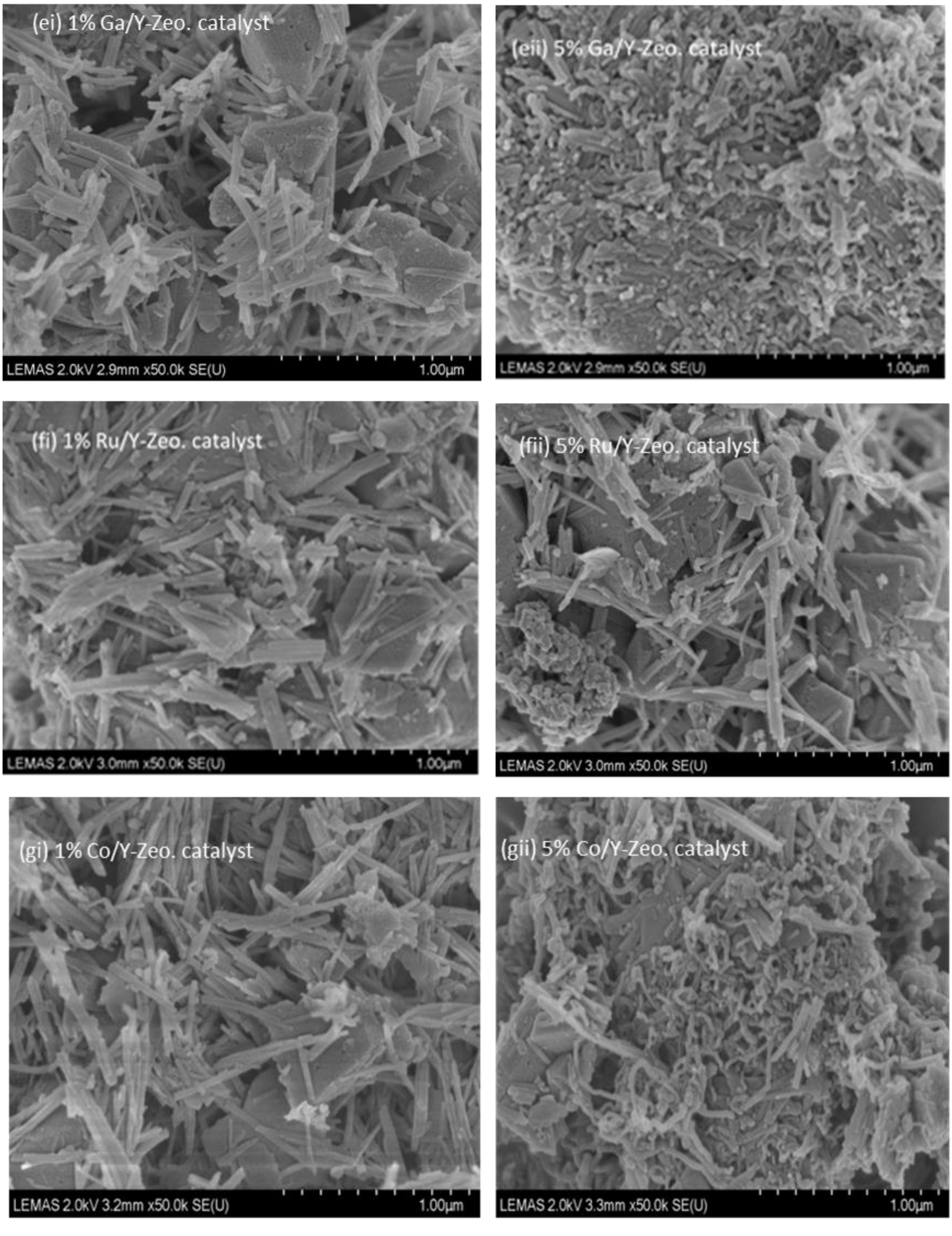

Figure 4.16. Scanning electron microscope images of the Y-zeolite, 1 wt% metal/Y-zeolite and the 5 wt.% metal/Y-zeolite catalysts after pyrolysis-catalysis of the HDPE.

4.5 Conclusions

High density polyethylene (HPDE) has been pyrolysed in a fixed-bed two-stage pyrolysis-catalysis reactor with a constant pyrolysis temperature of 600 ^{o}C. The catalytic bed temperature was varied from 600 to 900 ^{o}C to determine the effect of temperature on gas composition and aromatic oil yield. The experiments were conducted with and without catalysts. The results showed that as the catalyst temperature was increased, gas yield increased up to temperatures of 800 ^{o}C and then decreased at 900 ^{o}C. Also, the liquid yield decreased while the solid carbon deposition on the catalyst increased throughout the entire temperature range studied. The yield of hydrogen in the absence of catalyst was 0.35 mmol/g (4.95 vol.%) but increased to 2.41 mmol/g (25.40 vol.%) by introduction of Y-zeolite catalyst into the pyrolysis system at the initial catalytic bed temperature of 600 ^{o}C. The hydrogen and methane yield continuously increased as the temperature was increased through to the final temperature studied. Hydrogen increased to 15.34 mmol/g (41.05 vol.%) while methane increased to 15.49 mmol/g (41.44 vol.%) at catalytic temperature of 900 ^{o}C. Although the total liquid yield decreased, the content of aromatic hydrocarbons in the oil increased above 98% and there was a consistent decrease in aliphatic compounds as the temperatures increased. The effect of metal/Y-zeolite catalysts was investigated. In the non-catalytic pyrolysis process, the HDPE produced a high oil yield (~70 wt.%) comprised of almost 100% aliphatic hydrocarbon content. Introduction of the Y-zeolite catalyst caused a reduction of oil yield, but the composition of the oil was mostly aromatic hydrocarbons (~79%). Loading transition metals (including nickel, iron, molybdenum, gallium, ruthenium and cobalt) on the Y-zeolite catalyst promoted the formation of aromatic hydrocarbons (80-95%) in the product oil and increased hydrogen gas production. The aromatic hydrocarbons in the product oil using the metal-promoted Y-zeolite catalysts showed that the oil was composed of between 97-99% 1-2 ring aromatic compounds. The aromatic hydrocarbons in the oil were mostly toluene, ethylbenzene and xylene and the 2-ring aromatic hydrocarbons were naphthalene and alkylated naphthalenes. However, the introduction of the metal promoters to the Y-zeolite at 1 wt.% addition resulted in high carbon deposition onto the catalysts of between 14 – 26 wt.% and at the higher metal loading of 5 wt.% producing even higher carbon deposition. The carbon deposits were identified as mostly filamentous type carbon.

References

1. R.Miandada, et al., *Catalytic pyrolysis of plastic waste: Areview.* Process Safetyand Environmental Protection, 2016. **102**: p. 822–838.
2. Lopez, A., et al., *Influence of time and temperature on pyrolysis of plastic wastes in a semi-batch reactor.* 2011. **173**(1): p. 62-71.
3. Yoshioka, T., et al., *Pyrolysis of poly (ethylene terephthalate) in a fluidised bed plant.* 2004. **86**(3): p. 499-504.
4. Ji, L., A. Hervier, and M.J.C. Sablier, *Study on the pyrolysis of polyethylene in the presence of iron and copper chlorides.* 2006. **65**(7): p. 1120-1130.
5. Marcilla, A., et al., *Study of the catalytic pyrolysis behaviour of polyethylene–polypropylene mixtures.* 2005. **74**(1-2): p. 387-392.
6. Kim, B.-S., et al., *Catalytic copyrolysis of cellulose and thermoplastics over HZSM-5 and HY.* 2016. **4**(3): p. 1354-1363.
7. Singh, R.K. and B.J.F. Ruj, *Time and temperature depended fuel gas generation from pyrolysis of real world municipal plastic waste.* 2016. **174**: p. 164-171.
8. Jung, S.-H., et al., *Pyrolysis of a fraction of waste polypropylene and polyethylene for the recovery of BTX aromatics using a fluidized bed reactor.* 2010. **91**(3): p. 277-284.
9. Liu, J., et al., *Catalytic pyrolysis of polypropylene to synthesize carbon nanotubes and hydrogen through a two-stage process.* 2011. **96**(10): p. 1711-1719.
10. del Remedio Hernandez, M., et al., *Effect of the temperature in the nature and extension of the primary and secondary reactions in the thermal and HZSM-5 catalytic pyrolysis of HDPE.* 2007. **317**(2): p. 183-194.
11. Al-Salem, S., et al., *A review on thermal and catalytic pyrolysis of plastic solid waste (PSW).* 2017. **197**: p. 177-198.
12. Westerhout, R., J. Kuipers, and W. Van Swaaij, *Experimental determination of the yield of pyrolysis products of polyethene and polypropene. Influence of reaction conditions.* Industrial & engineering chemistry research, 1998. **37**(3): p. 841-847.
13. Scott, D., et al., *Fast pyrolysis of plastic wastes.* Energy & Fuels, 1990. **4**(4): p. 407-411.
14. Liu, J., et al., *Catalytic pyrolysis of polypropylene to synthesize carbon nanotubes and hydrogen through a two-stage process.* Polymer Degradation and Stability, 2011. **96**(10): p. 1711-1719.
15. Aguado, J., et al., *Feedstock recycling of polyethylene in a two-step thermo-catalytic reaction system.* 2007. **79**(1-2): p. 415-423.
16. Westerhout, R., et al., *Recycling of polyethene and polypropene in a novel bench-scale rotating cone reactor by high-temperature pyrolysis.* 1998. **37**(6): p. 2293-2300.

17. Mastral, F., et al., *Pyrolysis of high-density polyethylene in a fluidised bed reactor. Influence of the temperature and residence time.* Journal of Analytical and Applied Pyrolysis, 2002. **63**(1): p. 1-15.

18. del Remedio Hernández, M., Á.N. García, and A. Marcilla, *Study of the gases obtained in thermal and catalytic flash pyrolysis of HDPE in a fluidized bed reactor.* Journal of Analytical and Applied Pyrolysis, 2005. **73**(2): p. 314-322.

19. Chin, B.L.F., et al., *Kinetic studies of co-pyrolysis of rubber seed shell with high density polyethylene.* 2014. **87**: p. 746-753.

20. Xiao, X., et al., *Catalytic steam gasification of biomass in fluidized bed at low temperature: conversion from livestock manure compost to hydrogen-rich syngas.* 2010. **34**(10): p. 1505-1512.

21. Williams, E.A. and P.T. Williams, *The pyrolysis of individual plastics and a plastic mixture in a fixed bed reactor.* Journal of Chemical Technology and Biotechnology, 1997. **70**(1): p. 9-20.

22. Onwudili, J.A., et al., *Composition of products from the pyrolysis of polyethylene and polystyrene in a closed batch reactor: Effects of temperature and residence time.* 2009. **86**(2): p. 293-303.

23. Xue, Y., A. Kelkar, and X.J.F. Bai, *Catalytic co-pyrolysis of biomass and polyethylene in a tandem micropyrolyzer.* 2016. **166**: p. 227-236.

24. Lopez, A., et al., *Pyrolysis of municipal plastic wastes II: Influence of raw material composition under catalytic conditions.* Waste Manag, 2011. **31**(9-10): p. 1973-83.

25. Kaminsky, W. and J.-S. Kim, *Pyrolysis of mixed plastics into aromatics.* Journal of Analytical and Applied Pyrolysis, 1999. **51**(1): p. 127-134.

26. Uemichi, Y., Y. Makino, and T. Kanazuka, *Degradation of polyethylene to aromatic hydrocarbons over metal-supported activated carbon catalysts.* Journal of Analytical and Applied Pyrolysis, 1989. **14**(4): p. 331-344.

27. Guisnet, M., N. Gnep, and F. Alario, *Aromatization of short chain alkanes on zeolite catalysts.* Applied Catalysis A: General, 1992. **89**(1): p. 1-30.

28. MATSUI, H., et al., *Hydrocracking of Polycyclic Aromatic Hydrocarbons Catalyzed by Three Nickel-supported Different Zeolite Catalysts.* Sekiyu Gakkaishi, 1996. **39**: p. 120-128.

29. Serrano, D., J. Aguado, and J. Escola, *Developing advanced catalysts for the conversion of polyolefinic waste plastics into fuels and chemicals.* ACS Catalysis, 2012. **2**(9): p. 1924-1941.

30. Williams, P.T., E.A.J.E. Williams, and Fuels, *Interaction of plastics in mixed-plastics pyrolysis.* 1999. **13**(1): p. 188-196.

31. Williams, P.T.J.F.R., P.o.W.P.C.W.P.i. Diesel, and O. Fuels, *Yield and composition of gases and oils/waxes from the feedstock recycling of waste plastic.* 2006: p. 285-313.

32. Marcilla, A., et al., *Thermal Degradation of LDPE− Vacuum Gas Oil Mixtures for Plastic Wastes Valorization.* 2007. **21**(2): p. 870-880.

33. Auxilio, A.R., et al., *An experimental study on thermo-catalytic pyrolysis of plastic waste using a continuous pyrolyser.* 2017. **67**: p. 143-154.

34. Silva, A.O., et al., *Development of HZSM-12 zeolite for catalytic degradation of high-density polyethylene.* 2017. **244**: p. 1-6.

35. Almustapha, M.N., et al., *Sulphated zirconia catalysed conversion of high density polyethylene to value-added products using a fixed-bed reactor.* 2017. **125**: p. 296-303.

36. Huang, C., A. Gujar, and M. Rodgers, *Methods of Producing Liquid Hydrocarbon Fuels from Solid Plastic Wastes*. 2012, Google Patents.

37. Fricke, R., et al., *Incorporation of gallium into zeolites: syntheses, properties and catalytic application.* 2000. **100**(6): p. 2303-2406.

38. Chang, C.-S. and M.-D. Lee, *Effects of hydrogen pretreatment on the acidic and catalytic properties of gallium-supported H-ZSM-5 in n-hexane aromatization.* Applied Catalysis A: General 1995. **123** (1): p. 7-21

39. Uemichi, Y., Y. Makino, and T. Kanazuka, *Degradation of polypropylene to aromatic hydrocarbons over Pt-and Fe-containing activated carbon catalysts.* Journal of Analytical and Applied Pyrolysis, 1989. **16**(3): p. 229-238.

40. Zhang, H., et al., *Catalytic co-pyrolysis of biomass and different plastics (polyethylene, polypropylene, and polystyrene) to improve hydrocarbon yield in a fluidized-bed reactor.* Energy & Fuels, 2014. **28**(3): p. 1940-1947.

41. Kaewpengkrow, P., D. Atong, and V.J.E.t. Sricharoenchaikul, *Pyrolysis and gasification of landfilled plastic wastes with Ni− Mg− La/Al2O3 catalyst.* 2012. **33**(22): p. 2489-2495.

42. Acomb, J.C., C.F. Wu, and P.T. Williams, *Effect of growth temperature and feedstock:catalyst ratio on the production of carbon nanotubes and hydrogen from the pyrolysis of waste plastics.* Journal of Analytical and Applied Pyrolysis, 2015. **113**: p. 231-238.

43. Claridge, J.B., et al., *A study of carbon deposition on catalysts during the partial oxidation of methane to synthesis gas.* 1993. **22**(4): p. 299-305.

44. Alberton, A.L., M.M. Souza, and M.J.C.T. Schmal, *Carbon formation and its influence on ethanol steam reforming over Ni/Al2O3 catalysts.* 2007. **123**(1-4): p. 257-264.

45. Wu, C. and P.T.J.A.C.B.E. Williams, *Investigation of coke formation on Ni-Mg-Al catalyst for hydrogen production from the catalytic steam pyrolysis-gasification of polypropylene.* 2010. **96**(1-2): p. 198-207.

46. Zhang, Y., et al., *Pyrolysis−Catalytic Reforming/Gasification of Waste Tires for Production of Carbon Nanotubes and Hydrogen.* Energy & Fuels 2015. **29**: p. 3328−3334.

47. Fang, W., et al., *Ce–Ni mixed oxide as efficient catalyst for H 2 production and nanofibrous carbon material from ethanol in the presence of water.* 2012. **2**(25): p. 9626-9634.

48. Li, Q., et al., *Effect of hydrocarbons precursors on the formation of carbon nanotubes in chemical vapor deposition.* 2004. **42**(4): p. 829-835.

49. Zhang, Y., et al., *Pyrolysis–catalysis of waste plastic using a nickel–stainless-steel mesh catalyst for high-value carbon products.* 2017. **38**(22): p. 2889-2897.

50. Kumar, M., Y.J.J.o.n. Ando, and nanotechnology, *Chemical vapor deposition of carbon nanotubes: a review on growth mechanism and mass production.* 2010. **10**(6): p. 3739-3758.

51. Wu, C., et al., *Processing real-world waste plastics by pyrolysis-reforming for hydrogen and high-value carbon nanotubes.* 2014. **48**(1): p. 819-826.

52. Wu, C. and P.T.J.F. Williams, *Pyrolysis–gasification of plastics, mixed plastics and real-world plastic waste with and without Ni–Mg–Al catalyst.* 2010. **89**(10): p. 3022-3032.

53. Wu, C.F., et al., *Sustainable processing of waste plastics to produce high yield hydrogen-rich synthesis gas and high quality carbon nanotubes.* RSC Advances, 2012. **2**(10): p. 4045-4047.

54. Zhang, Y., P.T.J.J.o.a. Williams, and a. pyrolysis, *Carbon nanotubes and hydrogen production from the pyrolysis catalysis or catalytic-steam reforming of waste tyres.* 2016. **122**: p. 490-501.

Chapter 5

Pyrolysis-catalytic steam reforming of agricultural biomass wastes and biomass components for production of hydrogen/syngas

5.1 Introduction

In this chapter, the pyrolysis-gasification of six biomass samples namely: rice husk, coconut shell, sugar cane, palm kernel shell, cotton stalk and wheat straw as well as the three main biomass components namely: cellulose, xylan (hemicellulose) and lignin were investigated in a two stage fixed bed reactor with and without catalyst and steam. In addition, the main components of biomass, and their mixtures, were also investigated for hydrogen production using the pyrolysis-catalytic steam reforming process. The two stage fixed bed reactor consists of a first section where pyrolysis of the feedstock (2 g) takes place while the second section is the catalytic bed (1 g). The catalyst used was 10 wt.% nickel metal supported on alumina (Al_2O_3). The final pyrolysis temperature was 550 ^{o}C with a heating rate from ambient to 550 °C of 20 ^{o}C min^{-1}. The volatiles from the first section were passed to the second catalyst stage pre-heated with a catalytic bed temperature of 750 ^{o}C. Water at a flow rate of 5.7 g/h was injected into the second stage catalyst bed reactor for steam reforming reaction for a higher hydrogen yield. Nitrogen was introduced as the carrier gas. The gaseous products collected in a Tedlar gas bag were analysed immediately after each pyrolysis-gasification experiment using packed column gas chromatography (GC). Several other analyses such as proximate, ultimate and TGA were conducted for the biomass samples and components as well as SEM, TPO, XRD for both fresh and reacted catalyst. Different agricultural biomass wastes were investigated, and also the main bio-polymer components of biomass, cellulose, hemicellulose and lignin in relation to hydrogen/syngas yield.

5.2 Characterisation of Samples

5.2.1 Thermogravimetric analysis (TGA)

The biomass samples and biomass components were characterised with thermogravimetric analysis (TGA) for the determination of the characteristics of the thermal degradation of the samples. Figure 5.1 shows the TGA and the differential weight loss (DTG) thermograms of the individual biomass samples and the three main biomass components. In addition, the main components of the biomass, cellulose, hemicellulose and lignin were mixed and characterised by TGA to determine any interaction between components during the thermal degradation process, the results are shown in Figure 5.2. The TGA and DTG thermograms for the cellulose, hemicellulose and lignin are shown in Figure 5.1(a) and 5.1(b) respectively. Xylan, which is a representative of hemicellulose, decomposed between temperatures of 200-350 °C, cellulose decomposition was between 350-400 °C while that of lignin showed a wider decomposition temperature which started at about 250 °C and continued up to about 500 °C and beyond. Liu et al. [1], studied the thermal degradation of biomass components and reported the mass loss temperature range of hemicellulose to be between 200-327 °C, that of cellulose ranged between 327-450 °C while that of lignin ranged between 200-550 °C, in agreement with this study. Yang et al. [2], reported that lignin thermally decomposes to about ~ 40 wt.% mass yield from an ambient to a final temperature of 700 ^{o}C with a very slow heating rate (<0.15 wt.%/ ^{o}C) but above 750 ^{o}C, it was stated that the weight-loss rate increased slightly to 0.3 wt.%/ ^{o}C and about ~67 wt.% weight loss was achieved at 850 ^{o}C. This was attributed to the slow carbonization (with carbon suggested to be the main product) of lignin which is the major part of biomass components responsible for char production. The order of thermal degradation of the three components with the most difficult to the easiest to degrade is lignin > cellulose> hemicellulose [2]. Orfao et al. [3], confirmed that lignin produced the most char and the degradation continued up to a temperature of about 900 ^{o}C. According to Burhenne et al. [4], lignin is stated to be very stable and more difficult to decompose compared to cellulose and hemicellulose, and also degrades over a wide temperature range up to 1173 K (900 ^{o}C) [5].

From Figures 5.1 and 5.2, the cellulose weight loss peak (which is the mass fraction loss at that temperature) of cellulose was observed in this study to have the largest DTG peak compared to hemicellulose and lignin. This was also confirmed by Yang et al. [5], as cellulose was reported to have a higher decomposition peak than lignin. According to Mckendry [6], cellulose generally has the largest weight fraction of an entire biomass sample which is about 40-50%, while hemicellulose represent 20-40% of the materials by weight. This may account for the high DTG peak observed with the cellulose component. The decomposition range of biomass components was also reported to be 225-325 ^{o}C for hemicellulose, 325-375 ^{o}C for cellulose, and lignin with a wider decomposition temperature range of 250-500 °C [7]. Several studies have shown similar degradation temperatures for cellulose, hemicellulose and lignin [2, 5].

Furthermore, It has been reported [4, 5], that lignin is an aromatic polymer with three-dimensional linkages in an alkyl-benzene structure, and is very stable and more difficult to decompose compared to cellulose and hemicellulose, degrading over a wide temperature range. Hemicelluloses are branched polysaccharides that consist of a group of bio-polymers which are more complicated than cellulose, and are reported to be thermally unstable and degrade at a lower temperature compared to cellulose and lignin [8]. In addition, cellulose is a polysaccharide consisting of a linear polymer of $\beta(1\rightarrow4)$ linked D-glucose units which decomposes between 325-400 °C [9]. Yang et al. [2], have reported the structure of the three main biomass components, stating that hemicellulose is a random amorphous structure with little strength while cellulose is a long glucose polymer unit without branches but crystalline, strong and resistant to hydrolysis. Lignin is reported to be composed of polysaccharides and heavily cross-linked [2]. The three dimensional alkyl-benzene structure of lignin includes p-hydroxyphenyl (H), guaicyl (G) and syringyl (S) reported to vary in different lignocellulosic feedstock [10]. Furthermore, the chemical structure of the three main biomass components is known to have different functional groups. The functional group of OH and C-O was found with cellulose, while hemicellulose contains higher C=O compounds and lignin was observed to have high methoxyl-O-CH_3, C-O-C and C=C stretching (aromatic ring) containing compounds [5]. However, it may be considered that, the high content of the C-O chemical group leads to high CO in cellulose while hemicellulose with C=O chemical group seems to have more CO_2 production, as shown in previous studies [2, 5, 11].

The agricultural waste biomass samples in this study may be linked to the thermal decomposition of the cellulose, hemicellulose and lignin [5, 9, 12-15]. The mass loss thermograms of all the agricultural waste biomass samples (Figure 5.1) were between the thermal degradation weight-loss thermogram ranges of the three biomass components. The thermal decomposition (TGA) of the six waste biomass samples started at ~200 °C and the DTG thermograms showed more than one peak for all the biomass samples indicating the presence and a reflection of these main biomass components as seen in Figure 5.2(a) and 5.2(b). The DTG thermogram for wheat straw showed one major DTG peak at about 330 °C which suggested a composition of mainly cellulose and hemicellulose [15]. Sugarcane bagasse showed three DTG peaks, at temperatures of 240, 300 and 360 °C, with the major peak where cellulose decomposition is indicated, suggesting that sugarcane bagasse contains mainly cellulose and hemicellulose. Varhegyi et al. [16], also observed three peaks for sugarcane bagasse, reporting that the first two DTG peaks could be attributed to hemicellulose and the third peak attributed to cellulose. Thermal decomposition of rice husks showed two DTG peaks at temperatures of 300 °C and 360 °C, with the major peak linked to cellulose and hemicellulose, and with the presence of some lignin indicated. Other studies have also reported that the composition of rice husks consists mainly of cellulose and hemicellulose [15, 17, 18].

The thermal decomposition of palm kernel shells also showed two DTG peaks at temperatures of 280 °C and 370 °C, with the major peak similar to lignin decomposition, suggesting that the palm waste biomass contained more lignin than the other main components [19]. Other studies [20] have reported that palm shell waste is composed mainly of cellulose and lignin. The thermal decomposition of cotton stalks showed two DTG peaks between temperatures of 300 °C and 350 °C representing the temperature where hemicellulose and cellulose decompose. Other studies [21, 22] of the thermal decomposition of cotton stalks suggest a higher content of cellulose compared to hemicellulose and lignin. Coconut shell also showed two DTG thermal decomposition peaks at temperatures of 280 °C and 360 °C, suggesting a composition of higher cellulose and lignin content compared to hemicellulose [15].

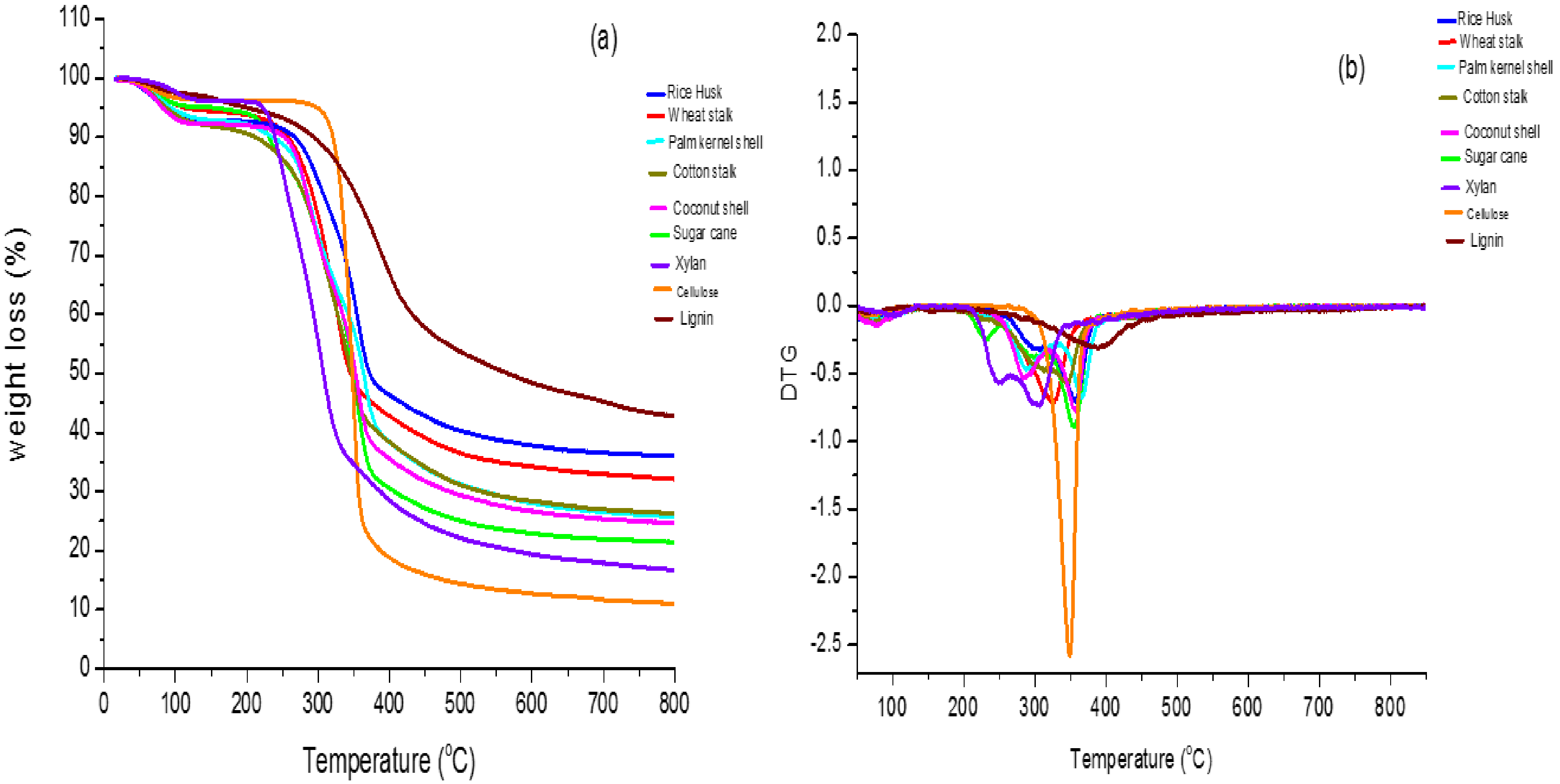

Figure 5.1. (a) TGA and (b) DTG thermograms of biomass samples and the main biomass components.

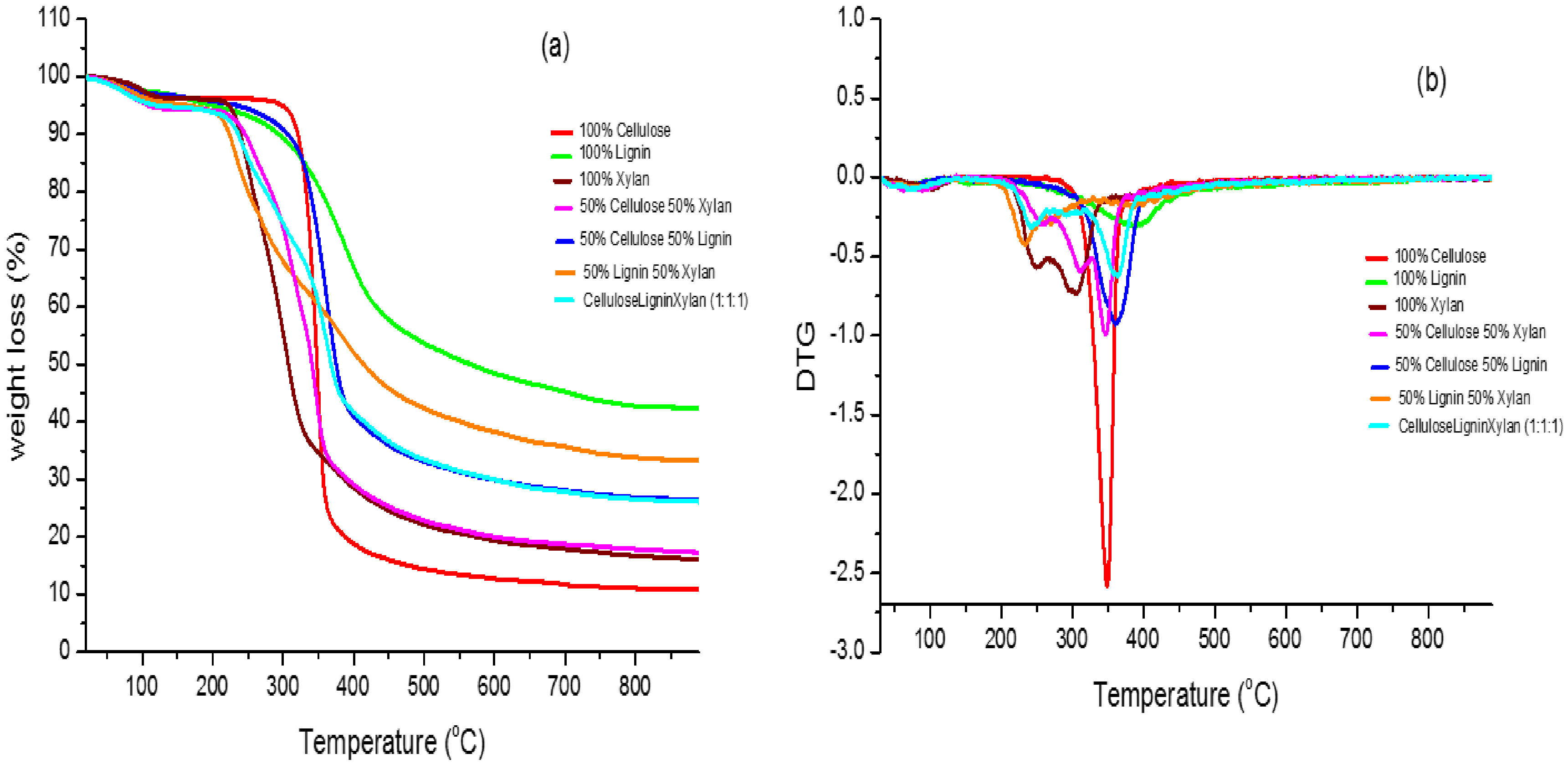

Figure 5.2. (a) TGA and (b) DTG thermograms of the main biomass components and their mixtures.

Figure 5.2(a) shows the TGA and Figure 5.2(b) shows the DTG thermogram of the mixtures of cellulose, hemicellulose and lignin. In the case of the 50:50 mixture of cellulose and lignin, there was a single DTG peak which occurred between the individual DTG peaks of cellulose and lignin. For the 50:50 mixture of xylan and lignin, two decomposition peaks were observed corresponding to the thermal decomposition of hemicellulose and lignin. However, the DTG thermogram peaks appeared to shift to lower decomposition temperatures, indicating interaction between the individual components. The mixture of 50:50 xylan and cellulose exhibited three peaks, which corresponded to the two decomposition DTG thermogram peaks of hemicellulose (although shifted to a higher temperature), and the cellulose decomposition DTG peak. A mixture of the three biomass components in equal proportions exhibited two separate DTG peaks, one at a temperature less than a temperature of 300 °C which may be attributed to the mass loss of xylan while the thermogram DTG peak above 300-400 °C could be the mass loss contribution by cellulose and some lignin. Yang et al. [2], analysed a mixture of hemicellulose, cellulose and lignin, it was suggested that virtually no significant obvious interaction existed between the biomass components but there was a shift in the thermal degradation to a higher temperature (about 10 ^{o}C) observed. It was also suggested that the pyrolysis of biomass could be regarded as a superposition of the three main components which perform separate roles during the biomass pyrolysis [2].

5.3 Product yield from the pyrolysis and pyrolysis-catalytic steam reforming of biomass sample wastes

Pyrolysis-catalytic steam reforming of the various agricultural waste biomass samples was conducted in the fixed bed, two stage reactor under a final pyrolysis temperature of 550 ^{o}C and the catalytic bed temperature of 750 ^{o}C, the resultant mass balance and gas concentration are illustrated in Table 5.1 and Figure 5.3. The product yields, which include the gas produced, liquid yield, residue and the carbon, were calculated with respect to the feedstock total weight (mass of biomass sample). Therefore, the mass balance was calculated as the total weight of the outputs (gases, liquid, char/residue and carbon) divided by total weight of inputs (these include the biomass feedstock sample and the water injected). Similarly, gas yield was calculated based on the results from the analyses of non-condensed gases injected into the gas chromatograph (GC-TCD/FID) after each experiment as conducted on the two stage fixed bed reactor. The gas concentration was calculated by the peak area obtained from the GC analysis and the molecular mass of each respective gas was used to compute the mass of the gas on an Excel spreadsheet. The liquid yield was calculated by differences in weight of condenser before and after each experiment, the same method of calculation was also applied to obtaining the weight of residue which is the difference in weight of the sample boat while carbon deposition is the difference in the weight of the reactor, before and after respectively. The calculations were discussed in Chapter 3.

The product yield and gas compositions from the pyrolysis (no catalyst) and pyrolysis-catalytic steam reforming of the agricultural waste biomass samples are shown in Table 5.1. The table shows the pyrolysis of the biomass wastes in the absence of the catalyst and without steam, but with silica sand in place of the catalyst bed. The results show that the sugarcane bagasse produced the highest total gas yield of 43.3 wt.%, palm kernel shell and coconut shell produced similar yields of gas at about 42 wt.% while rice husk and cotton stalk produced approximately the same gas yield of 39 wt.%. Also, wheat straw produced a gas yield of about 38 wt.% in the absence of catalyst. The highest char yield was produced by rice husk with a value of 37 wt.% and the lowest char production was cotton stalk at about 24 wt.%. Rice husks are known to have a high ash content which contributes to the char yield. From proximate analysis conducted (Chapter 3), rice husks had the highest ash content of about 18 wt.%, followed by the wheat straw of about 15 wt.% as compared to other samples with 1-5 wt.% ash content respectively.

The introduction of steam and the 10% $NiAl_2O_3$ catalyst to the pyrolysis-catalytic steam reforming process significantly increased total gas yield, with about 13-28 wt.% increment in gas yield observed across all the biomass samples. For example, palm kernel shell had a gas yield increase from 42 to 70 wt.% while rice husk and wheat straw had relatively the lowest gas yield value from 39 to 52 wt.% and from 38 to 51 wt.% which might be as a result of the high char produced by rice husk and wheat straw respectively. Several experimental investigations have also reported a higher total gaseous yield by introducing catalysts compared to absence of catalyst in the pyrolysis-catalytic steam reforming process [23, 24].

Similarly, Table 5.2 shows slight different in product yield and gas composition calculated based on dry-and-ash-free basis. Rice husks with the highest ash content produced slightly higher gas yield as compare with other feedstock.

Table 5.1. Mass balance and product yield from the pyrolysis and pyrolysis-catalytic steam reforming of biomass samples (as-received basis).

Feedstock	**Rice husk**		**Coconut shell**		**Surgarcane**		**Palm kernel shell**		**Cotton stalk**		**Wheat straw**	
	Sand	**Catalyst**	**Sand**	**Catalyst**	**Sand**	**Catalyst**	**Sand**	**Catalyst**	**Sand**	**Catalyst**	**Sand**	**Catalyst**
Product yield (wt.%)												
Gas	38.71	52.39	41.88	60.70	43.31	61.29	42.00	69.76	39.38	57.39	37.85	50.64
Char	36.50	39.00	26.00	29.00	25.50	25.00	30.00	27.50	24.00	25.00	30.50	30.50
Liquid*	24.79	7.11	32.12	7.80	31.19	10.71	28.00	2.74	36.62	17.61	31.65	15.86
Catalyst carbon	-	1.50	-	2.50	-	3.00	-	0.00	-	0.00	-	3.00
Gas composition (vol.%)												
CO	31.86	15.70	32.45	19.12	30.14	17.09	30.01	21.79	29.10	18.45	26.79	16.13
H_2	33.58	57.63	31.14	58.21	29.80	59.23	32.88	57.36	34.68	57.95	32.46	54.06
CO_2	20.38	23.99	17.56	20.74	22.50	21.50	19.79	18.49	18.53	21.09	21.48	22.35
CH_4	11.93	2.45	16.37	1.80	14.79	2.06	14.70	2.27	14.95	2.40	15.64	6.92
C_2-C_4	2.25	0.24	2.47	0.12	2.77	0.12	2.62	0.08	2.74	0.10	3.63	0.55

*By difference

Table 5.2. Mass balance and product yield from the pyrolysis and pyrolysis-catalytic steam reforming of biomass samples (dry-and-ash-free basis).

Feedstock	**Rice husk**		**Coconut shell**		**Sugarcane**		**Palm kernel shell**		**Cotton stalk**		**Wheat straw**	
	Sand	**Catalyst**	**Sand**	**Catalyst**	**Sand**	**Catalyst**	**Sand**	**Catalyst**	**Sand**	**Catalyst**	**Sand**	**Catalyst**
Product yield (wt.%)												
Gas	52.33	70.83	46.23	67.01	47.50	67.22	46.85	77.81	44.25	64.48	47.41	63.42
Char	49.35	52.73	28.70	32.02	27.97	27.42	33.46	30.67	26.97	28.09	38.20	38.20
Liquid*	33.52	9.62	35.46	8.61	34.20	11.74	31.23	3.06	41.15	19.79	39.64	19.87
Catalyst carbon	-	2.03	-	2.76	-	3.29	-	0.00	-	0.00	-	3.76
Gas composition (vol.%)												
CO	43.08	21.23	35.83	21.11	33.05	18.75	33.47	24.30	32.70	20.73	33.56	20.20
H_2	45.41	77.92	34.38	64.26	32.69	64.96	36.67	63.98	38.96	65.12	40.66	67.71
CO_2	27.55	32.43	19.39	22.90	24.68	23.58	22.07	20.63	20.82	23.70	26.90	27.99
CH_4	16.13	3.31	18.07	1.99	16.22	2.26	16.40	2.54	16.80	2.70	19.59	8.67
C_2-C_4	3.04	0.32	2.73	0.13	3.04	0.13	2.93	0.09	3.08	0.12	4.54	0.69
Gas composition (mmol g^{-1})												
CO	7.90	6.71	7.22	8.02	6.48	7.27	6.74	10.74	6.38	7.42	6.01	6.12
H_2	8.32	24.63	6.93	24.41	6.41	25.19	7.38	28.27	7.61	23.31	7.28	20.52
CO_2	5.05	10.25	3.91	8.70	4.84	9.14	4.44	9.12	4.06	8.48	4.82	8.48
CH_4	2.96	1.05	3.64	0.75	3.18	0.88	3.30	1.12	3.28	0.97	3.51	2.63
C_2-C_4	0.56	0.10	0.55	0.05	0.60	0.05	0.59	0.04	0.60	0.04	0.81	0.21

*By difference

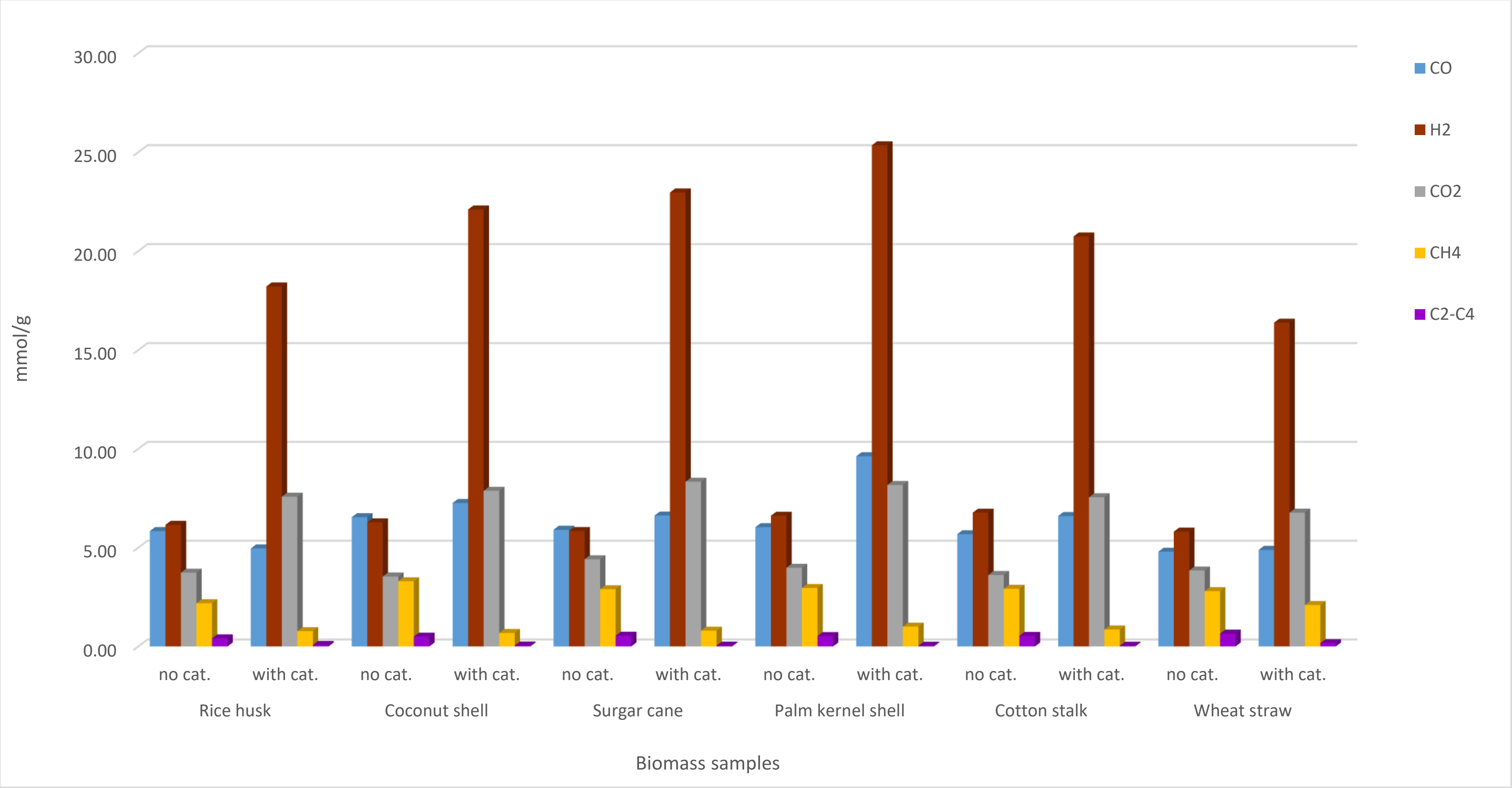

Figure 5.3. Gas composition yield pyrolysis-gasification catalysis of biomass samples (as-received basis).

Table 5.1 also shows the volumetric gas concentration from pyrolysis (without the addition of steam or catalyst) and in the presence of steam and the 10% $NiAl_2O_3$ catalyst. Pyrolysis produced a volumetric hydrogen concentration between 30-35 vol.%, carbon monoxide produced was between 27-32 vol.% for the different biomass samples. Furthermore, carbon dioxide was between 18-23 vol.%, methane was between 12-16 vol.% and C_2-C_4 hydrocarbon gases were between 2-4 vol.%. Consequently, the introduction of the 10% $NiAl_2O_3$ catalyst and steam to the pyrolysis-catalytic steam reforming process produced a marked increase in hydrogen production. The increase in the production of hydrogen resulted in an increase in the volumetric proportion of hydrogen, resulting in an increase in volumetric hydrogen in the product gas to 57.63 vol.%, 58.21 vol.%, 59.23 vol.%, 57.36 vol.%, 57.95 vol.% and 54.06 vol.% for rice husk, coconut shell, sugarcane, palm kernel shell, cotton stalk and wheat straw respectively. In terms of hydrogen yield, between 16.38 to 25.35 mmol/g was obtained from the mass of biomass feedstock pyrolysed. The hydrogen yield was in the order of wheat straw<rice husk<cotton stalk<coconut shell<sugarcane<palm kernel shell. There was an increase in carbon monoxide (CO) and carbon dioxide (CO_2), as shown in Figure 5.3 suggesting that water gas shift reaction and other reactions were promoted, as shown in Table 5.1. The carbon monoxide (CO) increased from about 5 to 10 mmol/g and carbon dioxide (CO_2) from ~ 4 to 8 mmol/g produced by the different biomass samples (see Figure 5.3). However, the methane (CH_4) yield and C_2-C_4 (tar) yield decreased which indicated that methane/hydrocarbon steam reforming and catalytic cracking reactions were dominant.

The pyrolysis process of biomass samples involves the production of water, permanent gases (such as H_2, CO, CO_2, and O_2), hydrocarbon (such as CH_4, C_2H_4, C_2H_6, etc.) and finally the production of carbonaceous solid-char shown in Table 5.2 and Equation 5.1. The production of H_2 yield as a desired product from the pyrolysis process usually involves a secondary reaction of volatile species which is suggested to occur at the vapour phase or between the vapour and solid phases [25]. The secondary gas phase reactions are suggested to be the most important factor in the formation of products during the pyrolysis process [13]. Also, several reactions are known to be at play during the pyrolysis and pyrolysis-catalytic steam reforming of biomass. For example, the methane/hydrocarbons steam reforming (Equation. 5.3) and water gas shift (Equation. 5.7) are known as gas-phase reactions due to the release of volatiles from pyrolysis at high temperatures which is the determinant of the final produced gas composition. Methane/hydrocarbons (Equation. 5.3) and tar (Equation. 5.2) equally undergo steam reforming as there are endothermic reactions to produce carbon-oxides and H_2. The thermal cracking of tar, which is also an endothermic reaction, leads to production of secondary lighter tar (hydrocarbon) and hydrogen is equally produced by the catalytic cracking as shown in Equation (5.4). Furthermore, there is conversion of the solid carbon (char) into gaseous products which are gas-solid reactions; water gas (carbon-water) and Boudouard reactions which equally leads to hydrogen production as shown in (Equations 5.8 and 5.9). Likewise, the pyrolysis process equally undergoes CO_2 reforming (Equations 5.5, 5.6 and 5.9) to produce syngas ($CO + H_2$) which is an important and desirable produced fuel as investigated in this study.

High temperatures have been reported to lead to increase gas composition such as H_2, CO, CH_4 and C_2H_4 from the biomass pyrolysis process. According to Dominguez et al. [26] a high pyrolysis temperature leads to a higher rate of total gas production while the liquid yield decreases due to the decomposition of heavier molecules into gaseous and lighter hydrocarbons. High temperatures were favoured in most of the reactions leading to hydrogen production [27, 28]. This is in accordance with the TGA results having a range of between 200-500 ^{o}C decomposition temperatures for all the biomass samples analysed in this study.

It has also been suggested that a longer residence time and higher temperature leads to an increase in the pyrolytic carbon formation resulting in higher yields of gaseous products due to continuation of a secondary reaction been favoured [29]. Higher heating rates are known to favour faster release of volatiles, increasing the liquid yield while the gaseous fraction and solid residue are being modified. It has been reported that the yield of volatiles increases with a decrease in particle size [10]. Likewise, smaller particles were reported to generate more hydrogen compared to larger particle sizes [30]. Additionally, catalysts added into the pyrolysis process has been equally reported to increase gaseous yield by decreasing the liquid fractions but with a positive up-grade effect on the quality of the oil composition [19].

Therefore, improving hydrogen yield from biomass pyrolysis thus involves modifying the process with the reactions as shown in Table 5.3 and, in addition, to the use of catalysts, temperature, particle size, feedstock composition, heating rate, residence time, etc. for the maximisation of hydrogen production.

Table 5.3. The main reactions of the pyrolysis-catalytic steam reforming of biomass.

Equation	**Reaction**	
$\text{Biomass} \rightarrow H_2O + H_2 + CO + CO_2 + \text{tar} + \text{hydrocarbon volatiles} + \text{char}$	Pyrolysis	(5.1)
$C_xH_yO_z + H_2O \rightarrow CO + H_2$	Tar steam reforming	(5.2)
$C_mH_n + H_2O \rightarrow CO + H_2$	Hydrocarbon volatiles steam reforming	(5.3)
$\text{Tars} \rightarrow H_2O + H_2 + CO + CO_2 + CH_4 + C_mH_n + C_xH_yO_z$	Catalytic cracking	(5.4)
$C_xH_yO_z + CO_2 \rightarrow CO + H_2$	Tar dry (CO_2) reforming	(5.5)
$C_mH_n + CO_2 \rightarrow CO + H_2$	Hydrocarbon volatiles dry (CO_2) reforming	(5.6)
$CO + H_2O \leftrightarrow CO_2 + H_2$	Water gas shift	(5.7)
$C + H_2O \rightarrow CO + CO_2 + H_2$	Char steam gasification	(5.8)
$C + CO_2 \rightarrow 2CO$	Char CO_2 gasification	(5.9)

5.4 Pyrolysis and catalytic-steam reforming of biomass components

The pyrolysis-catalytic steam reforming of lignin, cellulose, hemicellulose (xylan) and the components mixture were conducted in the two stage fixed bed reactor and the results are shown in Table 5.4 and Figure 5.4. In the absence of catalyst and steam, cellulose and hemicellulose pyrolysis generated a gas yield of about 50 wt.% and lignin about 30 wt.%. Pyrolysis of lignin marginally generated the highest hydrogen production compared to cellulose and hemicellulose, as also reported by Uddin et al. [19] and Yang et al. [5]. The highest char residue was observed with lignin at ~45%, while that of cellulose was ~20 wt.% and xylan ~18 wt.%. Since the first stage pyrolysis reactor was operated under the same conditions for the uncatalysed experiments (sand used in stage two) and for the catalysed experiments (catalyst used in stage two), the char residue yield was similar for both sets of experiments. The higher char yield for lignin pyrolysis compared with cellulose and hemicellulose char yield has been reported [3, 4]. According to Franco et al. [31], they suggested that the different behaviour of various biomass species could be due to the variation in reactivities of chars produced during the initial pyrolysis step depending on the cellulose or lignin content of the original biomass, the char reactivity varied significantly [32].

The introduction of the 10 wt.% $NiAl_2O_3$ catalyst and steam to the process showed an increase in gas yield for the three biomass components, at 55.45 wt.%, 55.44 wt.% and 50.48 wt.% for cellulose, hemicellulose and lignin respectively. The production of hydrogen from the catalytic steam reforming process was the highest for lignin and for cellulose and hemicellulose, CO and CO_2 yields were higher compared to lignin. The presence of methoxyl-O-CH_3 containing hydrocarbons in the lignin structure and their release during pyrolysis has been implicated in the enhanced production of H_2 from lignin [5, 11]. However, the presence of C – O and C = O structures in cellulose and hemicellulose results in enhanced production of CO and CO_2. In a study [5], lignin content was reported to generate a higher hydrogen and CH_4 gas than hemicellulose and cellulose, due to secondary reactions and catalytic reforming [11, 19, 33]. In addition, several authors have reported an increase in hydrogen production and carbon dioxide, carbon monoxide as well as a decrease in methane with traces of hydrocarbon (C_2-C_4) by catalytic reaction in the pyrolysis process of biomass. [34-36]. The increase in hydrogen production has been attributed to a higher temperature due to hydrocarbon decomposition

(CH_4, C_2-C_4) and endothermic reactions favoured at increasing temperature as well as the presence of a steam atmosphere and the use of catalyst that enhance the reforming reactions and char gasification leading to higher production of light gases such as H_2, CO and CO_2 [35, 37]. According to Kan et al. [38], the main reactions present are dehydrogenation, depolymerisation, and fragmentation prevailing at different ranges of temperature. Likewise, the high yields of hydrogen with an increase in CO_2, as well as decreased CO, CH_4 and C_2-C_4 from the catalytic pyrolysis-gasification process is suggested to be characterised by the water gas shift reaction, methane steam reforming and tar steam reforming, as shown in Table 5.3, which are the dominant reactions [27, 36, 39, 40]. The degradation of cellulose, hemicellulose and lignin significantly leads to the production of hydrogen and other gases during the pyrolysis process. Similarly, Table 5.5 shows slight different in product yield and gas composition calculated based on dry-and-ash-free basis. Likewise, lignin component slightly produced higher hydrogen as compared with cellulose and hemicellulose.

Table 5.4 Mass balance and product yield from the pyrolysis and pyrolysis-catalytic steam reforming of biomass components (as-received basis).

	Lignin		**Cellulose**		**Xylan**	
	Sand	**Catalyst**	**Sand**	**Catalyst**	**Sand**	**Catalyst**
Product yield (wt.%)						
Gas	29.92	50.48	50.71	55.44	49.56	55.45
Char	44.50	44.00	19.00	19.50	15.00	17.50
Liquid*	25.58	2.85	30.29	23.06	35.44	24.55
Catalyst carbon	-	2.67	-	2.00	-	2.50
Gas composition (vol.%)						
CO	29.38	16.34	43.48	20.69	38.23	18.15
H_2	40.23	64.02	26.48	56.43	28.70	58.77
CO_2	10.06	13.68	15.02	18.69	18.26	21.04
CH_4	18.20	5.84	11.40	3.95	11.61	1.92
C_2-C_4	2.13	0.12	3.62	0.24	3.20	0.11

*By difference

Table 5.5. Mass balance and product yield from the pyrolysis and pyrolysis-catalytic steam reforming of biomass components (dry-and-ash-free basis).

Feedstock	**Lignin**		**Cellulose**		**Xylan**	
	Sand	**Catalyst**	**Sand**	**Catalyst**	**Sand**	**Catalyst**
Product yield (wt.%)						
Gas	32.67	55.11	53.94	58.97	52.54	58.79
Char	48.58	48.03	20.21	20.74	15.90	18.55
Liquid*	27.92	3.11	32.22	24.53	37.56	26.02
Catalyst carbon	0.00	2.91	0.00	2.13	0.00	2.65
Gas composition (vol.%)						
CO	32.07	17.84	46.25	22.01	40.53	19.24
H_2	43.92	69.89	28.17	60.03	30.43	62.31
CO_2	10.98	14.93	15.97	19.88	19.36	22.31
CH_4	19.87	6.37	12.13	4.20	12.30	2.04
C_2-C_4	2.33	0.13	3.85	0.25	3.39	0.12
Gas composition (mmol g^{-1})						
CO	5.62	7.03	10.58	7.69	9.10	6.72
H_2	7.68	27.57	6.44	20.98	6.83	21.77
CO_2	1.92	5.84	3.65	6.95	4.34	7.79
CH_4	3.49	2.50	2.77	1.47	2.76	0.71
C_2-C_4	0.34	0.05	0.88	0.09	0.76	0.04

*By difference

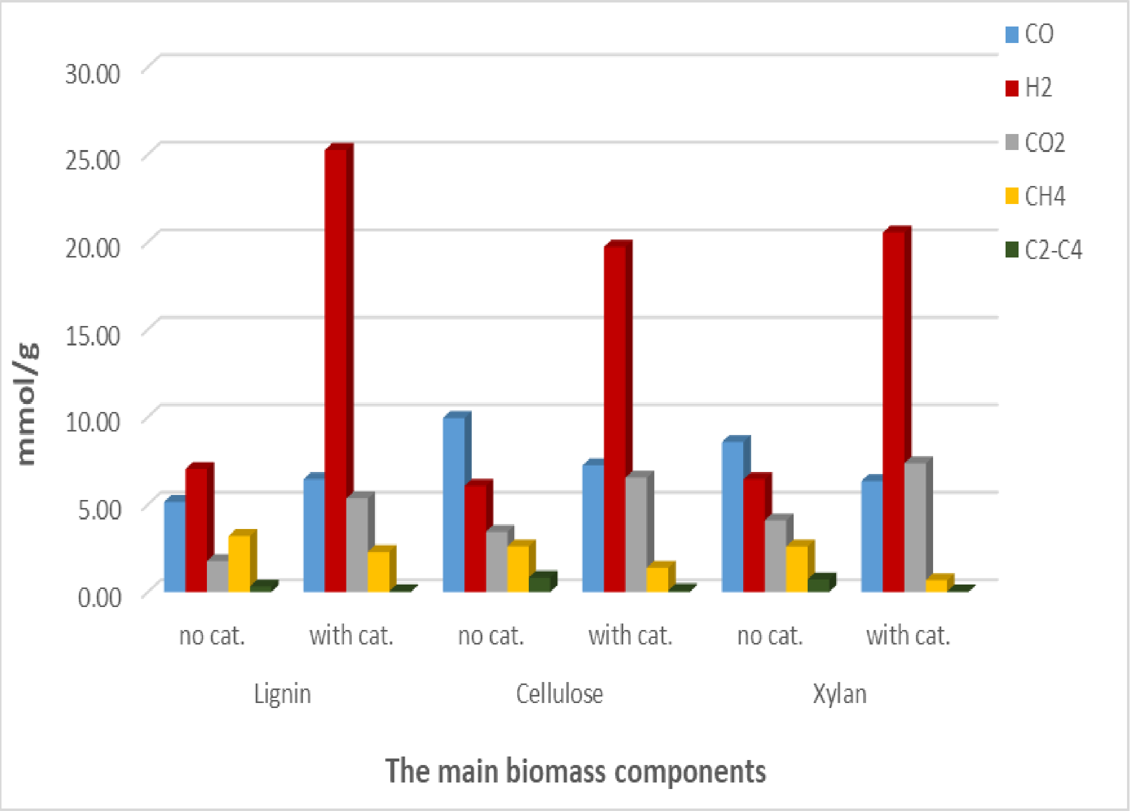

Figure 5.4. Gas composition/yields from the pyrolysis-gasification catalysis of biomass components (as-received basis).

Table 5.6 and Figure 5.5 show the influence of different mixtures of the main biomass components on the product yield and composition of gases for the pyrolysis and for the pyrolysis–catalytic steam reforming processes. The pyrolysis catalytic steam reforming of the lignin and xylan mixture (1:1) produced the highest gas yield of 63:19 wt.%. Also, the blend of lignin and xylan (1:1) produced the most char residue at ~36.0 wt.% compared with the cellulose and xylan mixture at ~19.5 wt.%. The mixture of the three biomass components lignin, cellulose and xylan with pyrolysis-catalytic steam reforming produced a gas yield of 59.31 wt.% and a char residue of 26.0 wt.%. The product yield, such as the gas yield and char production, observed for the three biomass component mixtures was a reflection of the superposition of the individual components. For example, a slightly higher hydrogen yield was produced with the mixture of lignin and cellulose as compared to other component mixtures respectively. Similar results of CO, CO_2 and CH_4 were observed and trace amounts of C_2-C_4 were produced comparable to the individual biomass components.

Table 5.7 and Figure 5.6 show the calculated value of product yield and gas composition of the different biomass component mixtures determined based on the proportion of each individual component product yield and gas composition generated by individual biomass components. The gas yield for the experimental data (Table 5.6 and Figure 5.5) showed a higher value than the calculated value, suggesting some interaction of the components during reaction.

There are several reports in the literature relating to interaction of cellulose, hemicellulose and lignin during the pyrolysis process [1]. Some have reported negligible interaction of biomass components. For example, Yang et al. [5] using a TGA-FTIR and a packed-bed with a micro gas chromatograph analytical system suggested negligible interaction of the components. They reported that superposition of the yields and composition of products from the individual biomass components reflected closely the composition of their mixtures [5]. Raveendran et al. [41] also researched the pyrolysis of biomass components using a TGA and a packed-bed pyrolysis reactor and reported no detectable interaction between the biomass components during pyrolysis.

However, other researchers have demonstrated significant interaction of the main components of biomass during pyrolysis. For example, lignin addition to cellulose has been reported to enhance the product yield of low molecular weight compounds and reduce the yield of char [42]. Also, Liu et al. [1] reported significant interaction of biomass components, particularly between lignin-hemicellulose and hemicellulose-cellulose. For example, they reported that lignin addition to hemicellulose decreased the yield of 2-furaldehyde and other aldehydes and ketones, and hemicellulose addition to cellulose decreased the yield of levoglucosan and increased the formation of hydroxyacetaldehyde.

However, it has also been concluded from a review of the composition of the products obtained from the pyrolysis of biomass, cellulose, hemicelluloses and lignin that the process operating conditions, such as heating rate, reactor temperature, particle size and gas residence time may have a more significant influence on the yield and composition of products [10].

Table 5.6 Product yield and gas composition from pyrolysis and pyrolysis-catalytic steam reforming of mixtures of biomass components.

	Lignin + Cellulose (1:1)		**Lignin + Xylan (1:1)**		**Cellulose + Xylan (1:1)**		**Lignin + Cellulose +Xylan (1:1:1)**	
Experimental	**Sand**	**Catalyst**	**Sand**	**Catalyst**	**Sand**	**Catalyst**	**Sand**	**Catalyst**
Product yield (wt.%)								
Gas yield	42.21	63.19	34.45	53.54	49.82	61.48	40.40	59.31
Char	30.50	29.50	35.50	36.50	19.00	20.00	28.50	26.00
Liquid*	27.29	5.81	30.05	7.96	31.18	16.52	31.1	12.19
Catalyst carbon	-	1.50	-	2.00	-	2.00	-	2.50
Gas composition (vol.%)								
CO	37.10	18.02	29.14	13.86	39.20	17.74	32.94	16.29
H_2	29.65	55.51	32.77	56.13	27.42	55.58	31.58	53.69
CO_2	14.23	20.00	20.60	22.99	18.54	24.63	19.13	23.28
CH_4	15.81	6.18	15.57	6.56	11.74	1.87	13.86	6.30
C_2-C_4	3.20	0.29	1.93	0.46	3.10	0.18	2.49	0.45

* By difference

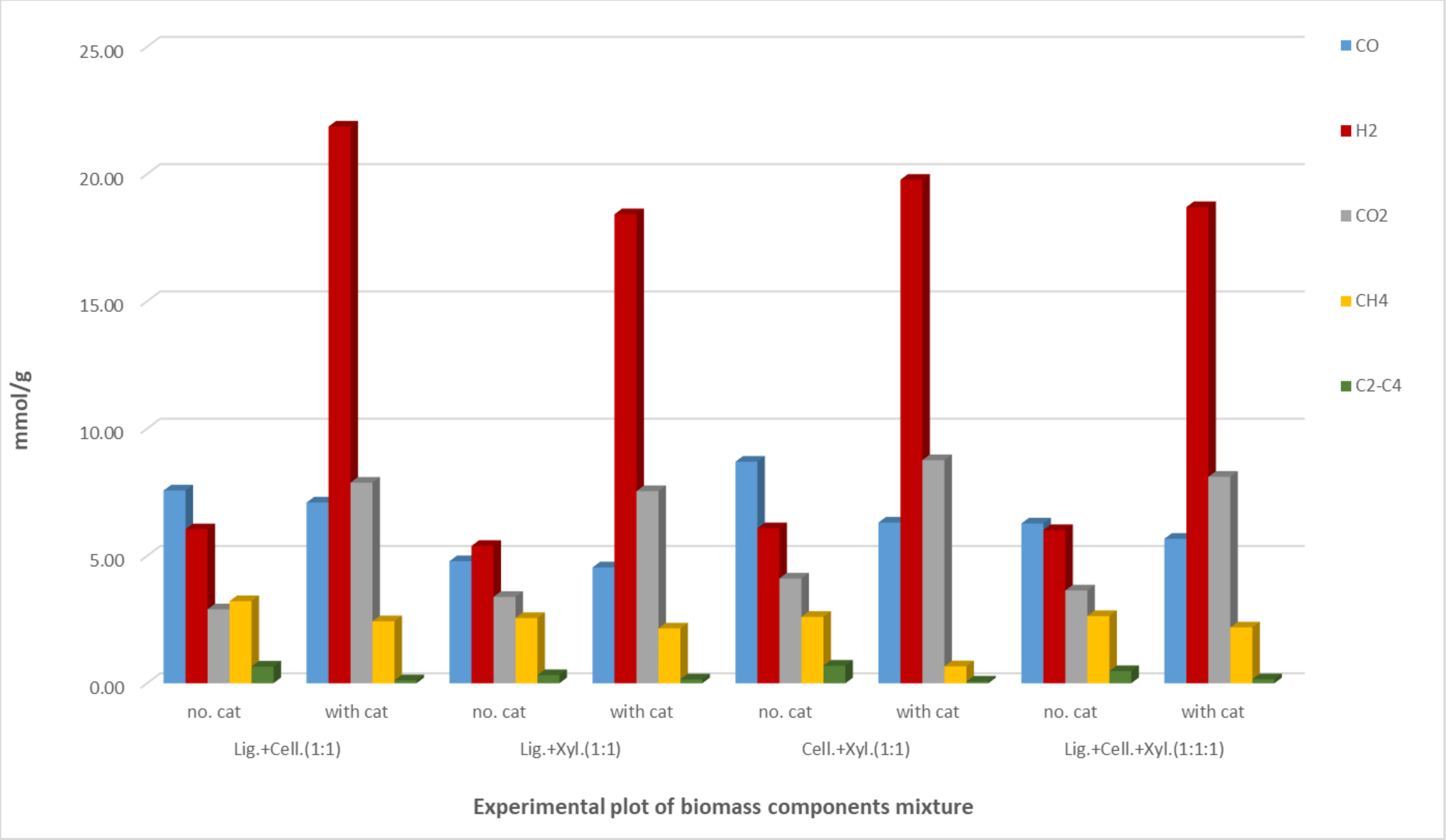

Figure 5.5. Illustration of experimental gas composition/yields from pyrolysis-gasification catalysis of biomass components mixture.

Table 5.7. Mass balance and product yield pyrolysis-catalytic steam reforming of biomass components mixture (calculated).

Calculated	**Lignin + Cellulose (1:1)**		**Lignin +Xylan (1:1)**		**Cellulose +Xylan (1:1)**		**Lignin + Cellulose + Xylan (1:1:1)**	
	sand	**catalyst**	**sand**	**catalyst**	**sand**	**catalyst**	**sand**	**catalyst**
Product yield (wt.%)								
Gas yield	39.81	52.30	39.24	57.00	50.14	58.82	43.06	56.04
Char	31.75	31.75	29.75	29.50	17.00	17.25	26.17	26.17
Liquid*	28.44	13.61	31.01	10.92	32.86	21.68	30.77	15.40
Carbon deposit	0.00	2.33	0.00	2.58	0.00	2.25	0.00	2.39
Gas composition (vol.%)								
CO	36.06	20.68	33.43	18.50	40.85	22.84	36.78	20.67
H2	33.96	61.15	35.06	60.11	27.59	57.24	32.20	59.50
CO2	12.61	13.99	14.23	17.25	16.64	17.55	14.49	16.26
CH4	14.33	4.07	14.43	4.00	11.50	2.23	13.42	3.43
C2-C4	3.05	0.12	2.84	0.14	3.41	0.14	3.10	0.13

*By difference

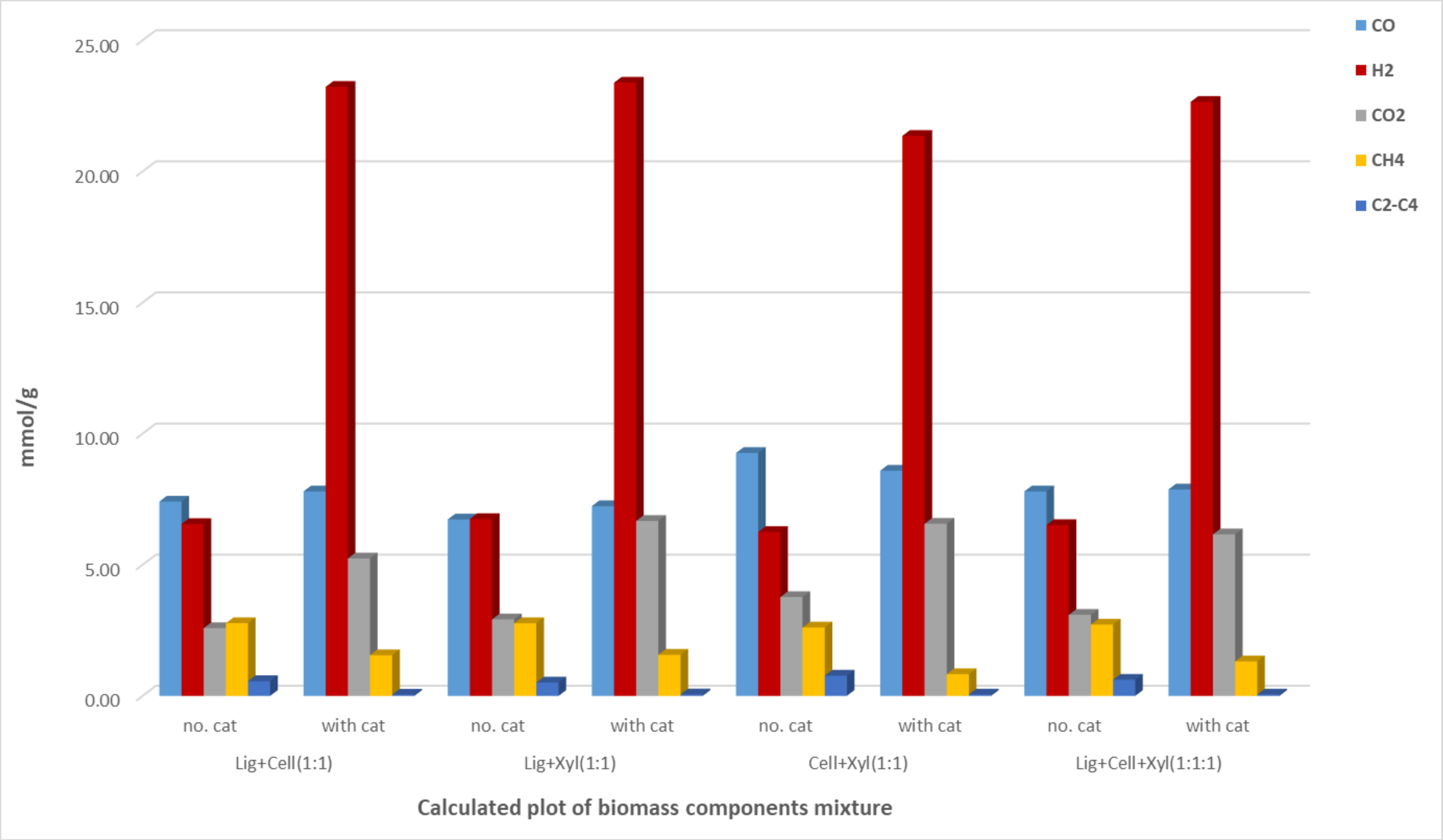

Figure 5.6 Illustration of calculated gas composition/yields from pyrolysis-gasification catalysis of biomass components mixture.

5.5 Hydrogen production in terms of lignin content

Table 5.8 and Figure 5.7 show the results of experiments to verify the effect of lignin content from the pyrolysis of various biomass component mixtures. The percentage of lignin was varied from 10, 50, 90 and 100 wt.% with a balance of equal quantities of cellulose and hemicellulose. The highest gas yield (40.66 wt.%) was obtained at the lowest lignin content of 10 wt.%, reflecting the higher gas yield from cellulose and hemicellulose in the absence of catalyst in the pyrolysis-catalytic steam reforming process. It was observed that as lignin content was increased, H_2 production increased and CO and CO_2 decreased. Burhenne et al. [4], studied the effect of biomass components in a fixed bed reactor and in a TGA with the observation that lignin content was the main controlling factor in relation to thermal decomposition temperatures and product yield. They also suggested that a high lignin content leads to higher yield of solid residue, lower product gas yield and a higher devolatilization temperature as compared to cellulose and hemicellulose. Zheng et al. [43], reported the role of lignin as the cementing medium of biomass via cross-linking between cellulose and hemicellulose resulting in a firm mechanical three-dimensional structure of the plant cell wall. Thereby, the higher the lignin content, the higher the resistance of the biomass to degradation and consequently, a higher char residue yield instead of a gases and volatiles yield.

Table 5.8 Product yield and gas composition from the pyrolysis of different mixtures of lignin with cellulose/hemicellulose.

Pyrolysis	**10 wt.% Lignin** **45 wt.% Cellulose** **45 wt.% Hemicellulose**	**50 wt.% Lignin** **25 wt.% Cellulose** **25 wt.% Hemicellulose**	**90 wt.% Lignin** **5 wt.% Cellulose** **5 wt.% Hemicellulose**	**100 wt.% Lignin**
Product yield (wt.%)				
Gas	40.66	38.97	33.56	29.92
Char	25.00	32.50	41.00	44.50
Gas composition (vol.%)				
CO	34.90	32.37	30.47	29.38
H_2	29.93	32.02	35.99	40.23
CO_2	20.19	18.09	14.05	10.06
CH_4	12.54	14.99	17.49	18.20
C_2-C_4	2.43	2.53	2.01	2.13

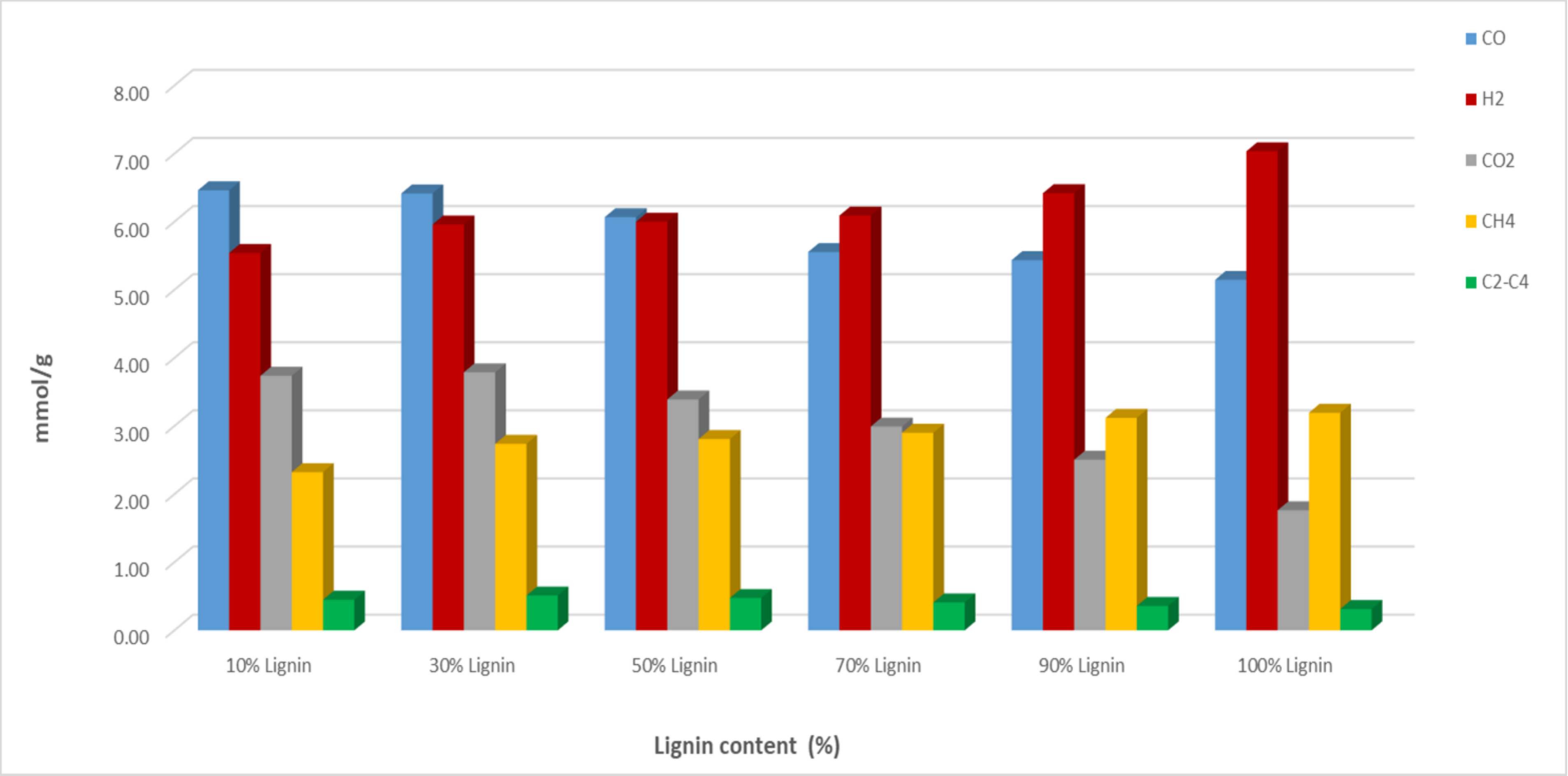

Figure 5.7 Illustration of gas composition/yields from pyrolysis-gasification catalysis of lignin content variation.

In a study conducted by Baumlin et al. [40], a high yield of hydrogen production which ranged between 40-50% from different types of lignin samples was produced [44]. Higher hydrogen production from woody biomass, as compared to agricultural residue, was also reported [19, 45]. This could be as a result of higher lignin content in woody biomass compared to agricultural wastes [46]. It was also reported that, softwood contains more lignin than hardwood and most agricultural residues [43]. These behavioural differences among the three biomass components could be as a result of the structure and the chemical nature of the individual components. However, there have been reports on cellulose and hemicellulose producing more hydrogen than lignin component of biomass sample [47]. According to Li et al. [47], in a study on fast pyrolysis, more hydrogen and carbon monoxide was produced due to the interaction of the fast pyrolysis of the biomass sample with the in situ steam gasification of the intermediate pyrolysis products such as char and bio-oil. Al Arni [48], investigated the effect of fast and slow (conventional) pyrolysis on biomass bagasse product yield, it was reported that fast pyrolysis leads to maximising production of liquid yield while the slow heating rate and longer residence time of conventional pyrolysis reduced liquid yield but leads to higher gas production. It was also reported in terms of higher hydrogen production with conventional pyrolysis as compared to fast pyrolysis at pyrolysis temperatures of 753 K and 853 K. Qu et al. [49], reported that the volume of H_2 fraction produced was found to be smaller when the temperature of pyrolysis is lower than 500 ^oC but the H_2 volume fractions increased rapidly when the pyrolysis temperature was above 550 ^oC. However, CO decreases at a temperature of about 500 ^oC and CO_2 also was stated to decrease between the temperatures ranging from 500-550 ^oC. High temperature is noted to favour hydrogen production [48, 49]. Different catalysts have been observed to react differently and the type of pyrolysis method, as explained, are possibly the main reason for the different results of either cellulose or lignin yielding higher hydrogen yield. Furthermore, many researchers have demonstrated the degradation temperature for the three biomass components, lignin was reported to degrade slower and at a wider temperature range than cellulose and hemicellulose [1, 7, 9]. Higher temperatures and residence times of volatiles can increase the pyrolytic carbon formation because of the extension of secondary reactions [19]. Therefore, it is suggested that with higher temperature and longer residence time, more hydrogen will be produced from lignin compared to cellulose and hemicellulose as demonstrated in this study [4, 5, 19, 44].

Table 5.9 Product yield and gas composition for different mixtures of lignin with cellulose/hemicellulose from the pyrolysis-catalytic steam reforming of biomass components.

Catalytic steam reforming	**10 wt.% Lignin** **45 wt.% Cellulose** **45 wt.% Hemicellulose**	**50 wt.% Lignin** **25 wt.% Cellulose** **25 wt.% Hemicellulose**	**90 wt.% Lignin** **5 wt.% Cellulose** **5 wt.% Hemicellulose**	**100 wt.% Lignin**
Product yield (wt.%)				
Gas	55.31	56.04	58.04	64.38
Char	24.00	32.50	40.50	43.50
Catalyst carbon	1.50	1.50	1.50	2.50
Gas composition (vol.%)				
CO	20.00	18.19	15.74	15.33
H_2	49.31	52.46	56.69	62.18
CO_2	23.44	21.62	20.09	18.02
CH_2	6.31	7.20	7.21	4.42
C_2-C_2	0.94	0.54	0.27	0.06

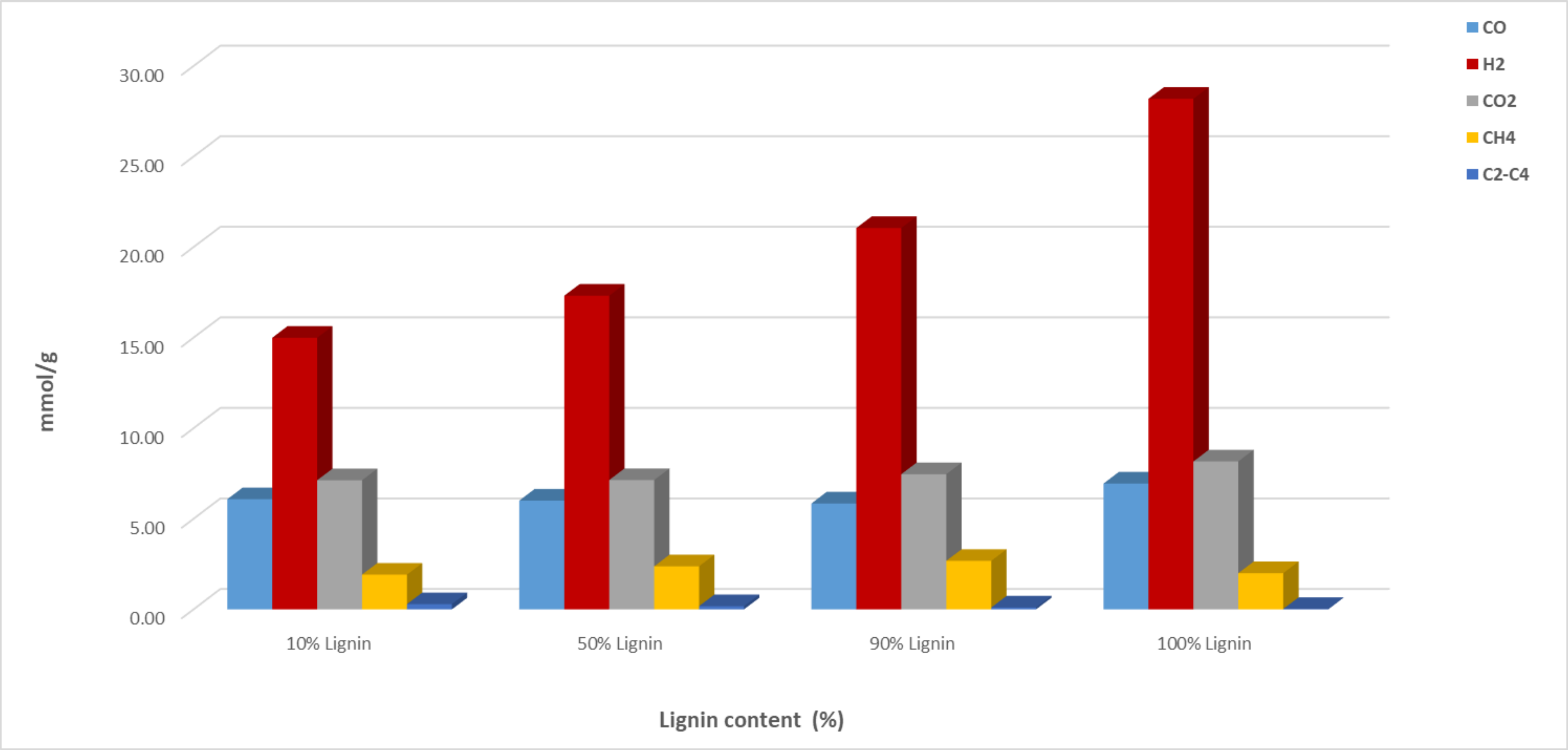

Figure 5.8 Illustration of gas composition/yields from pyrolysis-gasification catalysis of lignin content variation.

Table 5.9 and Figure 5.8 shows the effect of lignin content with a balance of equal quantities of cellulose and hemicellulose, 10, 50, 90 and 100% of lignin content for the pyrolysis-catalytic steam reforming process in the presence of the 10% $NiAl_2O_3$ catalyst. The presence of the 10 wt.% $NiAl_2O_3$ catalyst produced a marked increase in gas yield and, in particular, enhanced H_2 yield. Increasing lignin content produced an increasing total gas yield from 55.31 wt.% at 10 wt.% lignin to 64.36 wt.% at 100 wt.% lignin. In addition, higher hydrogen yield was produced with increased lignin content, rising from 14.99 mmol g^{-1} at 10 wt.% lignin content to 28.19 mmol g^{-1} at 100 wt.% lignin content. This suggests that catalytic steam reforming was active as gas yield increased at increasing lignin content in the presence of catalyst, as it was contrary in the absence of catalyst.

5.5.1 Correlation of hydrogen production in terms of lignin content

The derivation of an equation for the possible determination of hydrogen production with an estimated knowledge of lignin content in biomass components sample was investigated. Table 5.10 and Figure 5.9 shows a correlation equation that can be used to calculate hydrogen production with a known content of lignin as studied above. The correlation was obtained by a second order polynomial (non-linear regression). This correlation can be used to predict the influence of lignin content on hydrogen yield from the pyrolysis and pyrolysis-catalytic steam reforming. For instance, if the composition of lignin in biomass is known then an estimated hydrogen yield can be predicted. It is validated by comparing the experimental value and the calculated value based on the correlation, it shows a very close value to 1. The correction coefficient with R^2 (R-square) larger than 0.99 of similar equation for the calculation of the proportion of hemicellulose, cellulose and lignin in biomass sample had been reported [2]. Also, in the work of Biagini et al. [50], conducted on the devolatization of biomass fuels and biomass components using thermogravimetric-infrared spectroscopy (TG-FTIR), a similar correlation was derived for the prediction of biomass fuels based on the initial chemical composition.

In this study, the R-square value for the composition of hydrogen produced in volume per cent is about 96% while in mmol/g is estimated at 88% as shown in Table 5.10 and Figure 5.9, the hydrogen produced from lignin component for different contents both for the experimental and calculated values were in good agreement. A similar study had been carried out, such that correlation was developed based on the effect of organic composition (high lignin content) and the mineral element in biomass (e.g. potassium and zinc) on product properties and product distribution [51]. Qu et al. [49], equally investigated a similar trend by comparing calculated and experimental data. It has also been reported on the correlation between 16 milled wood lignin and several decomposition products from the result of TG-MS investigated [52]. Therefore, observing the plots of lignin content against hydrogen composition in volume per cent and mmol/g (Table 5.10 and Figure 5.9), shows that as lignin content increases, the higher the amount of hydrogen produced both for the experimental and for the calculated value. Additionally, there seems to be interaction as the experimental values were slightly higher than the calculated values, the contrary difference might be due to equipment and experimental error.

Tables 3.1 and 3.2 in Chapter 3 show both the physical properties and chemical composition of the biomass components indicated by elemental and proximate analyses. Lignin has the highest carbon content (~ 60 wt.%) compared to cellulose and xylan/hemicellulose of (~42 wt.%). The hydrogen content is relatively the same for all the three biomass components: lignin, cellulose and hemicellulose with a value of 5.5 wt.%, 5.6 wt.% and 6.0 wt.%. The pyrolysis decomposition of the biomass feedstock, with higher carbon content, suggested it produced more hydrogen yield as shown in Table 5.4. Likewise, lignin has the lowest oxygen content with a value of (~32 wt.%) among the other biomass components; cellulose and hemicellulose (~53 wt.% & 52 wt.%). The high oxygen content in cellulose and hemicellulose result in the production of more oxygenated compound in the bio-oil, whereas lignin produced better bio-oil quality yields due to the physical properties and chemical composition. The results in Table 5.4 give further explanation, such that higher liquid/oil production obtained from cellulose (~ 30 wt.%) and xylan (35 wt.%) as compared to lignin (~ 26 wt.%) in the pyrolysis process. In the catalytic reforming of lignin, the low liquid/oil yield of 3 wt.% is suggested to be due to higher hydrocarbon molecules (higher concentration of oxygenated compounds) such as phenol in the oil derived from lignin pyrolysis/gasification, reformed for increased hydrogen production as compared with cellulose and xylan having high liquid/oil (23 wt.% and 25 wt.%) concentration of oxygenated compounds. Therefore, hydrogen production increased for the lignin sample compared to cellulose and xylan [11]. Studies have shown that there is better quality bio-oil production from the pyrolysis of biomass with a high percentage of lignin content [53]. It has been reported that a high heating value (HHV) of biogas products from lignin is due to higher aromatic rings and methoxyl groups compared to cellulose and hemicellulose was obtained [54].

In Table 5.4, similar product yields and gas composition for cellulose and xylan except higher CO by cellulose and more CO_2 produced by xylan. On the other hand, lignin produced higher H_2 and CH_4 including a blend of the three components. Researchers have reported the higher production of CH_4 by lignin compared to cellulose and xylan [5, 33]. Therefore, it is suggested that higher production of hydrogen from lignin component compared with cellulose and xylan, might be due to steam methane reforming reactions being enhanced and this is favoured at increasing temperature [40, 55].

Likewise, Lignin has been characterised with higher char (~45 wt.%) production compared to cellulose and hemicellulose as shown in Table 5.4. Researchers have equally confirmed high residue and solid product from lignin compared to cellulose and hemicellulose [56]. Therefore, advantage can be taken in terms of gasification of biomass with high lignin content for increased hydrogen production due to char gasification that is favoured at high temperatures [57].

In Figure 5.9b, the plateau relationship between lignin content of 30 to 70% and hydrogen production, showed less synergetic effect between the blend of lignin content with the cellulose/hemicellulose components. For example, in the 50% lignin content, there is a balance of 50% from cellulose and hemicellulose (i.e. 25% of cellulose and 25% of hemicellulose) in the mixture, which signifies that there is equal contribution from lignin and cellulose/hemicellulose in the blend, and this shows no significant increase in hydrogen production (i.e. in the experimental value in mmol/g) at this point.

Table 5.10. Lignin content variation and hydrogen production (experimental and calculated value).

Lignin content Variation	**H_2 (Expt. value)**	**H_2 (Calc. value)**	**H_2 (Expt. value)**	**H_2 (Calc. value)**
%	**vol.%**	**vol.%**	**mmol/g**	**mmol/g**
10	29.93	30.19	5.54	5.66
30	30.70	30.44	5.96	5.73
50	32.02	31.74	6.00	5.88
70	33.93	34.07	6.09	6.11
90	35.99	37.44	6.42	6.42
100	40.23	39.52	7.03	6.61

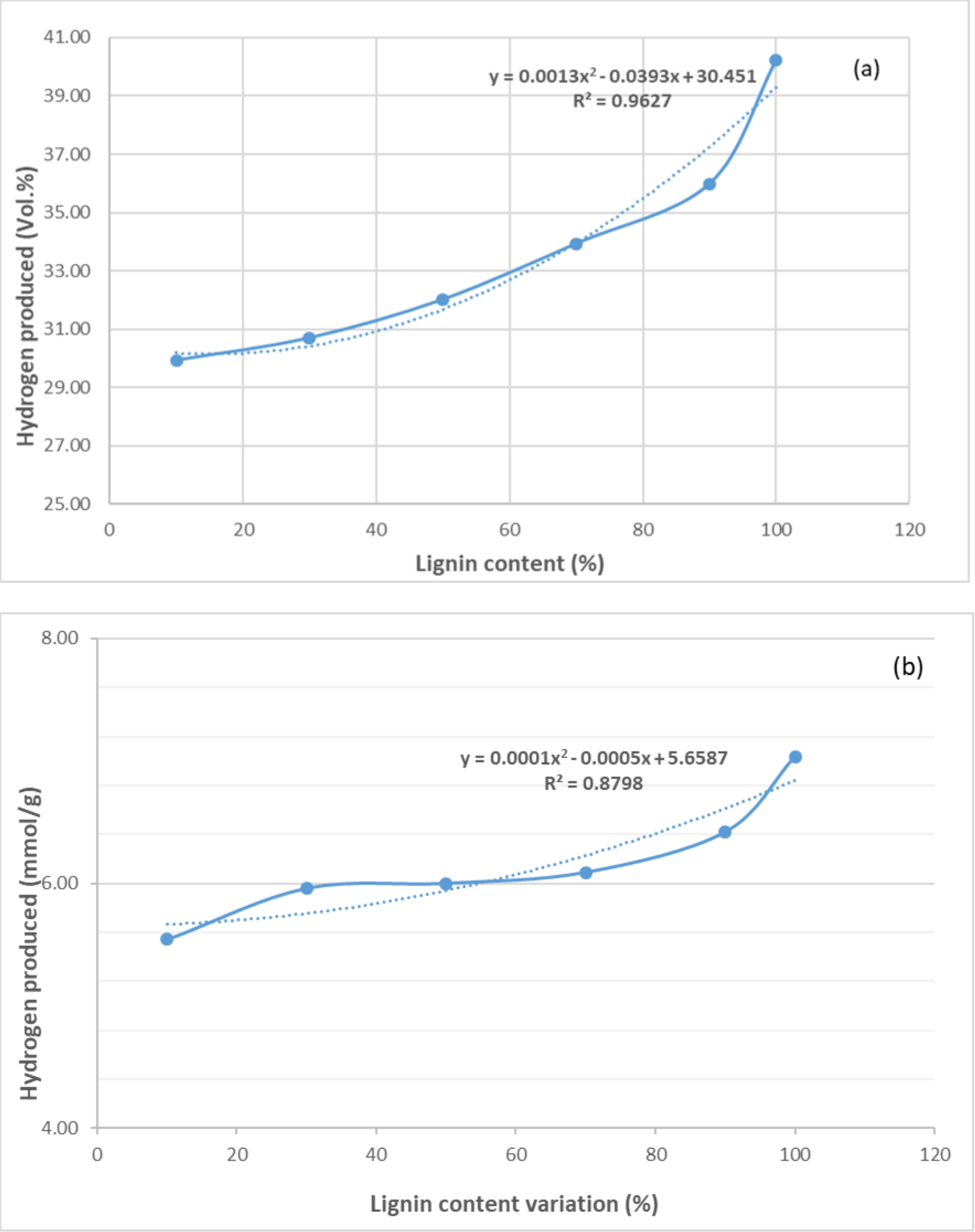

Figure 5.9 Illustration of lignin content variation and hydrogen production, (a) vol.%, (b) mmol/g (experimental).

5.6 Analysis of gases produced from lignin in relation to temperature and time

In a separate experiment and using a different experimental procedure, the gas composition evolved at specific temperatures throughout the pyrolysis process and the pyrolysis-catalytic steam reforming process for 100 wt.% lignin was investigated. Rather than collecting the evolved gases as a total gas yield in the gas sample bag, instead, several gas sample bags were used to collect the gases as the pyrolysis reactor was heated to 150 °C, then gas samples were collected at every 50 °C temperature increment until the required pyrolysis end temperature of 550 °C was reached. In addition, further gas samples were collected every 5 minutes at the pyrolysis temperature of 550 °C. For these experiments, in the case of pyrolysis, sand was used in the second stage reactor and for the catalyst experiment, the second stage contained the 10%$NiAl_2O_3$ catalyst maintained at 750 °C and where steam was introduced. The results are shown in Figures 5.10 and 5.11. The results show that the composition of each of the product gases, CO, H_2, CO_2, CH_4, and C_2-C_4, increases as the biomass feedstock undergoes pyrolysis or pyrolysis-catalytic steam reforming. The evolution of gases decreases as the thermal degradation of the biomass progresses and complete thermal degradation occurs, leaving the residual char. The highest yield of gases was released at 350 °C for the pyrolysis of lignin while for pyrolysis-catalytic steam reforming of lignin with the 10 wt.%$NiAl_2O_3$ catalyst, gas yield peaked between the temperatures of 250-300 °C, indicating a lower decomposition temperature for the lignin in the presence of the 10% $NiAl_2O_3$ catalyst. Studies have shown that the use of catalyst does lower the decomposition temperature of the pyrolysis process as well as increasing hydrogen production [39, 43, 47, 58, 59].

In this study, the gas yield increases in the presence of catalyst due to thermal and catalytic cracking of volatiles and water gas shift reactions. At a pyrolysis temperature of 300 °C and catalytic bed temperature of 750 °C, the results of the gaseous products show that the H_2 yield increased (from ~22 to 84 mmol/g), CO increased (~ 29 to 33 mmol/g), CO_2 increased (~10 to 25 mmol/g) while CH_4 decreased (14 to 10 mmol/g) and C_2-C_4 (~2 to 0.3 mmol/g) decreases comparing pyrolysis and pyrolysis-catalytic processes. For the increase in production of hydrogen yield, several reactions seem to be enhanced such as water gas shift, steam methane reforming, hydrocarbon reforming, tar reforming and Boudouard reactions which are favoured at high temperatures.

Likewise, there have been several reports on the mechanism for the catalytic steam reforming of biomass pyrolysis gases in order to understand the formation of CO and H_2. For example, Guan et al. [60], reviewed the catalytic steam reforming process for biomass tar, which is analogous to the catalytic steam reforming of the range of hydrocarbons produced during biomass pyrolysis. They suggest a mechanism where larger molecular weight hydrocarbons undergo several reactions including thermal and catalytic cracking, reforming (with CO_2 or H_2O), water gas shift, etc. on the catalyst to produce mainly CO and H_2. In addition, coke formation can occur on the catalyst due to larger molecular weight hydrocarbon polymerisation reactions. Su et al. [61], have further elucidated the catalytic steam reforming mechanism and have suggested that the hydrocarbons interact with the catalyst metals by dissociation and adsorption on the catalyst surface followed by metal-catalysed dehydrogenation. Introduction of steam input into the process, steam methane reaction is enhanced as water at the catalyst surface hydroxylates and the OH radicals formed migrate to the metal sites and oxidise the hydrocarbon intermediate fragments to form the CO and H_2.

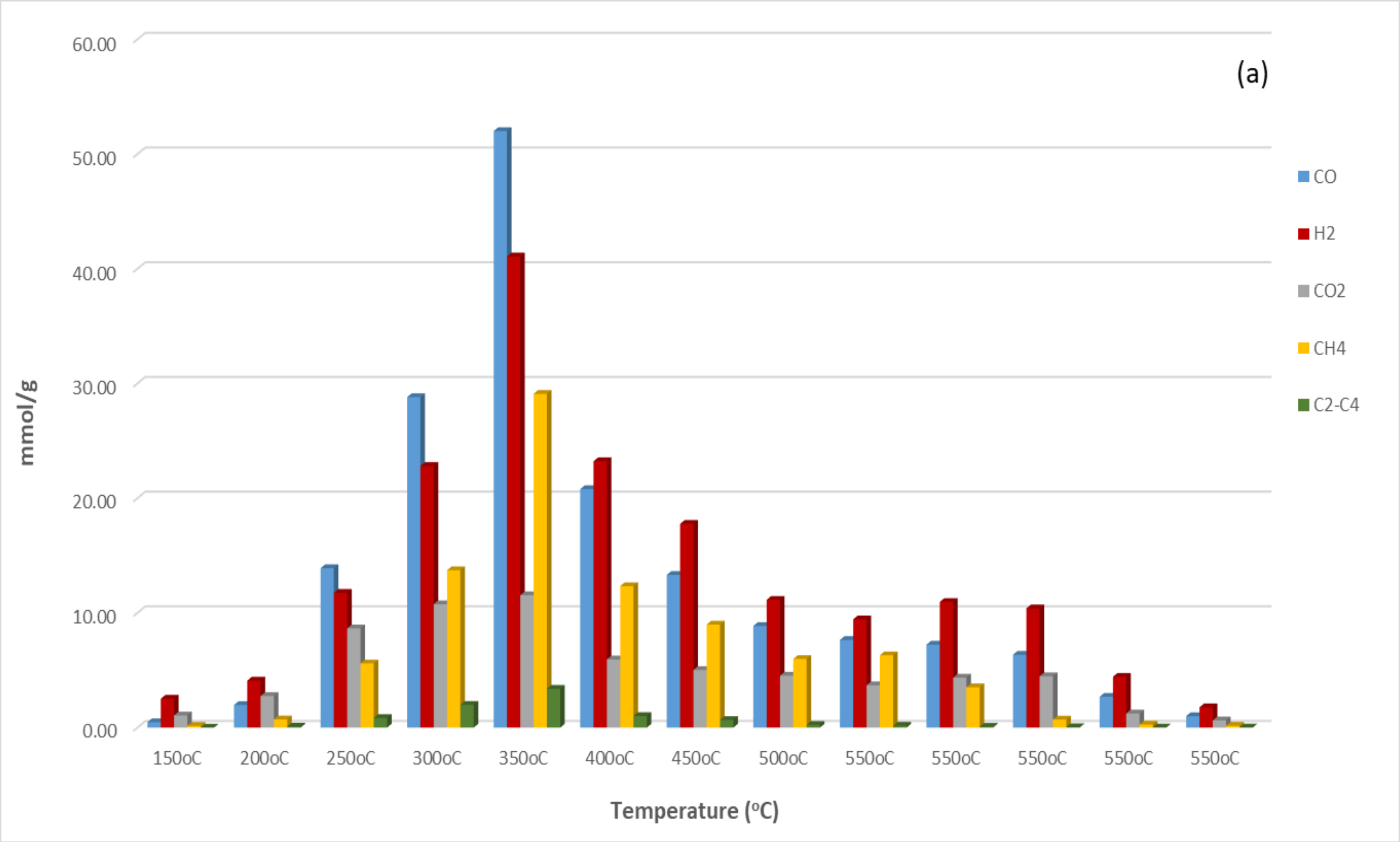

Figure 5.10 Illustration of gases released from pyrolysis of lignin at different temperature with time (a) without catalyst and steam.

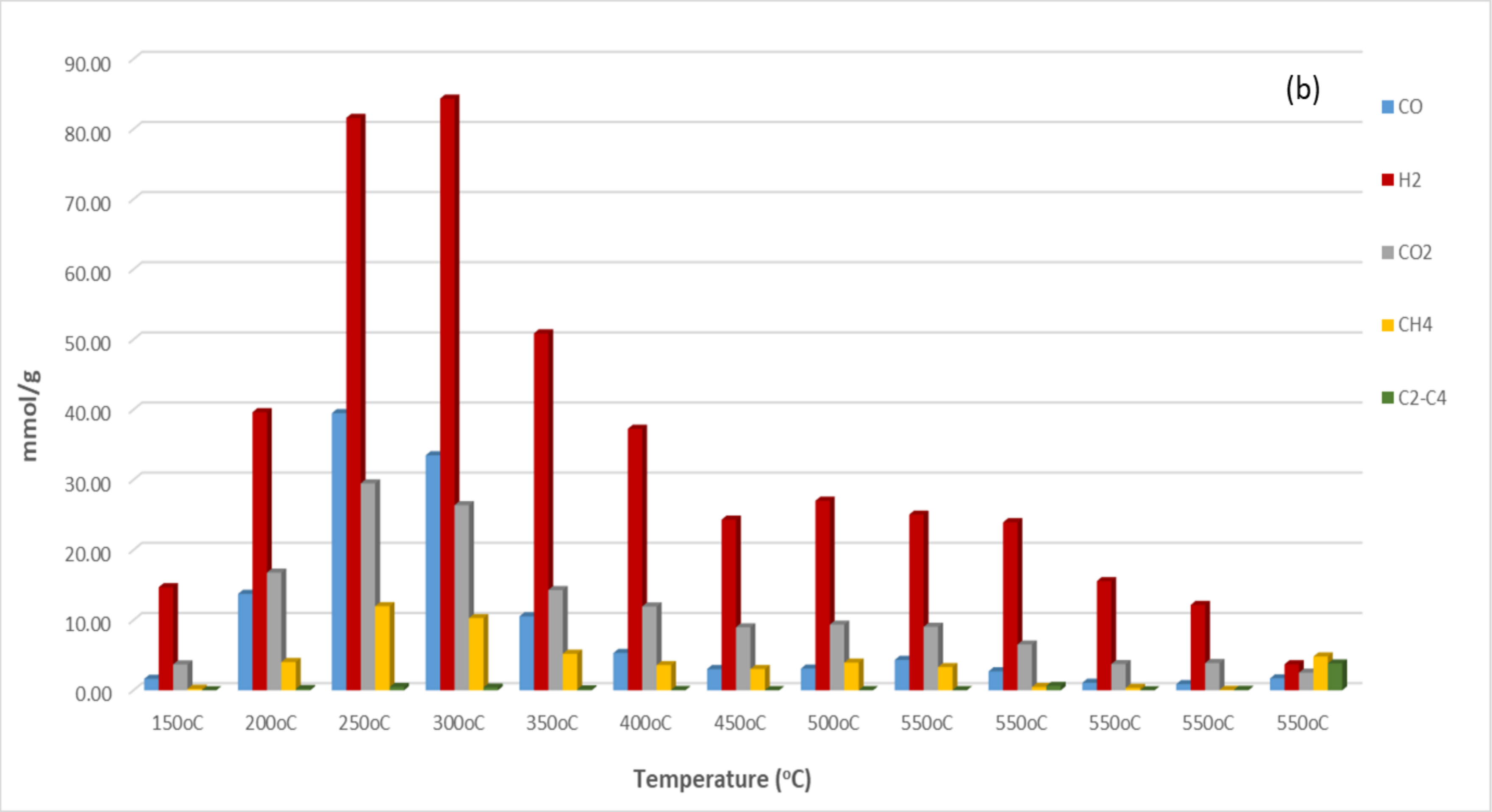

Figure 5.11 Illustration of gases released from pyrolysis of lignin at different temperature with time (b) with catalyst and steam.

5.7 Characterisation of reacted catalyst, fresh and char biomass sample components

Temperature program oxidation (TPO) analysis was conducted for the reacted catalysts used for the pyrolysis gasification of the six biomass samples and the biomass components. The TGA and DTG curves, as seen in Figure 5.12, show little or no oxidation of carbon, therefore, there seems to be negligible carbon deposition. The slight difference with some large weight loss, is the presence of biomass char/ash piece/drop in the catalyst during the pyrolysis–catalytic experiment. The TGA thermograms equally showed no appreciable weight loss for all the biomass samples except at 100-200 ^{o}C, which could be attributed to the weight loss due to moisture. The weight loss thermogram and DTG thermogram observed with some biomass samples might be as a result of the char or residue drop onto the catalytic bed during the experiment since the same catalyst, 10% $NiAl_2O_3$ was used for the steam pyrolysis-gasification process and therefore a similar trend was supposed to exist.

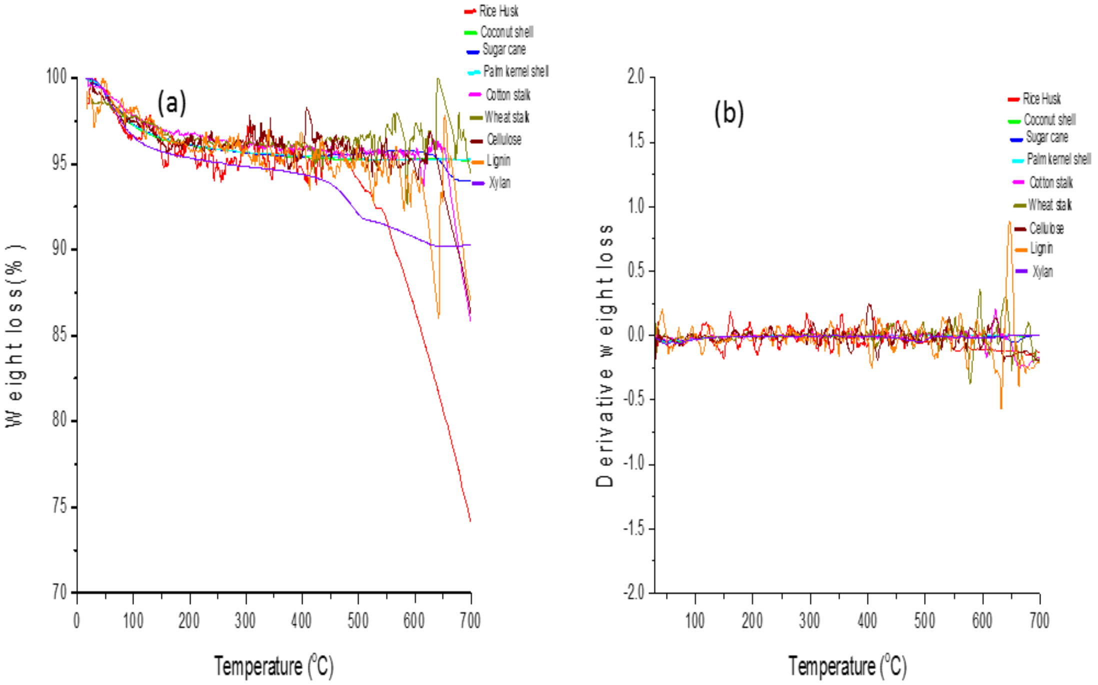

Figure 5.12 Reacted catalyst for pyrolysis-gasification of biomass samples and biomass compositions, (a) TGA plots (b) DTG plots.

The morphology of biomass samples and biomass components (both the fresh sample and the spent char) were taken before and after the pyrolysis-catalysis gasification experiment, the structure of the samples changed after the pyrolysis-catalysis experiment as shown by scanning electron microscope (SEM) in Figures 5.13-5.15. The morphologies of the biomass samples developed a porous structure as shown by lignin and xylan char after the pyrolysis-catalytic steam reforming process. It was suggested that the small holes inside the layer reveal the place through which gaseous products are liberated [44]. The cellulose char structure shows a smaller size as compared to the cellulose fresh sample. Sugarcane and coconut shell show a fibrous like structure before pyrolysis, while rice husk, cotton stalk, palm kernel shell, and wheat stalk showed a thick-like structure before pyrolysis which became a smoother and hollow-like structure after pyrolysis. Similar morphologies have been reported by other researchers suggesting bagasse and cellulose to have a fibrous structure before and after pyrolysis, while rice straw and rice husk had a lumpy structure during pyrolysis it became a porous structure after pyrolysis [14]. Similar morphology of lignin before and after pyrolysis was also studied in other research [44]. The EDXs results indicate the type of elements present in the biomass samples which was also investigated. Carbon and oxygen are high in the fresh biomass samples before pyrolysis but had a reduced peak in the biomass char after pyrolysis, suggesting the release of these elements. Likewise, from the SEM-EDXS image of 10% $NiAl_2O_3$ reacted catalysts (Figure 5.16), no appreciable carbon was seen and therefore negligible carbon deposit as this is in agreement with TPO result in this study. Also, the 10% $NiAl_2O_3$ reacted catalyst analysed on EDXs includes a composition of nickel (Ni), aluminium (Al), silica (Si) and oxygen (O) present in a significant form. The carbon (C) and iridium (IR) were also present in the analysed catalyst, this is as a result of the carbon tape used on the sample board.

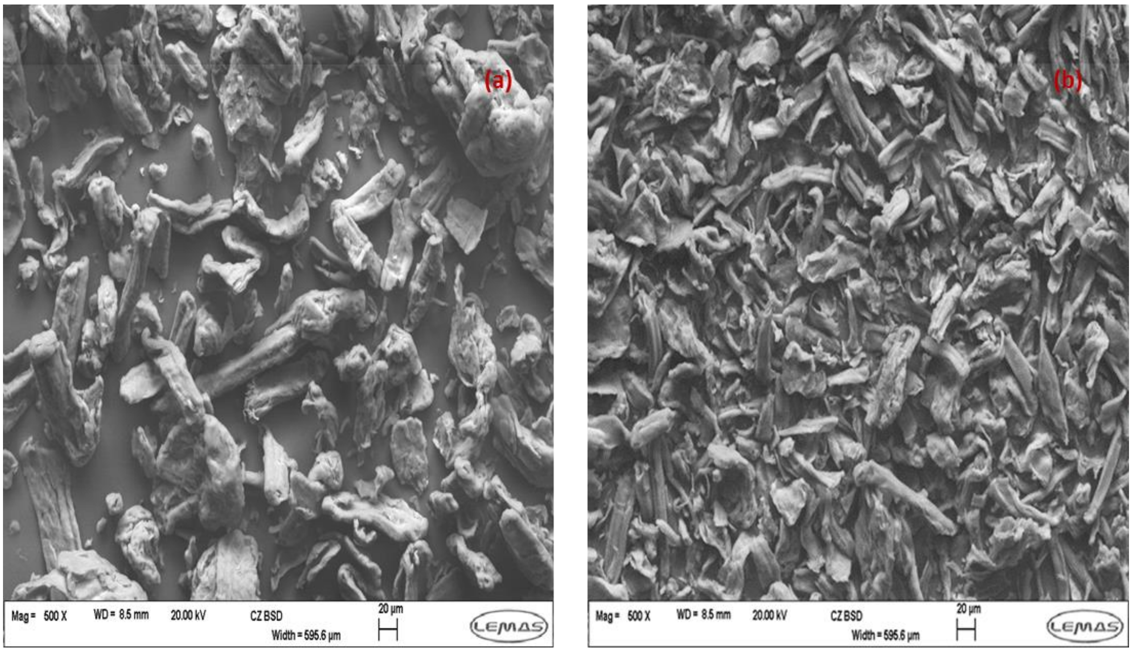

Figure 5.13. Illustration of biomass component sample on SEM (a) fresh cellulose, (b) cellulose char.

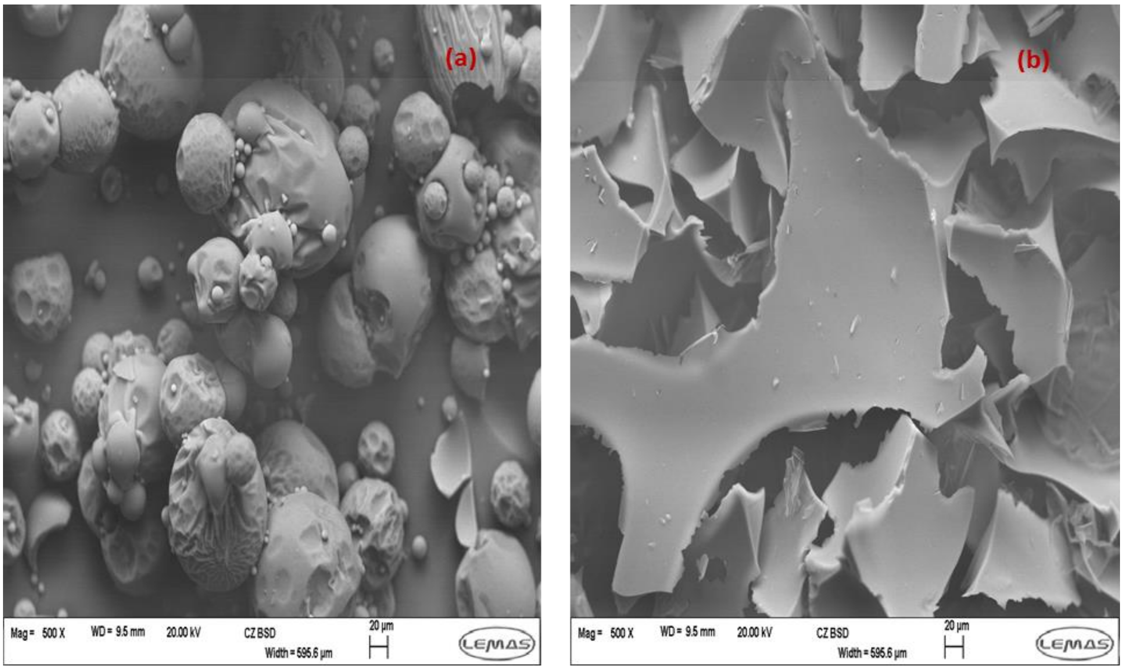

Figure 5.14. Illustration of biomass component sample on SEM (a) fresh xylan, (b) xylan char.

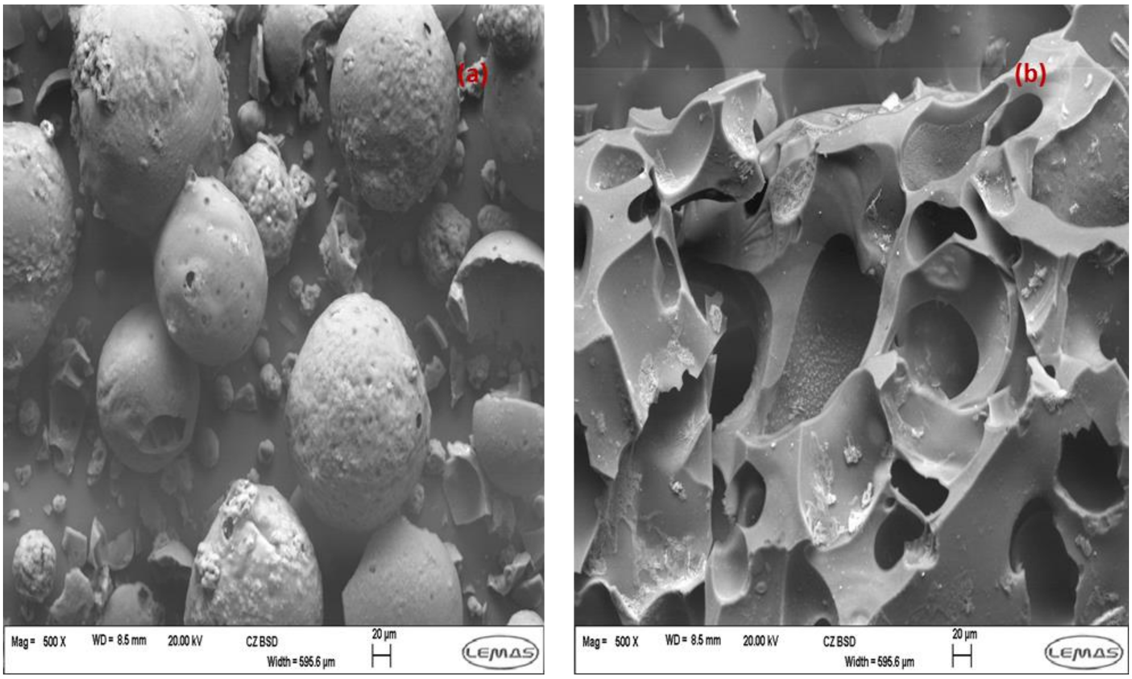

Figure 5.15. Illustration of biomass component sample on SEM (a) fresh lignin, (b) lignin char.

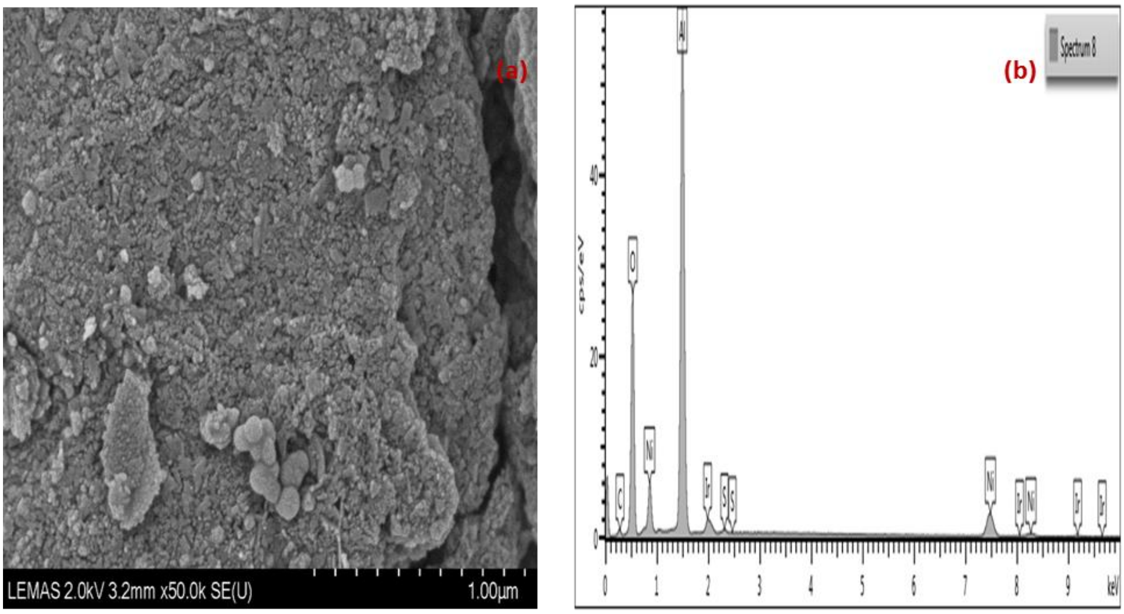

Figure 5.16. Illustration of 10% $NiAl_2O_3$ reacted catalyst for pyrolysis-gasification of lignin (a) SEM image, (b) EDXs.

5.8 Conclusion

The investigation carried out in this study involved the pyrolysis and the pyrolysis-catalytic steam reforming of six different biomass samples, namely: rice husk, coconut shell, sugarcane, palm kernel shell, cotton stalk and wheat straw. In addition, the pyrolysis and pyrolysis-catalytic steam reforming of the three main biomass components, cellulose, xylan and lignin were also investigated. The influence on the different types of biomass and the main biomass components on product yield and product gas composition, in particular hydrogen, was investigated. The results showed that introduction of steam and catalyst into the pyrolysis-catalytic steam reforming process significantly increased gas yield as well as product syngas hydrogen composition. Hydrogen yield from pyrolysis of the biomass types ranged from 5.81 mmol g^{-1} for wheat straw to 6.77 mmol g^{-1} for cotton stalks. For pyrolysis-catalytic steam reforming the hydrogen yield ranged from 16.38 mmol g^{-1} for wheat straw to 25.35 mmol g^{-1} for palm shell kernels. For pyrolysis of the biomass components, lignin produced the highest yield of hydrogen, whereas cellulose and hemicellulose favoured CO and CO_2 production, which was linked to the differences in chemical structure of lignin compared to cellulose and hemicellulose. It was also observed that by increasing the lignin content in mixtures of the biomass components, the hydrogen yield increased, suggesting that the lignin component of biomass sample is the main controlling factor for hydrogen yield.

The analyses of gasification processes performed on the different types of biomass samples investigated suggests that there were some variations in the gas composition and gas yield. However, there were no obvious major variations in the gas composition with the nature of biomass samples. Therefore, one type of biomass sample can replace another without any major consequences in the process, as this is an advantage due to seasonal production of biomass wastes.

References

1. Liu, Q., et al., *Interactions of biomass components during pyrolysis: A TG-FTIR study.* Journal of Analytical and Applied Pyrolysis, 2011. 90(2): p. 213-218.
2. Yang, H., et al., *In-depth investigation of biomass pyrolysis based on three major components: hemicellulose, cellulose and lignin.* 2006. 20(1): p. 388-393.
3. Orfao, J., F. Antunes, and J.L.J.F. Figueiredo, *Pyrolysis kinetics of lignocellulosic materials—three independent reactions model.* 1999. 78(3): p. 349-358.
4. Burhenne, L., et al., *The effect of the biomass components lignin, cellulose and hemicellulose on TGA and fixed bed pyrolysis.* Journal of Analytical and Applied Pyrolysis, 2013. 101: p. 177-184.
5. Yang, H., et al., *Characteristics of hemicellulose, cellulose and lignin pyrolysis.* Fuel, 2007. 86(12): p. 1781-1788.
6. McKendry, P., *Energy production from biomass (part 1): overview of biomass.* Bioresource Technology, 2002. 83: p. 37-46.
7. Di Blasi, C., *Modeling chemical and physical processes of wood and biomass pyrolysis.* Progress in Energy and Combustion Science, 2008. 34(1): p. 47-90.
8. Balat, M., *Mechanisms of thermochemical biomass conversion processes. Part 1: reactions of pyrolysis.* Energy Sources, Part A, 2008. 30(7): p. 620-635.
9. Williams, P.T. and S. Besler, *The influence of temperature and heating rate on the slow pyrolysis of biomass.* Renewable Energy, 1996. 7(3): p. 233-250.
10. Collarda François-Xavier and B. Joël, *A review on pyrolysis of biomass constituents: Mechanisms and composition of the products obtained from the conversion of cellulose, hemicelluloses and lignin.* Renewable and Sustainable Energy Reviews 2014. 38: p. 594-608.
11. Wu, C., et al., *Pyrolysis/gasification of cellulose, hemicellulose and lignin for hydrogen production in the presence of various nickel-based catalysts.* Fuel, 2013. 106: p. 697-706.
12. Williams, P.T. and S. Besler, *The pyrolysis of rice husks in a thermogravimetric analyser and static batch reactor.* Fuel, 1993. 72(2): p. 151-159.
13. McKendry, P., *Energy production from biomass (part 1): overview of biomass* Bioresource Technology 2002. 83: p. 37–46.
14. Dangzhen Lv, et al., *Effect of cellulose, lignin, alkali and alkaline earth metallic species on biomass pyrolysis and gasification.* Fuel Processing Technology 2010. 91: p. 903-909.
15. Vassilev, S.V., et al., *An overview of the organic and inorganic phase composition of biomass.* 2012. 94: p. 1-33.
16. Varhegyi, G., et al., *Kinetics of the thermal decomposition of cellulose, hemicellulose, and sugarcane bagasse.* Energy & Fuels, 1989. 3(3): p. 329-335.
17. Chornet, E. and R.P. Overend, *Biomass liquefaction: an overview*, in *Fundamentals of thermochemical biomass conversion*. 1985, Springer. p. 967-1002.

18. Prasara-A, J. and S.H.J.J.o.c.p. Gheewala, *Sustainable utilization of rice husk ash from power plants: A review.* 2017. 167: p. 1020-1028.

19. Uddin, M.N., W.W. Daud, and H.F. Abbas, *Effects of pyrolysis parameters on hydrogen formations from biomass: a review.* RSC Advances, 2014. 4(21): p. 10467-10490.

20. Daud, W.M.A.W. and W.S.W. Ali, *Comparison on pore development of activated carbon produced from palm shell and coconut shell.* Bioresource Technology, 2004. 93(1): p. 63-69.

21. Akpinar, O., et al., *Enzymatic production of xylooligosaccharides from cotton stalks.* Journal of agricultural and food chemistry, 2007. 55(14): p. 5544-5551.

22. Goksu, E.I., et al., *Production and characterization of films from cotton stalk xylan.* Journal of agricultural and food chemistry, 2007. 55(26): p. 10685-10691.

23. Kırtay, E., *Recent advances in production of hydrogen from biomass.* Energy Conversion and Management, 2011. 52(4): p. 1778-1789.

24. González, J., et al., *Investigation on the reactions influencing biomass air and air/steam gasification for hydrogen production.* 2008. 89(8): p. 764-772.

25. Ranzi, E., et al., *Chemical kinetics of biomass pyrolysis.* 2008. 22(6): p. 4292-4300.

26. Domínguez, A., et al., *Bio-syngas production with low concentrations of CO2 and CH4 from microwave-induced pyrolysis of wet and dried sewage sludge.* 2008. 70(3): p. 397-403.

27. Karnjanakom, S., et al., *Catalytic steam reforming of tar derived from steam gasification of sunflower stalk over ethylene glycol assisting prepared Ni/MCM-41.* 2015. 98: p. 359-368.

28. Yan, F., et al., *Hydrogen-rich gas production by steam gasification of char from biomass fast pyrolysis in a fixed-bed reactor: Influence of temperature and steam on hydrogen yield and syngas composition.* 2010. 101(14): p. 5633-5637.

29. Fernández, Y., et al., *Pyrolysis of glycerol over activated carbons for syngas production.* 2009. 84(2): p. 145-150.

30. Yin, R., et al., *Influence of particle size on performance of a pilot-scale fixed-bed gasification system.* 2012. 119: p. 15-21.

31. Franco, C., et al., *The study of reactions influencing the biomass steam gasification process☆.* 2003. 82(7): p. 835-842.

32. Orfão, J.J., F.J. Antunes, and J.L.J.F. Figueiredo, *Pyrolysis kinetics of lignocellulosic materials—three independent reactions model.* 1999. 78(3): p. 349-358.

33. Wang, S., et al., *Influence of the interaction of components on the pyrolysis behavior of biomass.* 2011. 91(1): p. 183-189.

34. De Filippis, P., et al., *Gasification process of Cuban bagasse in a two-stage reactor.* 2004. 27(3): p. 247-252.

35. Alauddin, Z.A.B.Z., et al., *Gasification of lignocellulosic biomass in fluidized beds for renewable energy development: A review.* 2010. 14(9): p. 2852-2862.

36. Luo, S., et al., *Hydrogen-rich gas from catalytic steam gasification of biomass in a fixed bed reactor: Influence of temperature and steam on gasification performance.* 2009. 34(5): p. 2191-2194.

37. Luo, S., et al., *Hydrogen-rich gas from catalytic steam gasification of biomass in a fixed bed reactor: Influence of particle size on gasification performance.* 2009. 34(3): p. 1260-1264.

38. Kan, T., V. Strezov, and T.J. Evans, *Lignocellulosic biomass pyrolysis: A review of product properties and effects of pyrolysis parameters.* Renewable and Sustainable Energy Reviews, 2016. 57: p. 1126-1140.

39. Xiao, X., et al., *Catalytic steam gasification of biomass in fluidized bed at low temperature: conversion from livestock manure compost to hydrogen-rich syngas.* 2010. 34(10): p. 1505-1512.

40. Waheed, Q.M. and P.T. Williams, *Hydrogen production from High temperature pyrolysis/steam reforming of waste biomass: rice husk, sugar cane bagasse, and wheat straw.* Energy & Fuels, 2013. 27(11): p. 6695-6704.

41. K. Raveendran, Anuradda Ganesh, and K.C. Khilar, *Pyrolysis characteristics of biomass and biomass components* Fuel Processing Technology 1996. 75(987-998).

42. Hosoya T., Kawamoto H., and S. S., *Cellulose–hemicellulose and cellulose–lignin interactions in wood pyrolysis at gasification temperature.* Journal of Analytical and Applied Pyrolysis 2007. 80(1): p. 118-125.

43. Zheng, Y., et al., *Pretreatment of lignocellulosic biomass for enhanced biogas production.* Progress in Energy and Combustion Science, 2014. 42: p. 35-53.

44. Baumlin, S., et al., *Production of hydrogen by lignins fast pyrolysis.* International Journal of Hydrogen Energy, 2006. 31(15): p. 2179-2192.

45. Jarungthammachote, S., B. Acharya, and A. Dutta, *Parametric effect of agricultural residues and woody biomass on hydrogen production through gasification process.* Proceedings of the International Agricultural Engineering Conference, Bangkok, Thailand, 3-6 December 2007. Cutting edge technologies and innovations on sustainable resources for world food sufficiency, 2007.

46. Liu, Q., et al., *Mechanism study of wood lignin pyrolysis by using TG–FTIR analysis.* Journal of Analytical and Applied Pyrolysis, 2008. 82(1): p. 170-177.

47. Li, S., et al., *Fast pyrolysis of biomass in free-fall reactor for hydrogen-rich gas.* Fuel Processing Technology, 2004. 85(8): p. 1201-1211.

48. Al Arni, S., *Comparison of slow and fast pyrolysis for converting biomass into fuel.* Renewable Energy, 2017.

49. Qu, T., et al., *Experimental study of biomass pyrolysis based on three major components: hemicellulose, cellulose, and lignin.* Industrial & engineering chemistry research, 2011. 50(18): p. 10424-10433.

50. Biagini, E., et al., *Devolatilization of biomass fuels and biomass components studied by TG/FTIR technique.* 2006. 45(13): p. 4486-4493.

51. Raveendran, K., A. Ganesh, and K.C. Khilar, *Influence of mineral matter on biomass pyrolysis characteristics.* Fuel, 1995. 74(12): p. 1812-1822.

52. Jakab, E., O. Faix, and F. Till, *Thermal decomposition of milled wood lignins studied by thermogravimetry/mass spectrometry.* Journal of Analytical and Applied Pyrolysis, 1997. 40: p. 171-186.
53. Jahirul, M.I., et al., *Biofuels production through biomass pyrolysis—a technological review.* 2012. 5(12): p. 4952-5001.
54. Zhao, C., E. Jiang, and A.J.J.o.t.E.I. Chen, *Volatile production from pyrolysis of cellulose, hemicellulose and lignin.* 2017. 90(6): p. 902-913.
55. Li, X., et al., *Biomass gasification in a circulating fluidized bed.* 2004. 26(2): p. 171-193.
56. Luisa Burhennea, et al., *The effect of the biomass components lignin, cellulose and hemicellulose on TGA and fixed bed pyrolysis.* Journal of Analytical and Applied Pyrolysis 2013. 101: p. 177–184.
57. Waheed, Q.M., C. Wu, and P.T. Williams, *Hydrogen production from high temperature steam catalytic gasification of bio-char.* Journal of the Energy Institute, 2016. 89(2): p. 222-230.
58. Nejat, T., et al., *Hydrogen production from steam reforming of ethanol over Ni-Co bimetallic catalysts and MCM-41 as support.* 2019. 97: p. 216-226.
59. Gaca, P., et al., *Catalytic Degradation of Polyethylene over Mesoporous Molecular Sieve MCM-41 Modified with Heteropoly Compounds.* Polish Journal of Environmental Studies, 2008. 17(1).
60. Guana Guoqing, et al., *Catalytic steam reforming of biomass tar: Prospects and challenges.* Renewable and Sustainable Energy Reviews 2016. 58: p. 450-461.
61. Su Shen, et al., *Analysis of the catalytic steam gasification mechanism of biomass.* International Journal of Hydrogen Energy 2015. 40(2): p. 935-940.

Chapter 6

Co-pyrolysis-catalytic steam reforming of biomass components with waste plastics in the production of hydrogen-rich syngas using novel catalysts

6.1 Introduction

In this chapter, co-pyrolysis-catalytic steam reforming of lignocellulosic biomass wastes with plastic wastes has been undertaken to optimise conditions in the production of hydrogen-rich syngas. The biomass components investigated were lignin and cellulose and the plastic wastes were high-density polyethylene (HDPE) and polystyrene (PS). The catalysts used were nickel, cobalt and molybdenum metals supported on MCM-41. The influencing process parameters such as temperature, catalyst staging, and steam flow rate were examined to optimize hydrogen and syngas production. Finally, the influence of different support materials, alumina and Y-zeolite were used to compare with MCM-41 support. The product gases were analysed using gas chromatography (GC). The equipment used for feedstock characterisation included thermogravimetric analyser (TGA) and elemental analyser. The catalyst characterisation included Brunauer-Emmett-Teller (BET) surface area and the used catalysts by temperature-programmed oxidation (TPO) and X-ray diffraction (XRD).

6.2 Characterisation of samples

6.2.1 Thermogravimetric analysis (TGA) of feedstock

The TGA analysis of individual feedstock as well as the mixture of feedstock, biomass components (cellulose, lignin) and plastic wastes (HDPE, PS) was conducted. Figures 6.1 and 6.2 show the thermograms of weight loss (TGA) and the differential weight loss (DTG) of the biomass components and plastic wastes. Figure 6.1a shows that there was weight loss around 100 ^{o}C which is ascribed to moisture content (water loss) in the biomass components (lignin and cellulose). In the case of the individual plastic wastes (HDPE and PS), no weight loss was observed at 100 ^{o}C since the plastics had no moisture content. In Figure 6.1, the TGA curve for HDPE, the degradation temperature was about 510 ^{o}C which is higher than the usual HDPE virgin plastics of about 482 ^{o}C. The high increase in degradation temperature might be due to contaminants in the waste plastics. The degradation temperature of polystyrene (PS) waste is within the range of 400 to 450

^{o}C as shown in Figure 6.1. Cellulose has a decomposition temperature ranging between 300 ^{o}C and 400 ^{o}C while lignin degrades over a wider temperature range of about 200 to 500 ^{o}C and the decomposition to the final temperature of 800 ^{o}C. Likewise, this trend has been reported by other researchers [1, 2].

The biomass components (lignin and cellulose) were individually mixed with plastic wastes (HDPE and PS) in a 1:1 ratio and were characterised by TGA to determine the thermal degradation of the blend samples. Figure 6.2, shows two peaks for the blend of cellulose with HDPE, the first peak was between temperatures of 300 to 400 ^{o}C which is attributed to the decomposition of the cellulose component while the second peak is within the temperature range of 450-510 ^{o}C which is attributed to the decomposition of HDPE plastics. In addition, the blend of cellulose with PS equally shows two major peaks, the first peak is between 300 to 400 ^{o}C and is attributed to degradation of cellulose while the second peak is between 400 to 500 ^{o}C, which is ascribed to PS decomposition. It appears that the weight loss for both peaks was reduced for the blend of cellulose and PS while in the case of cellulose with HDPE blend, the first peak which seemed to be cellulose decomposition had a reduced weight loss at a slightly higher temperature than the decomposition of cellulose alone but there was no effect on the weight loss as well as the temperature of the second peak ascribed to HDPE in the mixture with cellulose. This seems to be in agreement with Jakab and Blazso [3], who studied the thermal decomposition effect of additives (lignin, cellulose, wood and charcoal) on polystyrene (PS) and polyethylene (PE). It was reported that PS is more sensitive to the component mixtures resulting in a shift to a higher temperature for thermal decomposition and the product distribution changed significantly in the presence of the additives, which is interpreted in terms of free radical mechanism of the thermal decomposition. PE thermal decomposition curves only showed a small effect in the presence of the additives. The magnitude of the effect was approximately proportional to the quantity of char yield from the lignocellulosic additions [3].

On the other hand, the lignin component mixture showed one major peak in relation to the plastic degradation temperature, (Figure 6.2). The blend of lignin with HDPE had a small peak around a temperature of 350-450 ^{o}C while the major peak was within the range 450 to 550 ^{o}C. The lignin mixture with PS showed only one major peak as well between 350 and 500 ^{o}C, which was weight loss of the PS degradation temperature. The lignin component mixture with the plastics waste suggest that the decomposition temperature of these two blends has a common degradation temperature, which suggests that there might be interaction. Also, in the blend of lignin with the plastic wastes (HDPE and PS), there was a reduced weight loss compared to the plastic decomposition alone which had an increased weight loss as compared to the decomposition of lignin alone. According to Jakab et al. [2], they reported that the higher the lignin content of the mixture the lower the temperature at which PP starts to degrade, i.e. the maximum rate of decomposition of PP decreases with increasing lignin content. Likewise, the addition of PP to cellulose decreased the time it took the pyrolysis process to be completed and linked to the product distribution while hydrogen, hydroxyl and methyl abstraction were the most prevailing reactions in the conversion process [4].

Sorum et al. [5], observed that paper and cardboard have a similar degradation temperature as wood occurring between 200-500 ^{o}C. The decomposition of PS, PP, LDPE and HDPE took place at 350-500 ^{o}C while PVC with a more complex degradation occurred in two steps, first at 200-380 ^{o}C and second at 380-550 ^{o}C producing a char fraction. In addition, it was found that the reactivity of cellulosic material was increased in a blend of PVC with newspaper. Matsuzawa et al. [6] conducted thermal analysis of pure cellulose, PE, PP, PS, PVC and polyvinylidene chloride PVdC compared with the blend of these compounds. It was reported that there was good agreement between cellulose and PE, PP, PS mixtures but no interaction existed, however, there was interaction between cellulose and PVC/PVdC. Jimenez and Ruseckaite [7], found that there was interaction between polycaprolactone (PCL) and cellulose derivatives (solid-solid, solid-gas or gas-solid) with solid-gas being the major interactions in PCL and the microcrystalline cellulose (MC) contrary to sisal fibres (SF). Cai et al. [8], equally studied co-pyrolysis of HDPE, LDPE and PP and low volatile coal (LVC) in a thermogravimetric analyser, and the results showed that coal decomposed over a temperature ranging from 174-710 ^{o}C while that of the plastics was between 438-521 ^{o}C, the overlapping degradation temperature interval between the coal and plastics foster hydrogen transfer from the plastics to coal. It was also reported that there was a synergistic effect during the co-pyrolysis of plastic and coal at high temperature, expressed as the difference in weight loss (ΔW) between experimental and theoretical calculated as the sum of those from each individual component resulting in 2.0-2.7% at 550-650 ^{o}C. Brebu et al. [9], in a co-pyrolysis investigation via thermogravimetric analysis of PE, PP and PS with biomass (pine cone) showed that degradation starts around 200 ^{o}C with the cellulose, hemicellulose fraction of the biomass components. While decomposition of lignin at above 400 ^{o}C overlapped with the polyolefin plastics, which may lead to interaction between the component mixtures subsequently leading to a synergistic effect in the product yields. In addition, the temperature relative to the maximum rate of mass loss (Tmax) of each polymer was the same when analysed individually or in a mixture.

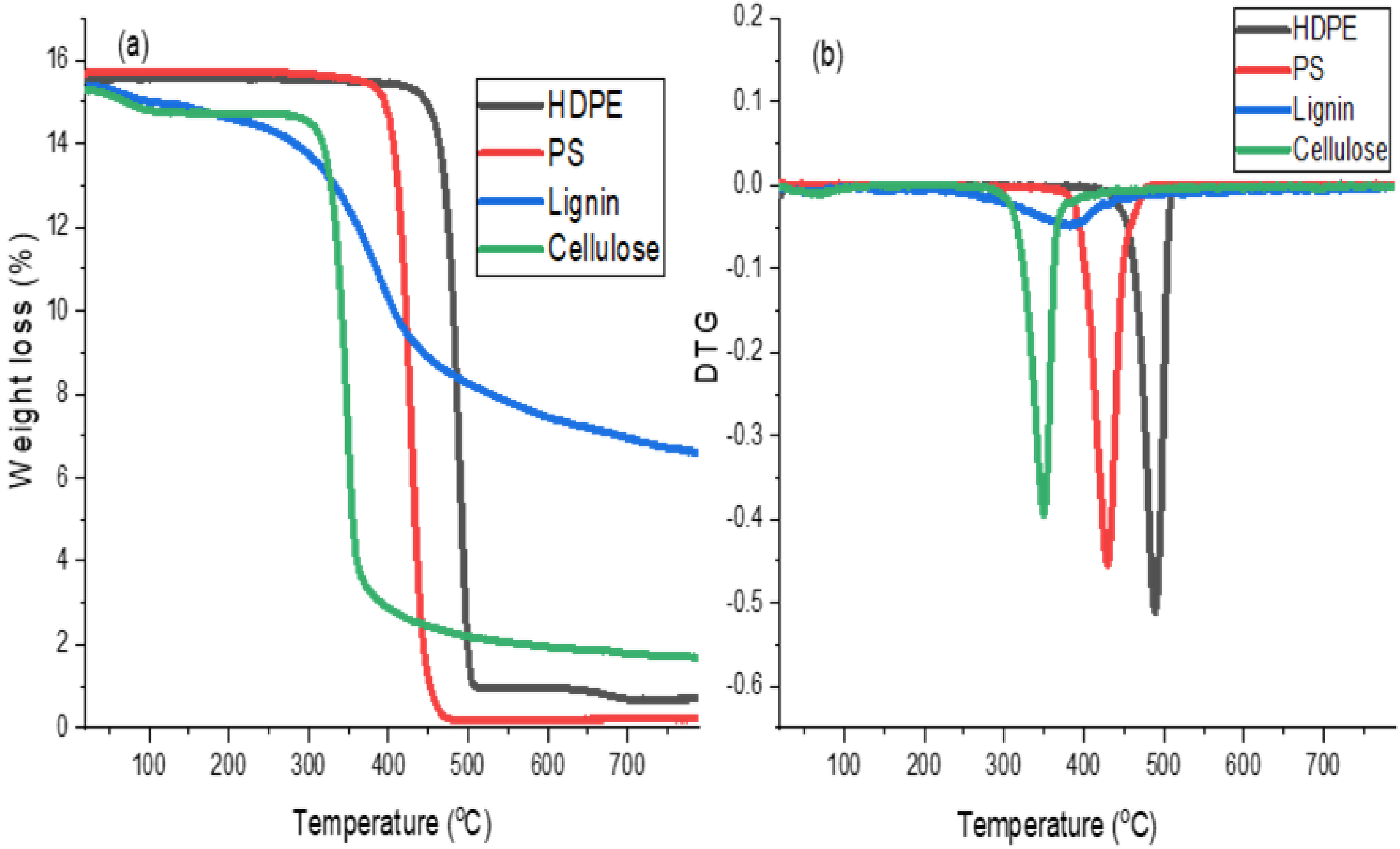

Figure 6.1. (a) TGA and (b) DTG of individual biomass components and plastic wastes.

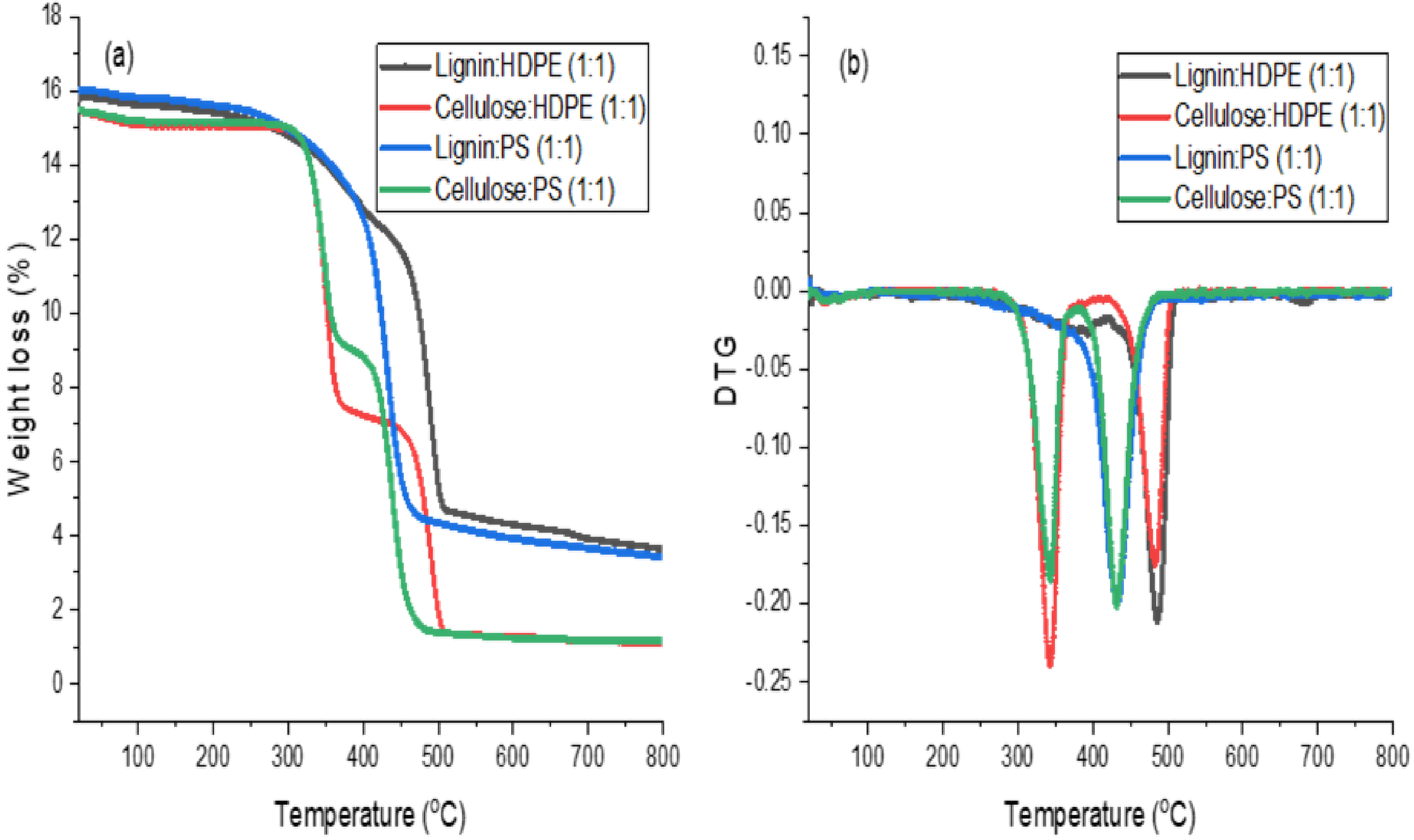

Figure 6.2. (a) TGA and (b) DTG of mixture of biomass components and plastic wastes.

6.2.2 Characterisation of fresh catalysts

The properties of the prepared fresh catalysts were determined to characterise the effects of the 10% metals addition on the MCM-41 and the different support catalysts. All the prepared catalysts were reduced under 5% hydrogen and balanced by nitrogen. Figure 6.3a shows the XRD patterns of the metal-MCM-41 catalysts. All the catalysts display a wide silica peak between 23^o and 30^o. The 10% Ni/MCM-41 catalyst showed three major peaks at about 45^o, 52^o and 77^o representing nickel (Ni) particles as the NiO was reduced. All the other metal catalysts, including the bimetal, showed smaller and weaker peaks at a similar position as the Ni/MCM-41. The 10% Mo/MCM-41 catalyst equally showed smaller, weaker and more dispersed peaks. The influence of metals and bimetals has been investigated and reported where iron (Fe) on MCM-41 showed a similar trend [10]. It seems that the three XRD peaks of Ni/MCM-41 catalyst were stronger compared to the other two metals on MCM-41 support which might suggest the reason for the higher yield by Ni/MCM-41 catalyst compared to the other Co and Mo metals on MCM-41 catalysts. All the metal oxides were previously reduced to metals prior to the XRD analysis and the co-pyrolysis experiments. In addition, the wide display of amorphous silica peaks between 20^o and 30^o for all the metals on the MCM-41 catalyst have been reported by other researchers [10, 11].

Figure 6.3b shows the XRD spectral patterns of the different supported nickel catalysts on MCM-41, alumina, Y-zeolite and dolomite, the 10% Ni/Y-zeolite catalyst showed a more dispersed pattern with strong narrow peaks compared to the other three support catalysts. The strongest observable peak obtained for 10% Ni/Y-zeolite was between 5-10^o [12, 13]. The results show that the dolomite primarily consisted of $MgCa(CO_3)_2$ as shown in the non-calcined dolomite while calcination of the dolomite resulted in a breakdown of the $MgCa(CO_3)_2$ into CaO and MgO as well as the addition of 10% nickel loading showed NiO and NiMgO in the catalyst [35]. Other authors reported similar results for dolomite catalysts [14, 15] as well as nickel alumina catalysts [16]. All the nickel-supported catalysts have similar XRD patterns with three identical peaks of nickel (Ni) metal at the same position.

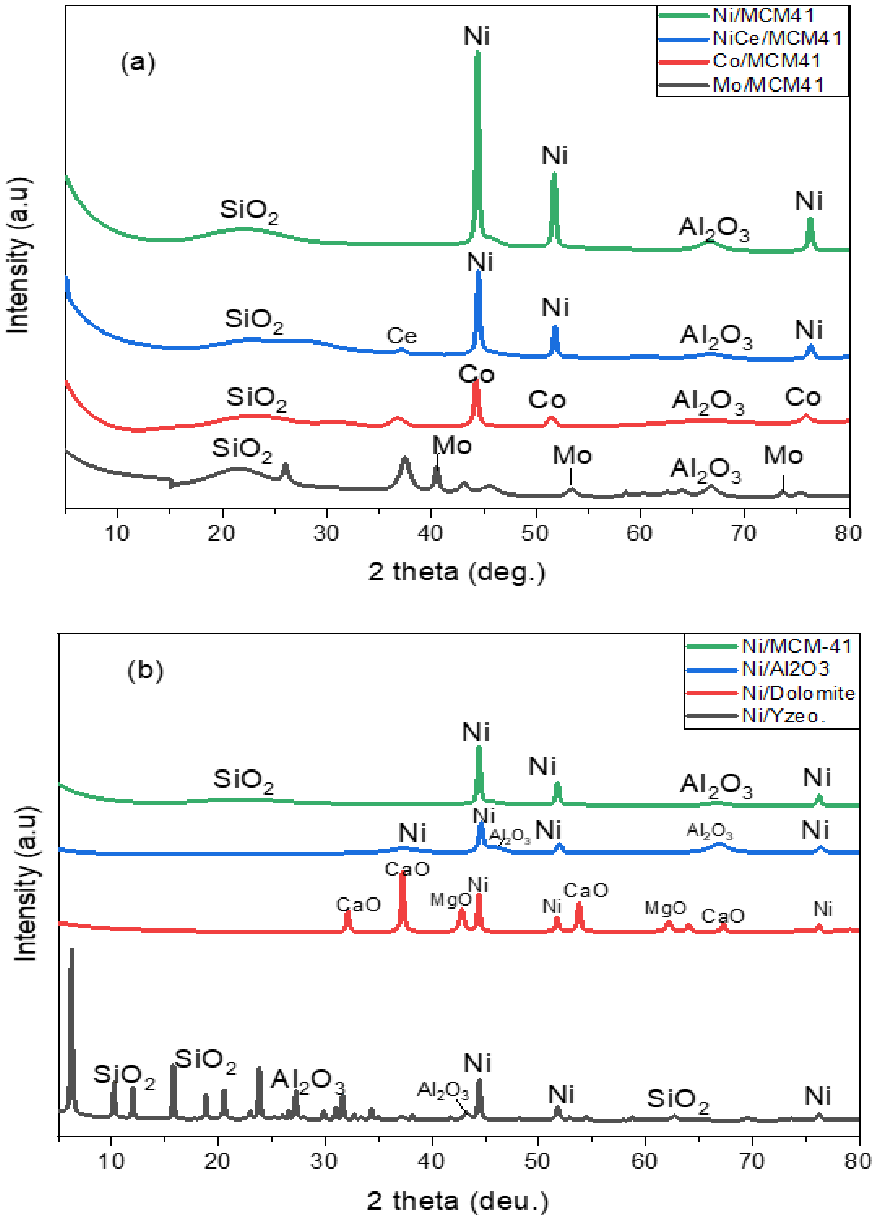

Figure 6.3. XRD patterns for (a) 10% metals loading on MCM-41 catalysts (b) 10% nickel metal on different support catalysts.

6.3 The co-pyrolysis-catalytic reforming of biomass components and plastic wastes (review)

The biomass components including cellulose and lignin were co-pyrolysed with high density polyethylene (HDPE) and polystyrene (PS) waste in the two-stage pyrolysis-catalytic steam reforming process. The essence of combining or mixing biomass with plastic wastes relates to the high hydrogen and carbon content of plastics which leads to an increase in gaseous yield, syngas and hydrogen production as desirable products.

However, the ratio of plastics in the co-pyrolysis is an important factor which determines the quantity as well as quality of the products produced. Researchers have varied the percentage of plastics content in co-pyrolysis gasification of biomass for increased gaseous yield and hydrogen production. For example Lui et al. [17], account on the investigation of the 1:4 ratio of biomass to plastics (LDPE) resulting in about 61.8 vol.% of hydrogen concentration over Ni-Pb-Al-MCM-41 catalyst. Alvarez et al. [18], equally carried out steam co-pyrolysis gasification of biomass (sawdust) and plastic (PP) in a two stage reactor with and without Ni/Al_2O_3 at the catalytic temperature of 800 ^oC. The plastics ratio was varied from 5-20%, it was observed that the 20% plastics blend to 80% biomass with catalyst gave the highest yield of hydrogen (27.27 mmol/g) attributed to be the synergetic effects between the feedstock as well as the catalyst which promotes steam reforming and water gas shift reactions. Lopez et al. [19] obtain a substantial effect in the co-feeding of biomass and plastics on gas composition, stating that at least 50% of the plastics content was ideal which led to about 57% of H_2 concentration which was just slightly lower than that with pure HDPE of 58% investigated. Also, Ahmed et al. [20], conducted co-gasification of biomass (woodchips) and plastics (PE) using high temperature steam as the gasifying agent in a semi-batch reactor. The highest yield of hydrogen, syngas, carbon and energy was obtained for 60-80% of plastics (PE) in biomass. The results confirmed that there was a synergistic interaction between the woodchips and PE plastics during the process of steam gasification at a high reactor temperature of 900 ^oC. Pinto et al. [21], equally obtained a high hydrogen concentration up to 50 vol.% with 20 wt.% content of PE added to pine sawdust co-pyrolysis. However, no increase in hydrogen production with PE content beyond 20% with increasing temperature from 730-900 ^oC was observed. This might be due to the absence of catalytic reforming as well as the cracking process of catalyst on the plastic to convert more hydrocarbon into hydrogen in the co-pyrolysis of the biomass (pine sawdust) with plastics (PE).

Onal et al. [22], reported a synergistic effect as two or more individual agents acting together to create an effect greater than that expected or predicted through the understanding of the separate effect of the individual agent, i.e. the difference between the experimental values and the calculated value based on individual yield being positive, leading to enhancement of the quality and quantity of the product obtained concludes that a synergistic effect exists between the biomass and the plastics blend [22]. Berrueco [23], suggested the existence of a positive synergistic interaction between the co-pyrolysis of biomass and HDPE plastics as the value of the experimental value 90.5 wt.% was higher than the calculated value of 76.6 wt.% at 850 °C. Across an increasing temperature range from 640 to 850 °C showed calculated values from 34.4 to 76.6 wt.% being lower than the experimental values from 55.4 to 90.5 wt.% respectively [23]. Ahmed et al. [20], equally reported a positive synergistic effect between the co-gasification of biomass (woodchips) and PE plastics. Lignocellulosic biomass such as cellulose and hemicellulose undergo dehydration, decarbonylation and decarboxylation to generate furan compounds while lignin decomposes into phenolic compounds [24, 25]. The plastics degradation route is describe to occur via two mechanisms: random and chain-end scission, thereby generating free radicals together with the long carbon chains (olefins), plastics donate hydrogen for the biomass-derived oxygenates which act as a strong acceptor [26]. According to the literature, polyolefin undergoes cracking as the initial step which occurs over the external surface and at the pore mouth of the catalyst, then the smaller molecules entering the pore were secondary reactions (such as hydrogen transfer, oligomerisation, cyclization and aromatisation, etc.) which take place inside the micropores of zeolites [27]. Illustration of reaction pathway for co-pyrolysis of biomass components with plastic wastes is shown in Figure 6.4.

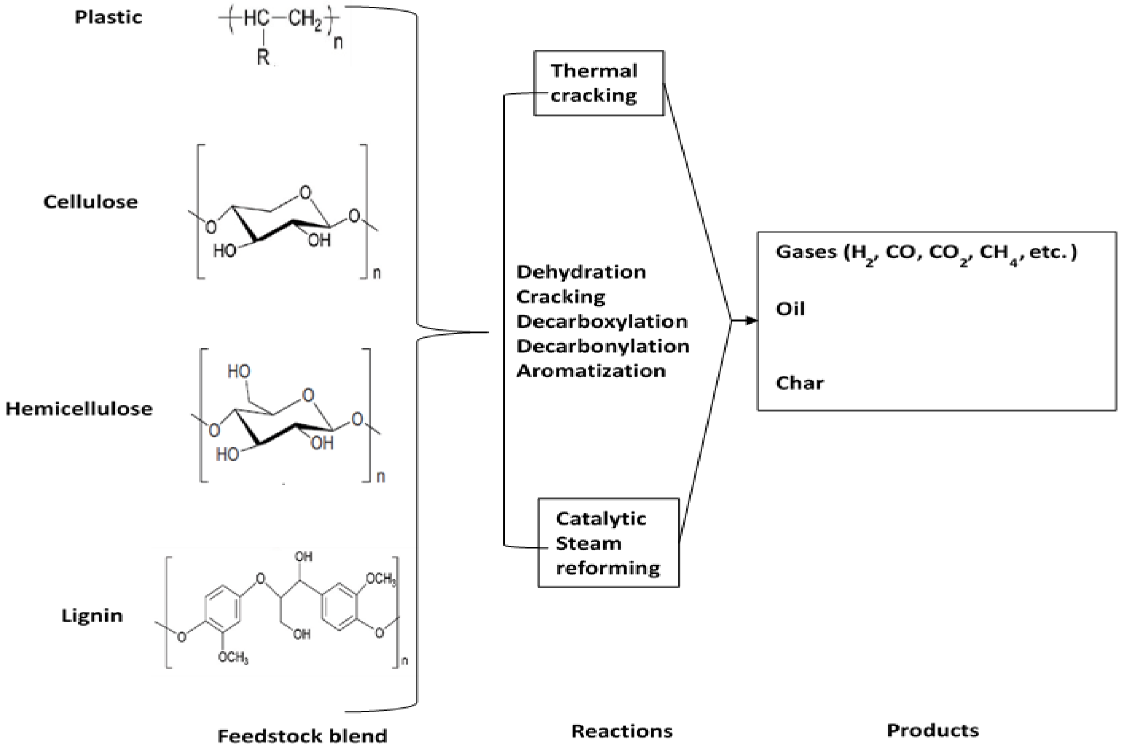

Figure 6.4. Illustration of a simple reaction pathway for co-pyrolysis of biomass components and plastic wastes in catalytic pyrolysis (Sketched).

Also, it has been reported that steam catalytic reforming at high temperatures up to 800 ^oC aid gas production instead of oil [28]. Therefore, under a high temperature of 850 ^oC and steam gasification investigated, more hydrogen and syngas were produced from the co-pyrolysis of biomass components (cellulose, lignin) and plastic (HDPE, PS) wastes. Both cracking and steam reforming reactions exist as shown in Equations 6.3-6.11 respectively. Onal et al. [22], highlighted co-pyrolysis reaction radicals as initiation, formation of secondary radicals [such as depolymerisation, formation of monomers, both favourable and unfavourable hydrogen transfer reactions, intermolecular hydrogen transfer (formation of dienes and paraffin), isomerization via vinyl groups], and termination by recombination of radicals or disproportionation [29].

6.4 Effect of metal catalysts on the co-pyrolysis, catalytic steam reforming of biomass components with plastics

6.4.1 Product yield

One very important influencing factor in co-pyrolysis with catalytic steam reforming is the use of catalysts. Three metal catalysts were investigated, 10 wt.% nickel-MCM-41, 10 wt.% cobalt-MCM-41 and 10 wt.% molybdenum-MCM-41 were investigated to determine the influence of the different catalyst metals on the production of hydrogen for co-pyrolysis, catalytic steam reforming of biomass components with plastic wastes (HPDE and PS). Also 5% cerium (Ce) metal was introduced as a catalyst metal promoter into the 10 wt.% Ni/MCM-41 which was investigated to improve product yield and hydrogen-syngas production. A reaction temperature of 750 ^oC and a steam rate of 5.7 g/h was kept constant for all the metal catalysts examined. The results in terms of product yield and gas composition as vol.% and mmol/g of biomass:plastic are shown in Table 6.1 for the mixture of cellulose with the plastics and in Table 6.2 for the lignin and plastics mixture. The product yield and the mass balance for all the catalysts investigated were all above 90% with the highest being about 98%.

The product yield calculations can be expressed by the following equations 6.1 and 6.2:

Products yield in relation to feedstock (biomass and plastic) plus reacted water, (wt.%) =

$$\frac{W_{product}}{W_{feedstock}+W_{steaminput}} X\ 100 \qquad \mathbf{6.1}$$

Products yield in relation to feedstock (biomass and plastics blend) only, (wt.%) =

$$\frac{W_{product}}{W_{feedstock}} X\ 100 \qquad 6.2$$

The total gas yield obtained from the feedstock (biomass:plastic blend) plus reacted water showed lower gas yield with a maximum of ~32 wt.%. However, the total gas yield with respect to only feedstock (biomass:plastic blend), showed an increase such that the gas yields were all above 100 wt.% for all the cellulose feedstock blends. These are also higher than the gas yields obtained from the lignin component blend as observed in the results (Tables 6.1 and 6.2). This shows that the reforming gas (steam) obviously contributed to the total gas yield in addition to the hydrocarbon gases from the catalytic co-pyrolysis of the biomass samples with plastics. A slightly higher gas yield was observed in the 10% Ni/MCM-41 catalyst for all the cellulose feedstock blends while the gas yield produced with 10% Co/MCM-41 and 10% Mo/MCM-41 catalysts were virtually the same results. Likewise, the gas yield obtained from the bimetal 10% Ni-5%Ce-MCM-41 catalyst was lower than that obtained from all the metal catalysts as shown in Table 6.1 and Figure 6.5. Likewise, in the gas composition, the H_2 yield was highest for 10% NiMCM-41 catalyst but the production of CO and CO_2 were relatively the same from all the feedstock blends and for all catalysts investigated. However, higher production of CH_4 and C_2-C_4 were obtained from the blend of HDPE and cellulose as compared with the PS and cellulose mixture/blend. This is suggested to be due to the chemical composition of the plastics, as HDPE is made from the monomer of ethylene while PS is made from the monomer of styrene. Therefore, the higher yield of CH_4 and C_2-C_4 from HDPE/cellulose blend than PS/cellulose blend could be due to the thermal and catalytic cracking reactions.

In this study, the nickel metal catalyst showed a better performance due to the higher gas yield, hydrogen and syngas produced than from the molybdenum and cobalt catalysts. In the blend of lignin with plastics waste result, higher hydrogen and syngas were produced, the CH_4 and C_2-C_4 were lower using 10% NiMCM-41 compared with 10% MoMCM-41. It is suggested that water gas reaction, methane steam reforming, hydrocarbon/tar steam reforming and Boudouard reactions were favoured at a high catalytic temperature using 10% NiMCM-41 as compared with 10% MoMCM-41.

Furthermore, the influence of catalyst on gas yield for the combination of lignin with plastics blend was less than that of the cellulose with plastics blend, but 10% Ni/MCM-

41 catalyst still produced the highest gas yield as compared with 10% Co/MCM-41 and 10% Mo/MCM-41 catalysts as shown in Table 6.2 and Figure 6.6.

In addition, the higher values of gas yield from the blend of cellulose compared to lignin mixture with the same plastics waste was possibly due to the synergistic effect between the feedstocks. Burhenne et al. [30], reported higher gaseous products and faster decomposition from cellulose and hemicellulose contained feedstock (herbaceous biomass) than lignin containing feedstock (woody biomass) as investigated in a TGA and fixed bed reactor. According to Vasile et al. [31], the presence of plastics (PVC) in a blend with biomass components (lignin, cellulose), co-pyrolysis increased gaseous yield and coke, while the waxy product decreased. Gunasee et al. [32], reported synergistic effects during co-pyrolysis of cellulose and plastic (LDPE), stating that gas-gas and/or solid-gas interaction exists as pyrolysis of the mixture of cellulose and LDPE increased the yield of the product as compared to a mixture of the products from pyrolysis of the individual components. In other research on co-pyrolysis of cellulose and PVC conducted in a fixed bed two stage reactor, the interaction between the cracking ratio and tar components became stronger at a higher temperature of 600 ^{o}C than at 500 ^{o}C [33]. The co-pyrolysis temperature might be another factor in the higher gaseous yield for the cellulose than lignin blend. Cellulose has been shown to decompose at a lower temperature than the lignin component of biomass sample. It has been reported that cellulose decomposes at temperatures up to 400 ^{o}C while lignin decomposes within a wider temperature range from about 200 ^{o}C up to 900 ^{o}C [2]. The catalyst bed temperature investigated in this study is 750 ^{o}C with catalytic steam reforming. It is suggested that the catalytic steam reforming reaction was more active with the cellulose blend since complete decomposition of cellulose occurs between 400 to 450 ^{o}C temperature, and cellulose might have totally decomposed before the investigated temperature of 750 ^{o}C to release more gases than the blend of lignin/plastics with a longer decomposition temperature pattern up 900 ^{o}C. Moreso, lignin presented a wider temperature range than plastic wastes [28, 34-37]. In the result obtained as shown in Table 6.1, the blend of cellulose:PS and cellulose:HDPE had a higher gas yield, especially with the nickel metal catalyst 10% Ni/MCM-41 compared with the results from the blend of lignin:PS and lignin:HDPE in Table 6.2. As observed in this study, the Ni on MCM-14 catalyst had a slightly higher performance in terms of gas yield. In support of this, Zhao et al. [38] reported that Ni on MCM-41catalyst as investigated, produced a higher gas yield compared to other Ni catalysts. Nickel-based catalysts have been reported to be one of the best metals for tar elimination by catalysing C-C bond breakage [38, 39].

Table 6.1. Product yield and mass balance showing the activity of metal catalysts on the co-pyrolysis steam reforming of biomass components with plastic waste blends.

	NiMCM41		**CoMCM41**		**MoMCM41**		**NiCeMCM41**	
	Cell:HPDE	**Cell:PS**	**Cell:HPDE**	**Cell:PS**	**Cell:HPDE**	**Cell:PS**	**Cell:HPDE**	**Cell:PS**
Gas yield in relation to feedstock (biomass:plastics) only (wt.%)								
Gas	112.49	119.22	107.52	113.64	107.54	115.35	89.09	89.33
Product yield in relation to feedstock (biomass:plastics) + reacted water (wt.%)								
Gas	29.68	32.40	26.95	30.63	28.60	30.88	23.98	24.08
Liquid	58.84	56.79	62.03	63.88	57.31	57.56	61.78	61.86
Char	2.77	3.26	2.76	3.23	3.72	3.08	3.23	3.23
Catalyst carbon	1.06	1.09	0.38	0.94	0.40	1.07	1.08	0.94
Mass balance	92.35	93.54	92.11	98.69	90.04	92.60	90.07	90.12
Gas composition (vol.%)								
CO	25.91	30.77	27.11	30.76	25.76	30.96	26.66	31.07
H_2	60.09	59.29	58.09	58.53	57.98	58.05	55.56	58.31
CO_2	8.37	7.98	7.03	7.57	7.38	7.57	6.96	7.05
CH_4	5.23	1.85	6.78	2.78	7.58	2.97	7.72	2.93
C_2-C_4	0.40	0.11	0.99	0.36	1.30	0.45	3.10	0.63
Gas composition (mmol g^{-1})								
H_2+CO	73.81	78.63	69.23	74.17	68.04	74.5	53.18	58.58

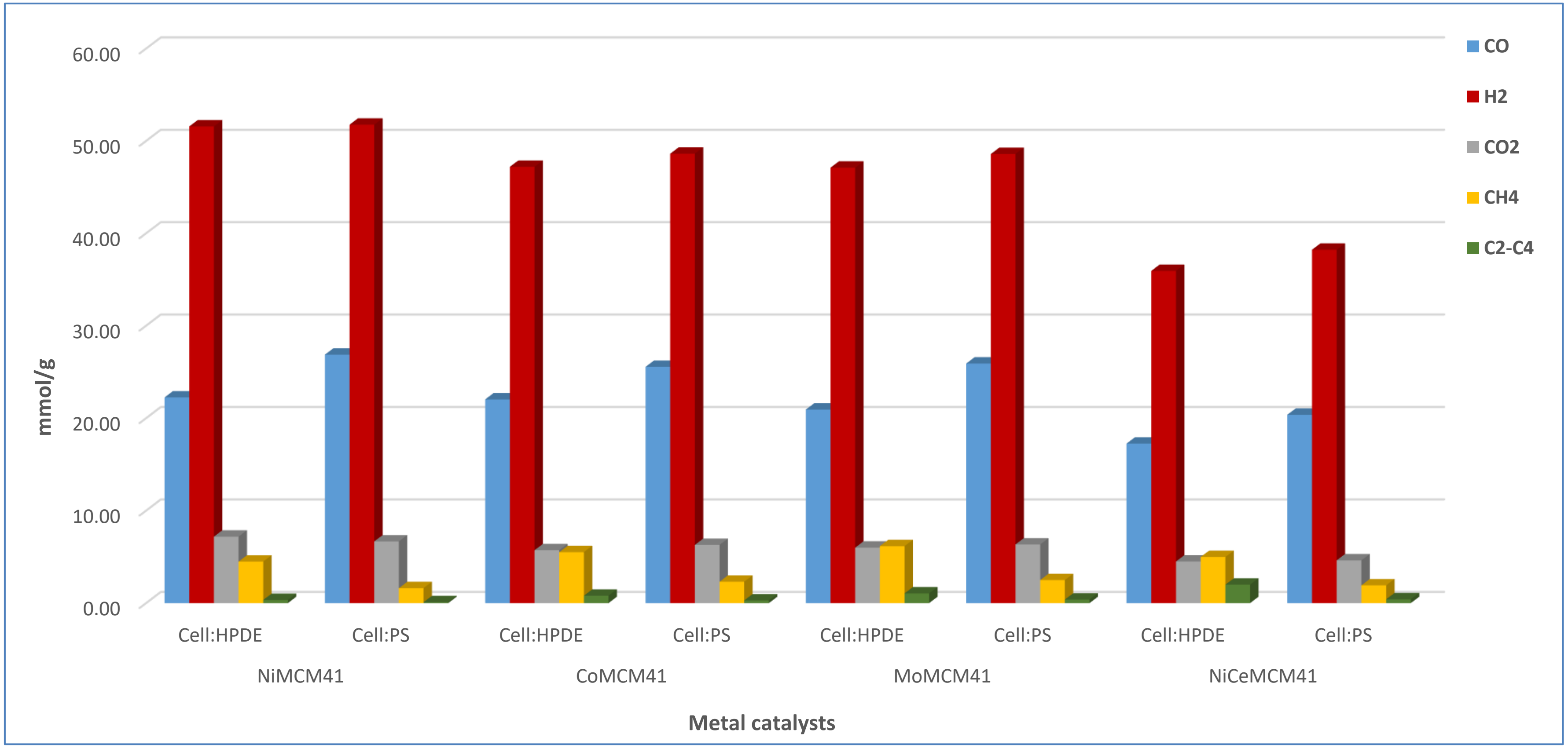

Figure 6.5. Gas composition yield showing the activity of metal catalysts on the co-pyrolysis steam reforming of biomass components with plastic waste blends.

Table 6.2. Product yield and mass balance showing the activity of metal catalysts on the co-pyrolysis steam reforming of biomass components with plastic waste blends.

	NiMCM41		MoMCM41	
	Lignin:HDPE	**Lignin:PS**	**Lignin:HDPE**	**Lignin:PS**
Product yield in relation to feedstock (biomass&plastics) only (wt.%)				
Gas	70.85	65.20	50.65	38.05
Product yield in relation to feedstock (biomass&plastics) + reacted water (wt.%)				
Gas	19.25	17.55	13.75	10.12
Liquid	70.65	72.54	69.20	70.48
Char	5.30	6.19	6.51	6.12
Carbon	0.95	1.08	1.76	3.06
Mass balance	96.15	97.36	91.22	89.77
Gas composition (vol.%)				
CO	24.17	29.31	16.47	22.19
H_2	51.56	55.18	47.22	56.24
CO_2	5.07	5.75	5.23	6.2
CH_4	13.55	7.73	20.25	11.61
C_2-C_4	5.66	2.03	10.84	3.76
Gas composition (mmol g^{-1})				
H_2+CO	38.82	40.32	22.69	22.96

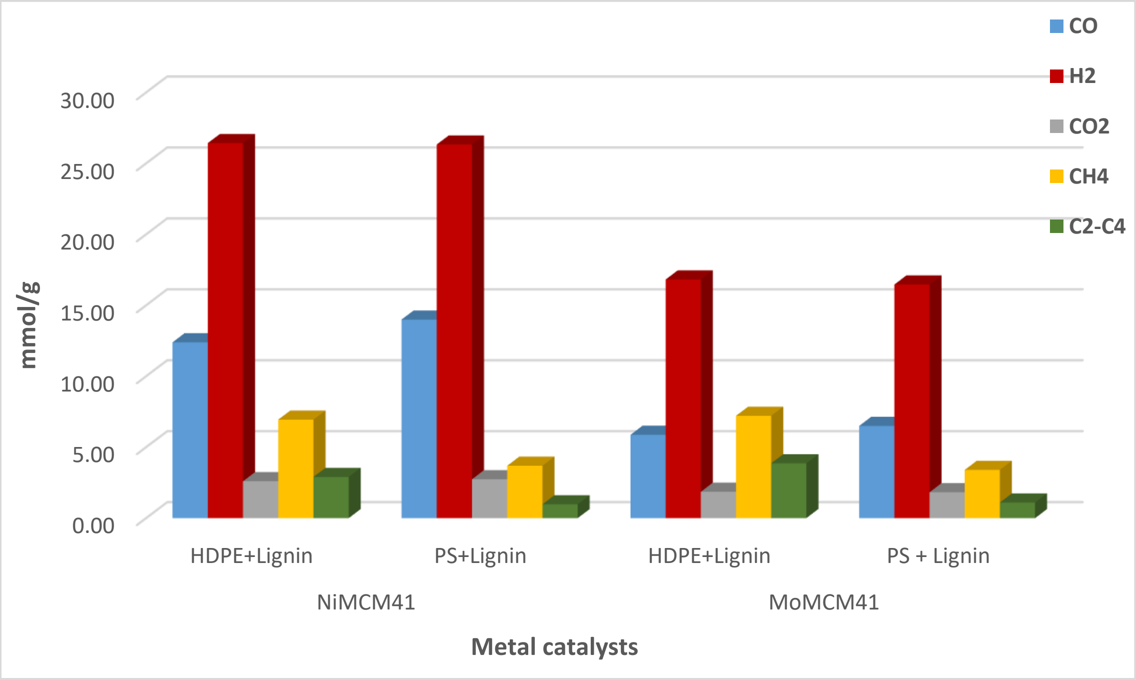

Figure 6.6. Gas composition/yields showing the activity of metal catalysts on the co-pyrolysis steam reforming of biomass components with plastic waste blends.

6.4.2 Influence of metal catalysts on gas composition and hydrogen yield

The investigation carried out with Ni-, Co-, Mo-MCM41 and bimetal NiCe impregnated on MCM-41 for co-pyrolysis of biomass components (cellulose and lignin) and waste plastics (HDPE and PS) blends, showed that the 10% Ni/MCM-41 catalyst resulted in a slightly higher yield of hydrogen. The nickel metal catalyst 10% Ni/MCM-41 performed better with a higher yield of hydrogen produced as compared with 10%Co/MCM-41, 10% Mo/MCM-41 and the bimetal catalyst of NiCe/MCM-41. In the results shown in Table 6.1 and Figure 6.5, hydrogen yield from the Ni/MCM-41 was approximately 52 mmol/g for both the co-pyrolysis of cellulose with PS and cellulose with HDPE. Likewise, Co/MCM-41 and Mo/MCM-41 catalysts produced 47 mmol/g of hydrogen for co-pyrolysis catalytic steam reforming of cellulose:HDPE and approximately 49 mmol/g of hydrogen was produced from cellulose:PS for both catalysts respectively. An overview of the syngas (H_2+CO) produced showed that the highest yield of 78.61 mmol/g was obtained by cellulose:PS, while ~ 74 mmol/g was produced by HPDE and cellulose co-pyrolysis catalytic steam reforming with the 10%NiMCM-41 catalyst. Similarly, the syngas yield of ~ 69 and 74 mmol/g for the mixture of cellulose:HDPE and cellulose:PS using 10%CoMCM-41 catalyst was obtained. And ~ 68 and 75 mmol/g was obtained from cellulose with HDPE and cellulose with PS using 10% Mo/MCM-41 catalyst. There was a drop in both hydrogen and syngas production with the bimetal catalyst of NiCe/MCM-41 with values of ~ 36 and 38 mmol/g for hydrogen yield and ~53 and 59 mmol/g for syngas yield from the co-pyrolysis catalytic steam reforming of cellulose:HDPE and cellulose:PS respectively.

Much research work has been conducted on the investigation of co-pyrolysis of biomass and plastics waste [18, 19, 40-42]. According to Alvarez et al. [18], the presence of Ni catalyst in the steam co-pyrolysis gasification of biomass (sawdust) and plastics (PP) produced a sharp increase in gas yield and hydrogen production compared to the non-catalytic process of the same co-pyrolysis gasification. Huang et al. [43], conducted studies in a two stage fixed bed reactor on co-pyrolysis of a cellulose with polyvinyl chloride (PVC) blend and there was an increase in hydrogen production with dolomite catalyst. Zhao et al. [38], investigated Ni on Al_2O_3 and MCM-41 supported catalysts using TG-MS for pyrolysis gasification of cellulose, it was reported that the MCM-41 supported Ni catalysts resulted in higher hydrogen production as compared with Ni on Al_2O_3. This was attributed to the large surface area and pore size of the MCM-41 catalyst, which was effective for tar cracking and reforming of the reaction. MCM-41 is described as having a large surface area of about 1000 m^2/g and pore size distribution ranging from 2-10 nm larger than zeolites, Al_2O_3 and other oxide supports, which further promote mass transfer as well as uniform distribution of the catalyst particles within the porous structure [44, 45]. The highly ordered hexagonal porous structure of MCM-41 enabled the incorporation of metals in the framework, thereby promoting both oxidizing and Lewis acidity properties [44]. According to Lucredio and Assaf [46], the mesoporous support MCM-41 with high surface area, uniform pore distribution facilitated a greater increase in metal dispersions within the framework of the support catalysts. Wu et al. [47], examined different nickel metal loading on MCM-41 ranging from 5 to 40 wt.% using a fixed bed two stage reactor for the pyrolysis-catalytic steam reforming of wood sawdust biomass with pyrolysis and a catalytic bed temperature of 550 ^{o}C and 800 ^{o}C. It was reported that an increase in gas yield from 38.9 to 62.8 wt.% and the hydrogen produced increased from 5.7 to 18.0 mmol/g with increased catalyst temperature. Different metal catalysts such as Ni, Co, Fe, etc. have been previously investigated for both biomass samples, plastics waste as well as co-pyrolysis of biomass with plastics [48-50]. Ni metal has been one of the most investigated metals and they have been found to be effective for reforming reactions, identified as the best metals for tar elimination by catalyzing C-C, O-H and C-H bond breakage [39, 51, 52]. Ni catalysts are known to be used for catalytic steam reforming of biomass due to their low cost, high activity for C-C bond rupture and formation of H_2 from H atom having a high degree towards water gas shift reaction [18]. It was suggested that a 10 to 15% Ni loading was ideal to provide maximum catalytic activity for tar gasification due to a higher Ni loading but which led to no significant increase in product yields [18, 53]. Ruoppolo et al. [54], investigated the effect of 5.5 wt.% of Ni metal on alumina, observing that there was a reduction of methane and light hydrocarbon (tar) yield indicating the effectiveness of the catalyst for reforming which led to an increase in hydrogen concentration of about 32 vol.%. The influence of cobalt (Co) catalytic activity has also been extensively studied, adequate for steam methane reforming [46, 55], active for C-C bond breakage, decomposition of tar and molecules with C and O [50]. Cobalt (Co) was reported to aid CO removal, improve the water-gas shift reaction which is essential for hydrogen production from biomass [50, 56] and, of course, co-pyrolysis of biomass with plastic wastes. According to Furusawa and Tsutsumi [49], investigation of cobalt and nickel on MgO support, the results showed that cobalt (Co) on MgO gave the highest catalytic activity for steam reforming of naphthalene as a model compound of tar derived from biomass. Other research equally showed the influence of cobalt (Co) metal on two different supports SBA-15 and MCM-41 for thermal decomposition of cellulose. The cobalt catalyst on MCM-41 (10 wt.% Co/MCM-41) was reported to have the highest selectivity as compared to cobalt (Co) on SBA-15 and alpha Al_2O_3 [50]. Lui et al. [17], emphasised the influence of the type of metal rather than the metal site of Ni and Pd on Al-MCM-41 catalyst for the co-pyrolysis gasification of biomass (pubescens) with plastics (low density polyethylene) resulting in a high increase in H_2 concentration up to 61.8 vol.%. It was suggested that steam reforming reactions over the Ni-Pd-Al-MCM-41 as well as the carbonium ions from the pyrolysis of LDPE formed by the acidic sites of the catalyst which undergo cyclization reaction leading to a high yield of hydrogen and aromatic hydrocarbons under vapour-catalysed co-pyrolysis catalytic steam reforming conditions [17]. In most of the literature [17, 18, 28, 54] on co-pyrolysis catalytic steam reforming of biomass and plastics, two major reactions were highlighted which includes the water gas shift reaction and steam reforming for increase yield of hydrogen production. The high production of hydrogen obtained from Ni on MCM-41 was suggested to be due to higher surface area and pore volume of the catalyst which aids high dispersion of metals on the surface or within the pores of the catalyst. It is suggested that different chemical reactions take place in the catalytic steam reforming of co-pyrolysis of biomass and waste plastics that are actively influenced by the presence of catalysts. According to Lopez et al. [19], the composition of products obtained in co-pyrolysis of biomass and plastics depend majorly on the individual chemical composition as well as the reaction during the catalytic steam reforming process. The main reaction pathways are as follows:

Biomass pyrolysis:

$$\rightarrow gas\ (H_2, CO, CO_2, CH_4, \dots) + tar\ (oxygnates, aromatics) + char \tag{6.3}$$

HDPE pyrolysis: $(CH_2)_m \rightarrow m/nC_2H_{2n} \rightarrow tar\ (aromatics)$ (6.4)

Tar cracking and reforming: $tar + H_2O \rightarrow CO + CO_2 + H_2 + CH_4 + C_{2+}$ (6.5)

Olefins/tar steam reforming $C_nH_m + nH_2O \leftrightarrow 2nH_2 + nCO$ (6.6)

Water gas reaction: $H_2O + C \leftrightarrow H_2 + CO$ (6.7)

Water-gas shift reaction: $H_2O + CO \leftrightarrow H_2 + CO_2$ (6.8)

Methane steam reforming: $CH_4 + H_2O \leftrightarrow CO + 3H_2$ (6.9)

Boudouard reaction $C + CO_2 \leftrightarrow 2CO$ (6.10)

Char steam gasification $C + H_2O \leftrightarrow CO + H_2$ (6.11)

The main products of co-pyrolysis are generally classified into three categories namely: gases (CO, CO_2, H_2, CH_4, C_2H_2, C_nH_n, etc.), liquids (tars, heavy hydrocarbons, oil, water) and solids (mainly char) [28]. The product obtained from co-pyrolysis catalytic steam reforming of biomass and plastics can be enhanced via operating conditions such as temperature, heating rate, residence time, gasifying agent (steam, CO_2, O_2, etc.), catalysts, etc. According to Block et al.[28], high temperature, low heating rate and long residence time favour solid-char production while at the same high temperature, low heating rate but a longer residence time favours gaseous conversion and subsequently at an intermediate temperature, fast heating rate and short residence time aid oil-liquid conversion [28]. Plastics (HDPE, PS) are known to be composed of long hydrocarbon chains, under the catalytic steam reforming process (with high temperature and heating rate) undergo cracking or pyrolysis as the first step which usually gives a high gaseous yield and a small amount of liquid product, mostly aromatics hydrocarbons [19]. It has been reported that the reforming of olefin plastics obtained during the thermal degradation of HDPE led to a greater increase in gas yield due to the introduction of steam, i.e. the steam reacted was more than 0.8 kg per kg of HDPE in the feed as shown in Equation (6.8). Whereas compared to the pyrolysis of pure biomass gasification shows only a partial reaction with steam resulting in a much lower gas yield [19]. Hence, plastics undergo thermal cracking of the polymeric chain generating a wide range of molecular weight hydrocarbons consisting of both light and stable hydrocarbon fractions which contributes to an increase in syngas yield and heating value of products, while the production of tar is more associated with heavy hydrocarbon fractions [54, 57-59]. Block et al.[28], highlighted the reaction steps in the pyrolysis gasification process as shown in Equations (6.3-6.10). In addition, it was reported that syngas production could be produced via dry reforming using CO_2 instead of methane as shown in Equation (6.8). Biomass pyrolysis-gasification is stated to breakdown into gases, tar and char while plastics pyrolyses into gases, liquid then tar and no char. The effect on the products from co-pyrolysis is usually the result of the products obtained from the individual mixture of the two feedstocks with a positive synergistic effect which, in this case, are biomass components (lignin, cellulose) and plastics waste (HDPE, PS) respectively.

6.5 Effect of different catalyst temperatures on the co-pyrolysis catalytic steam reforming of biomass components and plastics

6.5.1 Product yield

Catalyst temperature is one of the most influencing operational conditions that affects the product yield and gas composition from the pyrolysis, catalytic steam reforming process. In this section, the catalytic bed temperature was increased from 750 ^{o}C to 850 ^{o}C, while at the same time the final pyrolysis temperature was kept constant at 550 ^{o}C as well as the steam flow rate of 5.7 ml/min and the catalyst used was 10%Ni-MCM-41. The product yield and gas composition as vol.% and mmol g^{-1} biomass:plastic are shown in Table 6.3 and in Figure 6.7. The mass balances were all above 90% with the highest being about 98%. Observations on the result showed that the gas yield increased from ~ 112 wt.% at 750 ^{o}C to 125 wt.% at 850 ^{o}C with co-pyrolysis of cellulose with HDPE, as calculated based on Equations 6.1 and 6.2. The influence of temperature on gas yield for the combination of lignin with plastics is more intense than that of the cellulose blend. The mixture of lignin and HDPE showed an increase in gas yield from ~ 71 to 107 wt.% and from 65 to 103 wt.% for the blend of lignin:PS at an increased catalytic bed temperature ranging from 750 to 850 ^{o}C. The blend of lignin with the plastics waste (HDPE and PS) had a gas yield increment of about 36-38 wt.%, far higher than that of cellulose with about 0-13 wt.% with the plastic wastes (HDPE and PS) blend respectively. Therefore, the influence of temperature is more intense at higher temperature on lignin compared to cellulose, such that lignin produced more gases at 850 ^{o}C than at 750 ^{o}C catalytic bed temperature. The increase in gas yield in co-pyrolysis of biomass with plastics with an increase in temperature has also been reported. For example, Berrueco et al. [23], carried out co-pyrolysis of biomass (sawdust) with a HDPE plastic blend in a fluidised bed reactor and reported an increase in gas yield from 55.4 to 90.5 wt.% with a noticeable increase in the gas composition as the temperature increased from 640-850 ^{o}C. It was reported that the results of the gases produced from the co-pyrolysis of the biomass and HDPE showed an average heating value of the gases.

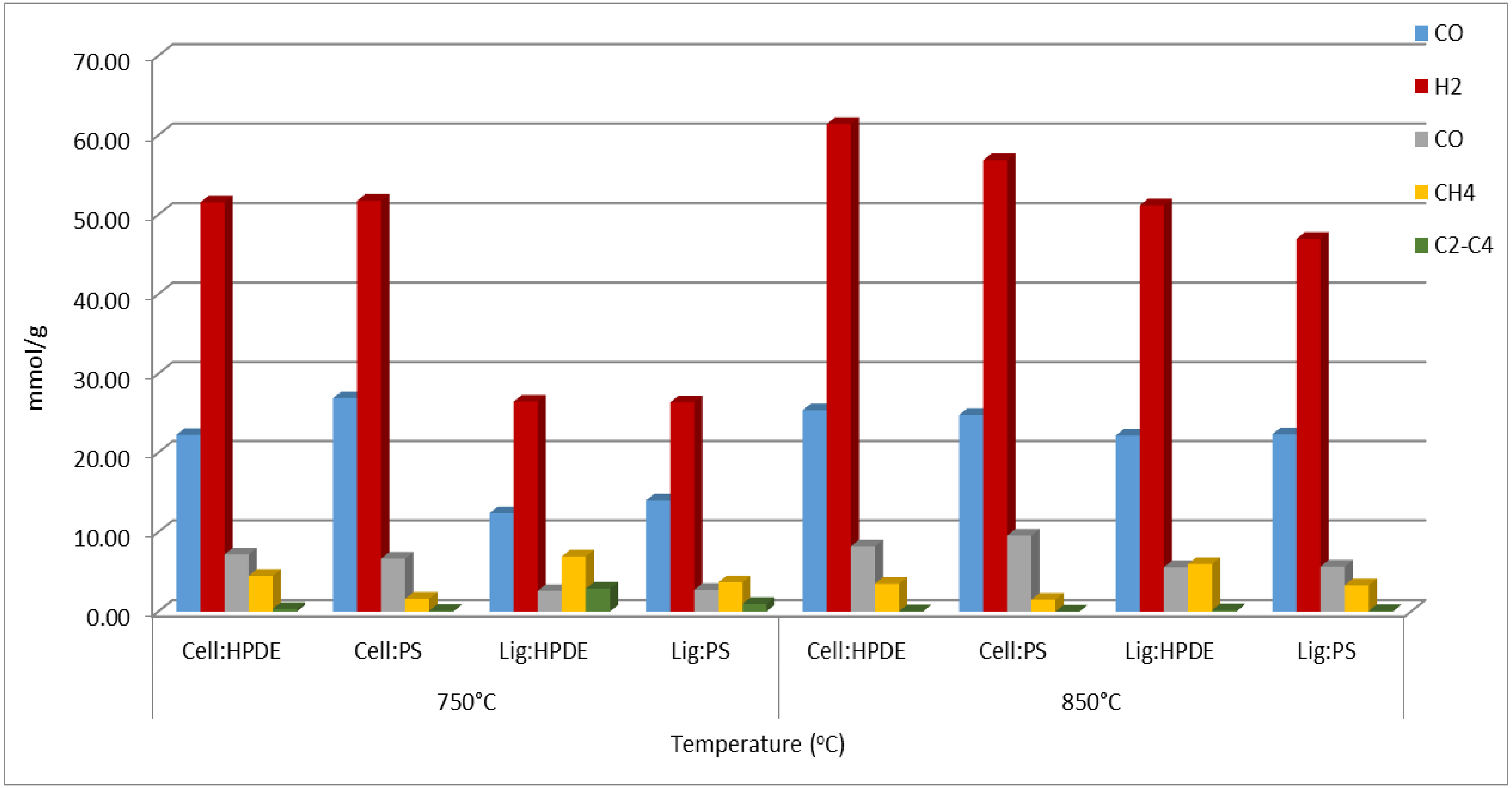

Figure 6.7. Gas composition yield showing the influence of temperature from the co-pyrolysis steam reforming of biomass components with plastics waste blend.

Table 6.3. Product yield and mass balance showing the influence of temperature on the co-pyrolysis steam reforming of biomass components with plastic wastes blend.

	Cell:HPDE	**Cell:PS**	**Lig:HPDE**	**Lig:PS**	**Cell:HPDE**	**Cell:PS**	**Lig:HPDE**	**Lig:PS**
Temp. (^{o}C)	**750**				**850**			
Product yield in relation to feedstock (biomass&plastics) only (wt.%)								
Gas	112.49	119.22	70.85	65.20	125.24	125.34	107.09	102.51
Product yield in relation to feedstock (biomass&plastics) + reacted water (wt.%)								
Gas	29.68	32.40	19.25	17.55	33.76	32.02	28.63	27.74
Liquid	58.84	56.79	70.65	72.54	58.49	56.70	59.36	57.92
Char	2.77	3.26	5.30	6.19	3.23	3.45	5.75	6.22
Catalyst carbon	1.06	1.09	0.95	1.08	0.40	1.66	1.20	0.95
Mass balance	92.35	93.54	96.15	97.36	95.89	93.83	94.94	92.83
Gas composition (vol.%)								
CO	25.91	30.77	24.17	29.31	25.73	26.7	26.04	28.48
H_2	60.09	59.29	51.56	55.18	62.34	61.35	60.15	59.93
CO_2	8.37	7.98	5.07	5.75	8.33	10.32	6.57	7.24
CH_4	5.23	1.85	13.55	7.73	3.56	1.63	7.03	4.24
C_2-C_4	0.4	0.11	5.66	2.03	0.04	0	0.21	0.11
Gas composition (mmol g^{-1})								
H_2+CO	73.81	78.63	38.82	40.32	86.76	81.64	73.34	69.28

6.5.2 Influence of catalyst temperature on gas composition

The effect of the increase in catalytic reforming temperature was also observed in the gas composition. Hydrogen and syngas yield increased from ~52 to 61 mmol/g of H_2 and from about ~ 74 to 87 mmol/g syngas for the blend of cellulose with plastics waste as the catalytic reforming temperature increased from 750 to 850 ^{o}C respectively. Likewise, the mixture of lignin and HDPE had an increased hydrogen yield from ~ 26 to 51 mmol/g and ~ 39 to 73 mmol/g of syngas at an increasing catalytic bed temperature from 750 to 850 ^{o}C as shown in Table 6.3 and Figure 6.7.

In the case of cellulose with plastics waste, there was a slight increase in hydrogen, CO and CO_2 while CH_4 and C_2-C_4 decreased. However, for the blend of lignin with plastics waste, there was higher H_2, CO and CO_2 production with almost a double fold increase while CH_4 and C_2-C_4 decreased as the catalytic bed temperature increased from 750 to 850 ^{o}C. The water gas shift reaction is suggested to increase the production of H_2 and CO_2 while water gas, methane and hydrocarbon steam reforming, and Boudouard reactions were all favoured as the temperature increased from 750 to 850 ^{o}C due to the increase in H_2 and CO, and the decrease in CH_4 and C_2-C_4 as shown in Equations 6.6-6.10. In addition, in the blend of lignin with the plastics waste, there was a decrease in the liquid yield and the char yield was higher as compared with the blend of cellulose with same plastics waste as the temperature increases from 750 to 850 ^{o}C. The decrease in liquid yield with the blend of lignin with plastics waste suggests that the higher concentration of oxygenated compounds in the oil derived from lignin blend were reformed for increased hydrogen production as compared with the blend of cellulose with the plastics waste. Thus, there was a greater production of hydrogen from lignin with plastics waste feedstock blend than cellulose with the same plastics waste blends.

Block et al. [28], highlighted the influence of temperature on product distribution, syngas and its composition as high temperature is mandatory for high carbon conversion as well as low tar content. Therefore, hydrogen concentration was stated to increase with increased temperature while methane (CH_4), tar and char yield decreased in the co-pyrolysis catalytic reforming of biomass with plastics process. The increase in catalytic reforming temperature led to an increase in gas yield, hydrogen and syngas production due to thermal cracking of volatiles, steam methane reforming and water gas-shift reaction which was favoured at high temperature [60].

The influence of catalytic bed temperature leading to an increase in hydrogen and syngas production has been reported in the literature. For example, Xie et al. [61] reported an increase in gas yield, hydrogen and syngas production with an increase in gasification temperature with maximum syngas production of 3.29 N m^3/kg biomass at 850 ^oC. It was explained that thermal cracking of the biomass was the major reaction that took place which is an endothermic reaction promoted as the gasification temperature increases. Other reactions reported at higher temperatures include decarbonylation, decarboxylation, depolymerisation in addition to thermal cracking of biomass pyrolysis [19, 62]. According to Berruecl et al. [23], the gas composition at an increasing temperature from 640-850 ^oC showed an increase in hydrogen and CO from 0.6 to 3.0 wt% and from 14.0 to 33.3 wt.% of feed respectively. The gases produced were stated to have an average heating value from the co-pyrolysis of biomass and HDPE mixtures. Pinto et al. [21] examined co-pyrolysis of biomass (pine sawdust) with plastics (HDPE) in a fluidized bed at a temperature range of 730-900 ^oC. Their observations included: H_2 concentration increases, CO_2 concentration increases slightly between 730-830 ^oC and then decreases at 830 ^oC, CO decreases at first and then increases from 830 ^oC, while CH_4, CnHm, tar and char yield decreases. This increase in H_2 concentration with temperature was explained by the reactions leading to H_2 i.e. water gas reaction, reforming reactions as shown in Equations (6.3-6.11) [28]. The increase in CO_2 and decrease in CO results were ascribed to a water gas shift reaction in the temperature range from 730-830 ^oC while at 830-900 ^oC suggested the water gas reaction dominating due to increasing CO and then Boudouard reaction explained the decrease as well as the increase of CO_2. Other products distribution due to endothermic cracking and reforming reactions were reported to decrease which include: CH_4, tar and char formation [21]. Many authors [21, 59, 63-65] have suggested the reaction pathways for increase in H_2 with temperature as well as other product distribution, except for some slight differences, could be explained based on different operating conditions, reactor design, etc.

6.6 Effect of different steam rate

6.6.1 Product yield

The influence of steam flow rate was investigated in relation to product yield and gas composition for the co-pyrolysis of biomass components (cellulose and lignin) and plastics waste (HDPE and PS) in relation to the pyrolysis, catalytic steam reforming process. The catalyst used was the 10 wt.% NiMCM-41 catalyst. The catalytic bed temperature was kept constant at 850 °C for all the experiments conducted with a different steam flow rate. The co-pyrolysis was 1:1 ratio of biomass components with plastics waste at different steam flow rates from 0, 3.7, 5.7, 7.7 and 9.7 ml/h representing steam to biomass ratios of 0, 1.85, 2.85, 3.85 and 4.85 were investigated. The product yield and gas composition as vol.% and mmolg^{-1} biomass;plastic are shown in Table 6.4 and Figure 6.8. The total gas yield was equally calculated based on Equations 6.1 and 6.2. The mass balances were all above 90 wt.% indicating the consistency of the results. The results showed that the increase in steam flow rate from 0 to 9.7 ml/h had a great influence on the product yields. For the gas yield in relation to feedstock plus reacted water (Table 6.4), showed a decrease in gas yield but the liquid yield increases as well as a decrease in char and carbon production with the increase in steam flow rate as shown in Table 6.4. This increase in liquid might suggest a decrease in gas yield. However, in the gas yield in relation to feedstock only, there is a consistent increase in gas yield from ~59 to ~129 wt.%, as the steam flow rate was increased from 0 to 7.7 ml/h as shown in Table 6.4. There was then a slight decrease to 125 wt.% at 7.7 to 9.7 ml/h steam flow rate for the co-pyrolysis gasification of cellulose:HDPE. In relation to the cellulose:PS mixture, the gas yield increased from about ~ 58 to ~147 wt.% as the steam input was increased from 0 to 7.7ml/h, then decreased slightly to 142 mmol/g as steam flow rate increased to 9.7 ml/h. The biomass components mixture with PS seems to have a slightly higher gas yield.

The higher gas yield with the increase in steam flow rate was obtained due to the higher steam rate, which promotes steam reforming of tar and other hydrocarbons from the co-pyrolysis-catalytic steam reforming of biomass components with the plastics waste leading to higher gas yield. Likewise, water gas reaction is also suggested to play a role in enhancing the gas yield [60]. In addition, there was a decrease in the liquid yield with the increase in steam flow rate. The decrease in liquid yield suggests that the higher concentration compounds in the derived oil were reformed for increased gas yield with the increase in steam flow rate.

Many researchers have investigated the influence of steam flow rate and reported an increase in gas yield at increasing steam rate and then a decrease [66, 67]. For instance, Lopez et al. [19] observed an increase in gas yield in the presence of steam flow rate in co-pyrolysis gasification with a positive synergistic effect leading to a decrease in both tar and char yield.

Table 6.4. Product yield and mass balance showing the influence of steam flow rate on the co-pyrolysis steam reforming of biomass components and plastics waste blend.

	Cell:HPDE	**Cell:PS**	**Cell:HPDE**	**Cell:PS**	**Cell:HPDE**	**Cell:PS**	**Cell:HPDE**	**Cell:PS**	**Cell:HPDE**	**Cell:PS**
Steam rate (ml/min)	**0**		**3.7**		**5.7**		**7.7**		**9.7**	
Product yield in relation to feedstock (biomass & plastics) only (wt.%)										
Gas	59.40	57.64	108.83	119.01	125.24	125.34	129.48	147.45	124.92	142.17
Product yield in relation to feedstock (biomass & plastics) + reacted water (wt.%)										
Gas	59.40	57.64	39.50	42.88	33.76	32.02	27.73	30.88	21.95	24.08
Liquid	0.00	0.00	45.92	40.54	58.49	56.70	63.49	60.52	70.56	65.20
Char	12.50	11.00	5.08	4.86	3.23	3.45	4.60	4.50	3.78	3.64
Carbon	18.00	22.50	2.36	4.14	0.40	1.66	1.07	1.05	0.88	0.85
Mass balance	89.90	91.14	92.86	92.43	95.89	93.83	96.89	96.95	97.17	93.76
Gas composition (vol.%)										
CO	24.62	32.46	25.59	29.19	25.73	26.7	25.51	27.44	26.55	29
H_2	61.92	61.86	61.12	60.8	62.34	61.35	62.34	61.05	64.64	60.27
CO_2	4.41	2.05	7.9	8.44	8.33	10.32	8.41	10.55	6.19	8.7
CH_4	8.99	3.64	5.21	1.57	3.56	1.63	3.57	0.96	2.61	2.02
C_2-C_4	0.05	0	0.18	0	0.04	0	0.16	0	0.01	0.02
Gas composition (mmol g^{-1})										
H_2+CO	44.54	45.98	73.93	80.11	86.76	81.64	89.41	95.16	95.84	94.04

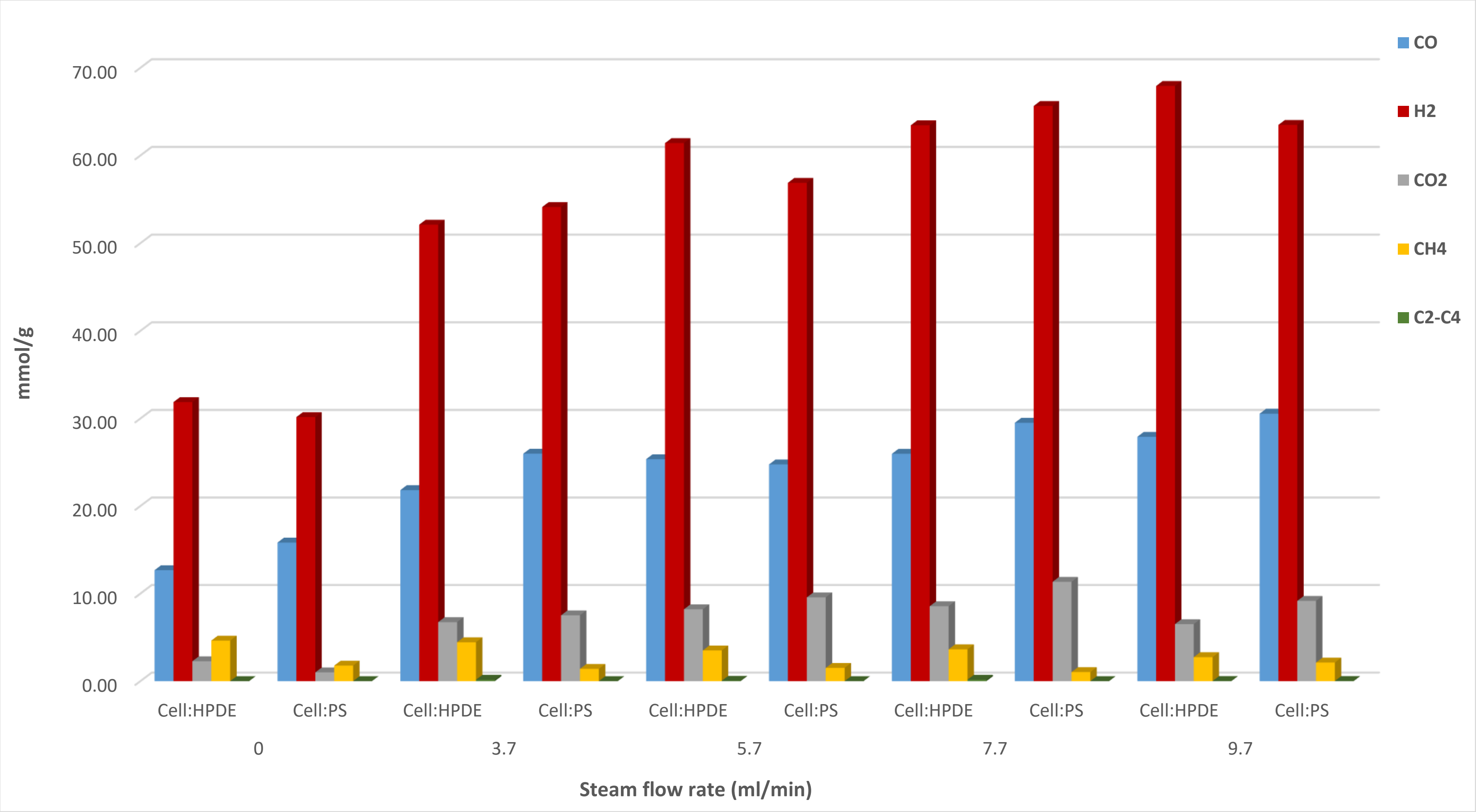

Figure 6.8. Product yield and mass balance showing the influence of steam flow rate on co-pyrolysis steam reforming of biomass components and plastics waste blend.

6.6.2 Influence of steam flow rate on gas composition and hydrogen yield

The gas composition in terms of hydrogen and syngas yield/production was positively enhanced with an increase in steam flow rate. For example, in the absence of steam (no steam injection) into the co-pyrolysis process, this resulted in ~ 32 and 30 mmol/g of hydrogen while the syngas yield was ~ 45 and 46 mmol/g for the blend of cellulose:HDPE and cellulose:PS respectively. The hydrogen production in the absence of steam is suggested to be the thermal and catalytic cracking process of the catalyst 10% NiMCM-41. Hence, as the steam flow rate was increased to 7.7 ml/h, the hydrogen yield increased to ~ 68 and ~ 66 mmol/g while the syngas yield increased to 96 mmol/g and 95 mmol/g for the blend of cellulose:HDPE and cellulose:PS. However, there was a decrease, with further steam flowrate increase to 9.7 ml/h for the blend of cellulose:PS, such that hydrogen decreased to 63 mmol/g while syngas yielded slightly to ~ 94 mmol/g.

Many studies have shown that there is an increase in hydrogen yield by co-pyrolysis gasification of biomass with plastics as compared to individual pyrolysis alone [19, 28]. H_2 concentration was reported to increase slightly, reaching a maximum point when the steam/fuel (S/F) ratio was studied, the steam flow rate was kept constant and the mass flow rate of the waste mixture was varied [21]. Ruoppolo et al. [54] also investigated the effect of steam for the co-pyrolysis of biomass and plastic and showed that there was an increase in hydrogen yield and H_2/CO and CO_2/CO ratios and a reduction in tar concentration suggesting that the presence of steam favoured the water gas shift reactions and reforming of hydrocarbons. Steam is known to be active for promoting water gas shift (WGS) reactions and steam reforming resulting in an increase in hydrogen production [11, 18].

In this study, water gas shift reaction and reforming reactions were promoted due to an increase in hydrogen yield. The concentration of CO increased for all the blended mixtures, this observation seems obvious at the point where steam (3.7 ml/g) was introduced into the pyrolysis-catalytic process with an increased yield ~ 10 mmol/g of CO. Likewise, CO_2 increases as steam flow rate increased from 0 to 7.7 ml/g for the entire feedstock blend. For example, the initial steam input recorded the highest CO_2 yield of ~ 4 to 6 mmol/g, as shown in Table 6.4 and Figure 6.8.

This suggests that both CO and CO_2 concentration in the co-pyrolysis catalytic steam reforming of biomass with plastics blend were mostly formed by the reforming reactions with oxygen being provided by the steam/reacted water.

According to Lopez et al. [19], it was also reported that the slight difference noticed in the concentration of CO and CO_2 may be ascribed to the decarboxylation and decarbonylation reactions from biomass pyrolysis as there is no oxygen present in the HPDE plastics [19]. It is consistent with this study as biomass component (lignin, cellulose) and plastics waste (HDPE, PS) were blended. Studies have shown that the high abundance of the functional group of OH and C-O are present in cellulose, while hemicellulose contained higher C=O compounds and lignin was found to be rich in methoxyl-O-CH3, C-O-C and C=C (aromatic ring) containing groups [35]. Therefore, it is suggested that high content of C-O chemical groups in cellulose leads to high CO, while hemicellulose with C=O chemical groups was observed to produce more CO_2 as shown in the results of previous studies [37, 68]. This might account for the slight increase in CO_2 with increasing steam flow, as observed in this study.

The increase in steam flow rate during gasification, introduces extra oxygen and hydrogen into the system [67]. At high temperatures such as 850 ^{o}C investigated in this study, water gas shift reaction is enhanced as steam input increases, therefore accounting for the increase in H_2 and CO_2. Likewise, the increase in H_2 and CO could be attributed to water gas and methane steam reforming reactions as steam flow rate increases while Boudouard reaction is suggested to increase CO production as shown in Equations 6.7-6.10. These reactions: water gas, methane steam reforming and Boudouard reactions are all favoured at the high catalytic reforming temperature of 850 ^{o}C studied, leading to an increase in H_2, CO and CO_2 as the steam rate increases up to 7.7 ml/h but decreases slightly at 9.7 steam rate. CH_4 yield decreases while C_2-C_4 is negligible at increasing steam rate. There are many reports by researchers on the influence of increasing steam flow rate leading to high hydrogen production [60, 69, 70]. This shows that the reforming gas (steam) obviously contributed to the total gas yield, hydrogen and syngas yield in addition to the hydrocarbon gases from the catalytic co-pyrolysis of the biomass samples with the plastics waste blend.

6.7 Conclusion

The co-pyrolysis-catalytic steam reforming of biomass components (lignin and cellulose) with plastic wastes (HDPE and PS) using novel catalysts in a fixed bed two-stage reactor have been investigated in this study. The yield of hydrogen and syngas was optimised by increasing steam injection and temperature increase as well as the presence of metal catalysts. Introduction of the different metal supported on MCM-41 catalysts suggests that nickel-based catalyst produced a slightly higher yield of hydrogen, the results showed that hydrogen yield from the 10%Ni/MCM-41 was approximately 52 mmol/g for both the co-pyrolysis of cellulose:PS and cellulose:HDPE while the highest yield of syngas (H_2+CO) produced was obtained at ~ 79 mmol/g for cellulose:PS and ~ 74 mmol/g for cellulose:HPDE co-pyrolysis catalytic steam reforming with the 10%NiMCM-41 catalyst.

Furthermore, hydrogen and syngas yield increased from ~52 to 61 mmol/g of H_2 yield and from about ~ 74 to 87 mmol/g of (H_2 + CO) as the catalytic reforming temperature increased from 750 to 850 ^{o}C respectively. Likewise, the mixture of lignin:HDPE had an increase in hydrogen yield from ~ 26 to 51 mmol/g and ~ 39 to 73 mmol/g of (H_2 + CO) at a catalytic bed temperature which increased from 750 to 850 ^{o}C.

In addition, the result on the effect of increase in steam injection flow rate from 0 to 9.7 ml/h had a great influence on the product obtained. As the steam flow rate was increased from 0 to 9.7 ml/h the hydrogen yield increased from ~ 32 to 68 mmol/g for the blend of cellulose:HDPE. Likewise, for the blend of cellulose:PS, hydrogen yield increased from ~ 30 to 66 mmol/g as steam flow rate increased from 0 to 7.7 ml/h but decreased slightly to 63 mmol/g as the steam rate increased to 9.7 ml/h respectively. The syngas yield increased from ~ 45 to 96 mmol/g as steam injection increased from 0 to 9.7 ml/h for the blend of cellulose:HDPE as well as from ~ 46 to 95 mmol/g at steam rate increase from 0 to 7.7 ml/h but decreased to ~ 94 mmol/g at 9.7 ml/h for the mixture of cellulose:PS respectively. The blend of lignocellulosic biomass with plastics waste in co-pyrolysis steam reforming with catalysis seems to be a novel option for tackling the problem of the waste disposal for production of petrochemical products and, in addition, generation of carbon neutral fuels.

References

1. Faix, O., et al., *Study on low mass thermal degradation products of milled wood lignins by thermogravimetry-mass-spectrometry.* 1988. 22(4): p. 323-334.
2. Jakab, E., et al., *Thermal decomposition of polypropylene in the presence of wood-derived materials.* 2000. 56(2): p. 273-285.
3. Jakab, E., et al., *Thermal decomposition of mixtures of vinyl polymers and lignocellulosic materials.* 2001. 58: p. 49-62.
4. Ojha, D.K. and R.J.R.A. Vinu, *Fast co-pyrolysis of cellulose and polypropylene using Py-GC/MS and Py-FT-IR.* 2015. 5(82): p. 66861-66870.
5. Sørum, L., M. Grønli, and J.J.F. Hustad, *Pyrolysis characteristics and kinetics of municipal solid wastes.* 2001. 80(9): p. 1217-1227.
6. Matsuzawa, Y., et al., *Acceleration of cellulose co-pyrolysis with polymer.* 2001. 71(3): p. 435-444.
7. Jimenez, A., R.A.J.J.o.t.a. Ruseckaite, and calorimetry, *Binary mixtures based on polycaprolactone and cellulose derivatives.* 2007. 88(3): p. 851-856.
8. Cai, J., et al., *Thermogravimetric analysis and kinetics of coal/plastic blends during co-pyrolysis in nitrogen atmosphere.* 2008. 89(1): p. 21-27.
9. Brebu, M., et al., *Co-pyrolysis of pine cone with synthetic polymers.* 2010. 89(8): p. 1911-1918.
10. Zhang, Y., et al., *Fe–Ni–MCM-41 Catalysts for Hydrogen-Rich Syngas Production from Waste Plastics by Pyrolysis–Catalytic Steam Reforming.* 2017. 31(8): p. 8497-8504.
11. Wu, C. and P.T. Williams, *Hydrogen production by steam gasification of polypropylene with various nickel catalysts.* Applied Catalysis B: Environmental, 2009. 87(3-4): p. 152-161.
12. Ma, Z., T. Kyotani, and A.J.C. Tomita, *Synthesis methods for preparing microporous carbons with a structural regularity of zeolite Y.* 2002. 40(13): p. 2367-2374.
13. Ma, Z., T. Kyotani, and A.J.C.C. Tomita, *Preparation of a high surface area microporous carbon having the structural regularity of Y zeolite.* 2000(23): p. 2365-2366.
14. Elbaba, I.F. and P.T.J.F. Williams, *High yield hydrogen from the pyrolysis–catalytic gasification of waste tyres with a nickel/dolomite catalyst.* 2013. 106: p. 528-536.
15. Srinakruang, J., et al., *Highly efficient sulfur and coking resistance catalysts for tar gasification with steam.* 2006. 85(17-18): p. 2419-2426.
16. Kim, J.-H., et al., *Effect of metal particle size on coking during CO2 reforming of CH4 over Ni–alumina aerogel catalysts.* 2000. 197(2): p. 191-200.
17. Liu, W.-W., et al., *Study on the effect of metal types in (Me)-Al-MCM-41 on the mesoporous structure and catalytic behavior during the vapor-catalyzed co-pyrolysis of pubescens and LDPE.* Applied Catalysis B: Environmental, 2013. 129: p. 202-213.
18. Alvarez, J., et al., *Hydrogen production from biomass and plastic mixtures by pyrolysis-gasification.* International Journal of Hydrogen Energy, 2014. 39(21): p. 10883-10891.

19. Lopez, G., et al., *Effect of polyethylene co-feeding in the steam gasification of biomass in a conical spouted bed reactor.* Fuel, 2015. 153: p. 393-401.

20. Ahmed, I., N. Nipattummakul, and A. Gupta, *Characteristics of syngas from co-gasification of polyethylene and woodchips.* Applied Energy, 2011. 88(1): p. 165-174.

21. Pinto, F., et al., *Co-gasification study of biomass mixed with plastic wastes.* Fuel, 2002. 81(3): p. 291-297.

22. Önal, E., B.B. Uzun, and A.E. Pütün, *Bio-oil production via co-pyrolysis of almond shell as biomass and high density polyethylene.* Energy Conversion and Management, 2014. 78: p. 704-710.

23. Berrueco, C., et al., *Experimental study of co-pyrolysis of polyethylene/sawdust mixtures.* Thermal Science, 2004. 8(2): p. 65-80.

24. Zhang, X., et al., *Renewable gasoline-range aromatics and hydrogen-enriched fuel gas from biomass via catalytic microwave-induced pyrolysis.* 2015. 17(7): p. 4029-4036.

25. Wang, K., K.H. Kim, and R.C.J.G.C. Brown, *Catalytic pyrolysis of individual components of lignocellulosic biomass.* 2014. 16(2): p. 727-735.

26. Zhang, X., et al., *Enhancement of jet fuel range alkanes from co-feeding of lignocellulosic biomass with plastics via tandem catalytic conversions.* 2016. 173: p. 418-430.

27. Serrano, D., J. Aguado, and J. Escola, *Developing advanced catalysts for the conversion of polyolefinic waste plastics into fuels and chemicals.* ACS Catalysis, 2012. 2(9): p. 1924-1941.

28. Block, C., et al., *Co-pyrogasification of Plastics and Biomass, a Review.* Waste and Biomass Valorization, 2018: p. 1-27.

29. Abnisa, F. and W.M.A.W. Daud, *A review on co-pyrolysis of biomass: an optional technique to obtain a high-grade pyrolysis oil.* Energy Conversion and Management, 2014. 87: p. 71-85.

30. Burhenne, L., et al., *The effect of the biomass components lignin, cellulose and hemicellulose on TGA and fixed bed pyrolysis.* Journal of Analytical and Applied Pyrolysis, 2013. 101: p. 177-184.

31. Vasile, C., et al., *Effect of some environmentally degradable materials on the pyrolysis of plastics II: influence of cellulose and lignin on the pyrolysis of complex mixtures.* 2010. 12(2): p. 147-153.

32. Gunasee, S.D., et al., *Co-pyrolysis of LDPE and cellulose: Synergies during devolatilization and condensation.* 2017. 126: p. 307-314.

33. Huang, Q., et al., *Effect of cellulose and polyvinyl chloride interactions on the catalytic cracking of tar contained in syngas.* 2016. 30(6): p. 4888-4894.

34. Jin, W., et al., *Evaluation of the co-pyrolysis of lignin with plastic polymers by TG-FTIR and Py-GC/MS.* 2016. 133: p. 65-74.

35. Yang, H., et al., *Characteristics of hemicellulose, cellulose and lignin pyrolysis.* Fuel, 2007. 86(12): p. 1781-1788.

36. Liu, Q., et al., *Interactions of biomass components during pyrolysis: A TG-FTIR study.* Journal of Analytical and Applied Pyrolysis, 2011. 90(2): p. 213-218.

37. Akubo, K., M.A. Nahil, and P.T.J.J.o.t.E.I. Williams, *Pyrolysis-catalytic steam reforming of agricultural biomass wastes and biomass components for production of hydrogen/syngas.* 2018.

38. Zhao, M., N.H. Florin, and A.T.J.A.C.B.E. Harris, *The influence of supported Ni catalysts on the product gas distribution and H2 yield during cellulose pyrolysis.* 2009. 92(1-2): p. 185-193.

39. Han, J. and H. Kim, *The reduction and control technology of tar during biomass gasification/pyrolysis: an overview.* Renewable and Sustainable Energy Reviews, 2008. 12(2): p. 397-416.

40. Matsuzawa, Y., M. Ayabe, and J. Nishino, *Acceleration of cellulose co-pyrolysis with polymer.* Polymer Degradation and Stability, 2001. 71(3): p. 435-444.

41. Solak, A. and P. Rutkowski, *Bio-oil production by fast pyrolysis of cellulose/polyethylene mixtures in the presence of metal chloride.* Journal of Material Cycles and Waste Management, 2014. 16(3): p. 491-499.

42. Zhang, H., et al., *Catalytic co-pyrolysis of biomass and different plastics (polyethylene, polypropylene, and polystyrene) to improve hydrocarbon yield in a fluidized-bed reactor.* Energy & Fuels, 2014. 28(3): p. 1940-1947.

43. Huang, Q., et al., *Effect of cellulose and polyvinyl chloride interactions on the catalytic cracking of tar contained in syngas.* Energy & Fuels, 2016. 30(6): p. 4888-4894.

44. Todorova, S., et al., *Metal states in cobalt-and cobalt–vanadium-modified MCM-41 mesoporous silica catalysts and their activity in selective hydrocarbons oxidation.* Microporous and Mesoporous Materials, 2008. 113(1-3): p. 22-30.

45. Szegedi, A., et al., *Cobalt-containing mesoporous silicas—Preparation, characterization and catalytic activity in toluene hydrogenation.* Applied Catalysis A: General, 2008. 338(1-2): p. 44-51.

46. Lucredio, A.F. and E.M. Assaf, *Cobalt catalysts prepared from hydrotalcite precursors and tested in methane steam reforming.* Journal of power sources, 2006. 159(1): p. 667-672.

47. Wu, C., et al., *Hydrogen production from biomass gasification with Ni/MCM-41 catalysts: influence of Ni content.* Applied Catalysis B: Environmental, 2011. 108: p. 6-13.

48. Zhao, M., et al., *Interaction between a bimetallic Ni–Co catalyst and micrometer-sized CaO for enhanced H2 production during cellulose decomposition.* International Journal of Hydrogen Energy, 2011. 36(1): p. 421-431.

49. Furusawa, T. and A. Tsutsumi, *Comparison of Co/MgO and Ni/MgO catalysts for the steam reforming of naphthalene as a model compound of tar derived from biomass gasification.* Applied Catalysis A: General, 2005. 278(2): p. 207-212.

50. Zhao, M., N.H. Florin, and A.T. Harris, *Mesoporous supported cobalt catalysts for enhanced hydrogen production during cellulose decomposition.* Applied Catalysis B: Environmental, 2010. 97(1-2): p. 142-150.

51. Sutton, D., B. Kelleher, and J.R. Ross, *Review of literature on catalysts for biomass gasification.* Fuel Processing Technology, 2001. 73(3): p. 155-173.

52. Davda, R., et al., *A review of catalytic issues and process conditions for renewable hydrogen and alkanes by aqueous-phase reforming of oxygenated hydrocarbons over supported metal catalysts.* Applied Catalysis B: Environmental, 2005. 56(1-2): p. 171-186.

53. Srinakruang, J., et al., *A highly efficient catalyst for tar gasification with steam.* Catalysis Communications, 2005. 6(6): p. 437-440.

54. Ruoppolo, G., et al., *H2-rich syngas production by fluidized bed gasification of biomass and plastic fuel.* Waste Management, 2012. 32(4): p. 724-732.

55. Furusawa, T. and A. Tsutsumi, *Development of cobalt catalysts for the steam reforming of naphthalene as a model compound of tar derived from biomass gasification.* Applied Catalysis A: General, 2005. 278(2): p. 195-205.

56. Mu, Z., et al., *Synthesis of mesoporous Co/Ce-SBA-15 materials and their catalytic performance in the catalytic oxidation of benzene.* Materials Research Bulletin, 2008. 43(10): p. 2599-2606.

57. Arena, U., L. Zaccariello, and M.L. Mastellone, *Tar removal during the fluidized bed gasification of plastic waste.* Waste Management, 2009. 29(2): p. 783-791.

58. Arena, U., L. Zaccariello, and M.L. Mastellone, *Fluidized bed gasification of waste-derived fuels.* Waste Management, 2010. 30(7): p. 1212-1219.

59. Mastellone, M.L., L. Zaccariello, and U. Arena, *Co-gasification of coal, plastic waste and wood in a bubbling fluidized bed reactor.* Fuel, 2010. 89(10): p. 2991-3000.

60. Qari M.K. Waheed, Chunfei Wu, and P.T. Williams, *Pyrolysis/reforming of rice husks with a Niedolomite catalyst:Influence of process conditions on syngas and hydrogen yield.* Journal of the Energy Institute 2016. 89: p. 657-667.

61. Xie, Q., et al., *Syngas production by two-stage method of biomass catalytic pyrolysis and gasification.* Bioresource Technology, 2012. 110: p. 603-609.

62. Fassinou, W.F., et al., *Pyrolysis of Pinus pinaster in a two-stage gasifier: Influence of processing parameters and thermal cracking of tar.* Fuel Processing Technology, 2009. 90(1): p. 75-90.

63. Pinto, F., et al., *Effect of experimental conditions on co-gasification of coal, biomass and plastics wastes with air/steam mixtures in a fluidized bed system.* Fuel, 2003. 82(15-17): p. 1967-1976.

64. Aznar, M.P., et al., *Plastic waste elimination by co-gasification with coal and biomass in fluidized bed with air in pilot plant.* Fuel Processing Technology, 2006. 87(5): p. 409-420.

65. Taba, L.E., et al., *The effect of temperature on various parameters in coal, biomass and CO-gasification: a review.* Renewable and Sustainable Energy Reviews, 2012. 16(8): p. 5584-5596.

66. Waheed, Q.M. and P.T. Williams, *Hydrogen production from High temperature pyrolysis/steam reforming of waste biomass: rice husk, sugar cane bagasse, and wheat straw.* Energy & Fuels, 2013. 27(11): p. 6695-6704.

67. Waheed, Q.M., C. Wu, and P.T. Williams, *Hydrogen production from high temperature steam catalytic gasification of bio-char.* Journal of the Energy Institute, 2016. 89(2): p. 222-230.

68. Wu, C., et al., *Pyrolysis/gasification of cellulose, hemicellulose and lignin for hydrogen production in the presence of various nickel-based catalysts.* Fuel, 2013. 106: p. 697-706.

69. Li, X., et al., *Biomass gasification in a circulating fluidized bed.* 2004. 26(2): p. 171-193.

70. Xiao, X., et al., *Two-stage steam gasification of waste biomass in fluidized bed at low temperature: Parametric investigations and performance optimization.* 2011. 102(2): p. 1975-1981.

Chapter 7

Conclusions and Future Work

The aim of this research work was the production of aromatic hydrocarbons and hydrogen/syngas using pyrolysis/pyrolysis-catalysis, pyrolysis/co-pyrolysis-catalytic, steam reforming of waste plastics and biomass in a two-stage fixed bed reactor. Optimisation of the process focused on the influence of different types of transition metals and support catalysts, and other process conditions such as temperature, steam injection rate, etc. Investigation of a series of different feedstocks such as plastics waste (HDPE and PS), six different biomass samples (rice husk, sugarcane bagasse, coconut shell, palm kernel shell, cotton stalk and wheat straw) and the three main components of biomass consisting of cellulose, hemicellulose and lignin. The improvement of catalytic activity was to promote aromatic fuel oil production from waste plastics and high-value fuels; hydrogen/syngas yield from the various biomass samples and a mixture of plastic wastes with biomass in co-pyrolysis.

7.1 Conclusions

The following conclusions were drawn considering the order of the chapters and experimental results presented in this research work.

7.1.1 Pyrolysis-Catalysis of Polyethylene Plastic with Metal-Impregnated Zeolite Catalysts for Aromatic Fuel Oil Production

The pyrolysis/pyrolysis-catalytic of HDPE (2 g) was conducted in a two-stage fixed bed reactor in the absence of catalyst and with the use of Y-zeolite catalyst (1 g) at a temperature of 600 ^{o}C with the same pyrolysis conditions. In addition, the catalytic bed temperature was varied from 600 to 900 ^{o}C to determine the effect of temperature on gas composition and aromatic oil yield. In the absence of catalyst at 600 ^{o}C, the total gas yield produced is ~ 21.09 wt.% and the liquid yield ~ 69 wt.% compared with the use of catalyst (Y-zeolite) total gas yield increase to ~ 22.49 wt.% and the liquid oil produced is ~ 71 wt.% respectively.

- The result showed that as the catalyst temperature was increased, gas yield increased up to a temperature of 800 ^{o}C and then decreased to 900 ^{o}C. The liquid yield decreased while the solid carbon deposition on the catalyst increased throughout the entire temperature range studied. Likewise, the yield of hydrogen in the absence of catalyst was 0.35 mmol/g (4.95 vol.%) but increased to 2.41 mmol/g (25.40 vol.%) after the introduction of Y-zeolite catalyst into the pyrolysis process at the initial catalytic bed temperature of 600 °C. The hydrogen and methane yield continuously increased as the temperature increased throughout the entire temperature studied. Hydrogen increased to 15.34 mmol/g (41.05 vol.%) while methane yield increased to 15.49 mmol/g (41.44 vol.%) at a catalytic temperature of 900 °C.

- Furthermore, in the non-catalytic pyrolysis process, HDPE produced a high oil yield (~70 wt.%) comprising of almost 100% aliphatic hydrocarbon. Introduction of Y-zeolite catalyst produced a slight increase in oil yield (~ 71 wt.%) and a decreased content of aliphatic oil yield (to 47.56%) while the aromatic yield increased to 52.44% at a temperature of 600 °C. Though, the total liquid yield produced decreases with increase in temperature, the composition of the hydrocarbon oil increases with aromatic hydrocarbon production above 98% and a consistent decrease in aliphatic compounds to 1.73% as the temperatures increases from 600-900 °C. This could be attributed to the thermal and catalytic cracking reactions as temperature increases due to heavier molecular hydrocarbons being converted into lighter compounds as well as secondary reaction, cyclisation, aromatisation reactions, etc.

Likewise, the effect of prepared novel metal/Y-zeolite catalysts on high-density polyethylene (HPDE- 2 g) plastics pyrolysed in a two-stage fixed bed reactor with a constant temperature of 600 °C for both the pyrolysis and catalytic bed were investigated.

- Pyrolysis of the HDPE (2 g) without a catalyst, but with a substitute of quartz sand of similar particle size, produced a mainly liquid product of ~70 wt.% and gas yield of 21 wt.%. Introduction of the Y-zeolite catalyst (4 g) into the second stage resulted in a significant increase in gas yield to 36 wt.% and a corresponding decrease in oil yield. Addition of metal promoters to the Y-zeolite showed only a small difference in oil and gas yield compared with the non-metal containing Y-zeolite. However, the loading of transition metals, which includes nickel (Ni), iron (Fe), molybdenum (Mo), gallium (ga), ruthenium (Ru) and cobalt (Co) on Y-zeolite catalyst (4 g), promoted the formation of aromatic hydrocarbons (80-95%) in the product oil and increased hydrogen gas production.
- The influence of the metal additions to the Y-zeolite further enhance the concentration of hydrogen in the product gas. The increase in hydrogen content of the product gases produced a consequent decrease in C_1-C_4 hydrocarbons respectively.

- The aromatic hydrocarbons in the product oil using metal-promoted Y-zeolite catalysts showed that the oil was composed of between 97-99% 1-2 ring aromatic hydrocarbon compounds. The aromatic hydrocarbons in the oil were mostly toluene, ethylbenzene and xylene and the 2-ring aromatic hydrocarbons were naphthalene and alkylated naphthalenes. These single and double ring aromatic hydrocarbons derived from the waste plastics are important petrochemical feedstock for the chemical industries.
- However, the introduction of metal promoters (1 wt.%) to Y-zeolite catalyst resulted in high carbon deposition onto the catalysts between 14 – 26 wt.%, and at a higher metal loading of 5 wt.% produced even higher carbon deposition. The carbon deposits were identified mostly as a filamentous type, which are of high value in carbon nanotube technology.

7.1.2 Pyrolysis-catalytic steam reforming of agricultural biomass wastes and biomass components for production of hydrogen/syngas.

The biomass samples and biomass components were characterised with thermogravimetric analysis (TGA) for the determination and characterisation of the thermal degradation profile.

- The cellulose weight-loss peak (which is the mass fraction loss at that temperature) was observed in this study to have the largest DTG peak compared to hemicellulose and lignin. Hemicellulose (xylan) decomposed between temperatures of 200-350 °C, cellulose decomposition takes place between 350-400 °C while that of lignin showed a wider decomposition temperature which started at about 250 °C and continued up to about 500 °C and beyond.
- A mixture of the three biomass components in equal proportion exhibited two separate DTG peaks, one at a temperature below 300 °C which may be attributed to the mass loss of xylan while the thermogram DTG peak above 300-400 °C could be the mass loss contribution by cellulose and some lignin. It is suggested that the pyrolysis of biomass could be regarded as a superposition of the three main components which perform separate roles during the biomass pyrolysis and decomposition.
- The agricultural waste biomass samples in this study were linked to the thermal decomposition of the three biomass components: cellulose, hemicellulose and lignin. The mass loss thermograms of all the agricultural waste biomass samples were between the thermal degradation weight-loss thermogram ranges of the three biomass

components. The thermal decomposition (TGA) of the six waste biomass samples started at ~200 °C and the DTG thermograms showed more than one peak for all the biomass samples indicating the presence, and a reflection of, these main biomass components as observed.

The product yield and gas compositions from the pyrolysis (no catalyst) and pyrolysis-catalytic steam reforming of the agricultural (six) biomass wastes and the three biomass components were investigated/conducted.

- In the absence of catalyst and steam, the results show that the sugarcane bagasse produced the highest total gas yield of 43.3 wt.%, palm kernel shell and coconut shell produced similar yields of total gas yield at about 42 wt.% while rice husk and cotton stalk produced approximately the same gas yield of 39 wt.% in the absence of catalyst. Also, wheat straw produced a gas yield of about 38 wt.% in the absence of catalyst. The highest char yield was produced by rice husk with a value of 37 wt.% and the lowest char production is cotton stalk of about 24 wt.%. Rice husks are known to have high ash content which contribute to the char yield.
- Consequently, introduction of steam and 10%$NiAl_2O_3$ catalyst to the pyrolysis-catalytic steam reforming process significantly increased total gas yield up to ~ 70 wt.% for palm kernel shell as well as ~ 13 - 28 wt.% increment in gas yield observed across all the biomass samples. In addition, there was a marked increase in hydrogen production as steam and catalyst were introduced into the process. The increase in the production of hydrogen resulted in an increase in the volumetric proportion of hydrogen in the product gas from about 54.06 to 59.23 vol.% for all the biomass samples (rice husk, coconut shell, sugarcane, palm kernel shell, cotton stalk and wheat straw) respectively. In terms of hydrogen yield, a range of 16.38 to 25.35 mmol g^{-1} was obtained from the mass of the biomass feedstock pyrolysed. However, methane (CH_4) yield and C_2-C_4 (tar) yield decreased which indicated that methane/hydrocarbon steam reforming and catalytic cracking were the dominant reactions.
- Likewise, in the absence of catalyst and steam, cellulose and hemicellulose pyrolysis generated a gas yield ~50 wt.% and lignin ~30 wt.%. The highest char residue was observed with lignin at ~45%, while that of cellulose was ~20 wt.% and xylan ~18 wt.%. The introduction of 10 wt.% $NiAl_2O_3$ catalyst and steam to the process showed an increase in gas yield for the three biomass components, at 55.45 wt.%, 55.44 wt.% and 50.48 wt.% for cellulose, hemicellulose and lignin respectively. The production of

hydrogen from the catalytic steam reforming process was slightly higher for lignin and for cellulose and hemicellulose, CO and CO_2 yields were higher compared to lignin. The presence of methoxyl-O-CH3 containing hydrocarbons in the lignin structure and their release during pyrolysis has been implicated in the enhanced production of H_2 from lignin. However, the presence of C – O and C = O structures in cellulose and hemicellulose results in enhanced production of CO and CO_2.

- The mixture of the three biomass components: lignin, cellulose and xylan with pyrolysis-catalytic steam reforming produced a gas yield of 59.31 wt.% and a char residue of 26.0 wt.%. The product yield, such as the gas yield and char production observed for the three biomass components mixture was a reflection of the superposition of the individual components. For example, a slightly higher hydrogen yield was produced from the mixture with lignin and cellulose as compared to other component mixtures respectively. Similar results for CO, CO_2 and CH_4 were observed and trace amounts of C_2-C_4 were produced comparable to the individual biomass components.

The results of the experiments analysing the effect of lignin content from the pyrolysis of various biomass component mixtures, the percentage of lignin was varied from 10, 50, 90 and 100 wt.% with a balance of equal quantities of cellulose and hemicellulose, are shown below:

- The highest gas yield (40.66 wt.%) was obtained at the lowest lignin content of 10 wt.%, reflecting higher gas yield from cellulose and hemicellulose in the absence of catalyst and no steam in the pyrolysis-catalytic steam reforming process. It was observed that as lignin content was increased, H_2 production increased and CO and CO_2 decreased. Therefore, the higher the lignin content, the higher the resistance of biomass to degradation and consequently, a higher char residue yield instead of a gases and volatiles yield. The presence of 10 wt.% $NiAl_2O_3$ catalyst produced a marked increase in gas yield and, in particular, enhanced H_2 yield, increasing lignin content produced an increasing total gas yield from 55.31 wt.% at 10 wt.% lignin content to 64.36 wt.% at 100 wt.% lignin content. In addition, higher hydrogen yield was produced with increased lignin content, rising from 14.99 mmol g^{-1} at 10 wt.% lignin content to 28.19 mmol g^{-1} at 100 wt.% lignin content. This suggests that catalytic steam reforming was active as gas yield increased at increasing lignin content in the presence of catalyst, as it was contrary in the absence of catalyst.

- A correlation equation was used to calculate hydrogen production with a known content of lignin, observed on the plots (with an R-square value up to 96%); showed that as lignin content increases, the higher the hydrogen produced as there seem to be interaction as the experimental values were slightly higher than the calculated values, the contrary difference might be due to equipment and experimental error.

In a different experimental procedure such that the gas composition evolved at specific temperatures (every 50 °C) gas samples were collected throughout the pyrolysis process and the pyrolysis-catalytic steam reforming process for 100 wt.% lignin was investigated.

- The results showed that the composition of each of the product gases, CO, H_2, CO_2, CH_4, and C_2-C_4, increases as the biomass feedstock undergoes pyrolysis or pyrolysis-catalytic steam reforming. The evolution of gases decreases as the thermal degradation of the biomass progresses and complete thermal degradation occurs, leaving the residual char. The highest yield of gases was released at 350 °C for the pyrolysis of lignin while for pyrolysis-catalytic steam reforming of lignin with the 10 wt. % $NiAl_2O_3$ catalyst, gas yield peaked between the temperatures of 250-300 °C indicating a lower decomposition temperature for the lignin in the presence of the 10% Ni/Al_2O_3 catalyst.

In addition, the morphologies of fresh and char biomass samples and components were equally investigated, the SEM analyser revealed porous structure on the char samples due to the release of gases especially as shown by lignin and xylan char after the pyrolysis-catalytic steam reforming process while cellulose char structure showed a smaller size as compared with the cellulose fresh sample.

7.1.3 Co-pyrolysis-catalytic steam reforming of biomass components with waste plastics for the production of hydrogen-rich syngas using novel catalysts

TGA experiments were conducted on the mixture of biomass components (lignin and cellulose) with plastics waste (HDPE and PS).

- It showed that there were two distinct peaks for the blend of cellulose with HDPE, the first weight loss peak was between temperatures of 300 to 400 ^{o}C which is attributed to the decomposition of the cellulose component while the second weight loss peak is within the temperature range of 450-510 ^{o}C which is attributed to the decomposition of HDPE plastics. Also, the blend of cellulose with PS equally shows two major weight loss decomposition peaks, the first is between 300 to 400 ^{o}C and attributed to the degradation of cellulose while the second weight loss peak is between 400 to 500 ^{o}C which is ascribed to PS decomposition. It appears that the weight loss for both peaks was reduced for the blend of cellulose and PS. In the case of cellulose with HDPE blend, the first peak seems to be cellulose decomposition which has a reduced weight loss at slightly higher temperature than the decomposition of cellulose alone but there was no effect on the weight loss as well as the temperature of the second peak ascribed to HDPE in the mixture with cellulose. This could suggest that the plastics waste might have a slight influence on the degradation of cellulose.

- The blend of lignin with HDPE had a small weight loss decomposition peak around a temperature of 350-450 ^{o}C while the major weight loss peak within the range 450 to 550 ^{o}C. The lignin mixture with PS showed only one major peak between 350 and 500 ^{o}C. The lignin component mixture with the plastics waste suggests that the decomposition temperature of these two blends have a common and overlapping degradation temperature, which suggests that there might be interaction. Also, in the blend of lignin with the plastics waste (HDPE and PS), there was a reduced weight loss compared to the plastic decomposition alone which had an increased weight loss as compared to the decomposition of lignin alone.

The steam reforming co-pyrolysis catalytic of biomass components (lignin and cellulose) with plastic wastes (HDPE and PS) using novel metal catalysts in a fixed bed two-stage reactor was also investigated in this study. The yield of hydrogen and syngas was optimised by increasing steam injection and temperature increase as well as the presence of metal catalysts.

- Introduction of the different metals (Ni, Co, Mo and the bimetal NiCe) supported on MCM-41 catalysts presented 10%Ni/MCM-41 to have a slightly higher yield of hydrogen compared with the other metals. The results showed that hydrogen yield from the 10%Ni/MCM-41 was approximately 52 mmol/g for both the co-pyrolysis of cellulose:PS and cellulose:HDPE. The syngas (H_2+CO) produced showed that the highest yield ~ 79 mmol/g was obtained by cellulose:PS and ~ 74 mmol/g was produced by cellulose:HPDE co-pyrolysis catalytic steam reforming with the 10%NiMCM-41 catalyst. The use of catalysts also aided in the selection of desired product as Ni based catalysts are known to be used for steam gasification of biomass due to their low cost, high activity for C-C bond rupture and identified as the best metals for tar elimination and hydrogen production.

- The mixture of lignin:HDPE had a gas yield of ~71 wt.% and ~65 wt.% for the blend of lignin:PS for 10%Ni/MCM-41 catalyst. For 10% Mo/MCM-41 catalyst, had a gas yield ~51 wt.% and ~38 wt.% for a blend of lignin:HDPE and lignin:PS respectively. The higher value of gas yield from the blend of cellulose compared to lignin mixture with the same plastic wastes was possibly due to a synergistic effect between the feedstocks. The reaction temperature might be another factor due to higher gaseous yield from the cellulose than lignin blend. Cellulose has been shown to decompose at a lower temperature than lignin component of biomass sample.
- Furthermore, on the influence of temperature, hydrogen and syngas yield increased from ~52 to 61 mmol/g of H_2 yield and from about ~ 74 to 87 mmol/g of syngas (H_2 + CO) as the catalytic reforming temperature increased from 750 to 850°C respectively. Likewise, the mixture of lignin:HDPE had an increase of hydrogen yield from ~ 26 to 51 mmol/g and ~ 39 to 73 mmol/g of syngas (H_2 + CO) at an increasing catalytic bed temperature from 750 to 850 °C. It was observed that at much higher temperatures lignin produced more gas yield than cellulose based on the incremental percentage at increasing temperature. Lignin degrades at a much higher temperature than cellulose. This shows that for biomass samples with higher content of lignin, such as woody plant wastes, will yield more hydrogen and syngas at higher temperatures compared with samples with more cellulose components. Additionally, lignin produced higher char than cellulose with plastic wastes blend.
- In addition, the result on the effect of increase in steam injection flow rate from 0 to 9.7 ml/h had a great influence on the product obtained. As the steam flow rate was increased from 0 to 9.7 ml/h the hydrogen yield increased from ~ 32 to 68 mmol/g for the blend of cellulose:HDPE. Likewise, for the blend of cellulose:PS hydrogen yield increased from ~ 30 to 66 mmol/g as steam flow rate increased from 0 to 7.7 ml/h but decreased slightly to 63 mmol/g at the steam flow rate of 9.7 ml/h respectively.
- Also, the syngas yield increased from ~ 45 to 96 mmol/g as steam flow rate increased from 0 to 9.7 ml/h for the blend of cellulose:HDPE as well as from ~ 46 to 95 mmol/g at steam rate increased from 0 to 7.7 ml/h but decreased to ~ 94 mmol/g at 7.7 to 9.7 ml/h for the mixture of cellulose:PS respectively. The blend of lignocellulosic biomass with plastics waste in co-pyrolysis steam reforming with catalysis seems to be a novel option for tackling the problem of the waste disposal, for production of petrochemical products and in addition generation of carbon neutral fuels. Furthermore, carbon

monoxide increases as the steam increased from 0 to 9.7ml/h, this suggest that as more steam is introduced into the process, more CO was produced, therefore, syngas yield increased across the entire steam flow rate investigated.

7.2 Future work

7.2.1 The process of two-stage pyrolysis-catalysis of high-density polyethylene (HDPE) to produce a high aromatic content feedstock for the production of fuels or chemicals has been demonstrated. However, further investigation is required to advance the process.

- There is particular interest in developing different types of catalysts, for example: hierarchical catalysts or staged catalysis where the large polymer hydrocarbon fragments from pyrolysis can be firstly cracked to smaller molecules which can then enter smaller pores to enhance the yield of aromatic hydrocarbons.
- Minimisation of catalyst deactivation through coke formation on the catalyst, which blocks active catalytic sites, is also an area for catalyst development. For real-world waste plastics, there is also the issue of contamination of the plastics and the potential release of sulphur and halogenated species which may poison the catalyst.
- Scale-up of the technology to a continuous system would also be required for larger scale plants. The two-stage system would require a continuous first stage such as a rotary kiln or screw kiln pyrolysis unit followed by the catalytic stage, where the catalyst could be quickly regenerated, such as a circulating fluidised bed, similar to a petroleum refinery catalytic cracking unit. Testing the product oil either for its potential as a substitute refinery-ready feedstock for further processing, direct application as a fuel for use as a boiler/furnace fuel or use in engines should also be assessed.

7.2.2 A two-stage reactor was employed in this study; therefore a three-stage reactor is recommended to further improve hydrogen production from the process pyrolysis-gasification of biomass by controlling the temperature of each section separately.

- The first stage for pyrolysis of biomass, second stage for catalytic steam gasification and for the third stage CO_2 absorption by CaO. Further conversion of CO into H_2 by water gas-shift reaction, methane reforming reaction and further modification of temperatures, steam injection rates, and different catalysts are suggested.
- Advantage can be taken in the area of char gasification of the biomass samples, especially feedstock containing more lignin content of biomass such as woody biomass

due to the largest char being produced by lignin with high carbon content. Reforming catalysts with the effect of support and promoter metals (such as Pd) are ideal for further investigation on co-pyrolysis of biomass with plastic wastes.

7.2.3 It was a biomass component (lignin and cellulose) mixture that was analysed in the co-pyrolysis of biomass with plastics waste in this study.

- Therefore, different biomass samples (such as rice husk, palm kernel shell, etc.) investigated in co-pyrolysis with waste plastics due to the synergistic effect of high gas yield and hydrogen. Likewise, only gases were analysed with respect to co-pyrolysis in this study, it would be advantageous to conduct further research to ascertain the component distribution in the oil produced from the co-pyrolysis of biomass components with plastic wastes. This could be a novel option for the improvement of bio-fuel production by deoxygenation, decarbonylation and decarboxylation reactions as well as aromatic hydrocarbons.
- In addition, different preparation of catalyst procedures such as sol-gel and co-precipitation method is suggested for further investigation of their effect on gas yield as well as hydrogen production from co-pyrolysis-catalytic steam reforming of biomass with plastics waste. Likewise, a kinetic and mathematical model could be developed for prediction of product yield and distribution.